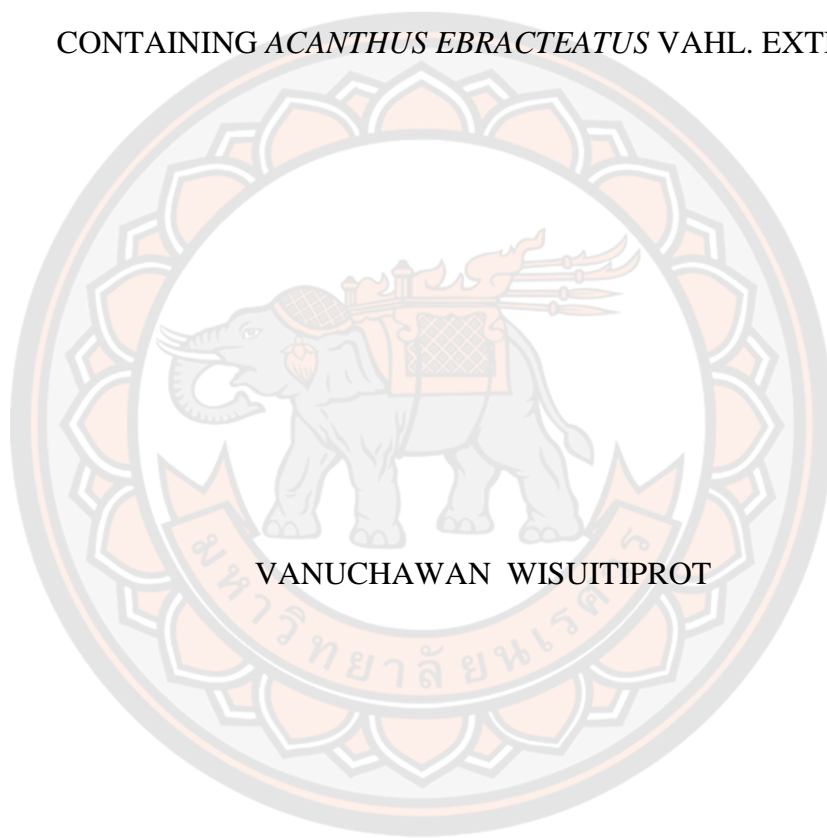




THE DEVELOPMENT OF HAIR GROWTH PROMOTING PRODUCT
CONTAINING *ACANTHUS EBRACTEATUS* VAHL. EXTRACT



VANUCHAWAN WISUITIPROT

A Thesis Submitted to the Graduate School of Naresuan University
in Partial Fulfillment of the Requirements
for the Doctor of Philosophy in Pharmaceutical Sciences

2022

Copyright by Naresuan University

THE DEVELOPMENT OF HAIR GROWTH PROMOTING PRODUCT
CONTAINING *ACANTHUS EBRACTEATUS* VAHL. EXTRACT



A Thesis Submitted to the Graduate School of Naresuan University
in Partial Fulfillment of the Requirements
for the Doctor of Philosophy in Pharmaceutical Sciences
2022

Copyright by Naresuan University

Thesis entitled "THE DEVELOPMENT OF HAIR GROWTH PROMOTING
PRODUCT CONTAINING *Acanthus ebracteatus* Vahl. EXTRACT"

By VANUCHAWAN WISUITIPROT

has been approved by the Graduate School as partial fulfillment of the requirements
for the Doctor of Philosophy in Pharmaceutical Sciences of Naresuan University

Oral Defense Committee

..... Chair
(Associate Professor Watcharee Khunkitti, Ph.D.)

..... Advisor
(Associate Professor Neti Waranuch, Ph.D.)

..... Co Advisor
(Associate Professor Kornkanok Ingkaninan, Ph.D.)

..... Co Advisor
(Assistant Professor Panlop Chakkavittumrong, M.D.)

..... Internal Examiner
(Associate Professor Tasana Pitaksuteepong, Ph.D.)

Approved

.....
(Associate Professor Krongkarn Chootip, Ph.D.)

Dean of the Graduate School

Title	THE DEVELOPMENT OF HAIR GROWTH PROMOTING PRODUCT CONTAINING <i>ACANTHUS EBRACTEATUS</i> VAHL. EXTRACT
Author	VANUCHAWAN WISUITIPROT
Advisor	Associate Professor Neti Waranuch, Ph.D.
Co-Advisor	Associate Professor Kornkanok Ingkaninan, Ph.D.
Academic Paper	Assistant Professor Panlop Chakkavittumrong, M.D. Ph.D. Dissertation in Pharmaceutical Sciences, Naresuan University, 2022
Keywords	<i>Acanthus ebracteatus</i> , androgenic alopecia, Anti-inflammation, Verbascoside, 5 α -reductase

ABSTRACT

Androgenic alopecia (AGA) is a serious skin disorder that leads to baldness. Testosterone metabolism catalyzed by 5 α -reductase results in dihydrotestosterone (DHT) production which triggers a chain reaction of the release of proteins that cause hair follicle damage, which induces hair follicle inflammation which, in turn, results in apoptosis of dermal papilla cells resulting in a reduction in the quantity of those cells. Miniaturization of the hair follicles, resulting from the decrease in the number of dermal papilla cell number makes the balding scalp evident.

Topical minoxidil and oral finasteride are approved medications for the treatment of hair loss. However, these synthetic substances sometimes manifest undesirable adverse effects such as itching, skin rash, loss of erectile function and libido, etc. Therefore, many medicinal plants, used as traditional remedies, have been investigated for anti-hair loss activity. The objective of our study was to develop an anti-hair loss application containing extract from *Acanthus ebracteatus* Vahl. (AE) which contains a prominent verbascoside (VB).

The development process was the evaluation of AE bioactivity associated with the pathogenesis of the AGA pathway. VB stability was evaluated by using Arrhenius' theory and shelf-life was then obtained. SLN loaded AE extract was developed for improving VB limitations. Finally, the application of the AE extract containing VB was evaluated for its safety and effectiveness with participating

volunteers. Regarding AE extract standardization, ethanolic extract showed the highest content of VB and did not present a cytotoxic effect on dermal papilla cells. It did, however, induce dermal papilla cell proliferation which occurred with AE extract 250 $\mu\text{g/mL}$ and VB 62.50 $\mu\text{g/mL}$. The number of G2/M and S phases increased within 24 hours of treatment. As well, both AE extract and VB showed a preventative effect on the dermal papilla cell apoptosis by decreasing the number of cells in the G1 phase. The anti-androgenic activity was demonstrated by the inhibition of 5α -reductase and prevention of testosterone induced dermal papilla cell apoptosis. The ethanolic extract of AE showed the IC_{50} value of the inhibition of 5α -reductase activity at 60.45 $\mu\text{g/mL}$ while VB did not show any inhibition activity. Interestingly, both AE extract and VB showed the preventative effect on dermal papilla cell apoptosis caused by 200 μM testosterone. In addition, 125 – 250 $\mu\text{g/mL}$ AE extract and 64.25 $\mu\text{g/mL}$ VB was effective in inhibiting the release of pro-inflammatory cytokines. IL- 1β , TNF- α , and nitric oxide were released from the RAW 267.4 cells, induced by the LPS. Also, IL- 1α and IL-6 were released from UV irradiated dermal papilla cells.

VB is a glycoside that is easily degraded when kept at a high temperature or dissolved in an alkaline solution. According to Arrhenius' theory, the result indicated a first-order reaction of VB degradation. Arrhenius' theory indicated an estimated shelf-life of VB in AE extract (semi-solid form) of 75 days and the estimated shelf-life of the AE extract in solution form of 12 days. However, our results indicated the real-time shelf-life of VB in solution form as 35 days, significantly longer than the estimated shelf-life.

VB in AE extract was encapsulated in SLN for improving the stability of VB and enhancing skin permeation. Compritol[®] ATO 888 (0.1%) was used as the lipid carrier and the particles formed and stabilized by using 0.50% Tween 80 and 3.0% Span 80. The optimized condition produced SLN with 32% entrapment efficiency and particle size of approximately 600 nm. The shelf life of SLN containing the AE extract was 172 days. Clearly, the SLN increased the VB stability significantly. The VB encapsulated in SLN also showed sustained release in both *in vitro* release and skin permeation studies. SLN loaded AE extract incorporated in the hydrogel was the subject of further study in a clinical trial for evaluating the product

safety and effectiveness. The result indicated that SLN loaded AE extract, including hydrogel base, showed non-skin irritation in 20 participating volunteers.

Seventy-two volunteers were allocated into 4 groups for evaluation of the effectiveness of hair serum and test products. Three of the groups were treated with a product that contained either minoxidil, or a hair serum containing SLN loaded AE extract, or a combined treatment (minoxidil + hair serum), while the fourth, control, group was administered a placebo. The results showed that the hair serum containing SLN loaded AE extract increased the number of hairs within 3 months as did both the combined treatment and the minoxidil. Anagen hair was significantly increased from baseline when the hair serum and the combined treatment were applied for 1 month while the minoxidil was significant at the 5th month. In all, the effectiveness of the hair serum in increasing the number of anagen hairs was significantly greater than that of the placebo. The effect of hair serum on anagen hair was not significantly different from the effectiveness of minoxidil. The effect of the hair serum, the combined treatment and the minoxidil on the increase of anagen hair density correlated with the effect on telogen hair that was significantly decreased from the baseline. In addition to the effect on hair numbers, the hair serum increased hair strength, as indicated by the decrease in hair fall in the hair comb test. No volunteer showed any adverse effect from the hair serum during the clinical study period.

Our study evaluated the bioactivities of AE extract including the evaluation of safety and the efficacy of hair serum containing AE extract. The results of *in vitro* testing indicates that AE extract containing VB is a promising ingredient for developing hair growth-promoting products. Furthermore, clinical data showed no adverse effects or reactions from the hair serum in volunteers with MPHL, thereby indicating that it can be safely used as a medicinal treatment for hair growth in AGA patients.

ACKNOWLEDGEMENTS

I would like to express my special thanks of gratitude to my advisor Assoc. Prof. Neti Waranuch for his encouraging guidance, advice and to provide me the opportunity to prepare the research throughout my study. I would also like to extend my gratitude to Prof. Kornkanok Ingkaninan, Assoc. Prof. Tasana Pitaksuteepong, Asst. Prof. Panlop Chakkavittumrong, and Assoc. Prof. Watcharee Khunkitti for their endless support whose valuable guidance, and kind supervision in this research. I would like to express my special thanks to my teacher Dr. Wudtichai Wisuitiprot for his continuous support and kindness which helped me to achieve this work.

I would like to thank the Faculty of Pharmaceutical Sciences, Naresuan University, Cosmetics, and Natural Products Research Center (CosNat), and Thammasat Skin Center, Thammasat University Hospital for providing all facilities and cooperation throughout my study period. The financial support of, Thailand Center for Excellence for Life Science (TCELS) is also acknowledged. I would like to extend my thank to Mr. Roy I. Morien of the Naresuan University Graduate School for his assistance in editing the English expression and grammar in this document. I am thankful to Ms. Juthamas Khampeepong, Ms. Sirintip Intharapasit, Mr. Somkiet Jaipan, and all staff in the Faculty of Pharmaceutical Sciences, Naresuan University for their kind assistance throughout my study. My appreciation also extends to my laboratory colleagues, especially Dr. Jukkarin Srivilai, Dr. Ekkarak Wongwad, Ms. Rattanaorn Chantakul especially Ms. Savitra Sittisuksomjai M.D., Ms. Pornpimon Jitanopajai, M.D., Ms. Korakoch Intarapisan, Ms. Suksri Naralert, Ms. Thapanee Kanvisat from Thammasat University Hospital for their friendship, and kindly support.

Finally, I am also grateful to my family for your love and unconditional support, my mother, my supportive husband who always was willing to provide management of our activities while I completed my thesis, and my lovely daughter. They all kept me going. Without whom this thesis would not have been possible at all.

VANUCHAWAN WISUITIPROT

TABLE OF CONTENTS

	Page
ABSTRACT.....	C
ACKNOWLEDGEMENTS.....	F
TABLE OF CONTENTS.....	G
LIST OF TABLES.....	L
LIST OF FIGURES.....	N
CHAPTER I INTRODUCTION.....	1
1. Background and rationale.....	1
2. Objectives of the study.....	2
3. Scope of the study.....	3
4. Keywords.....	3
CHAPTER II LITERATURE REVIEW.....	4
1. Introduction.....	4
1.1 Androgenic alopecia.....	4
1.2 <i>Acanthus ebracteatus</i> Vahl.....	7
1.3 Biological activities of Verbascoside.....	11
1.4 Hair follicle inflammation and androgenic alopecia.....	14
1.5 Reactive oxygen species.....	16
1.6 Human skin structure and function.....	21
1.7 Topical and Transdermal delivery.....	24
1.8 Trans follicular pathway for drug delivery systems.....	26
1.9 Skin absorption <i>in vitro</i> model.....	28

1.10 Microencapsulation	30
1.11 Preparation of microparticles	33
1.12 Spray chilling	34
1.13 High-speed homogenization (HSH)	36
1.14 Chemical and physical properties of Compritol® 888 ATO	37
1.15 The process in the measurement of anatomy properties of hair	39
CHAPTER III RESEARCH METHODOLOGY	42
1. Materials	42
1.1 Chemicals	42
1.2 Apparatus.....	42
2. Plant extraction	43
3. TLC fingerprint.....	43
4. Development of a method for standardization of AE extract	43
5. HPLC condition for determining VB	44
6. Standard VB preparation	44
7. Sample preparation	44
8. HPLC method validation	44
8.1 Precision	44
8.2 Accuracy.....	45
8.3 Linearity	45
8.4 Limit of detection and Limit of quantification	45
9. Determination of biological activities of AE leaves extract.	45
9.1 Cytotoxicity and cell proliferation testing	45
9.2 Cell cycle analysis	46
9.3 Anti-androgenic activity testing	46

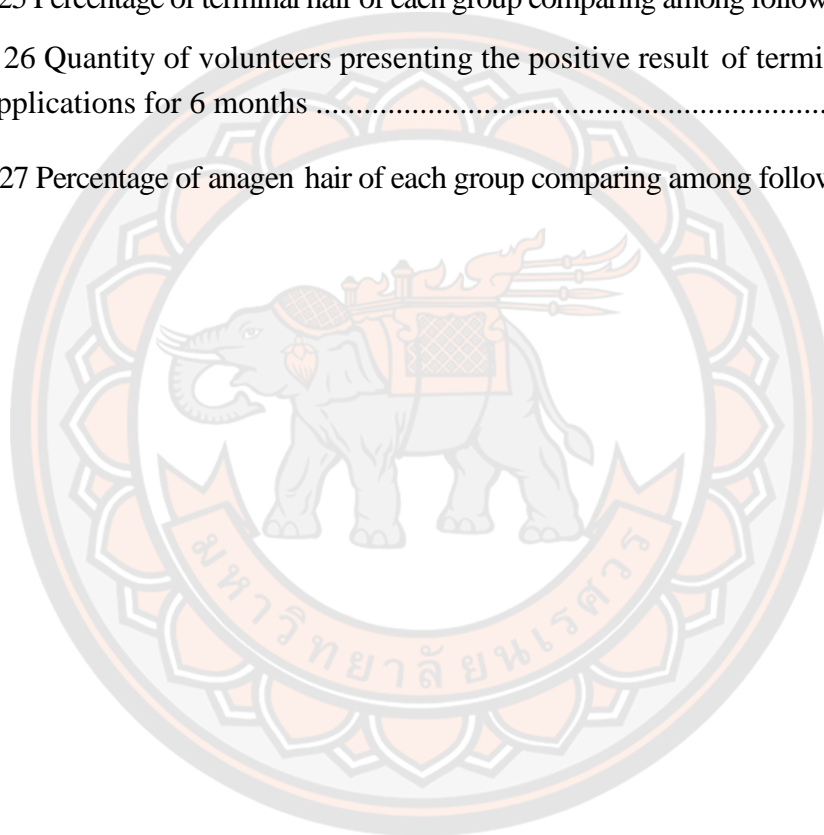
9.4	Anti-inflammatory activity study	46
9.5	Antioxidant activity	48
10.	Stability study of AE extract.....	49
10.1	The effect of temperature.....	49
10.2	The effect of pH.	49
10.3	Degradation kinetic analysis of VB in AE extract.....	49
11.	Microparticle preparation.....	49
12.	Hair tonic preparation	50
13.	Skin permeation study	51
14.	Evaluation safety of hair growth-promoting product containing AE extract ...	51
15.	Effectiveness of microparticle encapsulated AE extract in the hair-loss treatment.....	53
15.1	Subject selection.....	53
15.2	Study design	53
15.3	Clinical evaluation.....	55
	Hair sampling and hair clipping technique.	55
	Application of treatment.....	55
	Determination of total hair count	55
	Hair comb test	55
	Global photographic assessment	56
	Patient self-assessment	56
	Sample size calculation	56
	Clinical study process.....	57
16.	Statistical analysis.....	57
CHAPTER IV RESULTS.....		58

1. Plant extraction.....	58
2. Thin–layer chromatography fingerprint (TLC fingerprint)	58
3. VB determination by HPLC	60
3.1 HPLC method validation.....	60
3.2 Precision	60
3.3 Accuracy.....	61
3.4 Linearity	61
4. Bioactivities of AE extract.....	64
4.1 Antioxidant activity of AE extract	64
4.2 5 α –reductase Inhibition.....	64
4.3 Cytotoxic effect of AE extract and VB on DPCs.....	66
4.4 Cell cycle analysis	67
4.5 Anti-androgenic activity testing	68
4.6 Cytotoxicity effect of AE extract and VB on RAW 264.7 cells.....	69
4.7 Anti-inflammatory activity of AE extract and VB in LPS treated RAW 264.7 cells.....	70
4.8 Anti-inflammatory activity of AE extract and VB in UVB irradiated the DPCs.....	73
5. Stability study of AE extract	74
6. Solid lipid nanoparticle (SLN) loaded AE extract preparation.....	81
7. Particle release profile and skin permeation study	90
8. Evaluation of safety of hair growth–promoting product containing AE extract.....	93
9. Evaluation of the effectiveness of hair serum containing SLN loaded AE extract in the hair–loss treatment.	95
CHAPTER V DISCUSSION.....	109
REFERENCES	121
APPENDIX.....	138
BIOGRAPHY	160

LIST OF TABLES

	Page
Table 1 Natural chemicals identified in AE.....	9
Table 2 Preparation techniques for solid lipid Nano-and microparticles	33
Table 3 Formulation of hair serum containing SLN loaded AE extract	51
Table 4 Percentage yields of each AE leaves extract performed by different solvents	58
Table 5 Repeatability and intermediate precision which composes the precision parameter of the analytical method proposed	60
Table 6 Accuracy at three concentration levels covering the range of 80% to 120% of the expected concentration.....	61
Table 7 Amount of VB in each AE extract measured by HPLC method	63
Table 8 Antioxidant activity of each extract from AE and VB	64
Table 9 5 α -reductase inhibitory activity of AE extracts performed by different solvents	65
Table 10 The stability of VB in AE extract stored at 50°C	75
Table 11 Effect of temperature on the activation energy (E_a), reaction rate constant (K) values of VB in aqueous solution pH7.4 and semisolid form AE extract	79
Table 12 The estimated shelf life (T_{90}) of VB in solution form and semisolid form of AE extract at 25°C	79
Table 13 Percentage of remaining VB in AE solution pH 7.4 at 25°C (n=3).....	80
Table 14 The reaction rate constant of VB in various pH buffer solutions	80
Table 15 The detail of each formula in particle preparation.....	82
Table 16 Characteristics and entrapment efficiency of SLN loaded AE extract	82
Table 17 The effect surfactants combination on particles characteristics.....	84
Table 18 Ingredients of hair serum containing solid lipid nanoparticle loaded AE extract.....	87
Table 19 Remaining VB in hair serum containing AE extract or SLN loaded AE extract stored under various temperatures	88

Table 20 Percentage of VB in each part of Franz cell units after applied for 24 hours	92
Table 21 Skin evaluation by ICDRG guideline	94
Table 22 Skin evaluation by CTFA guideline	94
Table 23 Demographic data of volunteers recruited in research	96
Table 24 Quantity of volunteers presenting the positive result of hair number after applications for 6 months.....	99
Table 25 Percentage of terminal hair of each group comparing among follow-up times....	100
Table 26 Quantity of volunteers presenting the positive result of terminal hair density after applications for 6 months	100
Table 27 Percentage of anagen hair of each group comparing among follow-up times .	101



LIST OF FIGURES

	Page
Figure 1 Pictures of <i>Acanthus ebracteatus</i> Vahl. (a) and <i>Acanthus ilicifolius</i> L. (b)	8
Figure 2 Chemical structures: verbascoside (VB), hydroxytyrosol (HT), and caffeic acid (CA).....	12
Figure 3 Immunostaining of human hair follicles from a non-alopecia sample (left) and an alopecia sample (right)	14
Figure 4 The role of the NF- κ B signaling pathway in inflammation.....	18
Figure 5 Formation of active oxygen and nitrogen species, the targets of these reactive species, the reaction of ROS associated with the activation of NF- κ B, and transcription of pro-inflammatory cytokines.....	19
Figure 6 The structure of human skin in cross-section	23
Figure 7 A diagrammatical cross-section through human skin showing the different skin layers	26
Figure 8 Franz diffusion cell	29
Figure 9 Different structures of microcapsules and microspheres	31
Figure 10 Mini Spray Dryer B-290 with Dehumidifier B-296.....	34
Figure 11 Spray chilling accessory	35
Figure 12 Chemical structure of glyceryl dibehenate	37
Figure 13 Global photographs of an androgenic alopecia patient.....	40
Figure 14 Leviacam [®] and software for hair analysis	41
Figure 15 A marked areas using a tattoo to calculate hair density	41
Figure 16 Clinical study process flow chart	54
Figure 17 TLC fingerprint of AE extracts comparing among different solvents, fresh and dried leaves; (a) AE extracted by 95% ethanol, (b) AE extracted by 50% ethanol, (c) AE extracted by boiled water, (d) AE extracted by hexane, F= fresh leaves, D= dried leaves	59

Figure 18 Calibration curve of VB standard	62
Figure 19 Chromatogram of VB in AE extract 1 mg/mL.....	63
Figure 20 Dose respond curve of ethanolic extract of AE for 5 α -reductase inhibition activity.....	66
Figure 21 Relative cell viability of dermal papilla cells after being treated by AE extract and VB for 24 hours *significantly different versus the control cell (p<0.05, t-test)	67
Figure 22 The effects of AE extract (a), VB (b) on the dermal papilla cell cycle *significantly different versus the control cell (p<0.05, t-test)	68
Figure 23 Relative cell viability of dermal papilla cells when being treated with testosterone 200 μ M (T 200 μ M), testosterone 200 μ M plus AE extract 250 μ g/ml (T 200 μ M +AE), testosterone 200 μ M plus finasteride 75 nM (T 200 μ M + F) and testosterone 200 μ M plus VB 62.50 μ g/mL (T 200 μ M + VB); *significantly different versus the control cell (p<0.05, t-test)	69
Figure 24 Relative cell viability of RAW 264.7 cells treated with different concentrations of AE extract or VB for 24 hours; *significantly different versus the control cell (p<0.05, t-test)	70
Figure 25 Amount of IL-1 β from RAW 264.7 cells treated by lipopolysaccharide 5 μ g/mL (LPS), AE extract 250 μ g/mL plus LPS 5 μ g/mL (AE+LPS), Hydrocortisone 5 μ g/mL plus LPS 5 μ g/mL (HS+LPS) and VB 125 μ g/mL plus LPS 5 μ g/mL (VB+LPS); *significantly different versus the control cell (LPS) at (p<0.05, t-test) 71	
Figure 26 Amount of sodium nitrite from RAW 264.7 cells treated by lipopolysaccharide 1 μ g/mL (LPS), AE extract 250 μ g/mL plus LPS (AE+LPS), N(G)-monomethyl-L-arginine 10 μ g/mL (L-NMMA) plus LPS (L-NMMA+LPS), and VB 125 μ g/mL plus LPS (VB+LPS); *significantly different versus the control cell (LPS) (p<0.05, t-test)	72
Figure 27 Amount of tumor necrosis factor (TNF- α) from RAW 264.7 cells treated with lipopolysaccharide 1 μ g/mL (LPS), hydrocortisone 10 μ g/mL+LPS 1 μ g/mL (HS+LPS), AE extract 250 μ g/mL plus LPS 1 μ g/mL (AE250+LPS), and VB 250	

$\mu\text{g/mL}$ plus $1 \mu\text{g/mL}$ LPS (VB250+LPS). *significantly different versus the control cell (LPS) ($p < 0.05$, t-test)	72
Figure 28 The release of IL- 1α from dermal papilla cells following UVA 20 mJ/cm^2 irradiation and after treatment with hydrocortisone $5 \mu\text{g/mL}$, AE extract $250 \mu\text{g/mL}$ and VB $125 \mu\text{g/mL}$; *significantly different versus the irradiated cell ($p < 0.05$, t-test)	73
Figure 29 The release of IL-6 from dermal papilla cells following UVB 100 mJ/cm^2 irradiation and irradiated cell after treatment with hydrocortisone $5 \mu\text{g/mL}$, AE extract $250 \mu\text{g/mL}$ and VB $125 \mu\text{g/mL}$; *significantly different versus the irradiated cell ($p < 0.05$, t-test)	74
Figure 30 First-order plot between the logarithm of VB concentrations in the semisolid form of AE extract versus time at different temperatures	76
Figure 31 First-order plot between the logarithm of VB concentrations in solution form of AE extract versus time at different stored conditions	76
Figure 32 Plot of the natural log of rate constant versus the inverse of absolute temperature (Kelvin^{-1}) of VB in semisolid form of AE extract at various temperatures	77
Figure 33 Plot of the natural log of rate constant versus the inverse of temperature (Kelvin^{-1}) of VB in solution form of AE extract at various temperatures	77
Figure 34 pH rate profile of VB in AE aqueous solution at 25°C ($n=3$)	81
Figure 35 Particles loaded AE extract observed under the scanning electron microscope	84
Figure 36 The effect of homogenization times on particle size and polydispersity index	85
Figure 37 First-order plot between the natural logarithm of VB concentrations in SLN loaded AE extract versus time at different stored conditions	86
Figure 38 Plot of the natural log of rate constant versus the inverse of temperature (Kelvin^{-1}) of VB in SLN loaded AE extract at various temperatures, $\ln K$ (natural log of rate constant); $1/T$ (inverse of temperature)	87
Figure 39 First-order plot between the natural logarithm of VB concentrations in hair serum containing SLN loaded AE extract versus time at different stored conditions	89

Figure 40 Plot of the natural log of rate constant versus the inverse of temperature (Kelvin ⁻¹) of VB in hair serum containing SLN loaded AE extract at various temperatures, ln. K (natural log of rate constant); 1/T (inverse of temperature).....	90
Figure 41 Release profiles of VB permeated from SLN to different pH buffers	91
Figure 42 Skin permeation profile of VB from AE extract determined for 1–24 hours	93
Figure 43 Hair count of each group analyzed by Leviacam [®] comparing among follow up times.....	97
Figure 44 Percentage change of hair number from baseline at the 6 th month comparing among 4 groups.....	98
Figure 45 Percentage of volunteers presenting the increase of hair number after applications for 6 months.....	99
Figure 46 Percentage of volunteers presenting with increased anagen hair density after applications for 6 months	102
Figure 47 Percentage change of anagen hair of each treatment group compared to baseline after application for 6 months (*different from the placebo group; p<0.05; Mann–Whitney U Test)	103
Figure 48 Percentage of telogen hairs of each group comparing among following up times. *significantly different versus the baseline (p<0.05, Wilcoxon matched-pairs Signed–Rank)	104
Figure 49 The percentage of hair fall after combing compared among following–up times. *significantly different versus the baseline (p<0.05, t–test), #significantly different versus the baseline (p<0.05, repeated measures ANOVA).....	105
Figure 50 Characteristic and number of hairs at 6 th month(b) compared to baseline (a) of each treatment group; serum group (1a, 1b), Placebo group (2a, 2b), combination group (3a, 3b) and minoxidil group (4a, 4b)	106
Figure 51 Photograph comparing baseline(a) to 6 th month (b) of 4 groups; serum group (1a, 1b), placebo group (2a, 2b), combination group (3a, 3b) and minoxidil group (4a, 4b).....	108
Figure 52 Chemical structure and type of bound of VB	112
Figure 53 Proposed mechanism of AE for preventing androgenic alopecia	120

CHAPTER I

INTRODUCTION

1. Background and rationale

Alopecia is a symptom that impairs human confidence. Many researchers attempted to clarify the mechanism and treat this problem. There are different types of alopecia. One of the important hair loss is androgenic alopecia (AGA) that the mechanism that involves androgenic hormone metabolism. Testosterone is metabolized to dihydrotestosterone (DHT) by catalyzing with 5 α -reductase. DHT allows the synthesis of follicular hair damage proteins which in turn induce dermal papilla apoptosis. Presently, there are effective medications for anti-hair loss. These are finasteride and minoxidil. Finasteride is an approved oral medication for hair loss treatment. It inhibits 5 α -reductase activity, so testosterone metabolism has interfered. Due to the finasteride mechanism, adverse effects involving androgenic hormone impairment are evident. Decrease of libido and erectile dysfunction are often reported after using finasteride. Minoxidil, a vasodilator, can increase blood supply to hair roots. Moreover, a few reports revealed that minoxidil increased the proliferation of dermal papilla cells (DPC). Although minoxidil for hair loss treatment is a topical formulation, both locally and systematically adverse effects such as skin irritation and tachycardia also were concerned. Due to the adverse effect of these medications, a lot of researchers attempted to find promising natural compounds for treating AGA.

Our previous study demonstrated that *Acanthus ebracteatus* Vahl. (AE) extract significantly increased cell proliferation at concentrations between 125 – 500 μ g/mL. This was confirmed with cell cycle analysis in which AE extract increased cell proliferation by inducing mitosis processes, thus increasing daughter cells. Cell proliferation shown in cell cycle analysis was attributable to an increase in the S and G2/M phases (H.-J. Lee et al., 2005; L. Li et al., 2012). Moreover, this study also showed that AE extract improved cell viability when these cells were treated with 200 μ M testosterone. This anti-testosterone activity also correlated with the anti-5 α -reductase activity. The results indicated that AE extract inhibited 5 α -reductase

enzyme activity at an approximate IC_{50} value of $60 \mu\text{g}/\text{mL}$, while Dutasteride, a positive control, demonstrated an inhibitory effect $92.00 \pm 2.2 \%$ at a concentration of 100 nM or $0.19 \mu\text{g}/\text{mL}$.

In addition, AE extract also inhibited IL-1 β activity which is a major factor in an inflammatory pathway. Notably, there is a close association between hair follicle inflammation and alopecia. Thus, anti-inflammatory aspects in alopecia treatment are emerging. Based on the DPC viability improvement, anti-inflammation properties, anti-testosterone activity, and 5 α -reductase enzyme activity inhibition of AE extract, we hypothesized AE extract could be used it a part of the regiment for hair loss and to promote hair growth. Although AE extract showed the potential for anti-hair loss activity, its bioactivities were decreased after storage at 50°C for 3 months. Chemical components in the extract seem to be degraded by chemical reactions induced by heat (Khalid, Zhari, Amirin, & Pazilah, 2011). This could be a limitation of the plant extract in development for cosmetic or pharmaceutical applications. A solubility study found that AE extract can be dissolved in ethanol better than water about four times. Solid lipid particles can be used as delivery vehicles for the transdermal delivery system to improve extract stability. In addition, VB was reported in hair loss prevention effect and it had been determined in AE leaves. We expect that VB could be the biomarker of AE extract. Therefore, the extraction method was developed for providing a high amount of VB.

Therefore, further investigation is required for the development of AE extract products for stimulating hair growth.

2. Objectives of the study

2.1 To develop an extraction method for AE that can provide a high amount of VB.

2.2 To quantitate the hair growth-promoting activity of AE extracts.

2.3 To investigate the stability, chemical kinetic profiles, and skin permeation of VB in AE extract using VB as a marker.

2.4 To develop the suitable encapsulating carrier of AE extract for use as an active ingredient in hair growth promoting products and to formulate the hair care product containing AE extract.

2.5 To clinically evaluate the safety and efficacy of the hair growth-promoting product containing AE extract loaded in the developed carrier.

3. Scope of the study

AE leaves from Khaokhoherbary organic farm (Phetchabun, Thailand) were used in the study. The extract showing the highest amount of VB was selected for bioactivities determination. The extract was studied on hair growth promotion activity, anti-testosterone activity, antioxidant property, anti-inflammatory activity, and 5 α -reductase inhibition activity including formulation development. The stability of the extract and the finished product was tested in accelerated conditions recommended by WHO guidelines. The shelf life of AE extract was estimated using the Arrhenius equation and chemical kinetic principle. Finally, the formulated product containing AE extract was clinically evaluated for its effectiveness for hair growth promotion in healthy men.

4. Keywords

Acanthus ebracteatus, Verbascoside, Anti-hair loss, Hair loss prevention, Hair growth promotion, Hair follicle inflammation, Microparticle encapsulation, Skin permeation.

CHAPTER II

LITERATURE REVIEW

1. Introduction

1.1 Androgenic alopecia

AGA is a regular form of hair loss in both men and women. It is characterized by progressive hair loss with a distinctive, highly reproducible pattern where gradual conversion of terminal hairs into vellus hairs occurs. In men, it is also called male-pattern baldness, which is the most common type of hair loss. The pattern of male-baldness begins as the hair line moves backwards and forms an M shape. Finally, the hair becomes finer, thinner, shorter, and establishes a U-shape. Women's pattern of hair loss differs from male-pattern baldness. The hairs become thinner on the top and crown of the scalp and the front hair line is uninfluenced. The hair loss rarely progresses to total baldness as may be evident in men.

Genetic factors and androgens have a crucial role in stimulating androgenic hair loss (Kanchanapoom, Kasai, Picheansoonthon, & Yamasaki, 2001). Furthermore, a family study of balding patterns in 22 families showed that baldness has an autosomal dominant phenotype in men, whereas it has an autosomal recessive phenotype in women (Wisuitiprot, Ingkaninan, Wisuitiprot, & Waranuch, 2016). Another study identified 287 independent genetic signals associated with severe hair loss and summarized that genetic factors relate to male pattern baldness (Garlanda, Dinarello, & Mantovani). A family history of baldness was present for 48.5% of men and 45.2% of women with AGA in a study of 10,132 Koreans who visited the Health Examination Centre at Kyung Hee University Hospital between December 1997 and July 1999 (Schumann et al., 1998). Furthermore, a study that examined scalp hair condition in 572 participants over a wide age range confirmed that the frequency of balding of young men with balding fathers is increased and so there was a relatively high risk of going bald for young subjects with balding fathers (Mahesh, Bhuvana, & Hazeena Begum, 2009). Androgenic alopecia can develop and occur depending on the interaction of endocrine factors and genetic predisposition according to many studies

which have indicated that there are two major genetic risk factors for AGA. These are the X-chromosome AR/EDA2R locus and the chromosome 20p11 locus (S. Gregoriou et al., 2010; Philpott, Sanders, Bowen, & Kealey, 1996).

Androgens are important hormones for the expression of the male phenotype. They have characteristic roles in male sexual differentiation and the development of secondary male characteristics. The important androgens are testosterone and 5 α -dihydrotestosterone (DHT) (C. Bodemer et al., 2000).

Testosterone is the primary male sex hormone, which is synthesized from cholesterol in Leydig cells in the testis of males and to a lesser extent, the ovaries of females. Small amounts are also secreted by the adrenal glands. Approximately 5% to 7% of testosterone is metabolized by 5 α -reductase into 5 α -dihydrotestosterone (DHT), 5 α -DHT has a circulating level of about 10% of testosterone levels and so is a potent androgen. Both testosterone and DHT can bind to androgen receptors but DHT has a ten-fold higher affinity to androgen receptors than testosterone (Gil Ede, Enache, & Oliveira-Brett, 2013). Also, approximately 0.3% of testosterone is metabolized into estradiol by aromatase.

The conversion of testosterone to DHT is catalyzed by the enzyme 5 α -reductase, which has two isoforms (type 1 and 2), both of which are efficient in producing DHT from testosterone, although they have different biochemical and exact tissue-specific expression patterns. Thus, higher 5 α -reductase activity has been observed in bald scalps (Hausmann et al., 2007). It is fully understood that human hair follicles at specific body sites are responsive to the DHT androgen. In the beard, axillary and pubic areas, this androgen stimulates the conversion of vellus to terminal hairs, unless the frontal scalp areas of a genetically predisposed individual's androgens trigger miniaturization of hair follicles by conversion of the terminal to vellus hair follicles (Galvez Peralta, Martin-Cordero, & Ayuso, 2006). Dermal papilla cells from a balding scalp contain more androgen receptors and have higher levels of 5 α -reductase activity than a non-balding scalp (Rao, Fang, Hsieh, Yeh, & Tzeng, 2009). Presently, many researchers have found that not only genetic imbalance and excessive 5 α -reductase activities are responsible for AGA, but hair follicle inflammation also triggers AGA. Hair follicles of AGA patients were found to be associated with an inflammatory mechanism via a 2.0-2.5-time enlargement of the

follicular dermal sheath (Abdelouahab & Heard, 2008). Prostaglandin D2 (PGD2) and prostaglandin synthase are elevated in the bald scalps of AGA patients and the results have shown that PGD2 inhibits hair growth in both human hair follicles and when applied topically to mice. Besides, IL-6, IL-8, IL-1 α , IL-1 β , TNF- α are also over expressed in AGA (Jiménez, Villaverde, Riguera, Castedo, & Stermitz, 1989; Korkina, Mikhal'chik, Suprun, Pastore, & Dal Toso, 2007), suggesting that combining anti-inflammatory agents with 5 α -reductase inhibitors could enhance the efficacy of treatment for pattern hair loss.

Medical therapy using 5 α -reductase inhibitors (5ARIs) such as Finasteride and Dutasteride is effective but may cause side effects. The use of 5ARIs has been related to adverse sexual consequences, including erectile dysfunction, ejaculatory dysfunction, and decreased libido. These effects occur early in therapy and attenuate over time. The mechanism affecting sexual dysfunction relates to decreasing dihydrotestosterone. Finasteride is a synthetic 4-azosteroid that competitively inhibits the intracellular conversion of testosterone to DHT by selectively inhibiting the type 2 isoform of 5 α -reductases. Finasteride results in a reduction of plasma DHT levels by 75% to 80%. Dutasteride inhibits both type 1 and type 2 isoenzymes of 5 alpha reductases and reduces circulating DHT by more than 90%. The incidence of these sexual adverse effects by using Finasteride use is reported to be anywhere from 2.1% to 39% in published clinical studies (Akdemir et al., 2011).

Finasteride is prescribed in clinical dermatology at a lower dose (1 mg) than for benign prostate hyperplasia (BPH) (5 mg) for the treatment of alopecia (M. Pesce et al., 2015). Researchers also evaluated a dose-response effect of Finasteride on sexual function. In a double-blind study on 895 men with BPH, researchers evaluated the effect of two doses of Finasteride (1 mg and 5 mg) and a placebo, given once daily for 12 months. The rate of decreased libido, erectile dysfunction, and ejaculatory dysfunction was found to have increased in Finasteride compared with the placebo. However, the rate of sexually adverse effects between the two Finasteride groups was not significantly different (Hee Seung Lee et al., 2008). The sexual adverse effect profile of Dutasteride appears similar to Finasteride with regards to decreased libido, erectile dysfunction, and ejaculatory dysfunction, and gynecomastia.

In 2002, the first clinical study to report on the efficacy of Dutasteride found sexually adverse effect rates to be 7.3% for erectile dysfunction (4% placebo), 4.2% for decreased libido (2.1% placebo), and 2.2% for ejaculatory dysfunction (0.8% placebo) (Xiong, Hase, Tezuka, Namba, & Kadota, 1999). The adverse side effects of these medications create an opportunity for the development of an alternative efficient treatment agent with limited side effects, particularly from a medicinal plant. We would like to briefly summarize the causes of hair loss and focus on a medicinal plant for treatment, and the potential of the plant to be appropriate for a consumer's preference.

At present, we have various types of synthetic drugs to treat hair loss, but they have a lot of side effects. Medicinal plants may therefore be the starting material for any medical research. Many reports recommend herbal drugs for their beneficial effects while including fewer side effects when compared to synthetic drugs. Advanced research may reveal other beneficial compounds from natural sources that were helped resolve the hair loss problem.

1.2 *Acanthus ebracteatus* Vahl.

AE is a member of Acanthaceae family and has the English common name Holly Mangrove or namely Ngueak-Plaa-Mo in Thailand. This plant is found locally in the middle, northern, northeastern, and southern parts of Thailand. AE is a spiny and shrubby herb with dark green spiny leaves and is stiff and deeply lobed with sharp spines at each lobe's tip. The white flowers are composed of spikes at the branch tips, and it has flat seeds. The origin of the name Acanthus is derived from the Greek "Akanthos" meaning "thorn plant". Two species of Acanthus are commonly found in Thailand. They are *Acanthus ebracteatus* Vahl. which has white flowers and is generally localized in Thailand and *Acanthus ilicifolius* L. has purple flowers and is found in the mangroves of southern Thailand (Figure 1).



Figure 1 Pictures of *Acanthus ebracteatus* Vahl. (a) and *Acanthus ilicifolius* L. (b)

Source: <https://en.wikipedia.org/wiki/Acanthus-ebracteatus> (a),
<http://senthuerbals.blogspot.com/2014/10/acanthus-ilicifolius-kalutaimullisea.html> (b)

AE has been used as an ayurvedic traditional medicine for a wide range of tropical diseases. In India, whole plants are used as an astringent, stimulant, and expectorant, while the roots are used as a cough remedy, and the tender shoots and leaves are used as a snakebite cure (Liebezeit, & Rau, 2006). In China, the stem and roots are used for treating coughs, chronic fever, paralysis, asthma, hepatomegaly, hepatitis, and lymphoma (Prasansuklab, & Tencomnao, 2018). In Malaysia, the juice of the leaves is used to prevent hair loss (Liebezeit, & Rau, 2006). In Burma, the shoots are used to treat snake venom, and the leaves are used to treat rheumatism. In Vietnam, whole plants are used as a diuretic agent, and the roots are used to treat paralysis. In Thailand, it has been used in traditional medicine for treating arthritic inflammation and the decoction extract of the whole plant has been used to heal rashes and skin diseases. The fruit is taken orally to ease menstrual disorders (Laupattarakasem, Houghton, Hoult, & Itharat, 2003). In the Philippines, the decoction of leaves and roots is used to treat asthma patients (Liebezeit, & Rau, 2006).

A study of the decoction extract, a popular usage form in Thai traditional medicines of AE, shows it can be regarded as a potential enhancer of the innate immune response for macrophage activation. Therefore, it may have a beneficial role

in cancer treatment via stimulating immune responses. The antibacterial activity of the aqueous extract of the aerial part of AE has been investigated against various bacteria to evaluate the possibility of its use as a skin infection treatment remedy. The AE aqueous extract showed an inhibitory effect on the growth of *S. aureus*, *S. epidermidis*, *L. plantarum*, *K. pneumoniae* and *P. vulgaris* with the MICs in the range of 1-2 g/L and the MBCs in the range of 2-4 g/L against nosocomial pathogenic bacteria at low concentrations (Hokputsa et al., 2004). It could support the use of the extract for skin infection treatment and other nosocomial infections such as urinary tract and respiratory tract infections (Phisalaphong, Thu Ha, & Siripong, 2006).

The chemical constituents and polysaccharides of AE have been investigated. Twenty-seven compounds were isolated and identified from the aerial part of the plant (Kanchanapoom et al., 2001).

Table 1 Natural chemicals identified in AE

Categories	Chemical constituents
Flavonoids	Vecenin-2, Schaftoside, Luteolin-7- <i>O</i> - β -D- glucuronide, Apigenin-7- <i>O</i> - β -D-glucuronide
Phenylpropanoids	Verbascoside(acteoside), Isoverbascoside(isobascoside), β -Hydroxyacteoside, Cistanoside E, Leucosceptoside A, Martynoside
Lignans	(+)-Lyoniresinol 3 α - <i>O</i> - β -D glucopyranoside, (-)-Lyoniresinol 3 α - <i>O</i> - β -D-glucopyranoside, (8 <i>R</i> ,7' <i>S</i> ,8' <i>R</i>)-5,5'-Dimethoxylariciresinol 4'- <i>O</i> - β -D-glucopyranoside, (+)-Syringaresinol-4- <i>O</i> - β -D-apiofuranosyl-(1 2)- <i>O</i> - β -D-glucopyranoside, Magnolenin C
Megastigmane glycosides	Plucheoside B, Alangionoside C,

Categories	Chemical constituents
	Ebracteatoside A, Premnaionoside
Aliphatic alcohol glycosides	Ebracteatoside B, Ebracteatoside C, Ebracteatoside D
Benzoxazinoid glycosides	(2 <i>R</i>)-2- <i>O</i> - β -D-Glucopyranosyl-2H-1, 4-benzoxazin-3(4H)-one (HBOA-Glc, blepharin), (2 <i>R</i>)-2- <i>O</i> - β -D-Glucopyranosyl-4-hydroxy-2H-1,4-benzoxazin-3(4H)-one (DIBOA-Glc), 7-Chloro-(2 <i>R</i>)-2- <i>O</i> - β -D-glucopyranosyl-4-hydroxy-2H-1,4-benzoxazin-3(4H)-one (7-Cl-DIBOA-Glc)
Phenylethanol glycosides	2-Phenylethyl 8- <i>O</i> - β -D-glucopyranosyl-(1 2)- <i>O</i> - β -D-glucopyranoside, Benzyl alcohol 7- <i>O</i> - β -D-glucopyranosyl-(1 2)- <i>O</i> - β -D-glucopyranoside (zizybeoside I)
Nucleoside	Adenosine

Source: Kanchanapoom et al., 2001

A previous study revealed that the ethanolic extract of AE showed potential for hair loss treatment effect by its hair growth-promoting mechanism, anti-testosterone activity, 5 α -reductase activity inhibition, and IL-1 β inhibition activity. These results were indicated by significantly increased dermal cell proliferation at 125 – 500 μ g/mL concentrations (Wisutiprot et al., 2016). Cell cycle analysis was determined using flow cytometry technique, a Muse cell analyzer[®], also indicated that AE extract increased cell proliferation by inducing mitosis processes so that daughter cells were evident. This cell proliferation was identified by increasing S and G2/M phases (H.-J. Lee et al., 2005; L. Li et al., 2012). Further, the results of anti-testosterone activity also showed that AE extract improved cell viability when those cells were induced to apoptosis by 100 μ M testosterone. The anti-5 α -reductase activity was also correlated with the anti-testosterone activity. AE extract showed inhibition of 5 α -reductase enzyme activity with an approximate IC₅₀ value of 60 μ g/mL with Dutasteride as a positive control. In addition, AE extract also

demonstrated inhibition activity of IL-1 β (Wisuitiprot et al., 2016). IL-1 β is a major factor in inflammatory pathways (Garlanda et al.; Schumann et al., 1998). Several reports have demonstrated that IL-1 β played a crucial role in hair follicular inflammation in alopecia patients (Christine Bodemer et al., 2000; Stamatis Gregoriou et al., 2010; Yann F. Mahé et al., 2000; Philpott et al., 1996). However, both IL-1 β and IL-1 α are equally effective and they are the most potent inhibitors of hair growth and hair shaft elongation so far investigated *in vitro*. In addition, a researcher has found that hair loss may occur because proinflammatory cytokines such as IL-1 interfere with the hair cycle, leading to the premature arrest of hair cycling with inhibition of hair growth. Although the clinical sign of alopecia is gradual progress in affected areas of the scalp eventually leading to the total scalp, some hair regrowth is still possible. Thus, an anti-inflammatory agent could be expected for combined treatment with 5 α -reductase inhibitors for AGA. Due to the prevented apoptosis of DPC from testosterone, anti-inflammation properties, and inhibited 5 α -reductase enzyme activity, we hypothesized that the combined activities of AE extract could be used as a treatment for hair loss and as a promoter for hair growth. Some reports have revealed that AE extract contains many chemical compounds. In addition, a few research indicated that AE is composed of a high amount of verbascoside (VB).

1.3 Biological activities of Verbascoside

VB is interesting for use as a biological marker compound from the AE extract, as previous research indicated VB presenting prominently in this plant [29]. Verbascoside, also named as acteoside, is a hydroxycinnamic ester derivative widely distributed in plants, including diverse medicinal herbs, such as echinacea, lemon verbena (*Aloysia triphylla*), mullein (*Verbascum Thapsus*), Indian warrior (*Pedicularis densiflora*), savannah tea (*Lippia multiflora*) and olive fruits [37, 38]. Chemically, VB is a water-soluble phenylpropanoid glycoside, structurally characterized by caffeic acid (CA) linked by a - (D)-glucopyranoside to a hydroxytyrosol (HT) (Figure 2). While it is very water soluble (up to 30 mg/mL), in aqueous media it has been unstable, and it underwent degradation which was correlated to the pH. The main reaction involved in this process was the hydrolysis of the caffeic acid moiety which led to the formation of an inactive molecule. VB was also shown to be more active in scavenging activities by catechol groups that showed

prevention of oxidative stress than CA and HT in equimolar mixtures. Water solubility and the reducing properties were conferred by the sugar residues [39]. However, a study showed that VB weakly stability in buffered solution at basic condition while greater stability in a weak acid medium [40]. Different pH conditions should be investigated for VB in order to confirm its stability in cosmetic formulation due to the pH values can influence in the stability of VB.

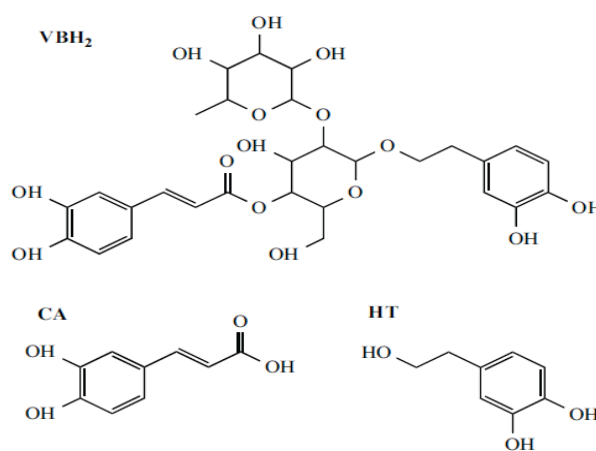


Figure 2 Chemical structures: verbascoside (VB), hydroxytyrosol (HT), and caffeic acid (CA)

Source: Gil Ede et al., 2013

VB was recently isolated from the aerial part of AE (Kanchanapoom et al., 2001), and studies have demonstrated its anti-inflammatory activity in several models, such as an intestinal inflammation model which revealed the effect of VB in decreasing pro-inflammatory molecule synthesis (Hausmann et al., 2007). An ear edema test for arachidonic acid and carrageenan-induced edema models showed inhibition of histamine and bradykinin production which was generated by VB (Gálvez, Martín-Cordero, & Ayuso, 2006). The anti-inflammatory effect of VB was demonstrated by potent inhibition of Nitric oxide, TNF- α , and IL-12 (Rao et al., 2009) and selective inhibition of COX-2 mediators which were induced by lipopolysaccharide and IFN- γ stimulated macrophages (Abdelouahab & Heard, 2008).

Furthermore, the anti-inflammatory activity of VB has been confirmed by an *in vitro* test performed on cell cultures of primary human keratinocytes (Korkina et al., 2007).

Due to the pharmacological activities of VB, plant extracts containing VB also displayed *in vitro* and *in vivo* anti-inflammatory properties (Gálvez et al., 2006; Hausmann et al., 2007; Jiménez et al., 1989; Korkina et al., 2007). This anti-inflammatory activity has affected the time required for wound healing and wound repair processes (Akdemir et al., 2011; Korkina et al., 2007). Furthermore, a report has indicated that VB can suppress pro-inflammatory mediators by inhibiting the enzyme activity of iNOS and 5-lipoxygenase (Mirko Pesce et al., 2015). Hepatoprotective effects against carbon-tetrachloride (H. S. Lee et al., 2008) and D-Galactosamine/ lipopolysaccharide have been reported in VB research (Xiong et al., 1999). Protection of human neuroblastoma SH-SY5Y cells against β -amyloid-induced cell injury (Wang et al., 2009), 1-methyl-4-phenylpyridinium ion-induced neurotoxicity (Sheng, Zhang, Pu, Ma, & Li, 2002), and rat cortical cells from glutamate-induced excitotoxicity (Koo, Kim, Oh, & Kim, 2006) are among the various neuroprotective effects of VB reported so far. The potential anticancer activity of VB is also evident from studies showing direct inhibition of human promyelocytic HL-60 leukemia cell proliferation (K.-W. Lee et al., 2007) and PMA-induced invasion and migration of human fibrosarcoma cells (Hwang et al., 2010). Antimicrobial effects including activity against multiple-drug-resistant strains of *Staphylococcus aureus* (Nazemiyeh et al., 2008) have also been reported for VB. The cytotoxicity assay in HepG2 and NIH cells were treated with different concentrations of VB demonstrated that the LD₅₀ value was greater than 5 g/kg which indicated that viability in all groups was greater than the IC₅₀ value. The acute and subacute toxicity of VB was evaluated in mice after a single intraperitoneal injection at the dose range of 0, 1, 2, and 5 g/kg body weight. (acute model) and 21 days administration at the dose range of 0, 10, 30, and 60 mg/kg body weight. (subacute model). In the subacute toxicity study, no statistically significant differences were observed in the values of hematological, biochemical, and pathological parameters in comparison with the control group. The report revealed that VB does not produce toxic effects in animals (Etemad et al., 2015). According to VB's pharmacological effects, the finding of it being a major constituent of AE could explain the reported medicinal value and

pharmacological effects of the plant. These previous findings were in good agreement with our previous reports which showed AE as a good source of pharmacologically active natural products. From this reported data VB exhibits anti-inflammatory mechanisms including anti-testosterone and anti-5 α - reductase activities. It suggests AE extract as a promising candidate for hair loss treatment applications. Moreover, the models of inflammation and testosterone metabolism studies using DPC provide insight regarding its feasibility for the treatment of AGA.

1.4 Hair follicle inflammation and androgenic alopecia

Presently, AGA is identified to be an alteration of hair growth or premature aging of the pilosebaceous unit. The various inflammation activators in the etiology of AGA have appeared recently in several studies (Kasumagic-Halilovic, Prohic, & Cavaljuga, 2011; Little, Westgate, Evans, & Granger, 1994; Mahe et al., 2000). A previous study referred to an inflammatory infiltrate of neutrophils and lymphocytes of the scalp samples of AGA which are characterized by the progression of alopecia (Anand & C., 1975). Scalp biopsies showed that perifollicular fibrosis generally occurs, consisting of connective tissue of fibrotic collage in follicular streamers (Figure 3), resulting in down growth of anagen hair follicles (Whiting, 1993).

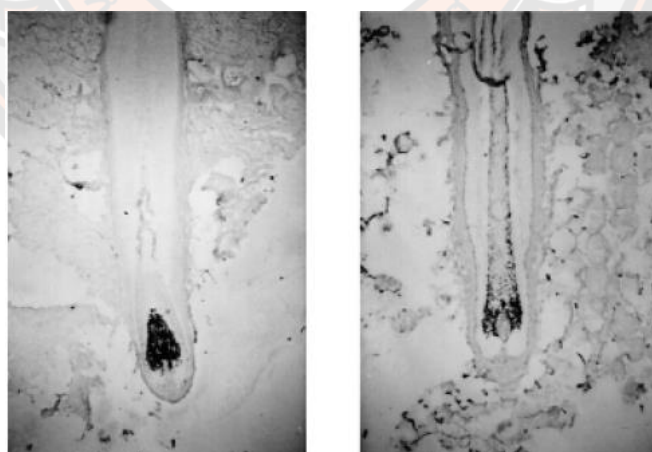


Figure 3 Immunostaining of human hair follicles from a non-alopecia sample (left) and an alopecia sample (right)

Source: Yann F. Mahé et al., 2000

The alopecia hair specimen in figure 3 from a volunteer in an *in vitro* study could be identified as exhibiting highly inflammatory IL-1 α production. Furthermore, the hair follicle growth was significantly inhibited by IL-1 α with the consequent effect of hair bulb degradation. These results indicate IL-1 α may negatively influence hair growth (Y. F. Mahé et al., 1996).

NF- κ B is a key regulator of inflammatory gene transcription. Pro-inflammatory cytokines, such as IL-1 α and IL-1 β trigger a signal transduction pathway leading to the activation of the transcription factor, nuclear factor- κ B (NF- κ B). NF- κ B induces a large number of target genes involved in many biological processes, such as inflammation, immunity, cell survival, and cell death (Kataoka, 2009). IL-1 α and IL-1 β both bind to the same IL-1 receptor (IL-1R) and are potent hair growth inhibition proinflammatory cytokines which are mainly produced by myeloid cells such as macrophages, monocytes, and dendritic cells. Production of proinflammatory (pro)-IL-1 α and pro-IL-1 β is induced by Toll-like receptor (TLR)-mediated NF- κ B activation. In most cell types, NF- κ B proteins are sequestered in the cytoplasm in an inactive form by the inhibitor I κ B (Q. Li & Verma, 2002). I κ B kinase (IKK) stimulates the degradation of I κ B. Therefore, the translocation and release of NF- κ B proteins occur into the nucleus, which activates the expression of target genes (Ghosh & Karin, 2002). Several studies have shown that secretion of pro-inflammatory cytokines is increased in AGA. These pro-inflammatory cytokines, such as tumor necrosis factor α (TNF- α) and interleukin-1 (IL-1), are potent activators of NF- κ B that activate phosphorylation and degradation of I κ B, which, in turn, stimulate the nuclear localization sequence of NF- κ B, resulting in NF- κ B nuclear translocation. In addition, stimulus involving activation of the inflammasome and caspase-1 is required for proteolytic cleavage and secretion of IL-1 β in its active form (Juráňová, Franková, & Ulrichová, 2017). Therefore, caspase-1 may act as a regulator of unconventional protein secretion. The study investigated the role of the inflammasome and caspase-1 on the expression of secreted and surface IL-1 α and found that surface expression was caspase-1 independent, whereas secretion of mature IL-1 α required activation of both inflammasome and caspase-1 (Fettelschoss et al., 2011). Hence, the secretion of these cytokines creates a positive feedback effect that induces constitutive NF- κ B activation (Parameswaran & Patial, 2010). IL-1 α

encourages transcriptional activation of NF- κ B, inducing the expression of IL-8, IL-6, TNF- α , and COX2 which can attract neutrophils to an inflamed area. Furthermore, the cytokines chemokine (IL-8) and ROS showed a consequential effect to NF- κ B activation by amplifying the inflammatory response (Figure 4) (Juráňová et al., 2017). The incidence of successful treatment with anti-inflammatory agents with AGA patients has been proven by comparing formulations containing Minoxidil alone, a placebo, and a microemulsion containing a nonsteroidal anti-inflammatory agent (Sakr, Gado, Mohammed, & Adam, 2013).

To determine the level of secretion of IL-1 α and IL-6 from DPCs, we performed ELISA analyses. Overexpression of interleukin-1 α (IL-1 α), IL-6, in response to UV radiation stimulated in DPC was performed. Consequently, the effect of the pro-inflammatory cytokine inhibition property of AE extract and its active compound (VB) also were determined.

1.5 Reactive oxygen species

A free radical is a molecule or atom that has one or more unpaired electrons and can exist independently. Consequently, it can react quickly with the other substances trying to catch the intended electron to obtain stability. Free radicals are composed of hydroxyl free radicals, superoxide free radical anions, lipid peroxy, lipid peroxide, and lipid alkoxy.

Reactive oxygen species (ROS) are radical derivatives such as singlet oxygen and hydrogen peroxide (Arulselvan et al., 2016). Under normal conditions, there is a balance between ROS formation, free radicals, and endogenous antioxidant defence mechanisms. ROS are produced in normal metabolic processes, and they serve important physiological functions. However, high levels of ROS may affect the cellular structure and functional integrity, by degrading the oxidation of key molecules, such as lipids, proteins, and DNA (Kumar, 2011).

DPCs are critical regulators of the hair growth cycle. The decrease of DPC numbers is an important factor of disorder characterized by hair loss, including alopecia, and evidence has indicated a significantly increased level of ROS in hair tissue and these cells in balding patients (Lim et al., 2015). There is growing evidence for the effect of oxidative stress on AGA. The causes of oxidative stress comprise oxidative metabolism, UVR, inflammation from microbial, pollutant, irritation,

chemical stress, and oxidized scalp lipid sources. Additionally, a previous study has also confirmed that oxidative stress is involved with the aging process in hair and skin. Oxidative stress directly affects the cell membrane and promotes the entrance of DHT and the other damaging factors into the cell. Furthermore, ROS also activates sebaceous gland hyperplasia, increasing DHT formation and promoting the increase of type I 5 α -reductase activities (Trüeb, 2015).

Oxidative stress and androgen signaling play an essential role in the DPC of balding scalps and AGA. DPCs from the balding scalp is significantly more sensitive to environmental stress than non-balding DPCs. One study showed DPCs from a balding scalp get premature senescence *in vitro* in association with the expression of p16INK4a, reduced cell proliferation and migration including increased ROS and senescence at 21% O₂. When DPCs from a balding scalp were protected from oxidative stress by performing cell culture at 2% O₂ they did not release the negative hair growth factor of TGF- β in response to DHT (Upton et al., 2015).

Oxygen metabolism produces ROS which is produced in the mitochondria as a by-product of the electron transport chain. Endoplasmic reticulum (through cytochrome P450), the plasma membrane (through the activity of NADPH oxidase) are sources of ROS as well (Bhandary, Marahatta, Kim, & Chae, 2013). The damaging effect of ROS species is induced both internally during normal metabolism and externally through exposure to various oxidative stresses from the environment. However, the body controls endogenous defence mechanisms such as antioxidant enzymes (superoxide dismutase, catalase, glutathione peroxidase) and non-enzymatic antioxidative molecules (vitamin C, vitamin E, glutathione, ubiquinone) by protecting cellular components from ROS by reducing and neutralizing processes (Ahmad, Jaleel, Salem, Nabi, & Sharma, 2010).

Concerning oxidative stress, the production of ROS during the inflammation process occurs by NF- κ B pathway activation Figure 4, 5 (Filippin, Vercelino, Marroni, & Xavier, 2008a; Juránová et al., 2017). Furthermore, much research has indicated high levels of production of ROS and ROS-generated molecules, including superoxide, peroxide, hydroxyl radicals, and ROS have been found in the synovial fluid and peripheral blood of patients exhibiting inflammation (Filippin, Vercelino, Marroni, & Xavier, 2008b; Winyard et al., 2011).

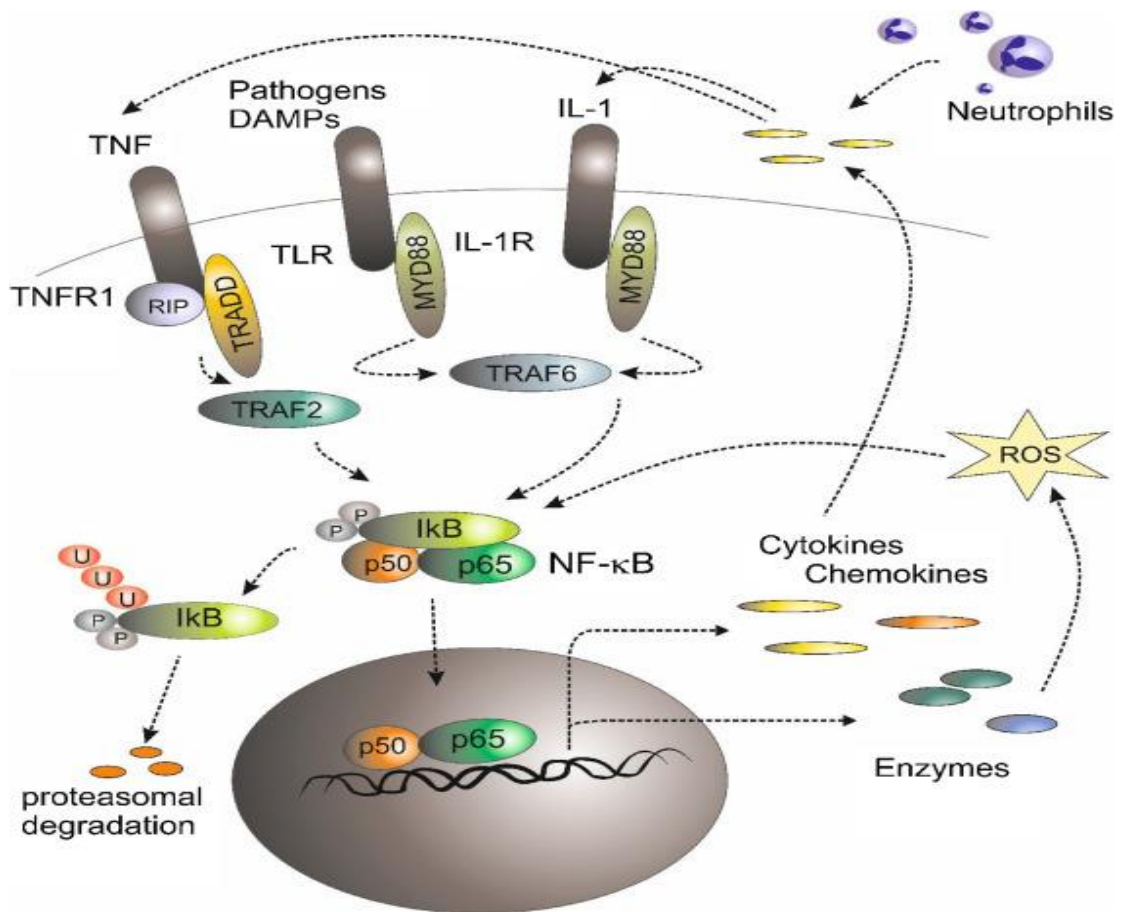


Figure 4 The role of the NF-κB signaling pathway in inflammation

Source: Juránová et al., 2017

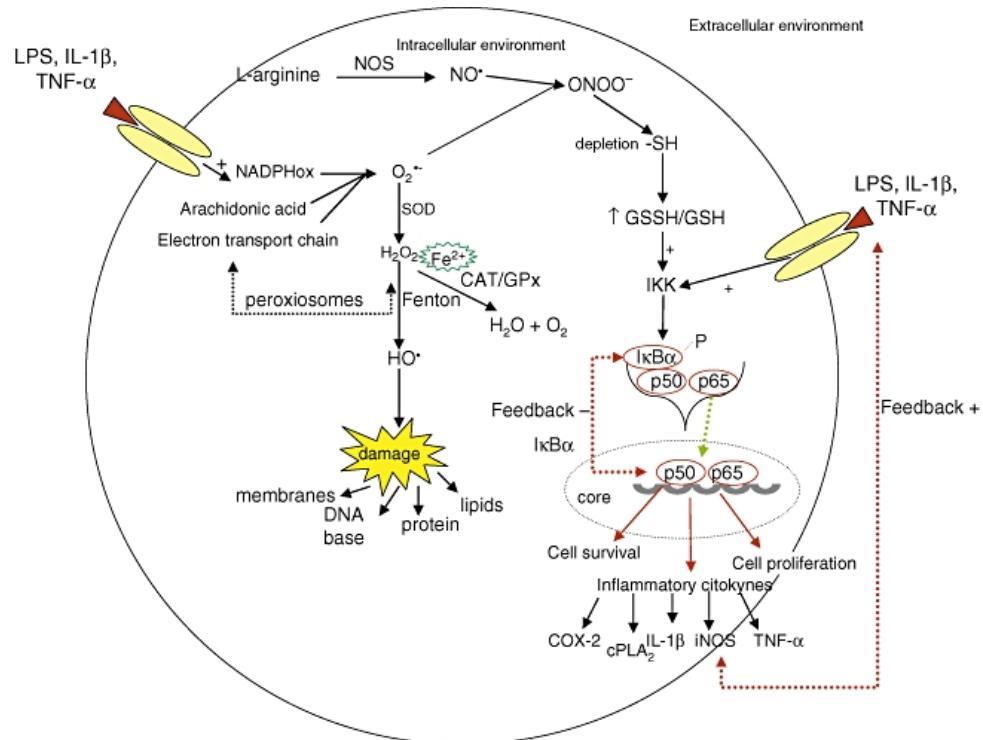


Figure 5 Formation of active oxygen and nitrogen species, the targets of these reactive species, the reaction of ROS associated with the activation of NF-κB, and transcription of pro-inflammatory cytokines

Source: Filippin et al., 2008a

An *in vitro* study showed balding DPCs grow slower than non-balding DPCs. Loss of proliferative capacity of balding DPCs was associated with changes in cell morphology, expression of senescence-associated β-galactosidase, upregulation of P16INK4a/pRb, and nuclear expression of markers of oxidative stress and DNA damage. The reduced proliferative activity of balding DPCs is associated with changes in the expression levels of senescence-associated (SA) β-galactosidase, oxidative stress markers, superoxide dismutase, and catalase. These findings indicate that oxidative stress is important in the loss of DPCs and hair production. Accordingly, balding DPCs are sensitive to environmental stress, and this may identify alternative pathways that could lead to novel therapeutic strategies for the treatment of AGA (Bahta, Farjo, Farjo, & Philpott, 2008).

Recently, a study of AGA and senescence alopecia using microarray analysis showed they differ in gene expression patterns suggesting they represent different entities. In AGA, the genes for anagen onset (TGF- α and TGF- β) require an epithelial signal from DPC (IGF-1), hair shaft differentiation genes (Msx2, KRTs, KAPs), and anagen maintenance genes (IGF-1) were downregulated, while the genes for catagen (IL-1) and telogen induction and maintenance (VDR, RAR) are upregulated. In senescent alopecia, genes involved in the epithelial signal to DPC (FGF5) are downregulated, while oxidative stress and inflammatory response genes are upregulated (Mirmirani & Karnik, 2010). In the case of hair aging, there is a decrease in hair pigmentation (graying) and a decrease in hair production (alopecia). Hair follicles are influenced by intrinsic and extrinsic aging. Intrinsic factors are related to genetic mechanisms with interindividual variation and extrinsic factors include smoking and UV radiation. Oxidative stress also plays an important role in the aging process of hair follicles. The production of free radicals increases into old age, with a lowering of endogenous defence mechanisms. This imbalance leads to progressive changes in cellular and molecular structures. Information on the role and prevention of oxidative stress could support a better understanding of the mechanisms involved in hair loss and open new strategies for intervention and reversal of age-dependent alopecia. The antioxidant potential of natural substances has been shown to reduce inflammation and could become a part of anti-inflammatory therapy (Nagulsamy, Ponnusamy, & Thangaraj, 2015). Not only genetic, hormonal, hair follicle inflammation and environmental factors are considered to affect the occurrence of alopecia but also oxidative stress at the DPCs of AGA patients have been recently proven to play a role. A study demonstrated total antioxidant activity and superoxide dismutase decreased and malondialdehyde and lipid peroxidation product levels in plasma increased in samples of patients with AGA (Prie, Iosif, Tivig, Stoian, & Giurcaneanu, 2016; Yenin, Serarslan, Yönden, & Ulutaş, 2014). These findings confirmed the important role of oxidative stress in the disease pathogenesis of AGA.

Free radical production from different biological and environmental sources creates an imbalance with natural antioxidants which leads to a progression of various inflammatory-associated diseases. The role of inflammation and its associated

adverse effects can provide a clear understanding in the development of innovative therapeutic targets from natural sources which are intended to reduce inflammation associated with diseases. In our study, we sought to evaluate the effect of antioxidants in the AE extract and VB using DPPH and ABTS assays.

1.6 Human skin structure and function

The human skin is an important organ of the body as it has the functions of protecting the body from the external environment by acting as a barrier to the absorption of exogenous molecules and preventing excessive loss of water. The skin is the largest organ of the body, comprising around 10% of the body mass and covering an area of approximately 1.8 m² in an adult, depending on the height and weight of an individual. The human skin consists of the epidermis, dermis, and subcutaneous tissue layers (see Figure 6).

The subcutaneous layer is typically thick throughout the body except for some areas such as the eyelids where it is absent. This subcutaneous layer of adipose tissue provides mechanical protection against physical shock, insulates the body, provides a store of high-energy molecules, and carries the principal blood vessels and nerves to the skin. The subcutaneous layer is an important barrier to transdermal and topical drug delivery.

The dermis is the major component of human skin. The dermis is composed of collagen types I and II, elastin, blood vessels, free nerve endings, lymph vessels, hair follicles, sebaceous glands, and sweat glands. The hair follicles and eccrine and apocrine sweat glands open directly to the outside on the surface of the skin. The dermis has a metabolic action and requires widely available vascular supply for regulation of body temperature, wound repair, delivery of oxygen and nutrients to skin tissue, and removing waste products from the skin. The blood supply reaches approximately 0.2 mm below the skin surface, near the dermis-epidermis boundary, and so most molecules passing through the outer layer of the skin are rapidly diluted and are carried systemically by the blood. This rich blood flow keeps the dermal concentration of most transdermally delivered drugs low, which in turn provides a concentration gradient from the outside of the body into the skin and it is this

concentration gradient (more accurately, it is the chemical potential gradient) that allows drug delivery through the skin (Williams, 2015).

The epidermis covers the dermis and is multiple layers containing various cell types, including keratinocytes, melanocytes, and Langerhans cells. Keratinocytes in the basal layer (stratum basale) undergo division and then differentiate as they migrate outwards, forming firstly the stratum spinosum, secondly the stratum granulosum and finally the stratum corneum. Differentiation is complex and essentially changes the metabolically active basal cells that contain typical organelles, such as mitochondria and ribosomes, into stratum corneum that comprises anucleate flattened corneocytes packed into multiple lipid bilayers.

The stratum corneum is the outer skin layer and is predominantly responsible for the barrier properties of human skin and limits drug delivery into and across the skin. The stratum corneum typically comprises only 10 to 15 cell layers and is around 10 μm thick when dry, although it can swell to several times this thickness when wet. The stratum corneum is thinnest on the lips and eyelids and thickest on the load-bearing areas of the body such as the soles of the feet and palms of the hands. The lipid bilayers in which the keratin-filled cells are embedded are uniquely different from other lipid bilayers in the body since they are comprised largely of ceramides, fatty acids, triglycerides, and cholesterol/cholesterol sulfate, whilst phospholipids are absent. The resulting structure can be likened to a brick wall (see Figure 6) where the keratin-filled cells act as the bricks in a mortar of multiply bilayer lipids. In normal skin, it takes approximately 14 days for a daughter cell in the stratum basale to migrate and differentiate into a stratum corneum cell, and these cells are then retained in the stratum corneum for a further 2 weeks before they are shed. Appendages can be viewed as shunt routes through which molecules can pass across the stratum corneum barrier. The important appendages are the hair follicles and sebaceous glands. The skin has 50 to 100 hair follicles per cm^2 except on the palms and soles. These shunt routes provide a potential route through intact skin. Furthermore, formulations can target these structures by delivering nano to micro-sized drug delivery systems to the follicles to target treatment (Williams, 2015). For drug delivery and therapy, the intact skin presents a formidable barrier and a difficult challenge for formulation scientists. The properties of the skin limit the range of active ingredients that can be delivered

through the barrier to achieving therapeutic levels. For this reason, a drug delivery system can be used to enhance the permeability of the drug or substance. However, skin can be relatively easily damaged through mechanical, chemical, or microbiological and UVR attacks.

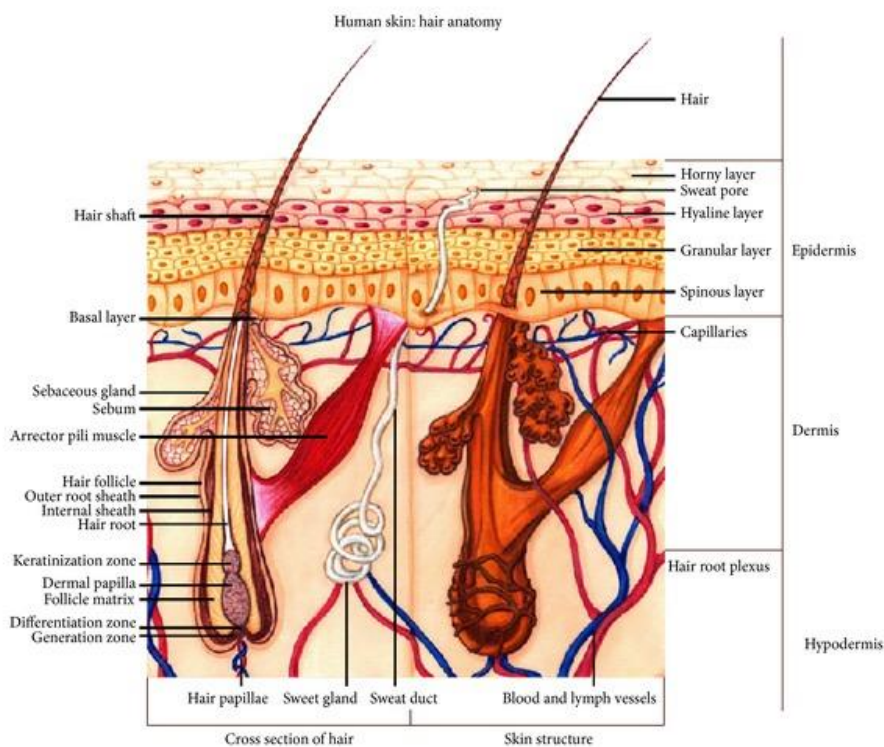


Figure 6 The structure of human skin in cross-section

Source: Schembri, Scerri, & Ayers, 2013

The ingredients of some cosmetic products include permeation enhancers which support the potential to affect skin structure integrity. For example, ethanol, oleic acid, and some surfactants are known to affect the thermodynamics of intercellular lipids in the stratum corneum, changing their organization from rigid gel crystalline structures to liquid. This process accelerates the penetration of the enhancers and other components in the formula. Delivery systems such as vesicles, nanoparticles, microparticles, and other solubilizers may also affect profiles of

partitioning. This means that two similar formulations containing the same percentage of active compound, but differing in the vehicle, can exhibit different penetration profiles through the skin.

There are three types of interactions between chemicals and skin. Firstly, a chemical substance can be transported from the surface of the skin into the skin and through systemic circulation. This process of skin absorption can be divided into three procedures: penetration, permeation, and resorption. Secondly, a chemical substance can induce local effects from skin irritation to skin corrosion. Skin irritation is the production of reversible damage to the skin following the application of a test substance while skin corrosion is the production of irreversible damage to the skin following the application of a test substance. Lastly, a chemical substance can generate allergic skin reactions through immune system responses at both the contact area and a referred response area (Klimová, Hojerová, Lucová, & Pažoureková, 2012).

Therefore, the study of skin penetration is a useful experiment for both the safety and efficacy assessment of topically formulations as it is considered an important route for topical delivery.

1.7 Topical and Transdermal delivery

Transdermal delivery represents an attractive tool delivery for drugs to the treatment target. Previously, people have placed substances on their skin for therapeutic effects and now a variety of topical formulations have been developed to treat local indications. Transdermal delivery has a variety of advantages compared with the oral route when it is used to achieve a significant first-pass effect of the liver that can perform the primary metabolism of drugs. Transdermal delivery also has advantages over hypodermic injections, which are painful and present a risk of disease transmission by needles. Furthermore, the transdermal system is non-invasive and can be self-administered. They can provide sustained release and improve patient compliance. In addition, the systems are usually inexpensive. However, transdermal delivery has a limitation in the number of possible drugs for administration and it is difficult to exploit the transdermal route to deliver hydrophilic drugs. Presently new generation transdermal delivery systems permit transdermal administration of

hydrophilic molecules. This skin permeation enhancement achieves increased skin permeability without providing an added driving force for transdermal transport. The increase of skin permeation causes by modification of skin barrier structure. So, chemical enhancers have limited use as they can destroy the stratum corneum structure. Successful transdermal delivery is based on accomplishing a suitable balance between delivery and safety to the skin (Prausnitz, & Langer, 2008).

An active molecule has three potential routes to cross the skin. Firstly, it can pass into the skin by the shunt routes. In this route, the molecules were partitioned into sweat or sebum and followed these fluids into the skin by diffusion against the outflow from the glands. The molecule was usually crossed the stratum corneum via an intracellular (also termed transcellular) route or intercellular route.

In terms of the intracellular route, the drug molecule partitions into a keratin-filled corneocyte, it can then diffuse through the corneocyte by partitioning into the intercellular lipid domains. In the case of transcellular transport, the molecule diffuses through the lipoidal region before repeatedly partitioning into the aqueous keratin in corneocytes and diffusing through the intercellular lipid. On the other hand, the intercellular route requires the molecule to partition into the lipid bilayers between the corneocytes and then passes via a sinuous route within the continuous lipid domain, like following the mortar in the brick wall model. While traveling through the stratum corneum, the molecule diffuses through the lower epidermal layers and then through the capillaries at the epidermal-dermal junction. In this way the permeant binds to skin components such as keratin and so, in this case, it may not reach the systemic circulation. Moreover, skin is metabolically active and contains esterase, peptidases, and hydrolases which can reduce the bioavailability of the topically applied molecules as described in Figure 7 (Williams, 2015). Importantly, the proportion of molecules crossing by these different routes was varied depending on the physiochemical properties of the permeant.

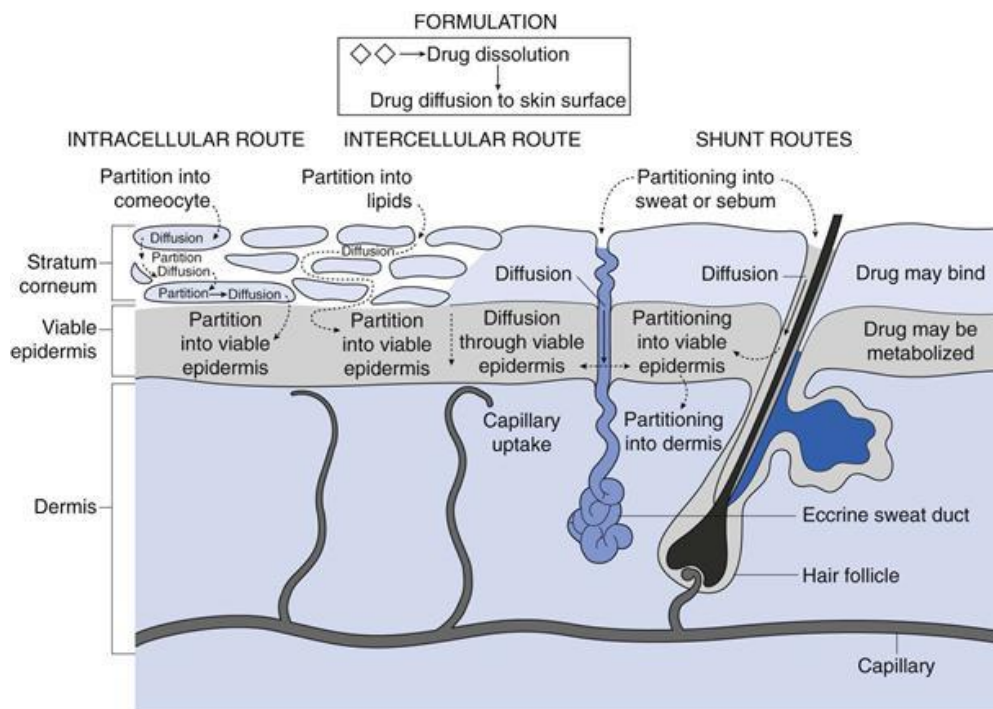


Figure 7 A diagrammatical cross-section through human skin showing the different skin layers

Source: Williams, 2015

Generally, to be a candidate for transdermal administration the properties of the substance should be nonionic, of low molecular weight (less than 500 Daltons), have a logP value between 1-4, and have both hydrophobic and hydrophilic properties (Benson, 2005).

1.8 Trans follicular pathway for drug delivery systems

The hair follicle openings rise through the epidermal layer but the section through the stratum corneum is thin at a depth of about 200 μm of the follicle duct. The pilosebaceous unit containing the hair follicle is closely surrounded by a high density of blood vessels, thus having a potential for high absorption of permeating substances into the systemic circulation. Lieb et al. demonstrated that permeation into hair follicles depends on the size and charge of the permeant and the formulation in which the permeant is applied (Lieb, Liimatta, Bryan, Brown, &

Krueger, 1997). Other chemical properties, like lipophilicity, might also play a significant role in follicular penetration. In addition, a degree of lipophilicity for compounds entering the hair follicle might be necessary due to the presence of sebum in the follicular duct from the sebaceous gland. Based on theoretical considerations, it has already been proposed by Scheuplein et al. that the follicular route plays an important role in the initial period of the transport process, but that at a later stage penetration occurs predominantly through the stratum corneum (Grams, 2005). Many reports (Mohd, Todo, Yoshimoto, Yusuf, & Sugibayashi, 2016; Todo et al., 2010) have been published describing how skin appendages such as hair follicles and sweat glands are an important permeation/penetration pathway, especially for hydrophilic compounds and macromolecules. Many researchers have already investigated the transfollicular permeation of topically applied chemicals. One study applied caffeine in a mixed solution of ethanol: propylene glycol (30:70 v/v) to volunteers before and after blocking all hair follicles with a varnish solution at the site of its application. The results reported that caffeine was observed in the blood 20 min after application on the hair follicle-varnish-blocked skin, but 5 min after topical application to normal skin. A possible reason for the more rapid appearance of caffeine in the blood may be the rapid absorption of the substance penetrating through hair follicles to blood capillaries (Nina et al., 2008). The hair follicular openings comprise only about 0.1% of the total skin area, but this can be as high as about 10% on the face around the mouth and scalp (Wosicka, & Cal, 2010). The lipoidal environment of the follicular canal may affect certain drugs and vehicles. In addition, follicular delivery may be enhanced by manipulating formulation factors. Recent studies have indicated that the particle size of drug carrier systems may be an important consideration in designing a follicular delivery system (C. Lauer, L. Flynn, Ramachandran, Weiner, & Margaret Lieb, 1995). Thus, this information is useful for chemical application to skin in evaluating the usefulness and safety of a crude extract and its subsequent formulation. In the present study, the contribution of the hair follicle pathway to the permeation of topically applied crude extract solution and formulation were determined.

1.9 Skin absorption *in vitro* model

The advantages of the *in vitro* method are that it can be used with both human or animal skin and synthetic membranes. Moreover, it does not need a live animal. Hence, this technique is suitable for screening the permeability of substances and cosmetic products. Furthermore, percutaneous penetration is an important parameter for the safety evaluation of cosmetic products and their ingredients.

Generally, skin is composed of several layers with the stratum corneum layer being the barrier to external substances. This layer provides the rate-limiting step for skin permeation. Hydrophilic compounds are usually limited in skin permeation. Many researchers have indicated that there are 3 routes of skin permeation. These are intercellular, intracellular, and trans-follicular routes. Skin absorption can be investigated using several models. The *in vitro* model is a practical method for estimating the skin permeation profile of permeants by determining the amount that permeates downward through the receptor compartment by diffusion force. *In vitro* skin, absorption methods exist in the Organization for Economic Co-operation and Development (OECD) guideline form No. 428. This method of access is used extensively by cosmeticians to predict the degree of systemic penetration of chemicals through the dermal route.

The Franz cell model is a well-known method with specific equipment that is solely used for determining skin absorption. According to Figure 8, a Franz cell is composed of a donor compartment that contains a certain amount of the drug or substance of interest. The membrane in the study can be animal skin or artificial membrane. The receptor compartment contains receptor fluid that dissolves the permeant which permeates from the donor compartment. It is measured by collecting it from the sampling port. The temperature of the receptor chamber is controlled by a water jacket (OECD, 2004). *In vitro*, Franz diffusion cells have been used in much research to assess skin permeability by providing the relationships between substance, skin, and formulation. The Franz diffusion cells are used not only for the development of novel formulations but also for quality control purposes (Ng, Rouse, Sanderson, Meidan, & Eccleston, 2010). *In vitro* techniques are ideal for screening percutaneous

penetration of topical formulations due to the low cost and time compared to *in vivo* experiments. In addition, ethical considerations are less than an *in vivo* technique.

In general, Franz diffusion studies usually use synthetic membranes to model real human or animal skin. Due to sufficient quantities of human tissues being difficult to obtain for performing permeation experiments, synthetic membranes may be preferred to skin tissue as they are easily resourced, less expensive, and have a simple structure. In addition, synthetic membranes exhibit permeation result reproducibility more than *in vivo* tissue which always shows variations due to skin age, race, sex, and anatomical site (Wester & Maibach, 1992). Synthetic membranes always used to mimic the skin include polydimethylsiloxane (PDMS) which shows similar hydrophobic and rate-limiting properties to the skin (J. Twist, & L. Zatz, 1988; J. N. Twist, & Zatz, 1986).

In vitro experiments are used to measure the penetration of test substances across skin or membranes during potentiality studies to predict the permeability of the same various substances passing through the skin in an *in vivo* evaluation in animal models.

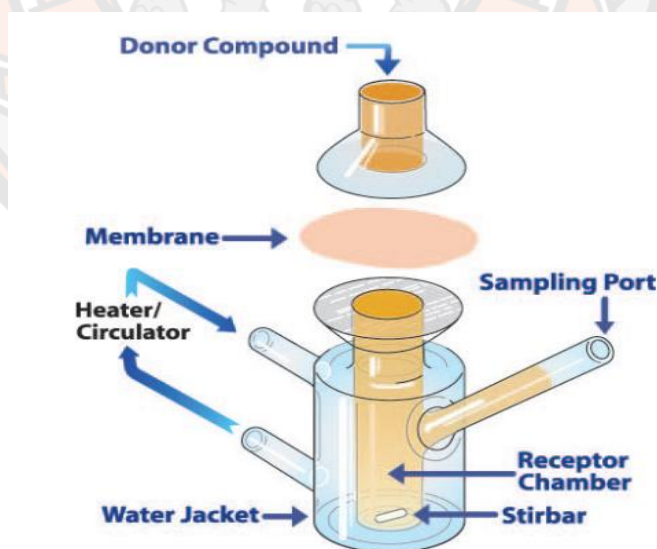


Figure 8 Franz diffusion cell

Source: Vats, Saxena, Easwari, & Shukla, 2014

The objective of the current study was to use the Franz-cell model to measure the penetration profile of the AE crude extract and hair product through a synthetic membrane for quality assessment.

1.10 Microencapsulation

Microencapsulation is a process in which tiny droplets or particles of liquid or solid material are surrounded or coated with a continuous film of polymeric material (Bansode, Banarjee, Gaikwad, Jadhav, & Thorat, 2010).

To achieve a final product some issues, need to be overcome, such as poor stability, solvent toxicity, and low solubility of the bioactive compound. Microencapsulation is one of the quality preservation techniques of sensitive substances. Microparticles provide various advantages as a drug delivery system, including effective protection of the encapsulated active substance against degradation, controlling the release rate of the substance over periods, controlling the rate of substance delivery to the target site, easy administration, and desired substance release profiles can be provided which are suitable for patients in need of treatment (Singh, Hemant, Ram, & Shivakumar, 2010). Microencapsulation can be described as the surrounding of a liquid droplet or solid particle core with a solid shell (Figure 9). The encapsulated ingredients include adhesives, drug substances, colors, fragrances, flavors, solvents, and oils. In the cosmetic industry, the capsules are designed to release the core by breaking the shell. Generally, a microparticle refers to a particle with a diameter of between 1- 1000 μm . The capsule size is estimated by the method used in production. These capsules are normally supplied in dry powder form which often needs to be dispersed into the cosmetic or pharmaceutical formulation.

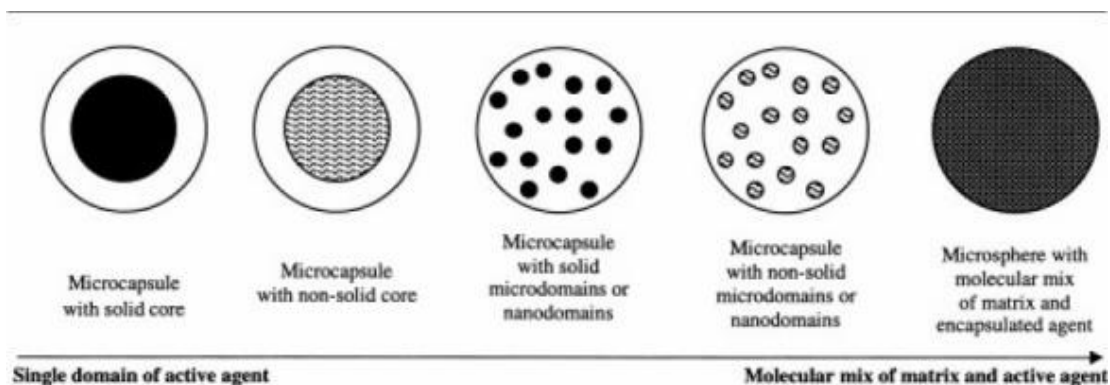


Figure 9 Different structures of microcapsules and microspheres

Source: Singh et al., 2010

Targeting drugs to specific organs and tissues has become one of the major endeavors of the new century. Microencapsulation systems can solve solubility problems, protect the drug from the external environment, for example from photodegradation and pH changes, control the release profile, control targeting at the target site of action, and reduce toxicity and side effects. Furthermore, they increase the efficacy of treatment and improve patient compliance (Gandhi, Mundada, & Gandhi, 2011). Biocompatibility forms the basis for important regulations regarding the use of cosmetic and pharmaceutical products. Formulation design to appropriately characterize the desired physicochemical properties of an active ingredient are a challenge for new drug forms (Martinho, Damgã, & Reis, 2011). The most common administration routes are oral, parenteral, transdermal, and inhalation. For the transdermal route, medical treatment is applied on the surfaces of the body such as mucous membrane or skin. This route is more significantly related to a local effect than to a systemic effect. Additionally, this route was transferred the active ingredients directly to the treatment target without gastrointestinal or liver metabolism (Gandhi et al., 2011).

Principally, the method used for the preparation of microspheres loaded with active components is composed of the following two techniques:

1. Formation of microspheres and
2. After formation, incubate them with the drug or protein.

The active component can be loaded by physical entrapment, chemical linkage, or surface adsorption. The entrapment and the release of the active constituent partly depend on the method of preparation, the physicochemical properties of the compound, and the properties of the carrier. There are three methods of drug release from the microspheres:

1. An osmotically driven burst mechanism,
2. A pore diffusion mechanism
3. Erosion or degradation of the polymer (Alagusundaram et al., 2009).

To administer an active compound at a therapeutic concentration to a target treatment site over some time is the major objective of a drug formulation. The physicochemical properties of a drug, its desired site of action, its duration of action, resolution of biological barriers, rapid drug metabolism, and information on related therapeutic effects are the required parameters for the appropriate formulation and delivery of a drug.

The stability and solubility of the substance are important physicochemical properties that should be considered when designing product formulation. The properties of the substance in both solid and liquid form play an important role at this stage. Although the solid form is more chemically and physically stable, easier to prepare, and more convenient to provide than the liquid formulation, it must be dissolved before it can be therapeutically active, therefore it should be chemically stable and sufficiently soluble in its solid form.

The therapeutic nature of many drugs determines the management of their administration. Transdermal drug delivery has many advantages, such as being non-invasive and having the possibility of providing high potency and rapid permeability through the stratum corneum. In terms of drug delivery, the three most important questions are the when, where, and how of drug delivery. Targeted drug delivery is often used when the site of action is located within a tissue and the release of the drug systemically would result in toxic or harmful effects.

The goal of any drug delivery system is to provide a therapeutic amount of the drug to its target site in the body, immediately if possible, and then to maintain the intended drug concentration. Moreover, a delivery system should also protect the chemical substance from degradation. Microparticulate drug delivery

systems are an interesting avenue for hair care product development to increase the efficiency of substance delivery, improve substance targeting and improve stability of the active substance.

This research was focused on the development of nano or microparticle encapsulated AE extract for hair tonic formulation to enhance solubility, permeability, and stability. These properties were achieved by protecting the encapsulated bioactive ingredients from degradation thus preserving their efficacy for a long period.

1.11 Preparation of microparticles

There are different techniques for the preparation of solid lipid nano/microparticles. Generally, the preparation of microparticles requires a dispersed system as precursor or template; otherwise, particles are generated using instrumentation (Table 2). The most important techniques which involve the use of specific instrumentation are the membrane contactor technique, spray-drying, spray-congealing, and electrospray (Battaglia et al., n.d.).

Table 2 Preparation techniques for solid lipid Nano-and microparticles

Precursor system	Technique	Nanoparticle type
Emulsion	Hot homogenization (high pressure homogenization, high shear homogenization, ultrasound homogenization)	SLN
	Melt dispersion	SLN
	Microemulsion cooling	SLN
	Coacervation	SLN
Supercritical fluid emulsion	Supercritical fluid extraction of emulsions	SLN
	Membrane contactor technique	SLN
	Cryogenic micronization	SLM
	Spray-drying	SLM
	Electrospray	SLN/SLM
	Spray-congealing	SLM

Source: Battaglia et al., n.d.

Different techniques have been developed to produce solid lipid particles providing the opportunity to obtain different sizes and shapes of microparticles. The current study concerned the practical method for encapsulating the active compound of AE extract. It has to be further developed for an industrial scale.

1.12 Spray chilling

In a spray chilling or spray congealing technique, lipids are heated to a temperature above their melting point and the drug is dissolved or suspended into the melted lipid. The hot mixture is then atomized through a pneumatic nozzle into a vessel, where the atomized droplets can solidify in the form of microparticles. The Mini Spray Dryer B-290 with Dehumidifier B-296 with spray chilling module connected with the spray chilling accessory has been used for preparing the microparticles See Figure 10. During spray chilling the carrier material and the active ingredients are heated above the melting point in the sample feed accessory Figure 11.



Figure 10 Mini Spray Dryer B-290 with Dehumidifier B-296

Source: Buchi, 2016



Figure 11 Spray chilling accessory

Source: Buchi, 2016

Spray chilling or spray congealing are forms of solid dispersion. The solid dispersion technique has proven to be the most successful in improving the dissolution and bioavailability of poorly water-soluble active pharmaceutical ingredients because it is a simple, economic, and advantageous technique. The melted mass is atomized into droplets, which quickly solidify in cool air. The advantage of spray chilling is not requiring an added manufacturing step to pulverize a solid dispersion. In pharmacies spray chilling has been used to prepare sustained-release formulations, to improve stability and to mask unpleasant tastes. In addition, this technique also has the advantage of being free from organic solvents when compared to spray drying. The method has also been used by the food industry, for example, to encapsulate vitamins and minerals. As an example, piroxicam (N-2-3-xylylanthranilic acid) is a poorly water-soluble drug. It has low aqueous solubility and therefore poor dissolution (K. Wu, Li, Wang, & Winstead, 2009). A previous study reported that spray chilled particles were prepared by melting the drug at $205 \pm 5^\circ\text{C}$. The melt was kept at $205 \pm 5^\circ\text{C}$ and chilled with a pneumatic nozzle where the air was kept at 20°C . The inner diameter of the pneumatic nozzle was 0.1 mm, the capillary length

was 5 mm, and the pressure was 1 Kg/cm². The particles were collected, separated, and stored in a desiccator (Dixit, Kini, & Kulkarni, 2010).

1.13 High-speed homogenization (HSH)

Homogenizer was initially used to produce solid lipid nano emulsions; this method is reliable. The process involves high-pressure homogenization which pushes the liquid with high pressure (100-2000 bar) through a narrow gap ranging in micrometer. Very high shear stress and cavitation forces disrupt the particles down to the submicron range. Two general approaches to achieve HSH are hot homogenization and cold homogenization. Hot homogenization is generally carried out at temperatures above the melting point of the lipid. A pre-emulsion of the drug-loaded lipid melt and the aqueous emulsifier phase (same temperature) is obtained by high shear mixing device. The resultant product is a hot o/w emulsion, and the cooling of this emulsion leads to the crystallization of the lipid and the formation of SLNs. Smaller particle sizes are obtained at higher processing temperatures because of lowered viscosity of the lipid phase. However, high temperature leads to the degradation rate of the drug and the carrier. Increasing the homogenization temperature or the number of cycles often results in an increase in the particle size due to the high kinetic energy of the particles. Generally, 3-5 homogenization cycles at a pressure of 500-1500 bar are used. Cold homogenization has been developed to overcome the temperature-related degradation problems, loss of drugs into the aqueous phase, and partitioning associated with the hot homogenization method. The drug is incorporated into melted lipid and the lipid melt is cooled rapidly using dry ice or liquid nitrogen. The prepared lipid microparticles are then dispersed in a cold emulsifier solution at or below room temperature. The temperature should be regulated effectively to ensure the solid state of the lipid during homogenization. However, compared to hot homogenization, larger particle sizes and broader size distribution are typical of cold homogenization samples.

In our study, nanoparticles were obtained using the hot melt homogenization method. The morphology, particle size, and substance loading capacity were optimized. Scanning electron microscopy (SEM) was used to characterize microparticles morphology. It is anticipated SEM images was illustrated

nanoparticles as spherical and fixed onto the carrier materials. Particle size analysis was evaluated using a particle size analyzer. Percentage entrapment of the active biomarker was determined using the HPLC method. Finally, *in vitro* skin permeation studies of nanoparticles using the Franz cell model were done.

1.14 Chemical and physical properties of Compritol® 888 ATO

Compritol® 888 ATO is the lipid composing of the hydrophobic mixture of mono-, di- and tri- behenate of glycerol. The name of the mixture for The International Nomenclature Cosmetic Ingredient (INCI) is Glyceryl Dibehenate/Tribehenin/Glyceryl. Behenic acid is prominent more than 80% It has melting point in the range 69-74°C and with hydrophilic-lipophilic balance (HLB) 2.

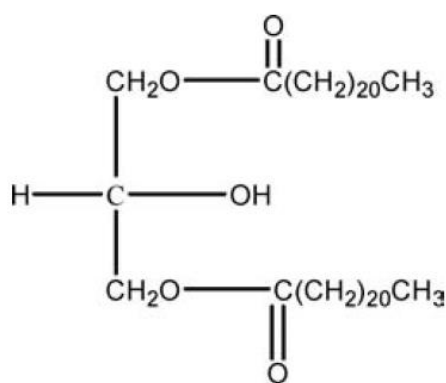


Figure 12 Chemical structure of glyceryl dibehenate

Source: Compritol® 888 ATO

Previously Compritol® 888 ATO has been used as a lubricant agent in tablet and capsule preparation. Many studies find that Compritol® 888 ATO is a good candidate as the carrier in micro/nano particle preparation. According to chemical structure analysis, several studies document that Compritol® 888 ATO shows the lipid polymorphism due to the difference of three-dimensional structures; they are unstable α , metastable β' , and stable β modification. The polymorphic form of Compritol® 888 ATO depends on crystallization, temperature, and storage condition. After melting,

each glyceride crystallizes and produces a complex structure containing 3 different lamellar phases that affect drug entrapment efficiency by each of the lamella cavities. After crystallization, the transformation of lipid particles from less stable to more stable is referred to as polymorphic transition. The structure transformation plays a crucial role in lipid application stability. Compritol[®] 888 ATO has been usually prepared as a particle by using homogenization technique incorporating drug by melting. Compritol polymorphism influences particle properties such as stability, drug incorporation, and release of the drug. Several researchers attempt to incorporate poor water-soluble drugs into a particle by melting and then emulsifying in an aqueous phase. The recrystallization was evident after particle formation. Compritol[®] 888 ATO, signifying that throughout the solidification process only the stable polymorph β is formed. However, there was study found that the lattice arrangement of Compritol[®] 888 ATO crystals generally comprised small amounts of the unstable α polymorphic form that disappeared after thermal stress at melting point. Recrystallization induces polymorphic transition; α structure is transformed to metastable β' and stable β respectively. Polymorphic transition causes drug expulsion and particle aggregation which is the instability of particles. Compritol[®] 888 ATO property also affects particle entrapment efficiency and release behavior. Lipophilic drug increases entrapment efficiency due to the ability to partition inside particle matrix. Lipid drug in Compritol[®] 888 ATO particle shows sustain release in aqueous media because the drug is limited water-soluble. Moreover, Compritol[®] 888 ATO showed sustained drug release due to it containing a long carbon chain length that allows less than 3% water up take inside. Although Compritol[®] 888 ATO can sustain the drug released from SLN, stability at high temperatures is also unsatisfactory. According to a long-term stability study of Compritol[®] 888 ATO at high temperature, the result reports that melting point and recrystallization index of Compritol[®] 888 ATO are increased. Those results can be used for predicting the structural transformation that causes drug expulsion and particle aggregation. Moreover, the gelling tendency at high temperatures also allows the release of drugs from SLN as like water permeating into the matrix.

1.15 The process in the measurement of anatomy properties of hair

A hair consists of two parts, a follicle, and a shaft. The follicle is a club-shaped structure in the skin. The lower part of the follicle has blood vessels that supply nutrients to the hair via the DPC. Surrounding the papilla is a bulb. A sebaceous gland, which secretes oil that helps to maintain hair moisture, is associated with the bulb. The erector muscle that causes the hair to stand upright attaches to the bulb. Nerve cells wind around the follicle and stimulate the erector muscle in response to changing environmental conditions. The hair shaft is composed of the protein keratin, which is produced in the skin. Keratin makes hair both strong and flexible. Like all proteins, keratin is made up of a chain of amino acids that forms a helical, or spiral shape. These helices are connected by strong bonds between amino acids. These bonds make hair strong. The hair shaft is made up of three layers: an inner medulla, a cortex, and an outer cuticle (Feughelman, 1997; Jones, 2001; Marie, 2007). Hence, the measurement of hair to monitor hair regulation or hair treatment effectiveness can be monitored its anatomical, biochemical, and physiological properties. Anatomical properties were measured and monitored in this clinical study.

1.15.1 Global photograph

Global photographic assessment is useful for determining overall clinical changes in a patient over time in a standardized manner. A patient is usually photographed from the front, top, sides, and back to show frontal hair line, temporal recession, the vertex, and the mid/frontal region. This basic photographic setup provides good, clear photographs suitable for recording a patient's hair loss and progress through hair growth during treatment. The same photographic position must be maintained when comparing the progress of hair loss or hair growth (Ishino et al., 2014; Elise A. Olsen et al.).



Figure 13 Global photographs of an androgenic alopecia patient

1.15.2 Hair density measurement

Hair diameter and density measurement are the in-situ methods that are always used to evaluate the effectiveness of hair treatment or to observe the progression of hair disease. This non-invasive method does not require staining because the staining process may affect the efficacy of the measurement. The method uses a light microscope or digital camera. Hair can be clipped from the target site, collected, and stored under ambient conditions. It is then divided into bundles and fixed at the proximal end. Ideally, the hair is captured by digital photography and then measured for length and diameter using the photographs (Vallotton & Thomas, 2008). Recently, research has determined hair diameter and hair thickness by using a Folliscope[®] or Phototrichogram[®]. These are easy to use and have software for the calculation of hair diameter and length (Buonocore, Nobile, Michelotti, & Marzatico, 2013; Ishino et al., 2014; Van Neste et al., 2000).

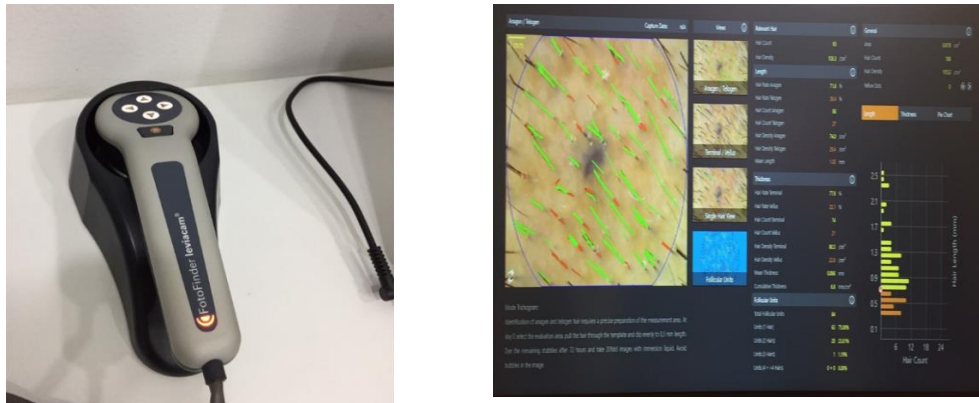


Figure 14 Leviacam® and software for hair analysis

A tattoo is a way to mark an area of observation. The result is analyzed using a digital camera at high magnification. The density of hair or total hair count can then be visually performed and calculated (Figure 15) (Elise A. Olsen et al.).



Figure 15 A marked areas using a tattoo to calculate hair density

1.15.3 Hair comb test

This protocol has been used for determining the number of shed hairs after combing for 60 seconds. The subjects were instructed to comb their hair for 60 seconds before shampooing in the morning, starting at the vertex, and combing forward. The hair was combed over a towel or pillowcase of contrasting color so that any shed hairs could be adequately visualized. The subjects then collected the shed hairs and recorded their number. This technique was often modified for evaluating hair shedding at visiting the site in the clinical study because the decreasing number of shed hair could imply the effectiveness of treatment (Wasko, Mackley, Sperling, Mauger, & Miller, 2008)

CHAPTER III

RESEARCH METHODOLOGY

1. Materials

1.1 Chemicals

1-(4, 5-Dimethylthiazol-2-yl)-3, 5-diphenylformazan, Thiazolyl blue formazan or MTT, Hydrocortisone were purchased from Sigma-Aldrich (St. Louis, USA). Dulbecco's Modified Eagle's medium or DMEM, 2.5% trypsin, fetal bovine serum, penicillin/streptomycin, Phosphate buffer solution pH 7.4 were obtained from Gibco (Auckland, New Zealand). Dimethylsulfoxide or DMSO (Analytical grad) was purchased from Labscan (V.S. Chemhouse, Thailand). Mouse IL-1 β ELISA Instant Kit was purchased from e-bio sciences (Bender-med systems GmbLt, Vienna, Austria). RAW 264.7 cells were purchased from ATCC (Manassas, Virginia, USA). Human follicle DPC and follicle DPC growth medium were purchased from Promo cell (Heidelberg, Germany). Verbascoside (VB), C₂₉H₃₆O₁₅ (MW = 624.61) was purchased from Abcam (Abcam, UK). Sodium dihydrogen orthophosphate, NaH₂PO₄·2H₂O (MW=156.01) was purchased from Ajax Finchem. Acetonitrile was HPLC grade (Mallinckrodt Baker Inc., Phillipsburg NJ). All reagents were of analytical grade. Water was produced from a Milli-Q water purification system (Millipore, Billerica, MA, USA). Interleukin-1 beta Human ELISA Kit was purchased from Abcam.). Mouse IL-1 β ELISA Instant Kit was purchased from e-bio sciences (Bender-med systems GmbLt, Vienna, Austria). RAW 264.7 cells were purchased from ATCC (Manassas, Virginia, USA).

1.2 Apparatus

Microplate reader (Eon, Biotek, Vermont, USA), CO₂ incubator (Forma Steri cult, Thermofisher Scientific, Ohio, USA), and laminar flow (1300 Series A2, Thermofisher Scientific, Ohio, USA) were purchased from Thermo Scientific, Thailand. Guava[®] easyCyte™ Flow Cytometry (Merck KGaA, Darmstadt, Germany). An HPLC system (Shimadzu Model. LC20AT System, Tokyo, Japan), an isocratic pump system, and an SPD-M10A diode array detector were used. C18 Luna Phenomenex, 250 mm length × 4.6mm ID with 5 μ m particle size was used.

Silverton Homogenizer L5 (Silverson Machines, AS Advancement, USA) and freeze dry machine (PowerDry LL3000, USA) were used. Leviacam® (Fotofinder system, Germany) was used.

2. Plant extraction

AE leaves were collected and purchased from Khaokhoherbary organic farm (Phetchabun, Thailand). The specimens were identified by Assistant Professor Dr. Pranee Nangngam, who is a Faculty of Science member at Naresuan University. A voucher specimen, with the collection number 004163, was deposited at the PNU herbarium, which is located at Naresuan University, Faculty of Science. Plant leaves were macerated with 95% ethanol, 50% ethanol, and hexane for 7 days. The extract solutions were filtered and removed the solvent using a rotary evaporator. Water extraction was done by boiling leaves in water for 15 minutes. A water extract solution was dried by using a freeze dryer machine. All the extracts were kept at -20 °C and protected from light.

3. TLC fingerprint

The chemical components of each extract were identified using a TLC fingerprint. A system of mobile phase composed of ethyl acetate, methanol, and phosphoric acid at a ratio of 50:3:3 was evaluated. The TLC plate was observed under UV light and the chemical reaction of the plate to vanillin spraying was determined.

4. Development of a method for standardization of AE extract

The bio-active compound in AE extract is VB which demonstrated interesting biological activities associated with the causes and mechanism of hair loss. The quantity of VB in the extract was determined using an HPLC method and VB was used as a marker for standardization of the extract. This study was also validated the HPLC method according to the Association of Official Analytical Chemists (AOAC) guideline. The evaluation consisted of measurement of linearity, precision, accuracy, and detection and quantitation limits.

5. HPLC condition for determining VB

The column was a C18 Luna Phenomenex, 250 mm length \times 4.6 mm ID with 5 μ m particle size. The mobile phase was an isocratic solution composed of the phosphoric buffer: acetonitrile (77:23, v/v). The flow rate was 1.5 mLmin⁻¹. The detection wavelength was 332 nm.

6. Standard VB preparation

Five milligrams of VB standard were added into a 5 mL volumetric flask. The mobile phase solution was then added as a diluent. The standard solution was sonicated to completely dissolve the standard powder. The volume was adjusted to 5 mL using diluent. VB standard solutions were prepared in various concentrations from the stock solution. All the solutions were filtered through 0.45 μ m filter paper before HPLC injection.

7. Sample preparation

Five milligrams of AE extract were added into a 5 mL volumetric flask and dissolved using 80% ethanol as a solvent. The extract solution was sonicated to completely dissolve the extract and the volume was adjusted to 5 mL by using 80% ethanol. The extract solution was prepared at various concentrations using the mobile phase as a diluent for making double dilution. Finally, all the sample solutions were filtered through 0.45 μ m filter paper before HPLC injection.

8. HPLC method validation

8.1 Precision

Precision is a measure of the degree of repeatability of an analytical method under normal conditions and is normally expressed as the RSD for a statistically significant number of samples. The experimental details are given below:

Fifty milligrams of AE extract were placed in a 5 mL volumetric flask and dissolved in 80% ethanol. Three concentrations of AE extract solutions (50, 500, 1,000 μ g/mL) were prepared and analyzed for determination of the content of VB. AE extracts solutions were prepared under similar procedures and VB was measured

3 times/day for intra-day reliability on three consecutive days to measure inter-day reliability. The percentage of RSD was evaluated.

8.2 Accuracy

Accuracy was evaluated by comparing the theoretical concentrations of standard spiked into the extract solution to the concentration obtained from the HPLC analysis.

Ten milligrams of AE extract were dissolved in 1 ml of 80% ethanol and then diluted to 250 $\mu\text{g/mL}$. Standard compounds of VB at a concentration of 20, 25, 30, and 50 $\mu\text{g/mL}$ were spiked into an AE extract solution. Finally, the percentage recovery of the VB standard was calculated.

8.3 Linearity

Linearity is the ability of a method to elicit test results that are directly proportional to the analyst concentration within a given range. It was evaluated by plotting concentration versus peak area of the marker over the whole range of the experiment and linearity was evaluated by the correlation coefficient (r^2) and standard deviation (SD). Five milligrams of VB were placed in a 5 mL volumetric flask and dissolved into the mobile phase solution (stock solution). Five concentrations of VB varied with double dilution (500 – 1 $\mu\text{g/mL}$) were prepared from a stock solution using the mobile phase solution as a diluent. The amount of VB was determined using HPLC and a standard curve was plotted.

8.4 Limit of detection and Limit of quantification

The sensitivity of this method was tested using LOD and LOQ which were calculated by using equations as $3.3\alpha/S$ and $10\alpha/S$, respectively, where α is the standard deviation of the y-intercept from the linear equation of standard curve and S is the slope of the regression line, which is recommended under the ICH guideline.

9. Determination of biological activities of AE leaves extract.

9.1 Cytotoxicity and cell proliferation testing

DPCs were added in 96 wells-plate with 1×10^5 cells/well and then incubated for 24 hours. The cells were treated with AE extracts and then re-incubated for 24 hours. Fifty microliters of 1 mg/mL an MTT solution were added to each well.

The incubation was done for formazan crystal formation for 3 hours. Formazan crystal was dissolved by adding 100 μ L DMSO. Cell viability was determined by measuring absorbance at 595 nm compared with the viability of control cells for determining the cytotoxic effect of the extract.

9.2 Cell cycle analysis

DPCs were added into 6 wells-plates with 1×10^6 cells/well and then incubated for 24 hours. The cells were treated with AE extracts and then re-incubated for 24 hours. After treatment, the cells were collected by trypsinizing and then fixed with 70% cold ethanol and kept at -20 °C for 24 hours. The fixed cells were stained using Guava[®] cell cycle analysis reagent and kept in a dark place for 30 minutes. The cell cycle was analyzed using Guava[®] easyCyte™ Flow cytometers and assigning the cycles into G0/G1, S, and M/G2 growth phases. The effect of the extract on each cell cycle phase was compared to the control cell.

9.3 Anti-androgenic activity testing

Anti-androgenic activity has been modified from previous research involving alopecia patient recruitment (Winiarska et al., 2006). DPCs were treated with 200 μ M testosterone and extract solution for 4 days. Cell viability was determined using an MTT assay. The anti-androgenic activity was evaluated by treating DPCs with testosterone combined with plant extract. Finasteride was used as a positive control.

9.4 Anti-inflammatory activity study

9.4.1 Anti-inflammatory testing by RAW 264.7 cell model

1) Cytotoxic testing of AE extract in macrophage RAW 264.7 cells Ten thousand RAW 264.7 cells were seeded into each well of a 96-well plate. The cells were incubated for 24 hours and then treated with AE extract solutions at various concentrations. The incubation time of treatment was 24 hours. One milligram per milliliter of MTT solution was added into each well and the plate was then incubated for 3 hours. Formazan crystals were dissolved into 100 μ L of DMSO. The absorbance was determined at 595 nm. The relative cell viability was calculated by comparing the treated cells with untreated cells (control cell).

2) Anti-inflammatory testing using RAW 264.7 cells model.

One hundred thousand RAW 264.7 cells were seeded into each well of a 24-well plate and then incubated for 24 hours, and the cells were then treated with 5 µg/mL of lipopolysaccharide (LPS), 250 µg/mL from an extract of AE or 125 µg/mL of VB. Five micrograms per milliliter of hydrocortisone were a positive control. After treatment, the cells were incubated for 24 hours. Supernatants were collected to determine the amount of IL-1β using a Mouse IL-1β ELISA Instant Kit. One hundred microliters of distilled water were added into the sample wells and 150 microliters of each supernatant were added in duplicate to the designated wells and the contents mixed. The plate was covered with an adhesive film and incubated at room temperature (25°C) for 3 hours and agitated using a shaker at 400 rpm. After incubation, the micro-wells were washed 6 times with approximately 400 µL of washed buffer per well, allowing the washed buffer to stay in the wells for about 10 – 15 seconds before aspiration. After the last washing, each micro-well was tapped onto absorbent paper tissues to remove the excess wash buffer. One hundred microliters of TMB solution were pipetted into all the wells, including the blank wells. The micro-wells were incubated at room temperature (25°C) for 10 minutes, avoiding direct exposure to intense light. The enzyme reaction was stopped by quickly pipetting 100 microliters of stopping solution into each well, including the blank wells. The absorbance was determined at 450 nm by a microplate reader. The IL-1β content was calculated using an IL-1β calibration curve.

9.4.2 Anti-inflammatory testing by using a human DPC model.

1) Inhibition of IL-1α and IL-6

One hundred thousand DPCs were seeded into each well of a 24-well plate and then incubated for 24 hours, the cells were then irradiated with ultraviolet A (UVA) 20 J/cm² was used for inducing the release of IL-1α from DPCs while ultraviolet B (UVB) 100 mJ/cm² was used as an inducer of IL-6 production. Two hundred and fifty micrograms per milliliter of AE extract or 125 µg/mL of VB were used for treating irradiated cells. Five micrograms per milliliter of hydrocortisone were used as the positive control. The treated cells were incubated for

24 hours. The Amount of IL-1 α and IL-6 were determined using an ELISA kit. The determination process was performed regarding the manufacturer's instructions.

9.5 Antioxidant activity

9.5.1 Antioxidant activity by DPPH assay

A DPPH radical scavenging assay is based on the reduction of DPPH which is a stable free radical. The antioxidant compound donates an electron and is bonded with DPPH. If the DPPH is reduced it changed in color from purple to yellowish. One hundred microliters of samples were reacted with 100 μ L 0.2 mM of the DPPH in a methanol solution. After 30 minutes of incubation period at room temperature under dark conditions, the absorbance of the resulting solution was measured at 517 nm using a spectrophotometer. Inhibition of free radical DPPH in percentage Inhibition (%) was calculated using the following equation:

$$\text{Inhibition (\%)} = (\text{Abs blank} - \text{Abs sample}) / \text{Abs blank} \times 100$$

9.5.2 Antioxidant activity by ABTS assay

An antioxidant is tested by ABTS assay giving the Trolox equivalent antioxidant capacity (TEAC). The ABTS assay is a decolorization assay that measures radical scavenging by electron donation to screen antioxidant activity. The ABTS radical cation reagent was prepared by mixing 7 mM ABTS^{•+} with 2.45 mM potassium persulfate for 12 hours in dark conditions at room temperature. The solution was then diluted with absolute ethanol to set the absorbance at approximately 0.70 \pm 0.02 at 732 nm as measured by spectrophotometer. Twenty microliters of the extracted sample were allowed to react with 180 μ L of the solution for 6 minutes in dark conditions. The absorbance was measured at 732 nm using a UV-VIS spectrophotometer. Antioxidant capacity was expressed as Trolox equivalents (μ M). The linear standard curve of Trolox is in the range of 0-200 μ M and the absorbance estimate is 0.3-0.7

10. Stability study of AE extract

10.1 The effect of temperature.

The samples were evaluated for the effect of temperature following WHO stability guidelines for evaluating the stability of ingredients and pharmaceutical finished products (WHO, 2017). AE extract and the formulation containing microparticles loaded with AE extract were incubated at 50°C for 3 months and measured every month for the remaining VB using an HPLC technique.

10.2 The effect of pH.

The AE extract was evaluated for the effect of varying pH values by dissolving in solutions as follows: pH of 2, 5.5, 7.4, and 8. The samples were kept in a saturated sodium chloride solution box at an ambient temperature for 1 month. The samples were collected on days 0, 7, 14, 21, 28, and 35. The percentage of remaining VB was measured by the HPCL technique.

10.3 Degradation kinetic analysis of VB in AE extract.

The AE extract in both semi-solid and solution forms was evaluated for the quantity of VB after a period of high-temperature conditions. The result was used to evaluate the kinetic parameters controlling the degradation of the active substance and to predict its shelf-life using the Arrhenius equation.

The influence of temperature on the kinetic parameters was studied at 60°C, 70°C, 80°C, and 90°C. Both semisolid form and solution form of AE extract were divided into sealed microtubes and stored in a hot air oven at an intended temperature under saturated sodium chloride solution conditions. The AE extracts were designed sampled on various days and sample degradation of total VB content was determined using an HPLC.

11. Microparticle preparation

AE extract was encapsulated into microparticles using the hot melt homogenization technique. The process of preparing the lipid phase containing Compritol® 888 ATO and Span 80 was melted 10°C above its melting point of Compritol. AE extract was added to the melted lipid. Distilled water containing

surfactant, Tween 80 (polyethoxylated sorbitan), was also heated to 80°C separately. Thereafter, the lipid part is added to the aqueous part maintaining the temperature at 80°C, with continuous stirring. The two-phase system is then homogenized using a high-speed homogenizer at 10,000 rpm for 15 minutes. Particles were let for solidification at room temperature with stirring at 400 rpm. The prepared solid lipid nanoparticle dispersion is lyophilized at 1.03 mbar and -80°C for 72 hours in the freeze dryer. The free-flowing powder was achieved using maltodextrin as a cryoprotectant. The encapsulation efficacy was calculated using the following formula:

$$n = \frac{F}{T} \times 100$$

where n is the efficiency of encapsulation, T is the total VB in the extract loading into the particle, and F is the determined VB in the particle (Ambrosone et al., 2014).

The particles were investigated for characteristics such as particle size, particle morphology, entrapment efficiency, and release profiles. The morphology, particle size, and substance loading capacity were optimized. Scanning electron microscopy (SEM) was used to characterize the microparticles morphology. Particle size analysis was evaluated using a dynamic light scattering (DLS) particle size analyzer. Encapsulation efficacy was determined as the percentage of VB encapsulated in particles to the original amount of VB loaded using HPLC analysis. To determine the drug release efficiency of the particles, lipid particles were suspended into buffer solutions pH 5.5 or 7.4. Free VB released from particles was determined by HPLC from the release medium.

12. Hair tonic preparation

The microparticles possessing appropriate characteristics were incorporated into hair serum that formulation, as illustrated in Table 3. The process of preparation was as follows; Hydroxy methylcellulose was dispersed in 10 mL of water and stirred until hydrogel formed. Other ingredients except SLN loaded AE extract were added

into the hydrogel and stirred until the mixture was homogenous. SLN loaded AE extract was scattered into the hydrogel and stirred until homogenously. The serum containing SLN loaded AE extract was kept at 4-6°C.

Table 3 Formulation of hair serum containing SLN loaded AE extract

	Ingredients	% (w/w)
1	Phosphate buffer (pH5.5)	92.85
2	SLN loaded AE extract	5.00
3	Phenoxyethanol	1.00
4	Hydroxy methylcellulose	0.75
5	Sodium EDTA	0.10
6	BHT	0.05

13. Skin permeation study

The permeation study of AE extract was performed using a Franz diffusion cell model. The procedure was followed according to OECD No. 428; it can be explained in brief as:

The membrane in this study was artificial. Hair serum-containing SLN loaded AE extract or AE extract solution was applied to the membrane and 1.0 mL of the receiver solution was collected at 0, 1, 2, 3, 4, 5, 6, 7, 8, and 24 hours respectively, and then receiver solution was replaced with fresh medium to the same volume. The sampling solution was measured for VB content using HPLC. After dismantling the Franz diffusion cell, the donor parts and membrane were washed and extracted using PBS solution and analyzed for remaining VB by HPLC technique.

14. Evaluation safety of hair growth-promoting product containing AE extract

Hair serum and its ingredients were evaluated for skin safety using a close patch test. Twenty healthy volunteers were recruited regard to the criteria as follows;

Inclusion criteria

1. Healthy male or female with 20-60 years old.
2. No wound or scar on the back skin.
3. Signed in the consent form.

Exclusion criteria

1. Have skin hyper allergenic history.
2. Have eczema and psoriasis history for 6 months.
3. Have steroids used history for 7 days.
4. Have topical treatment.
5. Have major operation history.
6. Have pregnancy and lactation period.
7. Have a cancer history.
8. Have a smoking and drinking history.

Withdrawal or termination criteria

1. Volunteers have severe skin irritation with sample products.
2. Volunteers have non-compliance.
3. Volunteers refuse to participate in the research project.

The upper portion of the back was used as the site of test materials with a 200 microliters application. On the appointment date, volunteers were visually evaluated their back skin and the treated area was photographed. Test products were randomly added to the patch channel of an IQ chamber (Chemo technique Diagnostic, Vellinge, Sweden). The patch test was attached to the selected back skin. The test products were used in the study as shown in the table below;

1	Hair serum	5	Hydrogel base
2	1% Particle + PBS	6	Hair serum+5% Minoxidil
3	5% Particle + PBS	7	5% Minoxidil
4	1% AE extract + PBS	8	5% AE extract + PBS

The patch was removed on the back skin for 48 hours. Tested skin was evaluated by a dermatologist and then photographed after removing the patch for 1 hour. Tested skin was evaluated again after removing the patch for 24 hours. Skin irritation was identified by using the International Contact Dermatitis Research Group (ICDRG) and CTFA guidelines.

Each sample ingredient was as below;

1. hair serum was composed of water, SLN loaded AE extract, phenoxyethanol, hydroxypropyl methyl cellulose, EDTA, and BHT.
2. 1% particle + PBS was SLN loaded AE extract suspended in PBS buffer.
3. 5% particle + PBS was SLN loaded AE extract suspended in PBS buffer.
4. 1% AE extract was 1 g AE extract dissolved in PBS buffer 100 mL.
5. Hydrogel base was the base of hair serum without SLN loaded AE extract.
6. Hair serum+5% Minoxidil was hair serum mixed with 5% minoxidil (Reten[®] 5, TO chemical, Thailand).
7. 5% Minoxidil was Reten[®] 5 (TO chemical, Thailand).
8. 5% AE extract was 5 g AE extract dissolved in PBS buffer 100 mL.

15. Effectiveness of microparticle encapsulated AE extract in the hair-loss treatment

15.1 Subject selection

Men aged 20–60 years old with Hamilton–Norwood types II–V AGA, who are in good health and are enrolled at Thammasat Hospital, and external volunteers were included. Subjects were excluded if they have known sensitivity to herbal applications. They were also excluded if they have had or used: (1) topical minoxidil within the previous 6 months; (2) topical botanicals/nutraceuticals for hair regrowth within the previous 3 months; (3) oral 5 α -reductase inhibitors, oral retinoids, radiation to the scalp, or chemotherapy within the previous 12 months; (4) systemic steroids for more than 14 days within 2 months of enrollment (5) stage VI–VII AGA (6) men with a history of hair transplant, scalp reduction, or hair weaves as well as uncontrolled hypertension, or untreated prostate cancer.

15.2 Study design

The study was a double-blind clinical study in men with male pattern hair loss. After giving informed consent, the history and baseline macro photography of the vertex scalp was obtained. At enrollment, subjects were block-randomized to receive one of the four preparations as detailed below. They were instructed to apply three sprays onto the front of parietal and vertex areas of the scalp, twice daily, gently

rubbing it in and allowing it to dry. Subjects were required to use the same shampoo received from this study for the standardization of shampoo used and to maintain the same hairstyle, hair length, and hair color during the entire study, and to refrain from cutting their scalp hair shorter than 1 inch in length. Subjects were returned to the center for compliance, efficacy, and safety evaluation monthly for 6 months. The effectiveness of the formulation was evaluated using a total hair count on the targeted area of the scalp, global view photographs, Comb-and-count in 60 seconds (Hair comb test), and a questionnaire. In this study, the subjects were allocated into 4 groups for treatment with: (1) 5%Minoxidil, (2) the test product containing AE extract, (3) a combination of minoxidil and test product, (4) a placebo. The process of study was followed in Figure 16.

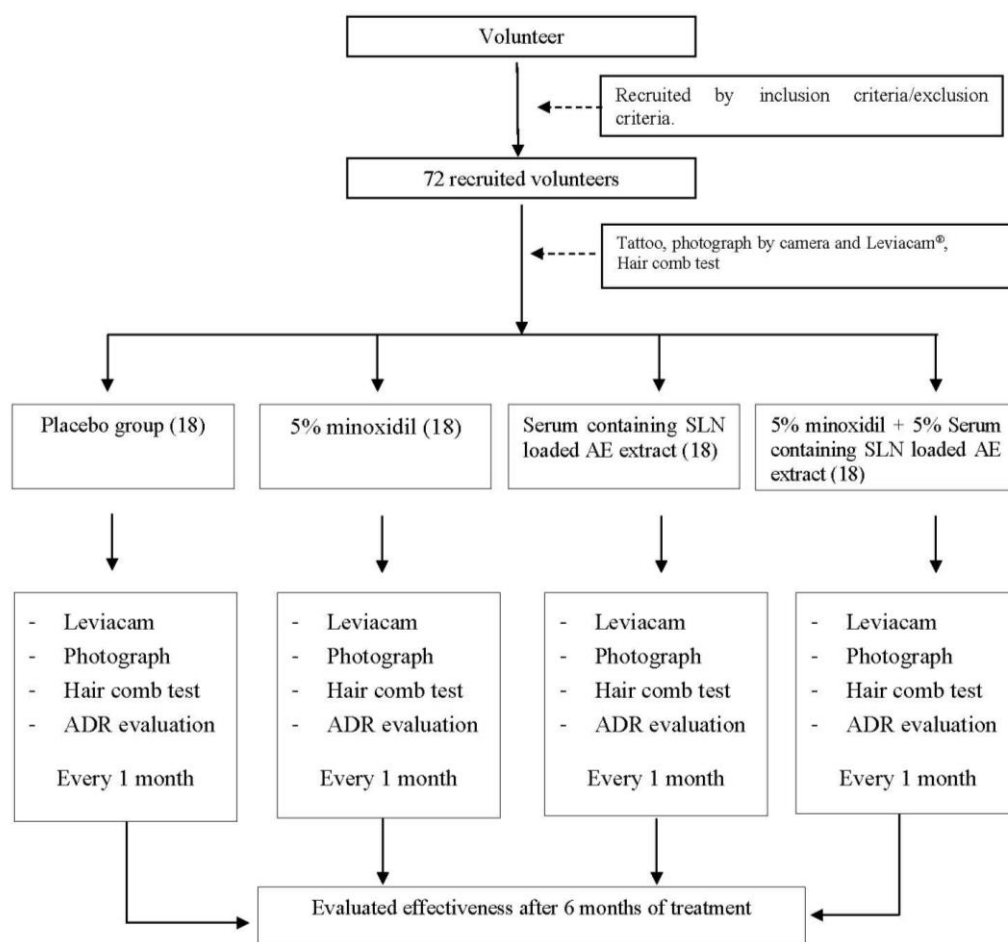


Figure 16 Clinical study process flow chart

15.3 Clinical evaluation

Hair sampling and hair clipping technique.

The vertex area of the scalp was selected for hair sampling that is most affected by AGA. Hair at the target area was marked permanently by the tattoo. One centimeter square of hair of the designed area was hand-clipped during initial baseline screening and monthly screening. The treatment was started immediately after the first clipping and continued for the 24-week study period.

Application of treatment

The subjects were provided with the test solutions in a randomized manner. The subjects were informed to use a test product for application by three sprays of each test product twice daily to the frontoparietal or vertex area of the scalp. Following application to the dry scalp, the subjects should gently massage using their fingertips.

Determination of total hair count

Subjects were taken of the hair at the target area using a Leviacam[®] with high magnification. Total hair count was visually performed and analyzed by Trichoscan[®] software that is used to determine the mean hair count, size of hair fibers, and the ratio of hair follicles in the anagen and telogen phase including the proportion of terminal and vellus hair follicles. The hairs in a 1 cm² are trimmed and a baseline photograph is taken. The target area on the scalp is marked with a central black tattoo. Every 1 month the same area of hair is trimmed again and taken photograph. This process is repeated until finish with the treatment time for 6 months.

Hair comb test

Subjects were assigned to comb their hair for 60 seconds over white paper, starting with the comb at the vertex of the scalp then moving the comb forward to the front of the scalp. The amount of hair falling on the paper was counted after combing. This technique is easy to perform and can estimate the amount of hair shedding.

Global photographic assessment

Subjects were taken a photograph of the frontal and vertex scalp using the stereotactic positioning device by fixing the chin and forehead of the subject, using consistent lighting, and camera to subject distance. The photographic evaluation was determined between baseline and post-treatment.

Patient self-assessment

Patient self-assessment concerning changes in their scalp hair after treatment was done to assess the efficacy of the treatment. The questionnaire was composed of multiple choices that indicated their satisfaction with the overall volume, appearance, and thickness of hair after treatment with assigned hair products.

Sample size calculation

The number of subjects in this clinical study was calculated using the equation below.

$$n = 2[(Z_{\alpha} + Z_{\beta}) S]^2 / d^2$$

Where

n = the number of populations

S = standard deviation that researcher estimate in each of the populations

d = the differentiation of standard deviation of each of the populations

Z_{α} = standard statistical value under a normal curve in type I error

Z_{β} = standard statistical value under q normal curve in type II error

The calculation of the number of subjects was referenced from the article entitled: “A multicenter, randomized, placebo-controlled, double-blind clinical trial of a novel formulation of 5% Minoxidil topical foam versus placebo in the treatment of androgenetic alopecia in men”.

“S” is the standard deviation of change in hair count in subjects who were type V of the Hamilton-Norwood pattern; the value was 21.7.

“d” is the differentiation of hair count of subjects who had the placebo and 5% minoxidil; The value was 21.4.

$$n = 2[(1.96+0.84) \times 21.7]^2 / 21.4^2$$

$$n = 16$$

In this clinical study, the subjects were allocated into 4 treatment groups; the total number of subjects was $16 \times 4 = 64$ subjects. The loss of follow-up was included 15% of each group ($16 \times 10\% = 1.6$). Finally, the total number of volunteers was $18 \times 4 = 72$ subjects.

Clinical study process

The study for evaluating hair serum containing SLN loaded AE extract effectiveness was done at Skin Center, Hospital of Thammasat University, Thailand. Seventy-two volunteers were recruited into the study. They were randomly allocated into 4 groups. The study period was 6 months. Each group was assigned to apply the product twice a day. They were evaluated clinical improvement by using Leviacam[®], combing test, photography, and questionnaire at baseline (T0) and monthly follow up (T1, T2, T3, T4, T5, and T6). Every follows up, all the volunteers were monitored adverse effects such as skin irritation, ejaculation function, and libido by a dermatologist.

16. Statistical analysis

All the analyses were performed in triplicate and values were reported as the mean \pm standard deviation. All results were confirmed from three independent experiments in the cell assay. An independent T-Test was used to determine significant differences between means, and ($p < 0.05$) was considered to indicate statistical significance. Statistical analysis was performed using SPSS 17.0. Clinical study data were analyzed using the Pair T-test for comparing before to after treatment. The different outcomes of each follow-up were analyzed by using repeated measure ANOVA.

CHAPTER IV

RESULTS

1. Plant extraction

AE leaves were extracted using an organic solvent with different polarities. Different percentage yields were obtained, as shown in Table 4. The fresh and dried leaves yielded different percentages of each extract. Fresh leaf showed a lower percentage yield than dried leaf due to the difference in water content in each leaf.

Table 4 Percentage yields of each AE leaves extract performed by different solvents

AE leaves	Percentage yield (% of weight leaves)			
	95% ethanol	50% ethanol	Boiled water	Hexane
Fresh leaves	6.03 ± 1.22	12.07 ± 3.14	4.38 ± 1.56	0.04 ± 0.01
Dried leaves	11.37 ± 2.33	28.11 ± 2.54	16.74 ± 1.34	1.33 0.51

2. Thin-layer chromatography fingerprint (TLC fingerprint)

TLC was used for identifying the basic chemical components in the AE extracts. A system of mobile phases composed of ethyl acetate, methanol, and phosphoric acid at a ratio of 50:3:3 was examined. The 8.0 cm of silica plates were developed which were then observed under UV light at 254 and 365 nm. The plates were further sprayed with vanillin solution and visually observed. (Figure 17).

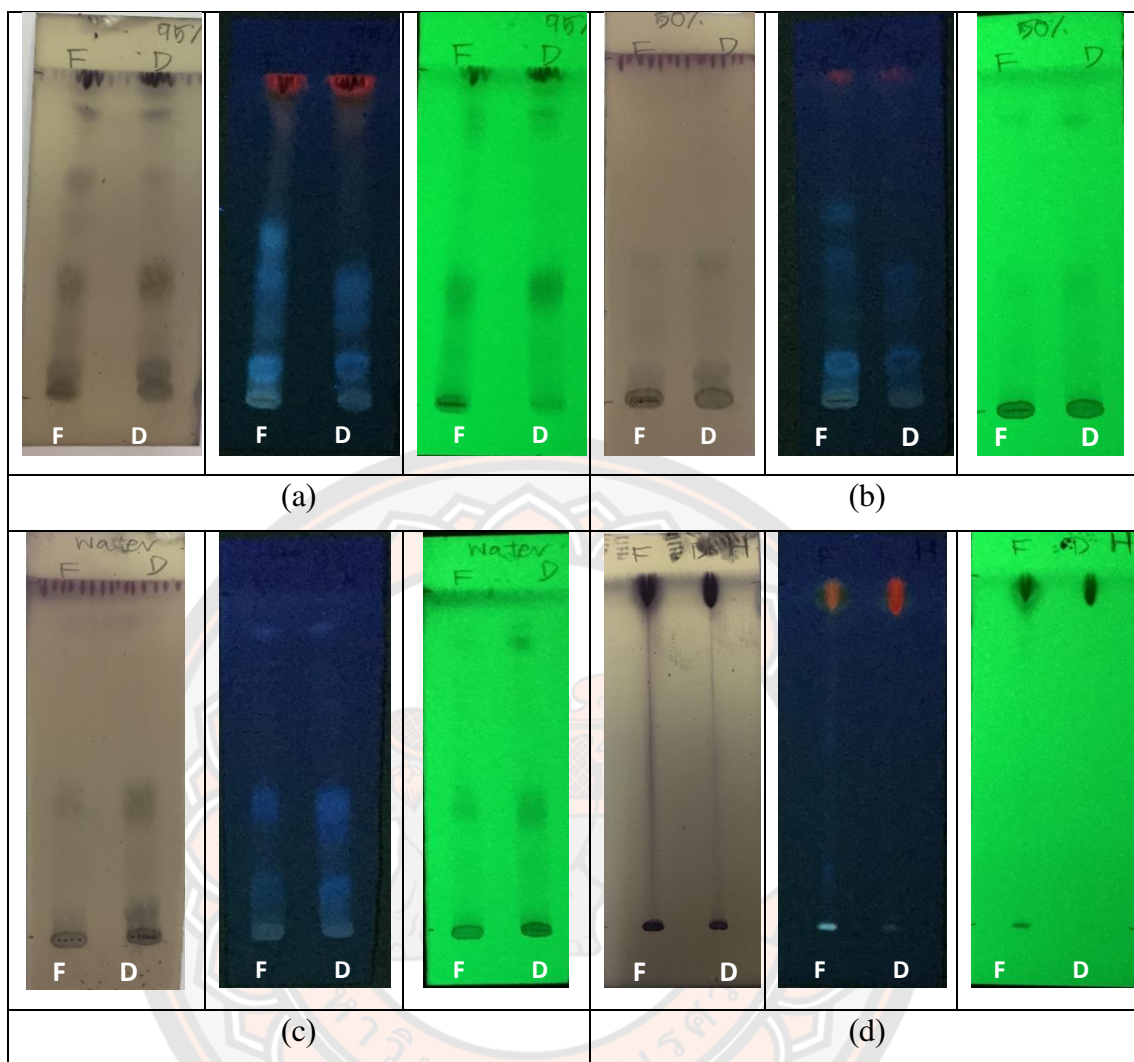


Figure 17 TLC fingerprint of AE extracts comparing among different solvents, fresh and dried leaves; (a) AE extracted by 95% ethanol, (b) AE extracted by 50% ethanol, (c) AE extracted by boiled water, (d) AE extracted by hexane, F= fresh leaves, D= dried leaves

The TLC fingerprint of the extracts revealed that different polarities of solvents could extract the chemical compounds from AE leaves differently. Dried and fresh leaves showed a quite similar fingerprint pattern. The extract using the polar solvent showed similar spots but with different intensities. Only the hexane extract of both the dried and fresh leaves showed no quenching or coloring spot when sprayed with vanillin solution.

3. VB determination by HPLC

One of the bioactive compounds in the AE extract was VB which demonstrates interesting biological activities associated with causes and mechanisms of hair loss. The quantity of VB in the AE extract was determined using the HPLC method. The chromatographic conditions included a C18 Luna Phenomenex column, 250 mm length \times 4.6 mm with 5 μ m particle size. The mobile phase was an isocratic solution composed of the phosphoric buffer: acetonitrile (77:23, v/v). The flow rate at 1.5 mLmin⁻¹. The detection is UV adjusted wavelength at 332 nm.

3.1 HPLC method validation

The HPLC method and condition were validated in terms of linearity, the limit of quantitation (LOQ), the limit of determination (LOD), accuracy, and precision. All validation parameters are discussed below.

3.2 Precision

The precision of the assay was measured as the percentage coefficient of variation over the concentration range of 50 – 1,000 μ g/mL. The result was represented as the percentage of recovery of VB and percentage relative standard deviation (%RSD). The amount of VB from the three replicates of each extract level was analyzed. The precision (inter and intra-day) is shown in Table 5. The values of %RSD showed less than 10%. It indicated the high precision of this method.

Table 5 Repeatability and intermediate precision which composes the precision parameter of the analytical method proposed

AE extract (μ g/mL)	Concentration (Mean \pm SD) (μ g/mL)		(%) RSD	
	Intra-day	Inter-day	Intra-day	Inter-day
1,000.00	104.85 \pm 3.26	102.83 \pm 2.37	3.11	2.31
500.00	53.02 \pm 1.85	51.00 \pm 1.76	3.50	3.44
50.00	4.44 \pm 0.26	4.71 \pm 0.24	5.84	5.05

Note: %RSD = 100% \times (SD/mean), RSD – Relative standard deviation

3.3 Accuracy

The accuracy of this method was indicated by the percentage recovery of VB that was calculated from the comparison of the measured concentration to the theoretical concentration. Percentage relative standard deviation was less than 5% (Table 6) and the lowest percentage relative standard deviation and highest percentage recovery implied the accuracy of this method.

Table 6 Accuracy at three concentration levels covering the range of 80% to 120% of the expected concentration

Spiked concentrations. ($\mu\text{g/mL}$)	VB Recovery		
	Measured conc. (Mean \pm SD) ($\mu\text{g/mL}$)	(%) RSD	%Recovery
20	20.12	1.70	100.61
25	25.85	1.03	103.41
30	31.04	0.22	103.46
50	52.44	2.11	104.87

Note: %RSD = $100\% \times (\text{SD}/\text{mean})$, RSD – Relative standard deviation

3.4 Linearity

Linearity was established by least squares regression analysis of the calibration curve. The calibration curve for the assay method was obtained over the calibration range from 3.9 – 125 $\mu\text{g/mL}$. The correlation coefficient (R^2) was 1. These results show that an excellent correlation existed between the peak area and concentration of the VB. The regression equation is;

$$y = 23816x + 4855$$

The linear calibration plotted for the VB obtained from the three sets of concentrations each cover the concentration range from 3.9 -125 $\mu\text{g/mL}$. The correlation coefficients (r) obtained were greater than 0.990. The regression equations for the three sets were as follows;

$$y = 22120x + 23153 \quad , r^2 = 0.9995$$

$$y = 23830x + 11623 \quad , r^2 = 1$$

$$y = 23791x + 3238.1 \quad , r^2 = 1$$

The results showed the specified acceptance criteria for the assay procedure (r is not less than 0.999). The standard curve of VB is shown in Figure 18.

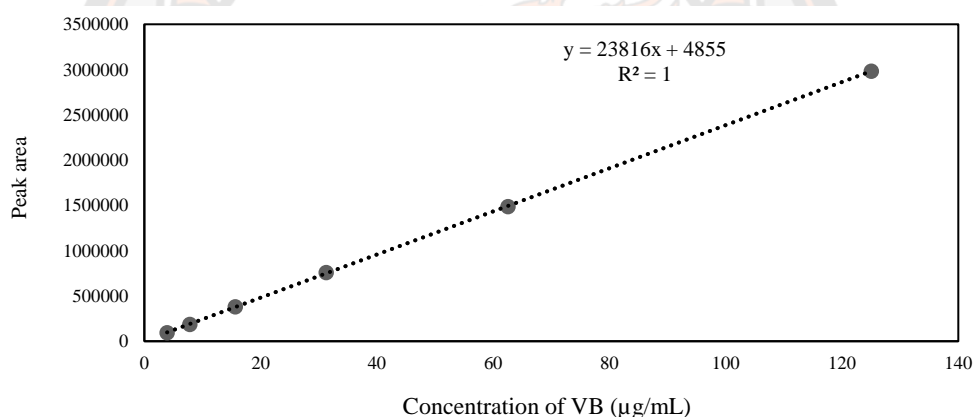


Figure 18 Calibration curve of VB standard

Evaluation of the method indicated that the method was precise with relative standard deviations (%RSD) of intra-day and inter-day of less than 5.84% and 5.05%, while accuracy was achieved by percentage recovery, ranging from 90% to 110%. These statistics indicated that the HPLC method was accurate and reliable for the determination of the contents of VB in AE extract. Chromatograms of VB in AE extract are shown in Figure 18 and VB content in each AE extract is shown in Table 7.

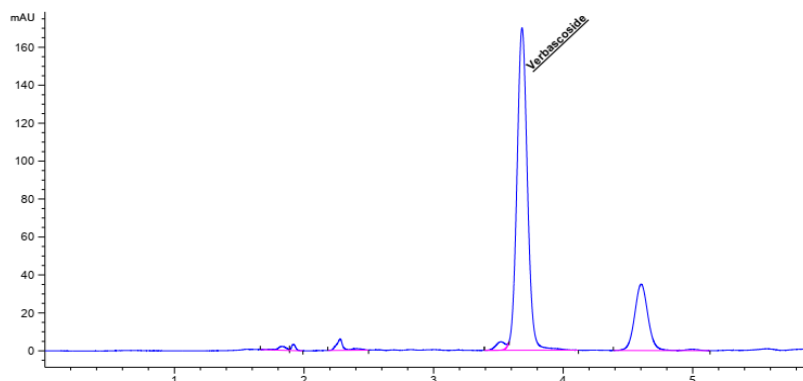


Figure 19 Chromatogram of VB in AE extract 1 mg/mL

Table 7 Amount of VB in each AE extract measured by HPLC method

AE extracts	VB (% \pm SD, w/w)
95% EtOH extract from fresh leaves	3.42 \pm 0.10
50% EtOH extract from fresh leaves	1.48 \pm 0.07
Water extract from fresh leaves	1.49 \pm 0.03
Hexane extract from fresh leaves	-
95% EtOH extract from dried leaves	9.58 \pm 0.65
50% EtOH extract from dried leaves	2.03 \pm 0.04
Water extract from dried leaves	3.10 \pm 0.10
Hexane extract from dried leaves	-

The HPLC analysis showed different amounts of VB in each extract. The highest content of VB was identified in extract performed using 95% ethanol of dried AE leaves (9.58 \pm 0.65%) while no VB was detected in the hexane extract from either the fresh or the dried leaves.

The HPLC results showed that each extract of dried AE leaves had a VB content higher than from the fresh leaves. Four extracts from the dried AE leaves were chosen to be screened for their bioactivities.

4. Bioactivities of AE extract

The bioactivities of the AE extracts and VB were examined and their results were as follows;

4.1 Antioxidant activity of AE extract

The AE extracts were evaluated for their antioxidant activity by using DPPH and ABTS assays, IC₅₀ of percentage inhibition was reported. Trolox was a positive control.

Table 8 Antioxidant activity of each extract from AE and VB

Samples	IC ₅₀ (µg/mL ± SD)	
	DPPH	ABTS
AE extracted by 95% ethanol	19.40 ± 4.11	1.00 ± 0.77
AE extracted by 50% ethanol	25.57 ± 6.41	0.61 ± 0.04
AE extracted by decoction method	3.33 ± 2.10	0.92 ± 0.01
AE extracted by hexane	ND	1,220.50 ± 62.93
VB	45.70 ± 1.57	48.85 ± 0.35
Trolox (Positive control)	1.17 ± 0.85	8.28 ± 0.26

Almost of the AE extracts exhibited high antioxidant activity. However, the antioxidant value of each extract by using the DPPH technique in hexane extract was undetectable. Water extract of AE, extracted by the decoction method, showed the strongest antioxidant activity. For both the VB and the four dried AE extracts, the antioxidant activity determined by DPPH showed similar results when determined by the ABTS assays.

4.2 5α-reductase Inhibition

One hundred micrograms per milliliter of each AE extract was tested for its 5α-reductase inhibitory activity. Finasteride was the positive control. The inhibitory activities of each AE extract are illustrated in Table 9. Comparing the inhibition activity of each extract showed that the AE hexane extract from the fresh leaves, showed the highest inhibition (75.89% ± 3.82), followed by the AE extract from the fresh leaves, extracted with 50%EtOH (42.23 ± 2.90). The AE extract from

the fresh leaves, extracted with 95%EtOH (40.26 ± 0.67) had the third highest inhibition, with the water extract having the lowest (40.82 ± 2.33).

For the dried leaves, the AE extracted by 95%EtOH, showed the highest inhibition (38.26 ± 4.90) followed by the AE extract in hexane ($36.92 \% \pm 2.41$), 50% ethanol ($13.72\% \pm 4.88$), and water ($6.75\% \pm 4.20$). However, no inhibitory activity of VB was observed.

It was also determined that, while the hexane extract of the fresh AE leaves expressed the highest 5α -reductase inhibitory activity, the other biological activities were not present. Given this, the dried leaves were selected for further study of their biological activities. To determine the percentage inhibition of 5α -reductase, the dried AE leaf extracts using 95% ethanol was chosen for further experiment and the IC_{50} of 5α -reductase inhibitory activity was determined to be $60.45\% \pm 2.45 \mu\text{g/mL}$ (Figure 20).

Table 9 5α -reductase inhibitory activity of AE extracts performed by different solvents

Samples	5α -reductase inhibition (% \pm SD)
Fresh leaves of AE in 95%EtOH	40.26 ± 0.67
Fresh leaves of AE in 50%EtOH	42.23 ± 2.90
Fresh leaves of AE in water	40.82 ± 2.33
Fresh leaves of AE in hexane	75.89 ± 3.82
Dried leaves of AE in 95%EtOH	38.26 ± 4.90
Dried leaves of AE in 50%EtOH	13.72 ± 4.88
Dried leaves of AE in water	6.75 ± 4.20
Dried leaves of AE in hexane	36.92 ± 2.41
VB	None
Finasteride	98.58 ± 1.96

Note: all AE extract was $100 \mu\text{g/mL}$, finasteride was $1.5 \mu\text{g/mL}$

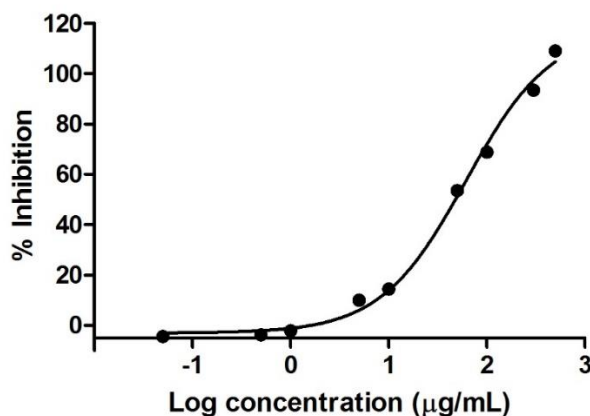


Figure 20 Dose respond curve of ethanolic extract of AE for 5 α -reductase inhibition activity

4.3 Cytotoxic effect of AE extract and VB on DPCs

DPCs were treated by AE extracts and VB with various concentrations. The results are shown in Figure 21 presented the non-cytotoxic effect of both AE extract and VB on DPCs. Moreover, concentrations of AE 62.50 – 500.00 $\mu\text{g/mL}$ and VB at 31.25 – 500.00 $\mu\text{g/mL}$ showed a significant increase in the cell viability more than the control. That indicated the proliferative effect of both AE extract and VB on DPC.

AE extract in 95% ethanol of dried leaves was the good candidate part for further study due to the highest content of VB and presented the proliferative effect on DPC which was selected for investigating further bioactivities.

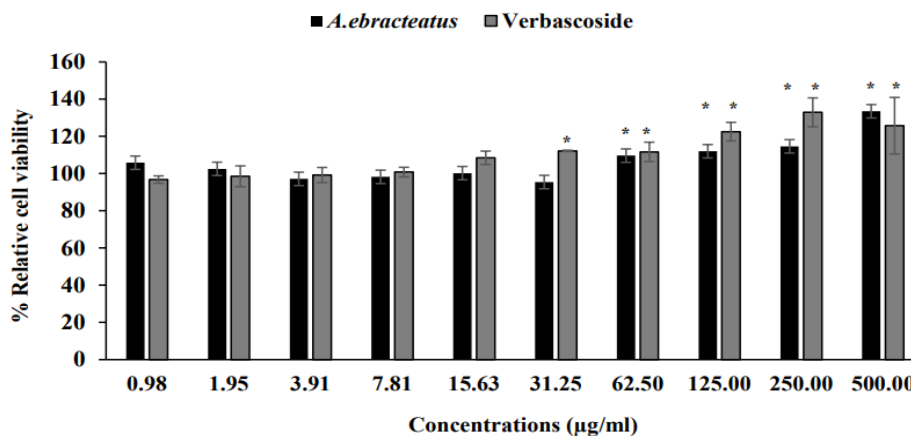


Figure 21 Relative cell viability of dermal papilla cells after being treated by AE extract and VB for 24 hours *significantly different versus the control cell ($p < 0.05$, t-test)

4.4 Cell cycle analysis

DPCs were treated with ethanolic AE extract or VB with a concentration between 31.25 to 500 µg/mL for 24 hours. Then we analyzed the DPCs at different phases in the cell cycle by propidium iodide staining. AE extract showed different effects on the DPC cycle depending on concentrations (Figure 22a). The G1 phase of the DPCs was stimulated by AE 500 µg/mL more than that control cells, however, the G2/M phase of the cell was significantly decreased when compared to the control cell. AE extract at 250 µg/mL and 125 µg/mL concentrations had a significantly increased number of cells in the G2/M phase compared to the control cells.

In the case of VB, VB 500 µg/mL significantly increased the number of cells in the G1 phase (Figure 22b) but decreased the number of cells in the G2/M phase compared to control cells. VB 62.50 µg/mL showed crucial effects on every phase of the G2/M and G1 phases of the DPC cycle. The number of cells in the G2/M phase was significantly increased, while the number of cells in the G1 phase decreased after being treated by VB 62.50 µg/mL. In addition, treating the cells with VB 125 µg/mL resulted in an increased number of cells in the G2/M phase compared

to the control cells. Almost of treatments had effect on the number of cells in the S phase of the cell cycle but not significantly different.

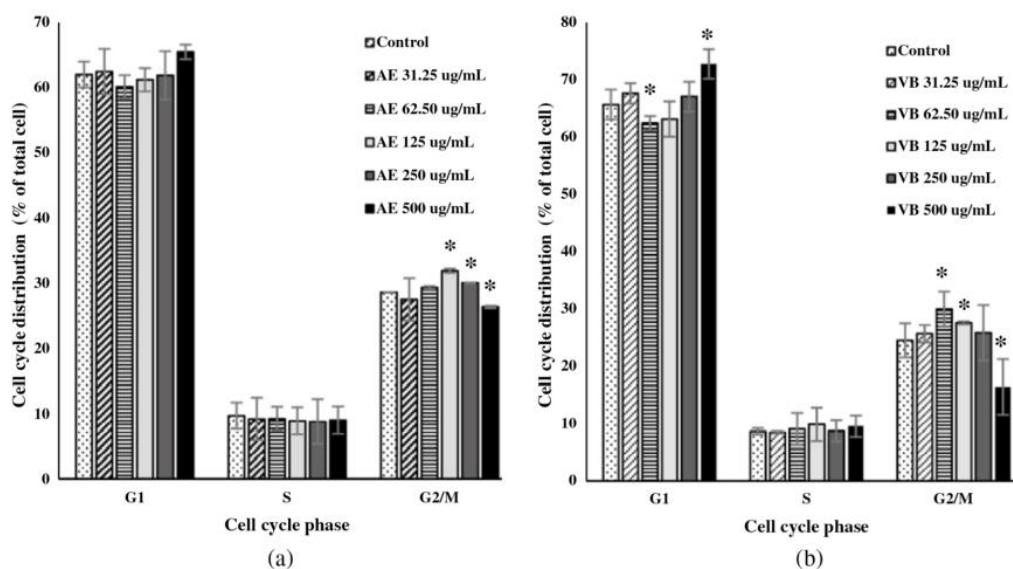


Figure 22 The effects of AE extract (a), VB (b) on the dermal papilla cell cycle
*significantly different versus the control cell ($p < 0.05$, t-test)

4.5 Anti-androgenic activity testing

DPCs were incubated with 200 μM testosterone solution for 4 days. Cell viability was then determined by using an MTT assay. About the cell cycle analysis, we treated DPCs with AE 250 $\mu\text{g/mL}$ or VB 62.50 $\mu\text{g/mL}$ and combined them with 200 μM testosterone. Our study results are shown in Figure 23. Two hundred micromolar concentrations of testosterone caused a decrease of DPC viability when the cells were treated for 4 days. Cell viability improved close to 100% when DPCs were combined with AE 250 $\mu\text{g/mL}$. VB 62.50 $\mu\text{g/mL}$ was also effective in improving cell viability, showing results similar to AE 250 $\mu\text{g/mL}$ or 75 nM finasteride.

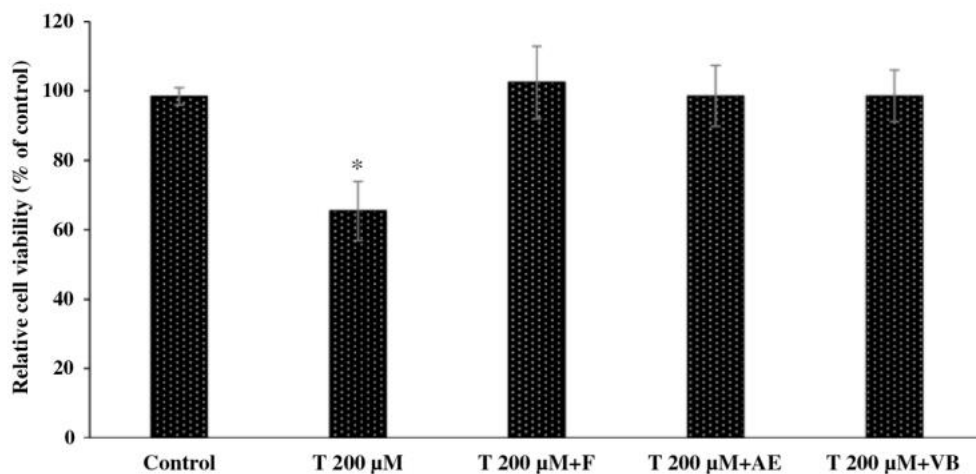


Figure 23 Relative cell viability of dermal papilla cells when being treated with testosterone 200 μ M (T 200 μ M), testosterone 200 μ M plus AE extract 250 μ g/ml (T 200 μ M +AE), testosterone 200 μ M plus finasteride 75 nM (T 200 μ M + F) and testosterone 200 μ M plus VB 62.50 μ g/mL (T 200 μ M + VB); *significantly different versus the control cell ($p < 0.05$, t-test)

4.6 Cytotoxicity effect of AE extract and VB on RAW 264.7 cells

The cytotoxicity of various concentrations of AE extract and VB on Raw 264.7 cells was determined using an MTT assay. The cytotoxicity results are shown in Figure 24. Before performing the bioactivity assay, a range of safety concentrations for Raw 264.7 cells was identified. Our study found that both AE extract and VB were safe at concentrations less than 250 μ g/mL. Thus, these concentrations were chosen to further anti-inflammatory activity study with macrophage cells.

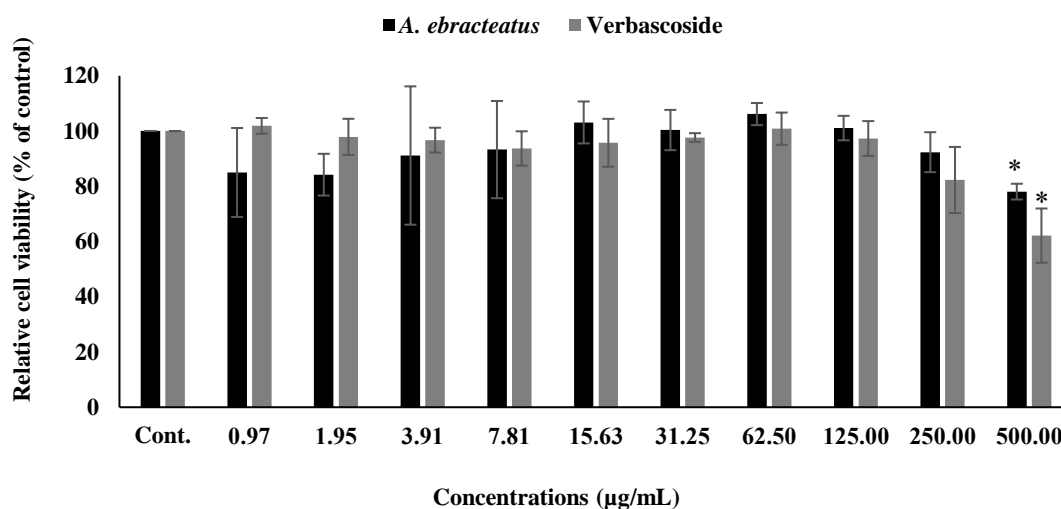


Figure 24 Relative cell viability of RAW 264.7 cells treated with different concentrations of AE extract or VB for 24 hours; *significantly different versus the control cell ($p < 0.05$, t-test)

4.7 Anti-inflammatory activity of AE extract and VB in LPS treated RAW 264.7 cells

The RAW 264.7 cells were treated by LPS to induce the release of IL-1 β , NO, and TNF- α . Then IL-1 β , NO, and TNF- α were measured using the ELISA technique. AE extract 250 µg/mL or VB 62.50 - 125 µg/mL was selected for treating RAW 264.7 cells induced by LPS. Hydrocortisone was a positive control. The Amount of IL-1 β released from macrophage cells and the inhibition of the treatments are shown in Figure 25 for IL-1 β inhibition, Figure 26 for Nitric oxide inhibition and Figure 27 for TNF- α inhibition. LPS treated RAW 264.7 cells successfully synthesized pro-inflammatory cytokines such as IL-1 β , NO, and TNF- α as shown in Figures 25-27.

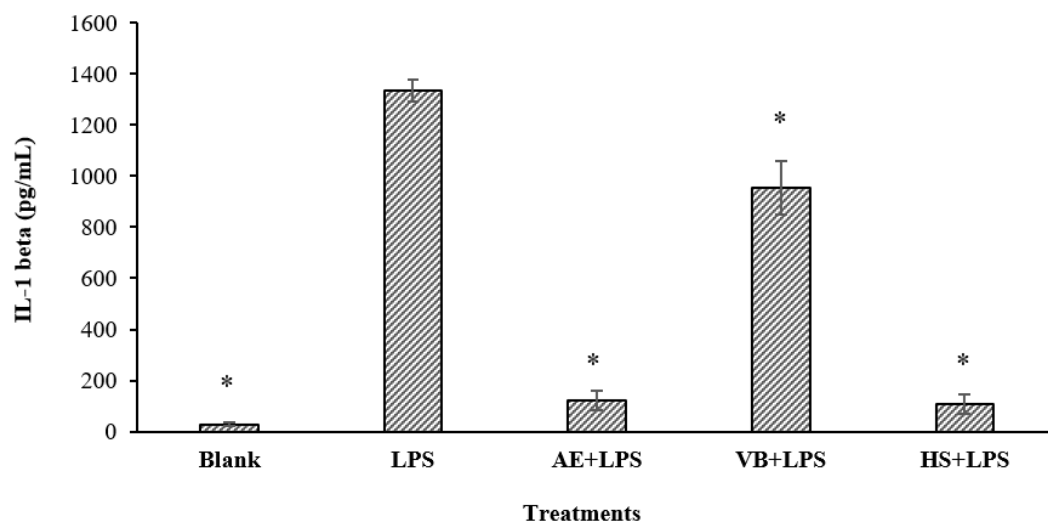


Figure 25 Amount of IL-1 β from RAW 264.7 cells treated by lipopolysaccharide 5 μ g/mL (LPS), AE extract 250 μ g/mL plus LPS 5 μ g/mL (AE+LPS), Hydrocortisone 5 μ g/mL plus LPS 5 μ g/mL (HS+LPS) and VB 125 μ g/mL plus LPS 5 μ g/mL (VB+LPS); *significantly different versus the control cell (LPS) at ($p < 0.05$, t-test)

The data in Figure 25 shows the successful downregulation of the release of IL-1 β from RAW 264.7 cells treated by LPS with AE 250 μ g/mL. Similarly, there was also inhibition of the release of IL-1 β from RAW 264.7 cells treated by LPS with VB 125 μ g/mL. The IL-1 β inhibition activity of AE extract was stronger than that of VB.

RAW 264.7 cells treated by LPS also produced nitric oxide, which was represented by sodium nitrite content. The nitric oxide inhibition activity is illustrated in Figure 26. N(G)-monomethyl-L-arginine (L-NMMA) was used as a positive control. In Figure 26, the results showed that LPS effectively induced the synthesis of sodium nitrite from RAW 264.7 cells. In contrast, L-NMMA inhibited the synthesis of NO. Both AE extracts 250 μ g/mL and VB 125 μ g/mL also showed significant, potent inhibition of nitric oxide secretion compared to control cells.

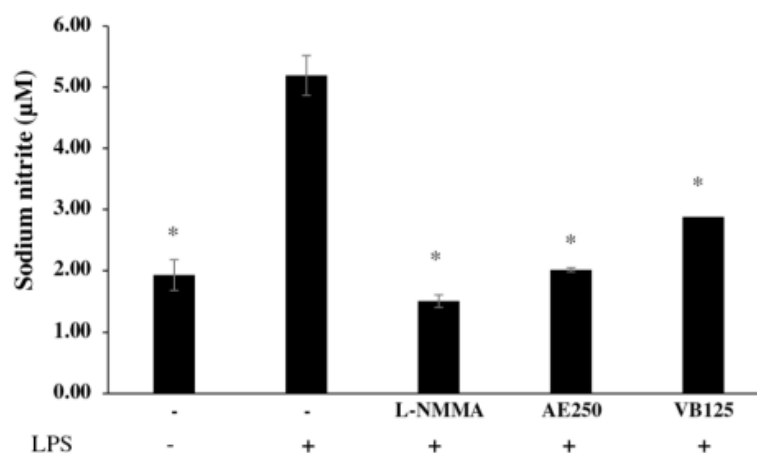


Figure 26 Amount of sodium nitrite from RAW 264.7 cells treated by lipopolysaccharide 1 µg/mL (LPS), AE extract 250 µg/mL plus LPS (AE+LPS), N(G)-monomethyl-L-arginine 10 µg/mL (L-NMMA) plus LPS (L-NMMA+LPS), and VB 125 µg/mL plus LPS (VB+LPS); *significantly different versus the control cell (LPS) ($p < 0.05$, t-test)

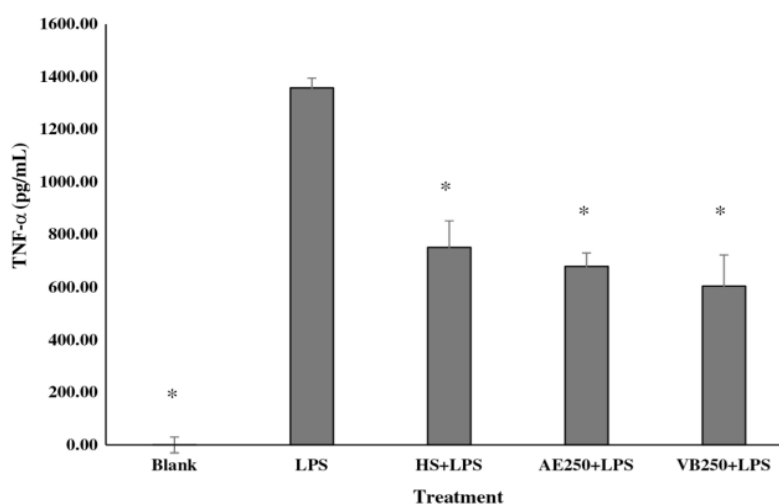


Figure 27 Amount of tumor necrosis factor (TNF-α) from RAW 264.7 cells treated with lipopolysaccharide 1 µg/mL (LPS), hydrocortisone 10 µg/mL+LPS 1 µg/mL (HS+LPS), AE extract 250 µg/mL plus LPS 1 µg/mL (AE250+LPS), and VB 250 µg/mL plus 1 µg/mL LPS (VB250+LPS). *significantly different versus the control cell (LPS) ($p < 0.05$, t-test)

The Tumor Necrosis Factor (TNF- α) released from LPS treated macrophage cells was strongly inhibited by hydrocortisone (Figure 27). AE extract and VB also significantly suppressed the release of TNF- α from murine macrophage cells.

4.8 Anti-inflammatory activity of AE extract and VB in UVB irradiated the DPCs

The DPCs released IL-1 α and IL-6 in the supernatant after being irradiated with 20 J/cm² UVA for inducing the release of IL-1 α or 100 mJ/cm² UVB for stimulating the release of IL-6. The cells were then treated with AE extract 250 μ g/mL or VB 125 μ g/mL. We measured the IL-6 and IL-1 α levels released by the cells into the supernatant using cytokine immunoassay (ELISA technique) according to the manufacturer's protocol.

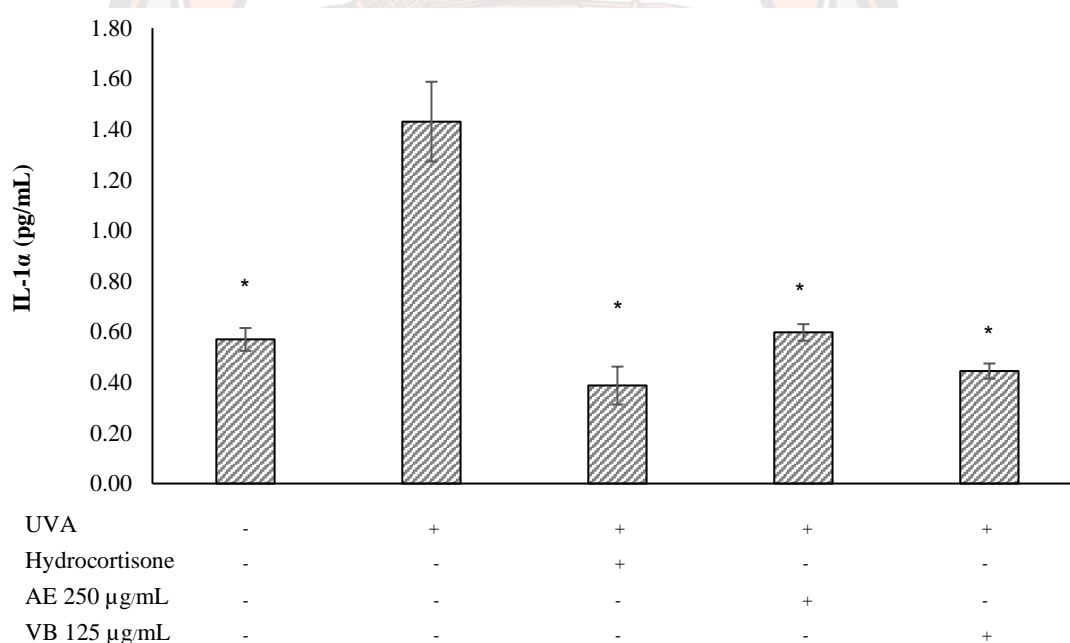


Figure 28 The release of IL-1 α from dermal papilla cells following UVA 20 mJ/cm² irradiation and after treatment with hydrocortisone 5 μ g/mL, AE extract 250 μ g/mL and VB 125 μ g/mL; *significantly different versus the irradiated cell ($p < 0.05$, t-test)

Hydrocortisone 5 $\mu\text{g/mL}$ was a positive control. The amounts of IL-1 α found in the cells are presented in Figure 28, and IL-6 release from the cells is shown in Figure 29. Figure 28 shows that AE extracts 250 $\mu\text{g/mL}$ or VB 125 $\mu\text{g/mL}$ decreased the amount of IL-1 α released from irradiated the DPCs. In Figure 29, we display that UVB 100 mJ/cm^2 induced a release of IL-6 from the DPCs. Hydrocortisone at 5 $\mu\text{g/mL}$ concentration powerfully suppressed the release of that cytokine. Similar to inhibition activity of IL-1 α , AE extracts 250 $\mu\text{g/mL}$ and VB 125 $\mu\text{g/mL}$ significantly suppressed the release of IL-6 as well.

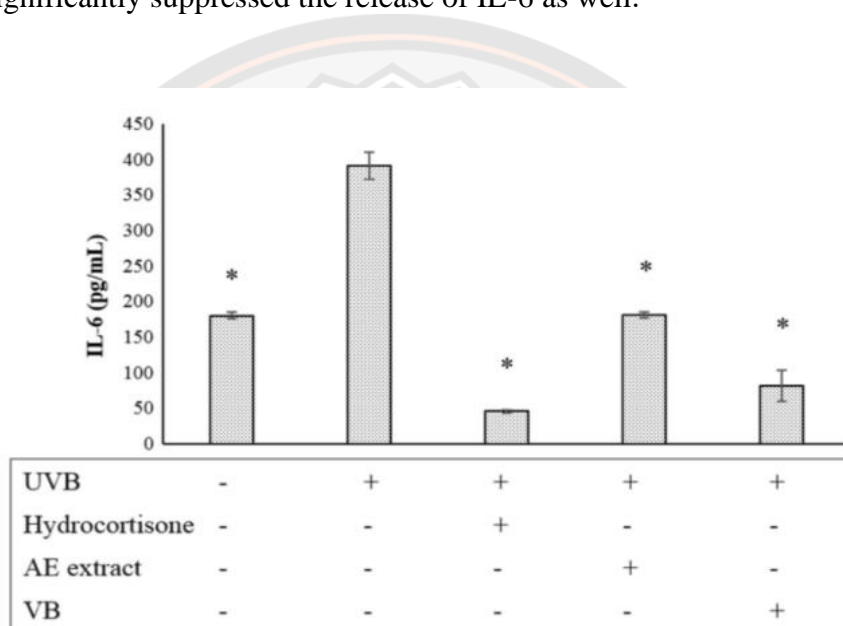


Figure 29 The release of IL-6 from dermal papilla cells following UVB 100 mJ/cm^2 irradiation and irradiated cell after treatment with hydrocortisone 5 $\mu\text{g/mL}$, AE extract 250 $\mu\text{g/mL}$ and VB 125 $\mu\text{g/mL}$; *significantly different versus the irradiated cell ($p < 0.05$, t-test)

5. Stability study of AE extract

VB in AE extract is a glycoside compound that is sensitive to the environmental factors affecting its stability. Semisolid form and solution form of AE extract performed by dissolving in PBS 7.4 were stored at 50°C for 3 months. The percentage remaining of the VB in the extracts stored at accelerated conditions for 3 months is shown in Table 10. These results indicate that the rate of

decomposition of VB was faster at elevated temperatures. The loss of the biomarker was more than 60% in the aqueous solution and more than 27% in the semisolid form of AE extract when stored at 50°C/75 %RH.

Table 10 The stability of VB in AE extract stored at 50°C

Storage time	% of remaining VB in solution form of AE extract	% of remaining VB in semi-solid form of AE extract
1 month	57.98±1.88	93.03±1.52
2 months	35.49±2.10	73.14±0.04
3 months	32.70±0.75	73.06±0.72

Table 10 shows that VB in semisolid form of AE extract was degraded by about 30% when stored at 50°C for 3 months. The results were found to be following the study mentioning the rise in decomposition with the increase in temperature. Our results are supported by findings of another study that the rate of a chemical reaction increases by a factor between 2-3 times for each 10°C rise in temperature.

The order of reaction of the biomarker in the extract was determined at each temperature and the curve with the best linearity was taken as order of the reaction. By comparing different curves, it was found that the degradation of VB followed the first-order reaction. The degradation profile of VB in semisolid form of AE extract was plotted logarithm concentration against time for finding reaction rate constant (K) that was estimated from the linear slope (Figure 30) while the degradation profile of VB in solution form of AE extract was plotted logarithm concentration against time for finding reaction rate constant (K) that was estimated from the linear slope (Figure 31)

Shelf-life was calculated using Arrhenius's equation that was a plot between the natural logarithm rate reaction constant versus the inverse of the absolute temperature of VB in semisolid form of AE extract at various temperatures (Figure 32) while the plot of natural logarithm rate reaction constant versus the inverse of the absolute temperature of VB in solution form of AE extract at various temperatures is shown in Figure 33.

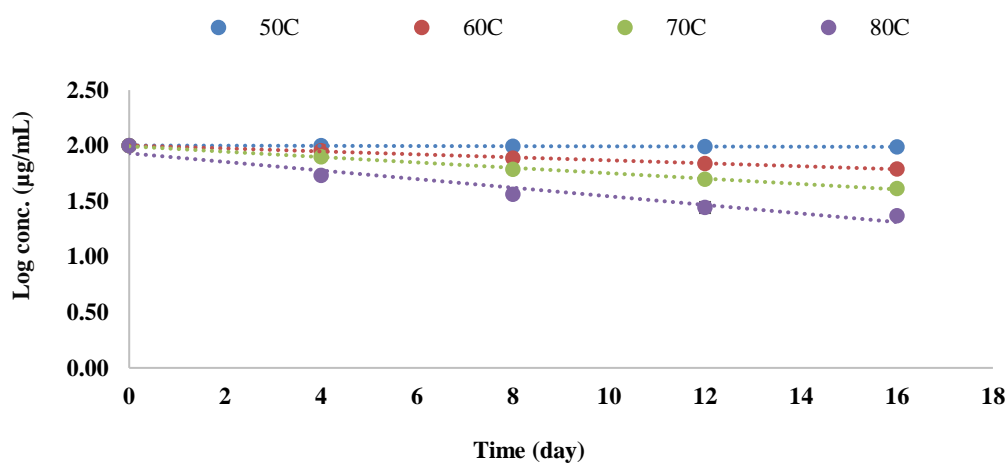


Figure 30 First-order plot between the logarithm of VB concentrations in the semisolid form of AE extract versus time at different temperatures

The % remaining of the marker versus time graphs showing the first-order reaction is given in Figure 30-31. These results indicated that the degradation of VB in both semi-solid forms of AE extract and AE extract solution was dependent on their initial concentration.

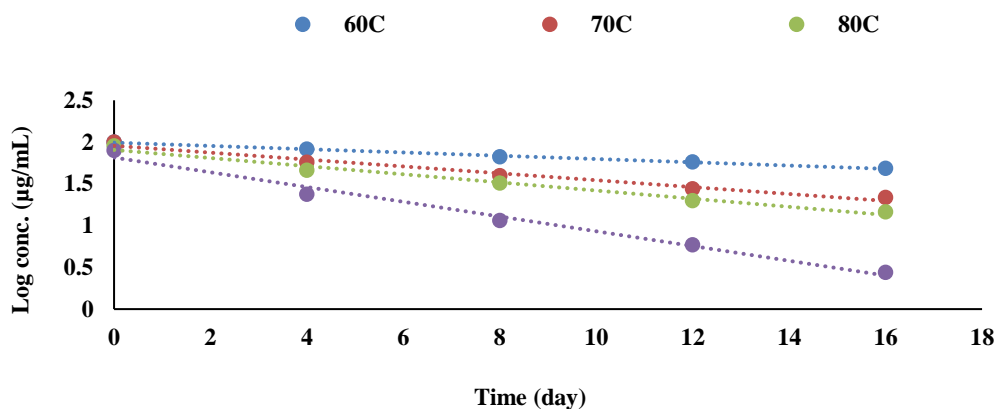


Figure 31 First-order plot between the logarithm of VB concentrations in solution form of AE extract versus time at different stored conditions

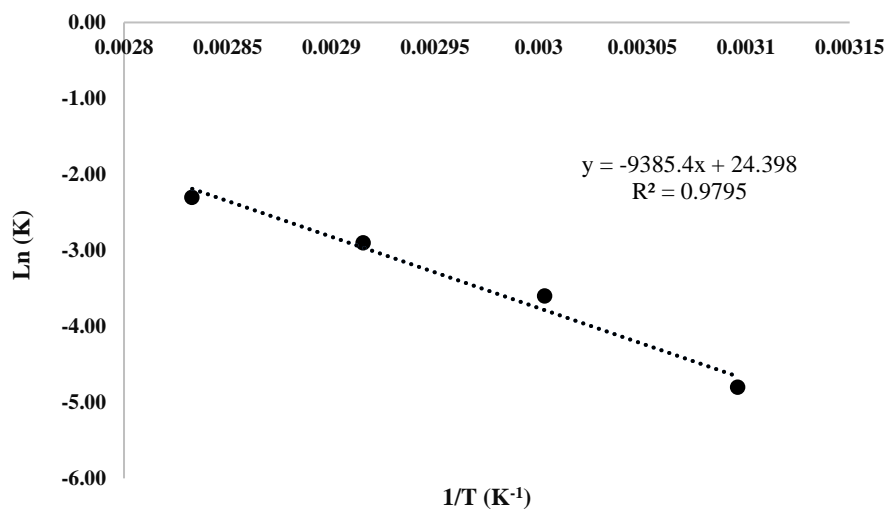


Figure 32 Plot of the natural log of rate constant versus the inverse of absolute temperature (Kelvin⁻¹) of VB in semisolid form of AE extract at various temperatures

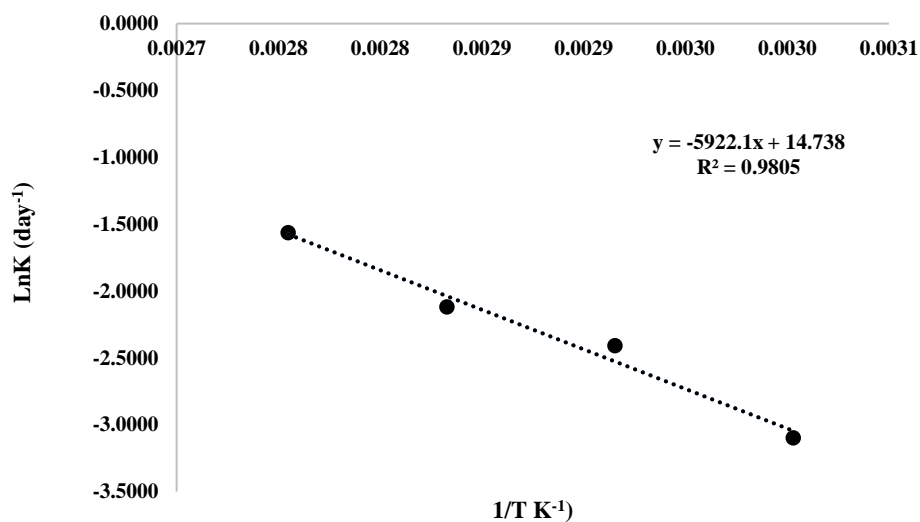


Figure 33 Plot of the natural log of rate constant versus the inverse of absolute temperature (Kelvin⁻¹) of VB in solution form of AE extract at various temperatures

From the detail in Figure 30-31, the reaction velocity or degradation rate constant (K) of VB was taken from the slope of the curves generated from the plot logarithm of the remaining percentage over time, and the rate constant of VB degradation at room temperature was determined by extrapolating the graph of (ln K) versus the inverse of absolute temperature ($1/T$ Kelvin⁻¹). The Arrhenius plots of VB are presented in Figures 32 and 33

The degradation rate constant (K) of each VB at different temperatures is shown in Table 11. The rate of reaction and activation energy more than doubled when increased by 10°C, demonstrating that the degradation reaction increases at elevated temperatures.

The activation energy (E_a), which is the energy required to move a molecule from the initial state to the transitional state or the fraction of molecules having sufficient energy at a given temperature and universal gas constant ($R = 8.314$ KJ mol⁻¹), of each of the marker, was determined from the slope of the straight line, whereas A was calculated from the intercept of the curve. The Arrhenius equation is given as follows:

$$K = A e^{-E_a / RT}$$

$$\ln K = \ln A - E_a / RT$$

Table 11 Effect of temperature on the activation energy (E_a), reaction rate constant (K) values of VB in aqueous solution pH7.4 and semisolid form AE extract

Temperature (°C)	K (day ⁻¹) x10 ⁻²		E _a (kJ/mol) x10 ⁻³	
	Solution form of AE extract	Semisolid form of AE extract	Solution form of AE extract	Semisolid form of AE extract
60	4.51	3.08	0.16	0.11
70	9.48	5.57	0.34	0.20
80	11.21	8.98	0.40	0.32
90	20.95	-	0.75	-

The reaction rate constant at 25°C can be estimated by a linear relationship between the natural logarithm of the rate reaction constant and inverse absolute temperature. Shelf-life (T_{90}) of VB at 25°C was then calculated by the equation as below;

$$T_{90} = 0.105/K$$

Table 12 The estimated shelf life (T_{90}) of VB in solution form and semisolid form of AE extract at 25°C

T_{90} at 25°C in solution form of AE extract (day)	T_{90} at 25°C in the semisolid form of AE extract (day)
12	75

The estimated T_{90} of VB in AE extract solution and semisolid form of AE extract at 25°C was calculated and the values presented in Table 12. The calculated shelf-life correlated with the stability study conducted at 50°C which indicated that VB in AE extract with semisolid form was more stable than that AE extract solution.

In addition, AE extract dissolved in PBS pH 7.4 was kept at 25°C for 3 months and then the remaining VB was measured to find the shelf life of VB. The remaining percentage of VB is shown in Table 13. The remaining percentage of VB was more than 90% from 1st week until the 5th week. The real-time shelf life of VB in solution is 35 days approximately while the estimated shelf life is 12 days. This indicates that the real-time shelf-life of VB in the AE solution was higher than that estimated shelf-life.

Table 13 Percentage of remaining VB in AE solution pH 7.4 at 25°C (n=3)

Storage time (weeks)	% of remaining VB
0	100.00±0.12
1	100.88±0.46
2	99.60±1.48
3	91.38±0.37
4	93.06±0.26
5	91.46±0.30
6	86.55±0.32
7	89.46±0.13
8	86.59±0.13
12	79.19±1.44

In addition to temperature, the stability of VB in AE extract was investigated in various pH values and then established its pH rate profile. Reaction rate constants of VB in various pH solutions were estimated by using a similar process according to Arrhenius's theory. The pH rate constant of each solution is shown in Table 14.

Table 14 The reaction rate constant of VB in various pH buffer solutions

pH	K (week ⁻¹) x10 ²
2.00	0.201
5.50	0.713
7.40	2.901
8.00	101.285
11.0	18.884

The natural logarithm of the rate of reaction constants against pH values was plotted and the pH rate profile of VB in AE extract dissolved in buffer solutions is shown in Figure 34. The results imply that VB is stable in acidic conditions. The degradation of VB increased with increased pH values. However, the degradation tended to decrease when the pH value was greater than 8.

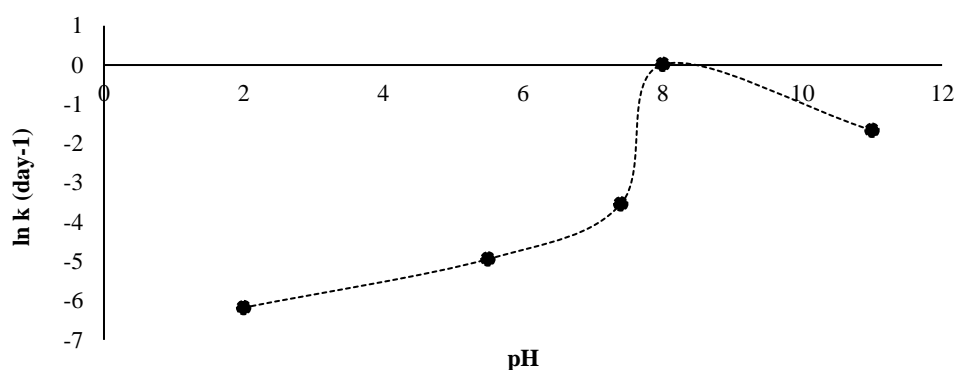


Figure 34 pH rate profile of VB in AE aqueous solution at 25°C (n=3)

6. Solid lipid nanoparticle (SLN) loaded AE extract preparation

Solid lipid nanoparticle-loaded AE extract was prepared using the hot melt homogenization technique. Our result showed that SLN loaded AE extract was successfully prepared with Compritol[®] used as a lipid carrier. The particles' characteristics and properties were different due to influencing factors during particle preparation. The amount of AE extract for particle loading and concentration of emulsifier affected particle properties. The details of the 14 formulas used for preparing SLN are shown in Table 15. Particle characteristics, including entrapment efficacy of SLN prepared according to 14 formulas, are shown in Table 16.

Table 15 The detail of each formula in particle preparation

Formula	Compritol (g)	Tween (g)	AE extract (mg)	Water (g)
F1	10.00	0.50	62.50	50.00
F2	10.00	0.33	62.50	50.00
F3	10.00	0.25	62.50	50.00
F4	10.00	0.13	62.50	50.00
F5	10.00	0.05	62.50	50.00
F6	10.00	0.25	7.81	50.00
F7	10.00	0.25	15.63	50.00
F8	10.00	0.25	31.25	50.00
F9	10.00	0.25	62.50	50.00
F10	10.00	0.25	125.00	50.00
F11	10.00	0.50	31.25	50.00
F12	10.00	0.50	62.50	50.00
F13	10.00	0.50	125.00	50.00
F14	10.00	0.50	250.00	50.00

Table 16 Characteristics and entrapment efficiency of SLN loaded AE extract

Formula	Particle size (μm)	Entrapment efficiency (% \pm S.D.)	Drug loading (%)	Zeta potential (mv)
F1	1.32	15.97 \pm 4.08	0.013	-23.86
F2	2.08	22.22 \pm 3.58	0.012	-38.49
F3	2.19	28.99 \pm 2.38	0.015	-34.60
F4	3.68	13.71 \pm 1.38	0.007	-31.14
F5	3.52	5.92 \pm 0.03	0.005	-44.21
F6	1.01	11.22 \pm 0.84	0.001	-30.31
F7	0.74	46.32 \pm 4.51	0.006	-46.33
F8	0.60	40.84 \pm 1.42	0.011	-23.10
F9	1.03	30.12 \pm 0.68	0.017	-29.37

Formula	Particle size (μm)	Entrapment efficiency (%\pmS.D.)	Drug loading (%)	Zeta potential (mv)
F10	1.55	17.60 \pm 1.59	0.020	-45.99
F11	1.24	4.21 \pm 2.01	0.001	-19.75
F12	1.32	19.13 \pm 1.16	0.011	-11.51
F13	0.95	10.23 \pm 4.10	0.011	-21.17
F14	0.73	15.21 \pm 3.25	0.034	-36.42

The result shown in Tables 15 and 16 indicate that SLN loaded AE extract exhibited a particle size between 0.60 – 3.00 μm approximately, demonstrating that loading of AE and emulsifier at various concentrations affects particle characteristics. Entrapment efficiency tends to decrease when the amount of AE loading is increased. Tween 80 is an emulsifier used for stabilized particle formation by enhancing entrapment efficiency. An increase in emulsifiers can change the solubility proportion of AE. Based on information regarding entrapment efficiency and percentage drug loading, F8 is appropriate for further development as an ingredient in topical formulations.

The morphology of the particles prepared by hot-melt homogenization were observed by scanning electron microscope. Lipid particles were a spherical shape with a smooth surface. Their morphology is shown in Figure 35.

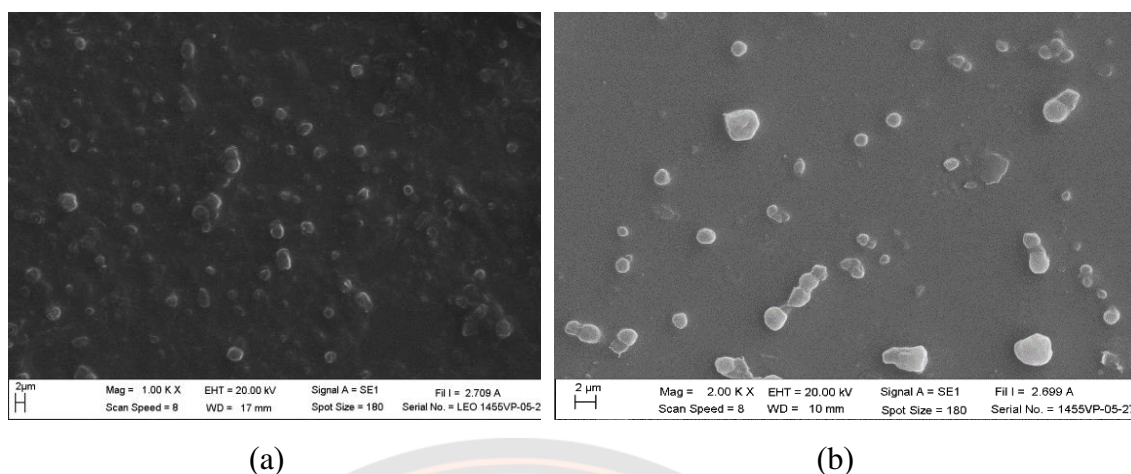


Figure 35 Particles loaded AE extract observed under the scanning electron microscope

Regarding the previous result, formula 8th was optimized by a varied amount of Tween80 and Span80 while Compritol was fixed at 1.50 grams because a high amount of wax had been shown to obstruct particle formation, evidenced by the presence of large particles. As well, a high amount of wax had been shown to cause drug expulsion due to the recrystallization process. To overcome this instability, SLNs were successfully prepared by using surfactant combination and their characteristics were then shown in Table 17.

Table 17 The effect surfactants combination on particles characteristics

Formulas	Parameters			Particle's characteristics			Entrapment efficiency (% ±SD)
	Compritol® ATO 888 (g)	Tween® 80 (%)	Span® 80 (%)	PS (nm) ± SD	PDI ± SD	ZP (mV) ± SD	
F8-1	1.50	0.50	0.25	2692.93±218.86	0.293±0.04	-31.42±2.06	13.51 ± 0.27
F8-2	1.50	0.50	0.50	2606.76±125.83	0.248±0.03	-31.09±0.61	18.24 ± 1.07
F8-3	1.50	0.50	1.00	2056.5±407.20	0.393±0.07	-39.07±3.33	15.87 ± 2.22
F8-4	1.50	0.50	2.00	1372.3±100.36	0.12±0.05	-37.48±0.90	21.73 ± 1.79
F8-5	1.50	0.50	3.00	628.06±159.36	0.21±0.04	-33.65±0.90	31.28 ± 0.98

Formulas	Parameters			Particle's characteristics			Entrapment efficiency (% ±SD)
	Compritol® ATO 888 (g)	Tween® 80 (%)	Span® 80 (%)	PS (nm) ± SD	PDI ± SD	ZP (mV) ± SD	
F8-6	1.50	0.50	4.00	1450.96±66.10	0.32±0.08	-32.77±0.86	24.99 ± 0.44
F8-7	1.50	0.50	5.00	1129.16±61.8	0.35±0.02	-34.46±1.12	25.37 ± 0.56

Note: PS= particle size, PDI= polydispersity index, ZP= zeta potential

A previous result showed that 0.50% of Tween 80 produced SLN with high entrapment efficiency. The concentration of Span 80 was varied, and the effect on the characteristics of the particle was observed. Span 80 affected entrapment efficiency with the increase of Span 80 causing an increase of entrapment efficiency, as illustrated in Table 17. However, entrapment efficiency was decreased when the concentration of Span80 reached 3%. The optimum condition for preparing particle-loaded AE extract was composed of Compritol® 888 15%, Tween 80 0.50%, and Span 80 3.00%. In addition, varying the homogenization times to 5, 10, and 15 minutes also affected particle size. The effect of homogenization time was evaluated based on particle size and the polydispersity index over time is shown in Figure 36.

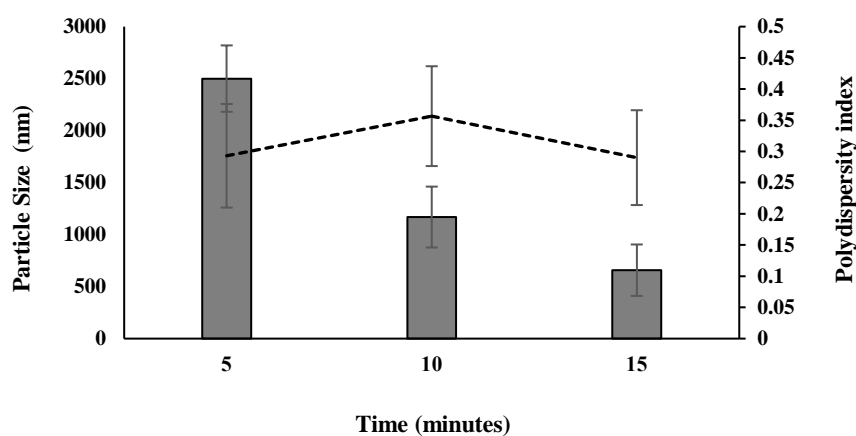


Figure 36 The effect of homogenization times on particle size and polydispersity index

Homogenization for 15 minutes effectively decreased particle size and approximately 600 nm particles with entrapment efficiency of $31.28\% \pm 0.98$ were obtained. SLNs were prepared in optimized conditions and then dried by using a freeze-drying machine. Two percent of maltodextrin was used as a cryoprotectant.

The SLN loaded AE extracts were then stored at various elevated temperatures to determine particle stability and shelf-life. The degradation behavior of the VB in the SLN was a first order reaction, the same as for the VB in AE extract and AE solution. The degradation profile is shown in Figure 37. The shelf-life of the VB in the SLN was calculated according to the Arrhenius plot presented in Figure 38; it was 154 days approximately.

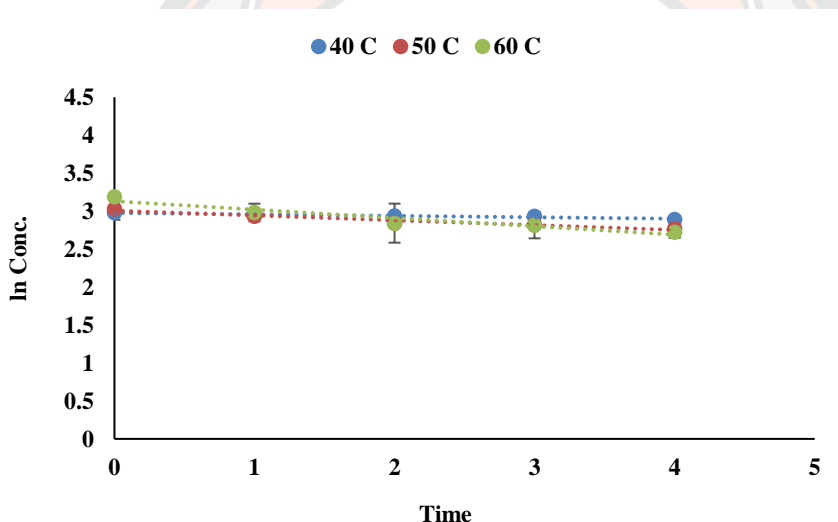


Figure 37 First-order plot between the natural logarithm of VB concentrations in SLN loaded AE extract versus time at different stored conditions

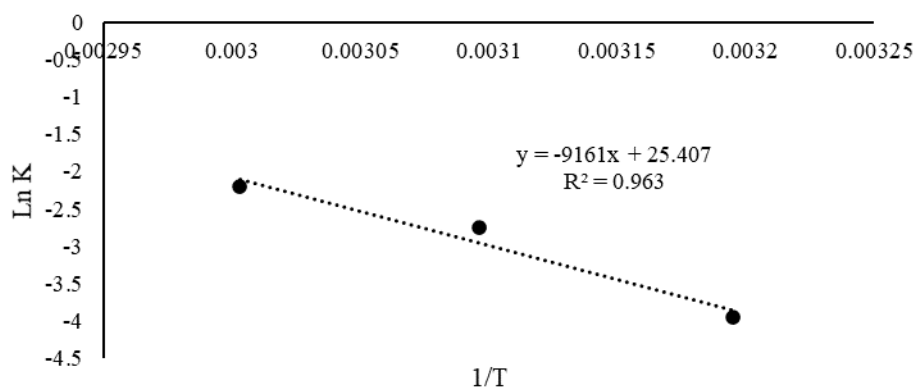


Figure 38 Plot of the natural log of rate constant versus the inverse of temperature (Kelvin⁻¹) of VB in SLN loaded AE extract at various temperatures, **ln. K** (natural log of rate constant); **1/T** (inverse of temperature)

The dried nanoparticle-loaded AE extract was incorporated into the formulation. The ingredients are shown in Table 18.

Table 18 Ingredients of hair serum containing solid lipid nanoparticle loaded AE extract

Ingredients	Amount (%)
Phosphate buffer (pH5.5)	92.85
Solid lipid nanoparticle loaded AE extract	5.00
phenoxyethanol	1.00
Hydroxypropyl methyl cellulose	0.75
Sodium EDTA	0.10
BHT	0.05

Hair serum-containing SLN loaded AE extract was a hydrogel that was quite stable due to HPMC being used as a suspending agent for preventing particle aggregation (Rostamkaleai, Akbari, Saeedi, Morteza-Semnani, & Nokhodchi, 2019). After formulating, hair serum containing SLN loaded AE extract was kept under 50°C

for 3 months and the amount of VB was compared to hair serum containing AE extract. The remaining VB in the tested samples was determined by HPLC assay. The remaining VB in the formulation at the end of each month, after being kept under stress conditions, is shown in Table 19.

Table 19 Remaining VB in hair serum containing AE extract or SLN loaded AE extract stored under various temperatures

Samples	Temperature (°C)	Percentage remaining of VB (% ± SD)			
		Baseline	1 st month	2 nd month	3 rd month
Serum with SLN loaded AE extract	4.00	100.00 ± 0.86	100.98 ± 1.67	101.45 ± 2.31	98.68 ± 2.34
Serum with SLN loaded AE extract	25.00	100.00 ± 1.93	100.45 ± 0.34	98.54 ± 1.32	95.44 ± 0.87
Serum with SLN loaded AE extract	40.00	100.00 ± 0.33	94.53 ± 0.10	95.23 ± 0.47	90.86 ± 1.89
Serum with SLN loaded AE extract	50.00	100.00 ± 2.34	74.34 ± 1.95	71.79 ± 2.30	72.44 ± 3.44
Serum with AE extract	50.00	101.21 ± 0.17	67.75 ± 0.68	52.11 ± 2.34	45.09 ± 1.47

The result indicated that temperature played a crucial role in VB degradation in both hair serum containing AE extract and SLN loaded AE extract. After 3 months, samples kept under 50°C showed the highest degradation however, SLN prevented VB degradation induced by temperature when compared to untrapped VB. VB in the hair serum that contained SLN loaded AE extract, remained at 72.44% ± 3.44 while VB in the hair serum that contained AE extract remained at 45.09% ± 1.47.

The VB in the serums containing SLN loaded AE extract that was kept at temperatures lower than 50°C for 3 months, showed high stability with more than 90% of the VB remaining. Although the hair serum containing SLN loaded AE extract showed good stability at temperatures between 4°C and 40°C, the stability of the VB at 50°C was also unsatisfactory.

The estimated shelf-life of the hair serum containing SLN loaded AE extract was examined by storing the formulation under various temperatures. The natural logarithm of VB concentrations was plotted against time for determining the rate reaction constant (Figure 39). The shelf-life was then predicted by plotting $\ln K$ against $1/T$. The plot and equation are shown in Figure 40.

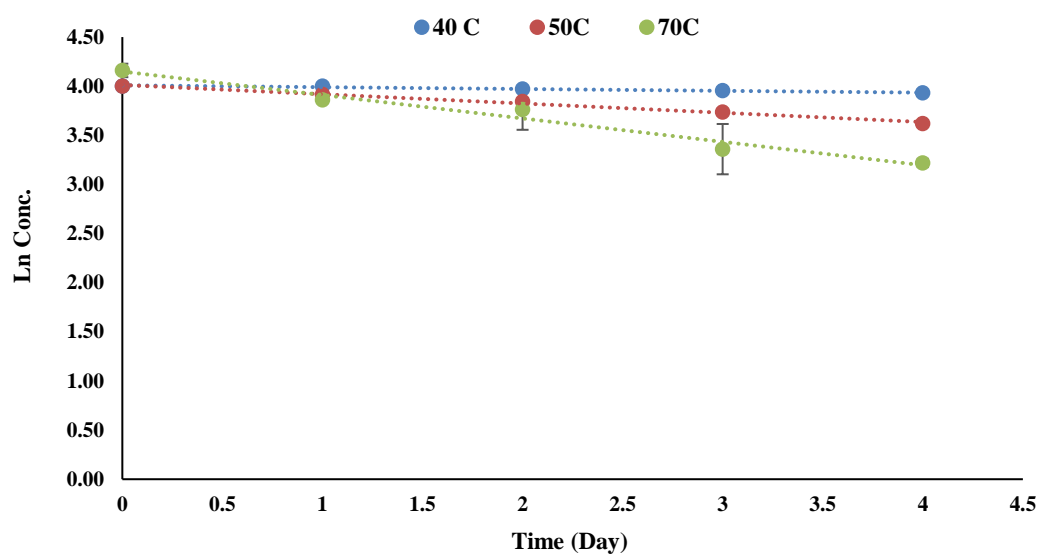


Figure 39 First-order plot between the natural logarithm of VB concentrations in hair serum containing SLN loaded AE extract versus time at different stored conditions

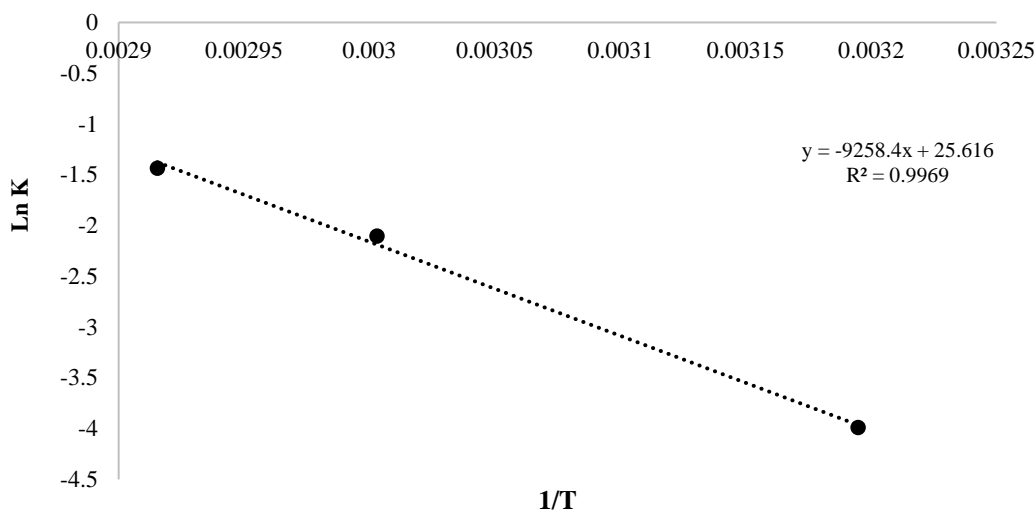


Figure 40 Plot of the natural log of rate constant versus the inverse of temperature (Kelvin⁻¹) of VB in hair serum containing SLN loaded AE extract at various temperatures, ln. K (natural log of rate constant); 1/T (inverse of temperature)

A shelf-life of 172 days was predicted at 25°C for VB in hair serum containing SLN loaded AE extract using an equation that is illustrated in Figure 40. These calculations indicate that the hair serum formulation could prevent the SLN loaded AE extract from degradation because the formulation contained ingredients such as antioxidant and chelating agents that prevented chemical reactions.

7. Particle release profile and skin permeation study

SLN loaded AE extract was dispersed into buffer solutions pH 5.5 or 7.4 and the amount of VB released from the particles was measured at the designed time. The amount of VB released at each pH level was plotted over time, as shown in Figure 41.

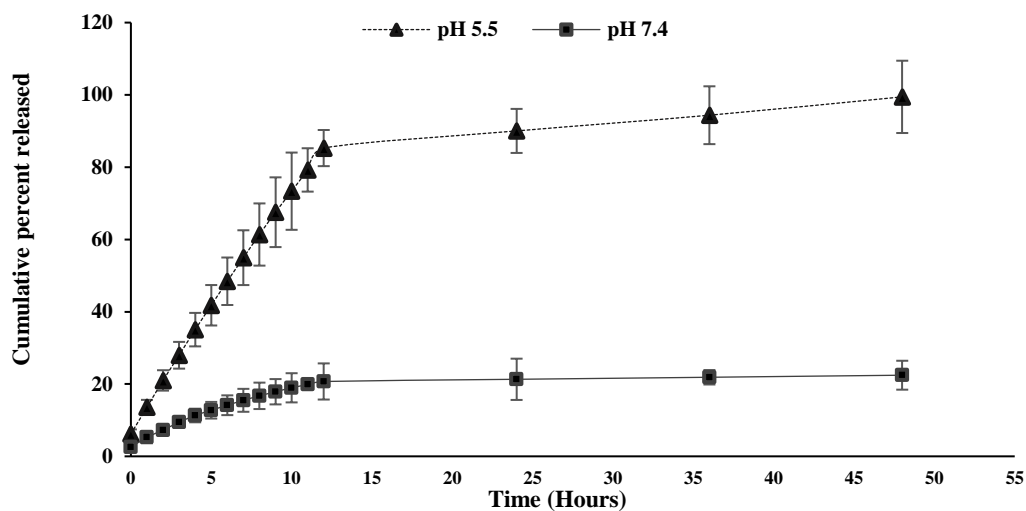


Figure 41 Release profiles of VB permeated from SLN to different pH buffers

The release profile indicated that VB permeated through the lipid wax within 10 - 12 hours and trended to a plateau from the 12th hour. VB showed a higher release in an acidic solution than in an alkaline solution. Remarkably, almost all VB from the particles was quantified in an acidic solution while 20% approximately of the VB could be determined in an alkaline solution. VB presented zero order release profile, which describe systems where the VB release rate is constant over a period of time and independent on the initial concentration of VB, in release medium at pH 5.5 while Korsmeyer peppas model, the release of VB from SLNs with both diffusion of the water into the particles, erosion and dissolution of the particles, was described the release profile of SLN loaded AE extract in release medium at pH 7.4.

The skin permeation profiles of the SLN loaded AE extract and the AE extract were examined according to OECD 428 using an artificial membrane. The permeation profiles were identified by determining the amount of VB that was collected from the receptor chamber at designated times. Table 20 illustrates the percentage of VB determined in each part of the Franz cell unit after 24 hours.

Table 20 Percentage of VB in each part of Franz cell units after applied for 24 hours

Samples	Quantity (% \pm SD)			
	Donor part	Membrane	Receiver part	Recovery
SLN loaded AE extract	59.80 \pm 8.78	21.45 \pm 8.89	Negligible	80.50 \pm 9.12
AE extract	43.98 \pm 10.56	34.30 \pm 2.89	4.46 \pm 8.55	82.75 \pm 16.45

VB remained in each part of Franz cell units but most VB from the AE extract remained in the donor part and the VB from SLN loaded AE extract remained in the membrane. The VB from the AE extract permeates through the membrane while the VB from the SLN was detected in negligible quantities in the receiver part. The percentage recovery of VB from both samples was less than 100% due to the instability of the VB in the receptor solution at pH 7.4. The skin permeation profile of the VB in the AE extract is shown in Figure 42. The highest permeation of VB through the artificial membrane was at the 8th hour and then trended to a plateau pattern at the 12th hour. However, the skin permeation profile the VB from the SLNs loaded AE extract could not be established because it could not be quantified in the receptor solution. A likely explanation for this is that the release of the VB from the SLN was prolonged; which caused the VB to be negligibly detectable. More than fifty percent of the VB in the SLN remained in the donor part due to the sustained release property of the nanoparticles.

A stability study of VB also documented that VB was unstable in neutral and alkaline solutions. Therefore, any VB remaining in the receptor fluid might be degraded due to physiological pH solution. Moreover, VB is a water-soluble compound that was limited skin permeation and partitioning into an aqueous phase. Hence, the VB from both the SLN and the AE extract tended to remain in the donor parts and membranes, indicating the hydrophobic property.

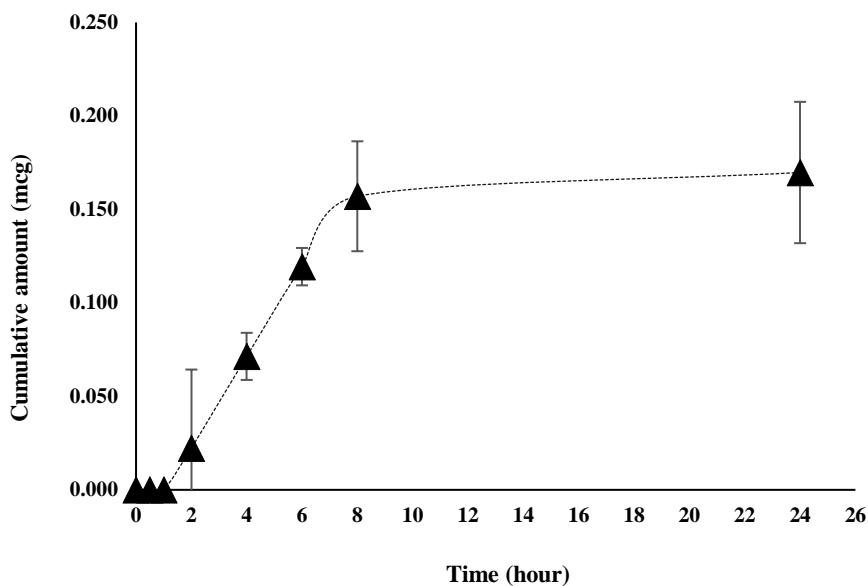


Figure 42 Skin permeation profile of VB from AE extract determined for 1–24 hours

8. Evaluation of safety of hair growth-promoting product containing AE extract

Skin irritation should be evaluated before starting a clinical study or launching a product to the consumer. The current study evaluated the skin safety of hair serum containing SLN loaded AE extract that included other ingredients associated with hair serum. Twenty volunteers were recruited for evaluating hair serum containing SLN loaded AE extract. After removing the occlusive patch test, the 20 volunteers were evaluated at 48 and 72 hours for any indication of skin irritation or damage by dermatologists who followed the ICDRG and CTFA guidelines. The evaluation results are shown in Tables 21 and 22.

Samples	Number of volunteers responding to the samples									
	48 hrs.					72 hrs.				
	-	+	++	+++	++++	-	+	++	+++	++++
1% AE extract in PBS	-	-	-	-	-	-	-	-	-	-
5% AE extract in PBS	-	-	-	-	-	-	-	-	-	-

Tables 21 and 22 show the results of the various treatments:

All four treatments which included 1% SLN in PBS, a combination of hair serum and 5% minoxidil, 5% SLN in PBS, and 5% minoxidil solution, showed positive reactions with minimal irritation (grade +) at 48 hours after removing the occlusive patch test.

However, a weak positive allergic reaction was observed from both the combination of hair serum and 5% minoxidil, and the 5% minoxidil, at 72 hours after removing the patch.

However, the hair serum formulation did not show any skin irritation or allergic reactions on human skin for the 20 participating subjects in the skin irritation testing. This result implies that hair serum containing SLN loaded AE extract is safe for further use as a test product for evaluating the effectiveness of hair serum in hair growth-promoting ability in the clinical trial.

9. Evaluation of the effectiveness of hair serum containing SLN loaded AE extract in the hair-loss treatment.

Seventy-two volunteers were recruited into this study; one volunteer was withdrawn from the research study due to non-compliance. Clinical research was performed at the Skin Center at Thammasat University Hospital over 6 months. Participating volunteers were randomly allocated into 4 groups each with a different treatment which were hair serum containing SLN loaded AE extract, 5% minoxidil, a combination of hair serum, SLN loaded AE extract and 5% minoxidil, and a placebo.

The treatments and their various outcomes were evaluated variously by hair comb testing, global photographs, and photographs of specific treatment sites, captured by a Leviacam[®] with those photographs then analyzed by Trichoscan[®]. The analysis using the Trichoscan[®] included total hair counts at the target area, the mean

hair diameter of the hair at the treatment's sites, the density of anagen hair and telogen hair, terminal hair density, and vellus hair density.

The demographic data of all volunteers is shown in Table 23. Participating volunteers made an appointment every 1 month for follow-up and evaluation of the effectiveness of the treatments. In addition, volunteers were not allowed to use other hair applications including shampoo but were required to use only the hair products assigned by the researcher during the study period.

Table 23 Demographic data of volunteers recruited in research

Items	Hair serum (17)	Placebo (18)	Combination (18)	Minoxidil (18)
Mean age (year \pm SD)	37.44 \pm 2.45	31.15 \pm 4.77	35.78 \pm 2.56	37.39 \pm 8.76
Baldness typed by Norwood –Hamilton	3.15 \pm 1.78	2.10 \pm 0.89	2.55 \pm 0.98	2.63 \pm 0.66
Total Hair count (mean unit \pm SD)	135.02 \pm 16.10	134.72 \pm 27.38	134.22 \pm 24.56	134.28 \pm 24.31
Anagen hair density (mean unit/cm ² \pm SD)	90.53 \pm 22.03	92.71 \pm 22.05	80.96 \pm 25.96	88.01 \pm 32.12
Telogen hair density (mean unit/cm ² \pm SD)	30.03 \pm 17.38	28.28 \pm 20.34	39.84 \pm 20.75	29.54 \pm 22.01
Hair falls after combing (mean unit \pm SD)	5.52 \pm 3.64	4.61 \pm 5.77	5.88 \pm 6.88	3.05 \pm 3.05

Total hair count was calculated by Trichoscan[®] at the tattoo area. The quantity of hair was counted every follow-up and compared to the hair count at baseline. The result of the hair count is shown in Table 24.

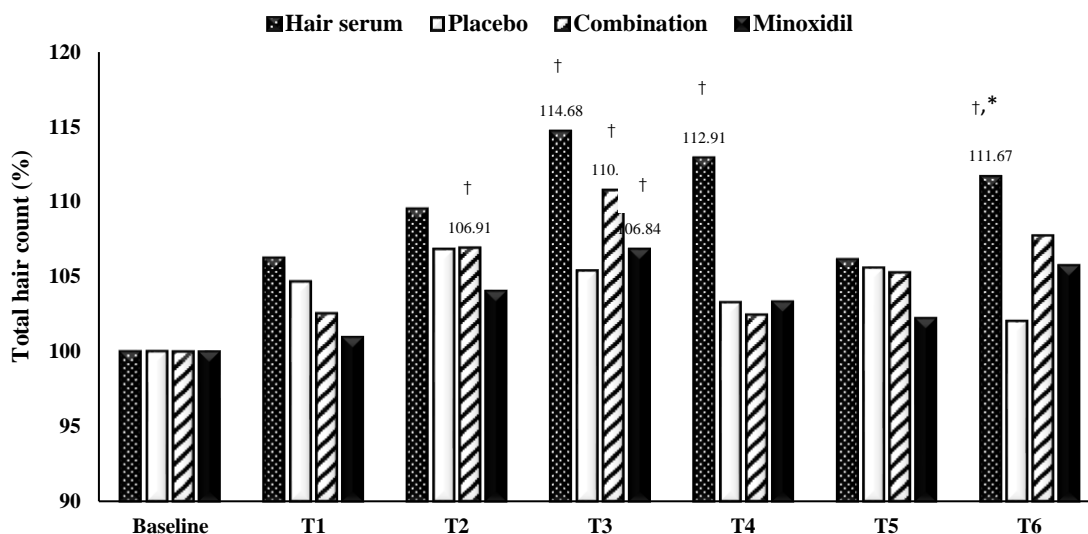


Figure 43 Hair count of each group analyzed by Leviacam® comparing among follow up times

Note: *significantly different versus the baseline ($p < 0.05$, t-test), † significantly different versus the baseline ($p < 0.05$, repeated measures ANOVA)

The data from Figure 43 indicated that the hair number of each group trended to increase when compared to baseline. However, volunteers who applied the hair serum, combination, and minoxidil had increased the hair number within the 3rd, 2nd, and 3rd months respectively while the hair number of the placebo group showed insignificantly increased as compared to baseline. However, the increased hair of combination and minoxidil groups was insignificant from the 4th month until the 6th month.

The percentage change of hair number at the 6th month compared to baseline is shown in Figure 41. Although at the 6th month only hair serum group showed a significant increase in hair number from baseline, the percentage change of hair number in the other groups also increased as well. The highest percentage change of hair number was hair serum group (12.21%) following with combination (8.61%), minoxidil (6.76%), and placebo (4.21%) groups respectively.

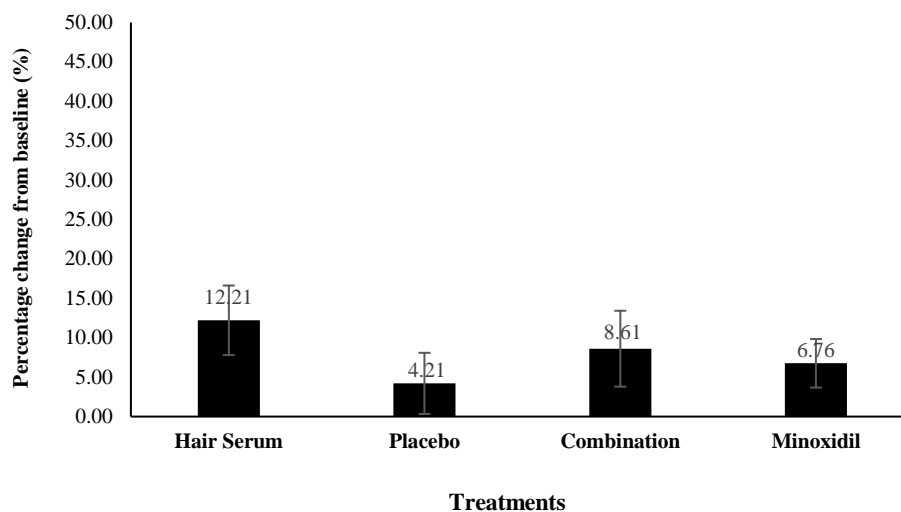


Figure 44 Percentage change of hair number from baseline at the 6th month comparing among 4 groups

After 24 weeks of the treatment, eleven volunteers (64.71%) in the hair serum group showed an obvious increase of hair numbers from baseline while other volunteers in this group did not show any improvement. Twelve volunteers (66.67%) of the minoxidil group showed a significant increase in hair number from baseline. The combination group also showed a positive effect on 13 volunteers (72.22%). In the placebo group, 8 volunteers (44.44%) showed a significant increase of hair number from baseline while other volunteers (66.66%) showed a decrease of hair number from baseline. The combination group showed the highest improvement in hair count (72.22%), followed by the minoxidil group (66.67%), the hair serum group (64.71%), and placebo group (44.44%) (Table 24).

Figure 45 illustrates the percentage of volunteers presenting positive results for hair numbers within each treatment group, at each follow-up time. These results indicate that the hair serum group had an increased number of volunteers showing a positive result from the 1st month until the 3rd month, after which the number of volunteers showing the positive result gradually decreased. The combination treatment group and the minoxidil group showed a fluctuation over time of the percentage of volunteers experiencing positive results. This fluctuating result might be caused by hair shedding induced by minoxidil (E. A. Olsen et al., 2002). The

placebo group showed different results from the other groups with the number of volunteers who presented positive results tending to decrease at every follow-up. It implied that a placebo application might induce the progression of AGA when continuously used for a long period.

Table 24 Quantity of volunteers presenting the positive result of hair number after applications for 6 months

Groups	Quantity of volunteers (%)					
	T1	T2	T3	T4	T5	T6
Hair serum	11 (64.71)	12 (70.59)	14 (82.35)	13 (76.47)	12 (70.59)	11 (64.71)
Placebo	12 (66.67)	12 (66.67)	9 (50.00)	12 (66.67)	10 (55.56)	8 (44.44)
Combination	11 (61.11)	13 (72.22)	13 (72.22)	11 (61.11)	11 (61.11)	13 (72.22)
Minoxidil	12 (66.67)	12 (66.67)	13 (72.22)	11 (61.11)	10 (55.56)	12 (66.67)

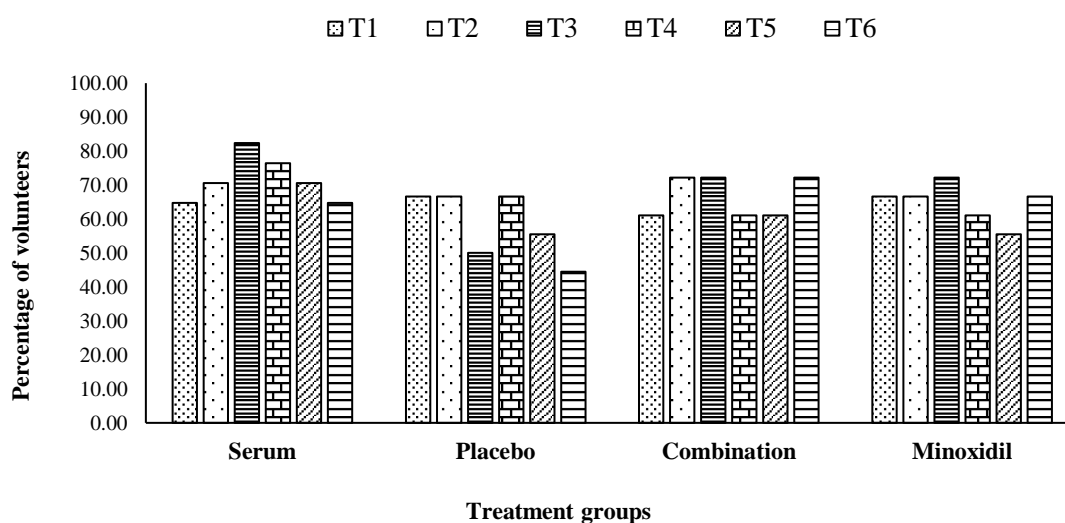


Figure 45 Percentage of volunteers presenting the increase of hair number after applications for 6 months

In addition to total hair count, the number of terminal hairs has been used for predicting the progression of hair loss. The increase of terminal hair might predict the improvement of hair loss treatment. The result was compared each follow-up to baseline. The density of terminal hairs is shown in Table 25.

Table 25 Percentage of terminal hair of each group comparing among follow-up times

Time	Terminal hair (%)			
	Serum	Placebo	Combination	Minoxidil
Baseline	100.00±00.00	100.00±00.00	100.00±00.00	100.00±00.00
T1	100.51±14.27	109.66±28.59	100.62±15.75	102.22±16.49
T2	99.33±17.18	113.51±31.33	106.14±18.45	111.27±24.81
T3	101.65±18.18	113.75±28.65	114.32±15.55*†	114.20±15.85*†
T4	104.46±17.43	114.58±26.32	107.28±18.93	112.62±22.26*†
T5	101.09±18.93	115.00±28.85	108.55±21.16	113.61±21.41*†
T6	102.84±19.69	109.70±28.97	116.29±42.44*†	111.58±20.59*†

Note: *significantly different versus the baseline ($p < 0.05$, t-test), † significantly different versus the baseline ($p < 0.05$, repeated measures ANOVA)

The percentage of terminal hair of each of the hair serum group and the placebo group at each follow-up time was not significantly different from baseline, but the combination treatment group showed a significant difference in percentage of terminal hair from baseline at 6th months. Showing a different pattern, the minoxidil group was more effective in increasing terminal hair within 3 months.

Table 26 Quantity of volunteers presenting the positive result of terminal hair density after applications for 6 months

	Quantity of volunteers (%)					
	T1	T2	T3	T4	T5	T6
Hair serum	11 (64.71)	12 (70.59)	12 (70.59)	12 (70.59)	10 (58.82)	10 (58.82)
Placebo	11 (61.11)	8 (44.44)	13 (72.22)	13 (72.22)	11 (61.11)	11 (61.11)
Combination	9 (50.00)	11 (61.11)	16 (88.67)	12 (66.67)	12 (66.67)	14 (77.78)
Minoxidil	10 (55.56)	10 (55.56)	16 (88.89)	15 (83.33)	15 (83.33)	14 (77.78)

Although the hair serum treatment did not significantly increase percentage of terminal hair at every follow-up, Table 26 revealed that more than 50% of the volunteers in the hair serum group showed the increase of terminal hair from baseline at the 1st month with a gradual increase thereafter. The combination group and the minoxidil groups showed a similar trend.

In addition to the terminal hair, the phase of the hair growth cycle has been used for estimating alopecia progression. The anagen and telogen phases are usually used for predicting the effectiveness of treatment and the severity of baldness. Our study classified the anagen and telogen phases by analysis using the Trichoscan[®]. The percentage of anagen hair of each group was compared at each follow-up time, and the comparisons are shown in Table 27. Similarly, the comparison results of the telogen hair density are shown in Table 28.

Table 27 Percentage of anagen hair of each group comparing among follow-up times

Time	Anagen hair (%)			
	Serum	Placebo	Combination	Minoxidil
Baseline	100.00±00.00	100.00±00.00	100.00±00.00	100.00±00.00
T1	132.61±25.28*†	121.01±41.16	147.96±59.33*†	135.50±62.44
T2	133.88±33.25*†	118.71±40.42	139.94±66.21*†	136.70±77.15
T3	133.35±35.40*†	120.69±40.08	146.92±66.77*†	131.48±56.08
T4	133.22±38.28*†	111.89±27.42	140.89±55.07*†	136.32±71.67
T5	135.31±33.16*†	125.04±37.65*†	151.75±75.11*†	146.87±72.73*†
T6	138.55±32.43*†	120.59±32.97*†	151.99±58.03*†	148.04±70.54*†

Note: *significantly different versus the baseline ($p < 0.05$, t-test), † significantly different versus the baseline ($p < 0.05$, repeated measures ANOVA)

An increase of anagen hair is an indicator of alopecia improvement. Hair shedding tends to decrease when the duration of the anagen phase is extended. Table 27 shows that both the hair serum and combination groups showed a significant increase of percentage of anagen hair over that of the baseline within the 1st month,

whereas the minoxidil group showed a significant increase of anagen hair at the 5th month which was a similar result to the placebo group.

From Figure 46, it can be seen that 80% of the volunteers in the hair serum group showed an increase of percentage of anagen hair that was evident from the first month after application and the percentage of anagen hair of these volunteers was quite stable up to the end of the study. As well, 50% of the volunteers in the combination and minoxidil groups also showed a positive result. The placebo group showed a lower percentage of volunteers having positive results than the other groups.

In the 6th month, the hair serum group showed anagen hair improvement, with 15 volunteers (88.23%) in that group showing an increase of anagen hair from baseline. In the minoxidil group, 15 volunteers (83.33%) showed an increase of anagen hair from baseline while the placebo group also showed a positive effect on anagen hair with 12 volunteers (66.67%) from that group showing increased anagen hair from baseline at the 6th month (Figure 46).

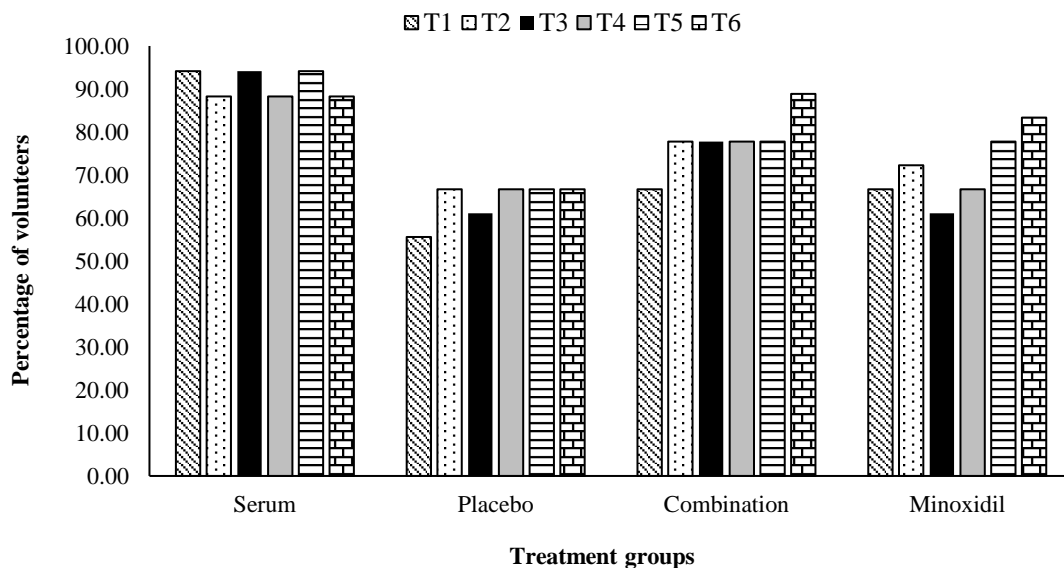


Figure 46 Percentage of volunteers presenting with increased anagen hair density after applications for 6 months

The anagen phase has been used for predicting the effectiveness of the treatment. Our results showed that the percentage change of anagen hair density showed no difference between the hair serum, combination, and minoxidil groups, with the percentage change of anagen hair of those groups being significantly different from the placebo.

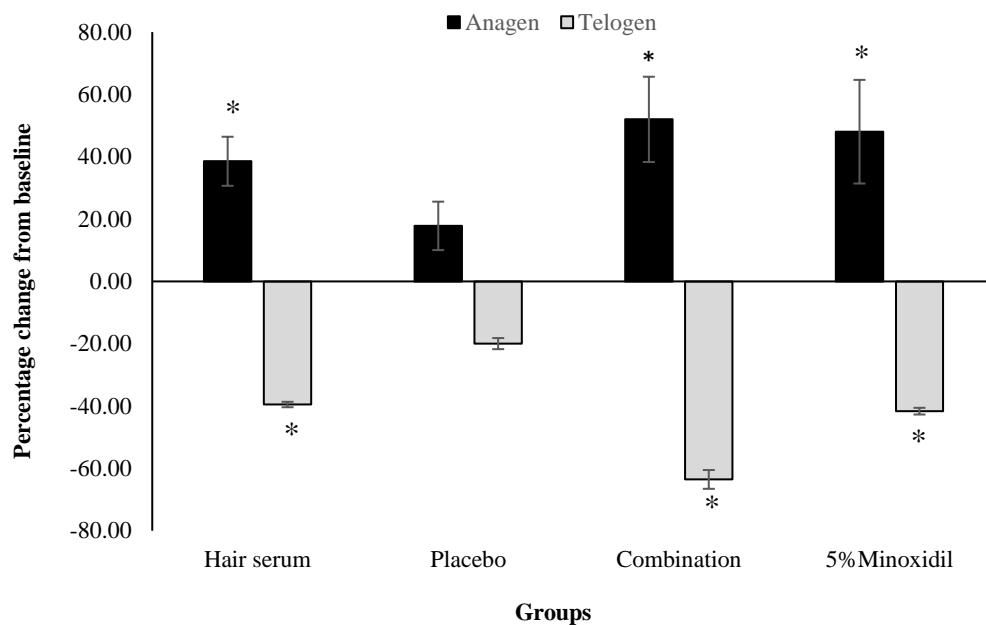


Figure 47 Percentage change of anagen hair of each treatment group compared to baseline after application for 6 months (*different from the placebo group; $p < 0.05$; Mann–Whitney U Test)

The percentage change in the density of anagen hairs from baseline indicated that the hair serum, the combination, and the minoxidil groups all showed a significant increase of anagen hair density, greater than that of the placebo group. In addition, both anagen hair and telogen hair densities are a significant parameter used for predicting alopecia improvement. The telogen phase is shortened which causes anagen acceleration that benefited from the hair loss treatment. The decrease of telogen hair is illustrated in Table 29. Since the number of telogen hairs was not a

normal distribution, the statistic for analyzing the comparison of telogen hair between baseline, and at each follow-up, was the Wilcoxon matched-pairs Signed-Rank.

The percentage change of telogen presented in Figure 47 also correlated to the result of anagen hair. At the 6th follow-up, both the hair serum and combination groups showed a decrease of telogen hair when compared to baseline (39.5% and 63.53% respectively) while the placebo group showed a slight decrease of telogen hair (19.95%). Minoxidil also decreased telogen hair density with a percentage change of 41.63%. In addition, the percentage change of telogen hair in the hair serum, combination, and minoxidil groups was significantly different from the placebo group.

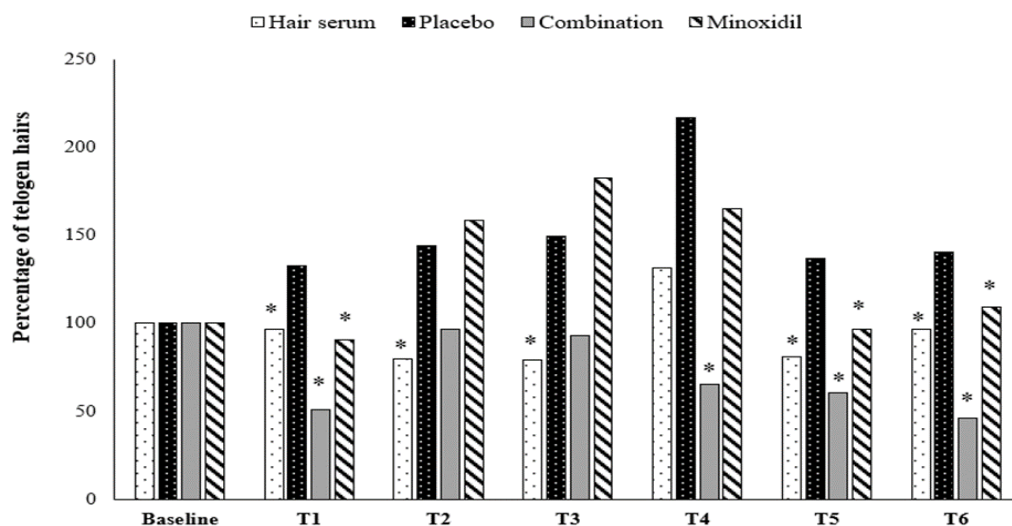


Figure 48 Percentage of telogen hairs of each group comparing among following up times. *significantly different versus the baseline ($p < 0.05$, Wilcoxon matched-pairs Signed-Rank)

Figure 48 shows that the percentage of telogen hairs of the hair serum group significantly decreased within 1 month while the combination and minoxidil groups showed similar patterns of a significant decrease of telogen hair at the 1st, 5th, and 6th month. The placebo group showed an insignificant difference in telogen hair density from baseline. This result indicated that hair serum, combination, and minoxidil effectively decreased telogen hair density within 1 month after application.

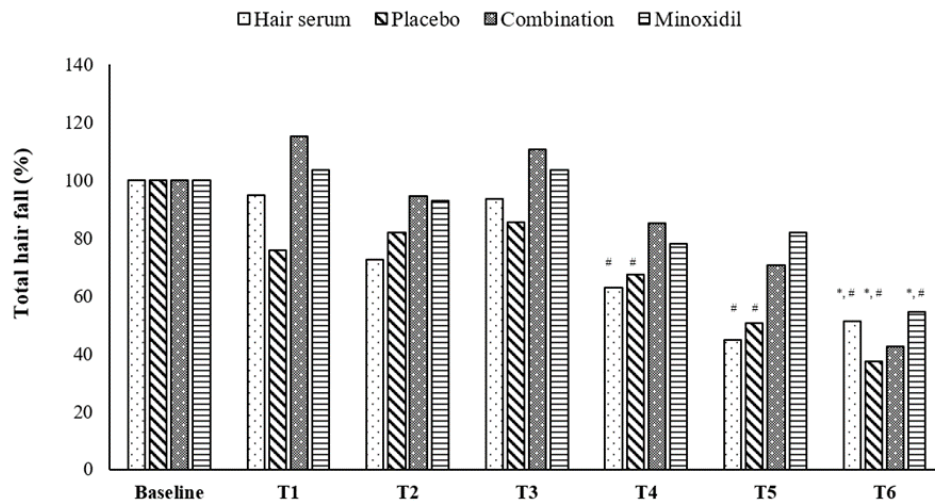


Figure 49 The percentage of hair fall after combing compared among following-up times. *significantly different versus the baseline ($p < 0.05$, t-test), #significantly different versus the baseline ($p < 0.05$, repeated measures ANOVA)

The percentage of hair fall after combing for 60 seconds could be used for estimating the hair strength. The results in Figure 48 show that volunteers of hair serum and placebo groups showed a decreased percentage of hair fall after combing. The quantity of hair fall after combing decreased significantly from the baseline activity by the 4th month while the minoxidil group showed a significant decrease of hair fall by the 6th month. The combination group did not show any significant difference in hair fall over the 6 months period. These results indicated that the hair serum, the minoxidil, and the placebo improved hair strength. The placebo effect was perhaps due to the greater attention paid to hair care by the participants in the placebo group during the experimental period.

In addition to the result analyzed from the Trichoscan[®], the pictures captured by the Trichoscope[®] also were compared between the baseline situation and after application for 6 months. The comparisons of the physical appearance of the hair are shown in Figure 49. The pictures show that the application of hair serum, combination, and minoxidil improved the quantity of hair and hair thickness while the application of placebo showed an indifferent hair appearance between baseline and 6 months of the application.

A global photograph is an effective tool for evaluating the improvement in hair loss due to the treatment. The pictures compare the results from applying the treatment for 6 months with the baseline. They are presented in Figure 50.





Figure 51 Photograph comparing baseline(a) to 6th month (b) of 4 groups; serum group (1a, 1b), placebo group (2a, 2b), combination group (3a, 3b) and minoxidil group (4a, 4b)

The volunteers who applied the hair serum containing SLN loaded AE extract presented with increased hair thickness at the 6th month (Figure 50 (1a, 1b)). Combination (Figure 50 (3a, 3b)) and the minoxidil groups (Figure 50 (4a, 4b)) also showed effects similar to the serum group; hair density was increased more than that at baseline. Differently, the placebo group showed a decrease in hair thickness when compared to baseline (2a, 2b). Skin irritation or severe adverse drug event was not evident during the study period.

CHAPTER V

DISCUSSION

AE is a medicinal plant that has been traditionally used as an anti-inflammatory agent which has been recommended for incorporating into the traditional recipe that is used for treating skin and hair disorders (Liebezeit, & Rau, 2006). VB has been reported as a composition in *Acanthus spp* (Kanchanapoom et al., 2001), and has been documented as having various bioactivities such as being an antioxidant, anti-inflammatory, and inhibition of testosterone activities (Alipieva, Korkina, Erdogan Orhan, & Georgiev, 2014; Attia, El-Kersh, Wagdy, & Elmazar, 2018; Vertuani et al., 2011).

Our study selected VB as the biomarker for evaluating the effectiveness of AE extract and standardizing the extract. AE extracts are performed by macerating with different organic solvents. Ethanolic extract showed the highest content of VB and is then selected for further studying bioactivities. The DPC is the important key of AGA pathogenesis (Han et al., 2004; Lu, Cai, Wu, & Zheng, 2006). Apoptosis of DPCs leads to hair miniaturization which causes hair baldness progression. AE extract and VB show beneficial non-cytotoxic effects on DPCs by increasing cell viability. Our results showed that 250 $\mu\text{g/mL}$ AE extract increases DPC proliferation by increasing the number of cells in the S and G2/M phases. The decrease of DPC number in the G1 phase indicated that AE extract can prevent DPC apoptosis. VB also shows a similar effect on the DPC cycle. G2/M of DPC is stimulated by 62.50 – 125.00 $\mu\text{g/mL}$ VB. The effects of AE extract and VB on the DPC cycle explain how the treated cells demonstrated greater proliferation than the untreated cells. The results from the cell cycle analysis also correlate with the preventative effect of AE extract and VB on testosterone-induced DPC apoptosis. The results show that AE extract 250 mg/mL and VB 62.50 mg/mL prevented DPCs apoptosis induced by testosterone 200 μM .

The decrease of DPC viability is related to the cell damage caused by testosterone metabolism induced by the 5 α -reductase enzyme (Winiarska et al., 2006). The prevention of cell apoptosis might be caused by the inhibitory activity of AE extract and VB on 5 α -reductase activity. The *in vitro* study for determining 5 α -reductase inhibition using 5 α -reductase performed from LNCaP cell showed that ethanolic extract of AE inhibited 5 α -reductase activity with IC₅₀ of 60.45 μ g/mL, an outcome of the AE extract improving DPC viability. However, VB presented no effect on 5 α -reductase activity. A likely explanation for this discrepancy between the results achieved by AE extract and VB is that AE extract contains various chemical compounds that could inhibit 5 α -reductase activity such as apigenin, β -sitosterol, and luteolin (Garre Contreras, Piquero-Casals, Trullas, & Martinez, 2018; Kanchanapoom et al., 2001; Koseki et al., 2015; Y. Wu et al., 2017). In addition, VB in AE extract might inhibit testosterone activity by a different mechanism that decreases the expression of cAMP by reducing TGF- β expression that causes DPC apoptosis (Liu, Zhang, Li, Zhang, & Hu, 2015).

Although VB might not be an appropriate biomarker due to the non-inhibitory activity in the 5 α -reductase enzyme, the beneficial effect on DPC was both increased cell proliferation and prevention of cell apoptosis induced by testosterone indicated that VB is an interesting biomarker for anti-hair loss product development. Many articles showed that hair loss occurred due to hair follicle inflammation (Yann F. Mahé et al., 2000; Trüeb, 2002). A combination of 5 α -reductase inhibition and anti-inflammatory agents has been recommended for treating AGA (Kaufman et al., 1998; Varothai & Bergfeld, 2014). VB is reported as an anti-inflammatory agent by inhibiting the inflammation process in several mechanisms (Mirko Pesce et al., 2015; Speranza et al., 2010; Yang, 2016). The anti-inflammatory activity of AE extract and VB have been examined by using LPS treated RAW 267.4 macrophage cells and UV irradiated DPC models. Those studies showed that AE extract and VB can significantly inhibit the release of IL- β , NO, TNF- α from LPS induced RAW 267.4 at concentrations of 250 μ g/mL and 62.50 – 125.00 μ g/mL. The mechanism of inflammatory inhibition might be the cause of the reduction of NF- κ B activity and iNOS stimulation (Mirko Pesce et al., 2015; Qiao, Tang, Wu, Tang, & Liu, 2019; Speranza et al., 2010). There have also been some studies that have documented that

VB inhibits inflammatory cytokines by inducing the downregulation of cleaved-caspase-3 and apoptosis regulator Bax, and upregulation of Bcl-2 and inhibiting IL-1 β -induced activation of JAK/STAT pathway (Qiao et al., 2019).

All mechanisms reported in the previous study might cause the decrease of those pro-inflammatory cytokines in RAW 267.4 cells. DPC inflammation induced by UV radiation, AE extract and VB might diminish the release of IL- α and IL-6 by similar mechanisms mentioned above. The 5 α -reductase inhibition of AE extract combined with the anti-inflammatory activity of both AE extract and VB indicates that AE extract containing VB is a promising agent for treating AGA. Additionally, the preventive effect of AE extract containing VB on testosterone-induced DPCs apoptosis can extend the anagen phase in the hair growth cycle, which is an interesting effect indicating that AE extract as a natural agent for hair loss treatment.

Although VB demonstrated a beneficial effect on DPCs, its stability was a limitation for its topical application development. Chemical kinetic studies of VB have shown that VB is degraded when exposed to high temperatures and water. VB in AE extract (semi-solid form) is more stable than AE extract in solution form. VB remains in the semi-solid form of AE extract for twice as long as in solution form after being kept under 50°C for 3 months. VB in AE extract solution has an estimated shelf-life of about 12 days when stored at 25°C, according to Arrhenius' theory while the shelf-life of VB in the semi-solid form of AE extract is 75 days.

The instability of VB dissolved in aqueous might be caused by a hydrolysis reaction at the glycoside structure (Brito-Arias, 2007). VB is very unstable in water, particularly in a basic pH, and acquires a brown color over time as the caffeic acid moiety undergoes oxidation after hydrolysis which produces caffeic acid ortho-quinone. As well, the ester bond between caffeic acid and rhamnose also may have hydrolyzed (Figure 48) (Isacchi et al., 2017; Su et al., 2016). In solution form, VB in AE extract is more stable in an acidic solution than in the biological or basic solution. This finding indicated that VB is a phenolic glycoside that might be subject to basic hydrolysis (Brito-Arias, 2007; Vernon & Perutz, 1967).

The stability of bioactive compounds can be improved by several strategies such as formulation design, use of antioxidants, chelating, and using preservative agents. In addition, given that a drug delivery system is usually used for increasing

drug effectiveness and improving drug stability, nano/micro-particles have been developed for reducing drug limitations. The current study improves the stability of VB by using solid lipid nanoparticles. Although VB shows hydrophilic properties due to the glycone group, AE extract is solubilized in oil to a greater extent than occurs in an aqueous phase. The oil-soluble property of AE extract allows the preparation of the oil phase of SLN by a homogenization technique.

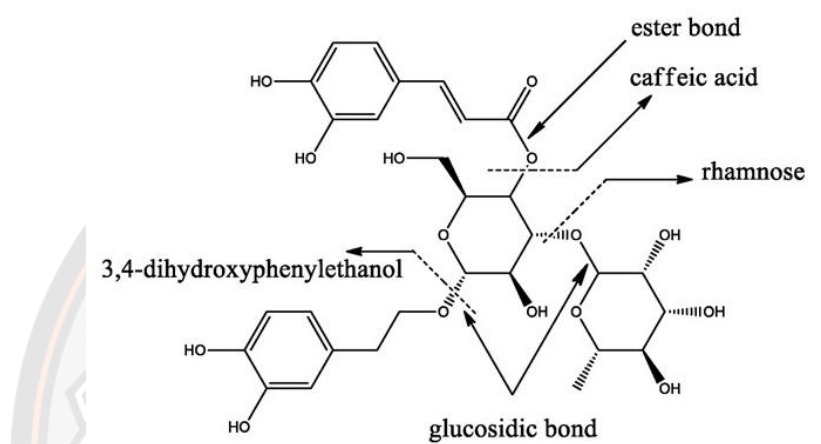


Figure 52 Chemical structure and type of bound of VB

SLN was developed for preventing VB in AE extract from degradation and thereby reducing its limitations. Compritol® ATO 888 was used as a carrier, preparing the lipid particles by a hot melt homogenization method. SLN loaded AE extract was successfully prepared with a size of between 0.60 μm and 3.00 μm . Loading of AE and emulsifier concentration both affect particle characteristics. Entrapment efficiency decreases as the amount of AE loading is increased. A decrease in entrapment efficiency might be due to limited particle capacity. The solubility of VB in water is also an important factor influencing particle encapsulation. The decrease of drug loading also causes the reduction of entrapment efficiency of particles because VB, the hydrophilic compound, may be diffused and dissolved in an aqueous phase during preparation processes due to sinking conditions.

Tween 80 is an emulsifier used for stabilized particle formation; it also affects entrapment efficiency. Generally, Tween 80 can decrease the surface tension energy of the lipid phase and induce particle formation. Encapsulated VB is prevented from aqueous partitioning by Tween 80 locating at the interfacial layer. Although Tween 80 can increase entrapment efficiency by being the barrier to VB partitioning, an increase of Tween 80 changes the solubility of VB in AE extract due to the increase of HLB value. VB is solubilized in an aqueous phase and entrapment efficiency is then decreased.

Although the previous conditions containing Compritol® ATO 888 and Tween 80 can produce SLN with high entrapment efficiency, the stability of particles is the important factor to be considered. SLNs are prone to instability due to their complex crystallization behavior based on polymorphic transition. The polymorphic transition of lipid particles induces a change of particle structure and shape which increases the surface area of the particles which in turn leads to uncovered hydrophobic patches that will aggregate and may eventually form as a gel.

Aggregation and polymorphic transition can be prevented by adding a high concentration of surfactant that will quickly adsorb to the newly formed surfaces upon polymorphic transition. However, a high concentration of surfactants is usually restricted in pharmaceutical applications. Co-surfactant has been considered to improve particle property and stability (Salminen et al., 2014). Co-surfactant allows particle formation and increases the curvature of the interfacial layer by using a lower concentration of specific surfactants. 0.50% Tween 80 and 3.00% Span 80 are used as co-surfactant for improving particle formation including entrapment efficiency.

Although the co-surfactant system can improve particle stability, the increase of Span 80 by more than 3.0% results in the decrease of entrapment efficiency because Span 80 alters the layer formation of Tween 80. Layer alteration leads to an increase of the VB solubility into the outer phase (Ngwuluka, Kotak, & Devarajan, 2017). On the other hand, a decrease of Span 80 of less than 3.0% reduces VB entrapment efficiency because the decrease of Span 80 allows HLB to increase, allowing VB to solubilize into the aqueous phase. Where the Tween 80 proportion is optimized at 0.50% and the Span 80 proportion is optimized at 3.00%, the highest

entrapment efficiency is 35.25% with a particle size of about 628 nm, and the particles are smooth and spherical.

The development of SLN is intended to improve VB stability because the major advantage of SLNs is the entrapment of both hydrophilic and hydrophobic bioactive ingredients inside the solidified lipid matrix. The lipid particles prevent the diffusion of VB to the outer phase. VB degradation induced by influencing factors is limited. The result indicated that VB incorporated into SLN was more stable than the AE extract. The shelf-life of free VB was extended to 154 days when encapsulated into SLN. However, VB-loaded SLNs degraded when the temperature increased, similarly to the free VB in AE extract. The stability of SLNs is dependent on temperature, and some studies have revealed that a high temperature affects the particles' lipid structure. After heating, solid lipid then recrystallizes as the temperature system decreases to room temperature. Recrystallization alters the chemical structure of the lipids and their melting point is usually decreased (Freitas, & Muller, 1999; Uner, Wissing, Yener, & Muller, 2005). When SLNs are gelled VB is released from the particles when the SLN is kept under high temperatures (Makoni, Wa Kasongo, & Walker, 2019; Uner et al., 2005). Pharmaceutical dosage forms are always used for not only administrating but also protecting the active drug from degradation (Ekoja, 2017).

SLN loaded AE extract is incorporated into hydrogel by using hydroxypropyl methylcellulose as a suspending agent. The hydrogel containing SLN loaded AE extract and hydrogel containing AE extract were kept under various conditions for 3 months. The remaining VB indicated that hydrogel containing SLN loaded AE extract is more stable than the hydrogel containing AE extract. In the case of hydrogel containing SLN loaded AE extract, more than 90% of VB remained in the hydrogel when kept at between 4°C and 40°C while VB is degraded by more than 30% when the hydrogel was kept at 50°C. Degradation of VB caused by high temperatures induced SLN to a gelled state and the recrystallization process is triggered. VB is then expelled from the particles and degraded when exposed to the influenced environment. Hence, an application containing SLN kept under a cool place is recommended.

At ambient temperature (25°C), SLN can prevent the active compound from degradation reaction. Our study reveals that the shelf-life of VB can be extended from 75 days in the semisolid form of AE extract to 154 days in SLN. Although SLN can extend the shelf-life of VB, the modification of the SLN component might increase the shelf life of VB even more. Lipid particle is a barrier to degradation reaction induced by influenced factors (Müller, Mäder, & Gohla, 2000). However, the shelf-life of VB-loaded SLN, which was expected to be in excess of one year, was found to be only 172 days in this experiment.

Lipids have a low recrystallization index which increases particle stability with the perfect formation structure evident during the recrystallization process. However, the entrapment efficiency might decrease due to there being no space between the lipids in the perfect formation. Lipids in combination or lipids composed of multi-structures, are often considered for increasing entrapment efficiency. Compritol® ATO 888 should be combined with other lipids composed of multi-structures, such as Dynasan114 (Glycerin trimyristate). The lipids in combination have a low recrystallization index and, importantly, their structure also prevents the perfect structure formation, Dynasan114 and Compritol® ATO 888 are composed of mono-, di-, and triglycerides containing fatty acids of different chain lengths which makes recrystallization difficult and enables high encapsulation efficiency (Ruktanonchai et al., 2009).

Combination lipids can modify the HLB system, for instance where the mixture of Compritol® ATO 888 (HLB =2) and Dynasan 114 (HLB = 4) demonstrates an increase in HLB, depending on their ratio (Devi & Agarwal, 2019). The increase of the HLB system decreases the hydrophobic property of the lipid and allows VB partitioning into the lipid phase, resulting in an increase in entrapment efficiency.

Co-surfactants containing Tween 80 and Span 80 are also an appropriate system for stabilizing the solid lipid particles. However, a polymer such as Poloxamer should be considered to increase particle stability because of its steric hindrance. Tween 80 and Span 80 can stabilize the lipid particles by balancing the HLB value and performing the perfect formation of surfactant localized at the surface interface of the lipid and aqueous phases (Salminen et al., 2014).

Low crystallization index lipid demonstrates sustained release behavior. One study has indicated that low crystallization index lipids show sustained release where 40% of the drug is released from SLN for 50 hours. Hence, the combination of Compritol® ATO 888 and Dynasan 114 is recommended as SLN lipid carrier. The co-surfactant containing Tween 80 and Span 80 is also recommended as an emulsifier for stabilizing particle formation. Poloxamer is considered a stabilizer. However, the ratio of all components should be further optimized for producing the SLN loaded AE extract with appropriate characteristics.

Although VB is encapsulated in a solid lipid particle, VB could be liberated from particles and then diffuses into the outer region. The release profile of VB liberated from SLN indicated that the behavior of VB in various pH conditions was different. The cumulative release of VB in basic solution was lower than in an acidic solution which is caused by the instability of VB in a basic solution (Alipieva et al., 2014; Vertuani et al., 2011). VB degradation was evident when released from SLN into a basic medium.

VB is a weak basic compound that is unionized in alkaline solution (Fini, Cavallari, Rabasco Alvarez, & Rodriguez, 2011) meaning that the release of VB in neutral or alkaline solution is less than that in an acidic solution. Similarly, in the skin permeation study, the permeation profile of VB decreased when it penetrated to the receptor solution. This is due to the degradation of VB in a basic solution. Degradation of VB in a receptor fluid also affected the percentage recovery in a skin permeation study with about an 80% recovery. In addition, VB is a water-soluble compound that has limited skin permeation. Most of the VB in SLN loaded AE extract and free VB in AE extract localized at the donor part and membrane. The VB in SLN showed sustained release and remained in the donor part longer than the VB in the AE extract. Those effects are caused by lipid carriers preventing VB partitioning through the outer medium, and solid lipid is like a reservoir storing VB and gradually releasing it from particles.

Although SLN loaded AE extract does not show cytotoxic effects on DPCs, hair serum containing SLN loaded AE extract was also evaluated for skin irritation in humans in the clinical study to ensure guaranteed skin safety. Twenty participants were recruited into the skin irritation study and the results indicated that hair serum

containing SLN loaded AE extract formulation ingredients are safe for use as the test products in the clinical study and for developing as a topical application.

A clinical study for evaluating the effectiveness of serum containing SLN loaded AE extract examined 72 male participants with male pattern baldness. Participants are allocated into 4 groups and an evaluation was done comparing the Hair Serum containing SLN loaded AE extract group, the Placebo group, the 5% minoxidil group and the combination group (hair serum containing SLN loaded AE extract and 5% minoxidil) group.

The results from that clinical study showed that the Hair Serum group and the 5% minoxidil group significantly stimulated hair growth within 3 months while the combination group increased the number of hairs within 2 months. This implies that 5% minoxidil and Hair Serum show a synergistic effect on hair numbers by accelerating the hair regrowth period. Although 5% minoxidil increased the number of hairs within 3 months, the number of hairs decreased during and after the 4th month, but this was not significantly different from the baseline.

Prior publications have documented the use of topical minoxidil as causing hair shedding at 1st - 3rd months of use. This might be caused by the shortening of the telogen phase (Mori & Uno, 1990; E. A. Olsen et al., 2002). The number of hairs decreased sequentially. The hair shedding effect of minoxidil also influenced the combination group as well. The participants in the Hair Serum group experienced an increase in hair numbers after application, indicating a trend showing a gradual increase in hair numbers at every follow-up. The promising effect of Hair Serum is different from the other treatments that resulted in a stable number of participants who showed a positive result. A likely explanation for this is that the Hair Serum improves hair loss without hair shedding periods similar to the effect of 5% minoxidil.

In the case of terminal hair, participants in the Combination group and 5% minoxidil showed increased terminal hair density within 3 months which implies that minoxidil plays a crucial role in an increase of terminal hair density (Elise A. Olsen, Weiner, Delong, & Pinnell, 1985), However, the treatment does not involve the conversion of vellus hair to terminal hair (Hugh Rushton, Norris, & Van Neste, 2016) because both groups do not significantly change the number of vellus hairs. Although the Hair Serum group showed an increase in the total hair number, the terminal hair

did not significantly increase from the baseline. However, the percentage of the participants who experienced a significant increase of terminal hair from baseline (64.71%) is close to the result of the 5% minoxidil group (77.78%) and the Combination group (77.78%).

The density of anagen and telogen hair is usually used for predicting the hair regrowth cycle. Medical treatments of hair loss such as finasteride and minoxidil shorten the telogen phase of the hair cycle and accelerate the evidence of the anagen phase (S. W. Lee, Juhasz, Mobasher, Ekelem, & Mesinkovska, 2018; Mori & Uno, 1990; York, Meah, Bhojrul, & Sinclair, 2020). Our study showed that the Hair Serum group and the Combination group demonstrated significantly increased density of anagen hair within 1 month; the results correlate with the decrease of telogen hair density. Telogen hair density also significantly decreased within 1 month after application. Those results imply that both the Hair serum and the Combination applications are effective in hair loss prevention and hair regrowth.

Minoxidil prevents hair loss by increasing anagen hair density and decreasing telogen hair density. The positive result is observed within 5 months after application. Similar to the effect of minoxidil on the density of terminal hair, the delay effect on anagen hair density might be caused by the hair shedding that affects hair regrowth in 1-3 months after use. Although the Combination treatment contains 5% minoxidil, the effect on anagen hair density was not delayed which might be caused by the effect of VB in SLN loaded AE extract that prevents hair loss by preventing DPCs from apoptosis and increasing the number of DPCs through G2/M stimulation. Anagen phase of hair is then extended as a consequence. The growth of new anagen hair also affects telogen hair that was pushed out (Randall & Botchkareva, 2009). Hence, the treatments which increase anagen hair also decrease telogen hair.

Given the importance of anagen hair density, the percentage change of anagen hair density at the 6th month from baseline can be used to indicate the effectiveness of the treatment. Hair serum was effective in showing an increase in the anagen hair density significantly greater than the Placebo group, and its effectiveness is not significantly different from the 5% minoxidil group. The Hair Serum, the Combination and the 5% minoxidil all showed similar effectiveness that was not significantly different.

The hair comb test is used to check the health of hair by testing its ability to resist combing force (Dhurat, & Saraogi, 2009). The result revealed that hair fall caused by combing significantly decreased within 4 months in the Hair Serum group and the Placebo group while the 5% minoxidil group shows a significant decrease of hair fall at the 6th month. The effect of the Hair Serum and the Placebo on the decrease of hair falling might be explained by the possibility that VB in the Hair Serum induces the regrowth of anagen hair which possesses healthy and strong fibers thereby being more able to resist combing force. In the Placebo group, the placebo effect might be caused by changes in the behavior of the participants who became more concerned about hair hygiene when participating in the study. By applying the solution to the skull, blood supply is increased by massaging after application. The Combination group showed no significant hair fall because the treatment contains 5% minoxidil which induces hair shedding. As well, the increase in hair strength is caused by the physical integrity of anagen hair that waited for 3-6 months (E. A. Olsen et al., 2002).

Our study evaluated the bioactivities of AE extract for its effectiveness in promoting hair growth and therefore its efficacy in product development using AE extract. The results of the *in vitro* tests indicate that AE extract containing VB is a promising ingredient for developing hair growth-promoting products. Both the inhibition of the 5 α -reductase activity of AE extract and the anti-inflammatory activity of VB can be used for promoting hair regrowth and preventing hair loss (Figure 51).

In addition, VB can extend DPC viability by preventing cell apoptosis induced by testosterone metabolism. Although VB is degraded by the influenced factor, SLN prevents it from degradation.

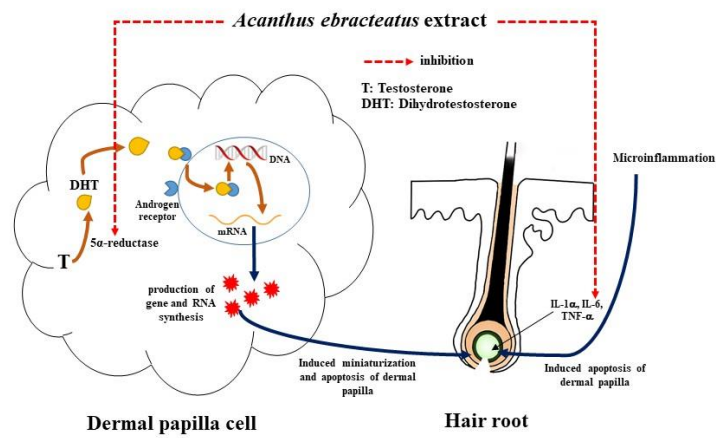
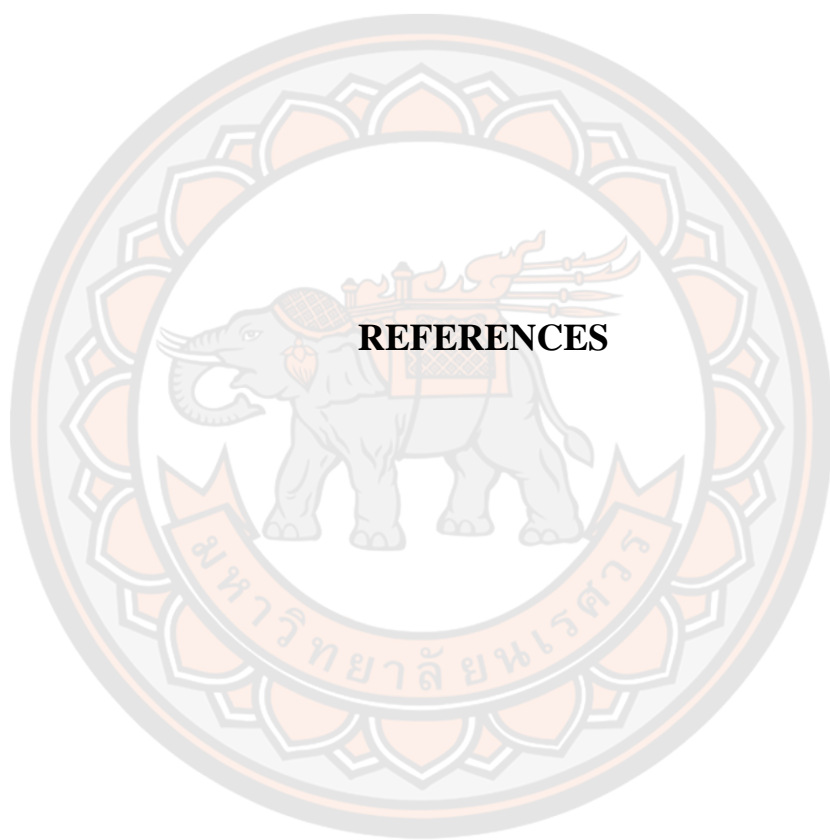


Figure 53 Proposed mechanism of AE for preventing androgenic alopecia

Hair serum-containing SLN loaded AE extract successfully improved hair regrowth in the clinical study and showed a satisfying result without severe adverse effects or reactions. The Hair Serum increased both terminal and anagen hair density which are important for stimulating hair regrowth and preventing hair loss. Hence, the Hair Serum containing SLN loaded AE extract is a good candidate for treating AGA alternating to current medication.



REFERENCES

REFERENCES

- Abdelouahab, N., & Heard, C. (2008). Effect of the major glycosides of *Harpagophytum procumbens* (Devil's Claw) on epidermal cyclooxygenase-2 (COX-2) in vitro. *J Nat Prod*, 71(5), 746-749. doi:10.1021/np070204u
- Ahmad, P., Jaleel, C. A., Salem, M. A., Nabi, G., & Sharma, S. (2010). Roles of enzymatic and nonenzymatic antioxidants in plants during abiotic stress. *Critical reviews in biotechnology*, 30(3), 161-175.
- Akdemir, Z., Kahraman, C., Tatlı, II, Küpeli Akkol, E., Süntar, I., & Keles, H. (2011). Bioassay-guided isolation of anti-inflammatory, antinociceptive and wound healer glycosides from the flowers of *Verbascum mucronatum* Lam. *J Ethnopharmacol*, 136(3), 436-443. doi:10.1016/j.jep.2010.05.059
- Alagusundaram, M., Madhu Sudana Chetty, C., Umashankari, K., Badarinath, A. V., Lavanya, C., & Ramkanth, D. S. (2009). *Microspheres as a novel drug delivery system - A review* (Vol. 1).
- Alipieva, K., Korkina, L., Erdogan Orhan, I., & Georgiev, M. (2014). Verbascoside – A review of its occurrence, (bio)synthesis and pharmacological significance. *Biotechnology Advances*, 32, 1065-1076. doi:10.1016/j.biotechadv.2014.07.001
- Ambrosone, L., Guerra, G., Cinelli, M., Filippelli, M., Mosca, M., Vizzarri, F., . . . Costagliola, C. (2014). Corneal Epithelial Wound Healing Promoted by Verbascoside-Based Liposomal Eyedrops. *BioMed Research International*, 2014(Article ID 471642), 8.
- Anand, L., & C., J. W. (1975). Male Pattern Alopecia A Histopathologic and Histochemical Study. *Journal of Cutaneous Pathology*, 2(2), 58-70. doi:doi:10.1111/j.1600-0560.1975.tb00209.x
- Arulselvan, P., Fard, M. T., Tan, W. S., Gothai, S., Fakurazi, S., Norhaizan, M. E., & Kumar, S. S. (2016). Role of Antioxidants and Natural Products in Inflammation. *Oxidative Medicine and Cellular Longevity*, 2016, 5276130. doi:10.1155/2016/5276130

- Attia, Y. M., El-Kersh, D. M., Wagdy, H. A., & Elmazar, M. M. (2018). Verbascoside: Identification, Quantification, and Potential Sensitization of Colorectal Cancer Cells to 5-FU by Targeting PI3K/AKT Pathway. *Scientific reports*, 8(1), 16939. doi:10.1038/s41598-018-35083-2
- Bahta, A. W., Farjo, N., Farjo, B., & Philpott, M. P. (2008). Premature senescence of balding dermal papilla cells in vitro is associated with p16(INK4a) expression. *J Invest Dermatol*, 128(5), 1088-1094. doi:10.1038/sj.jid.5701147
- Bansode, S. S., Banarjee, S. K., Gaikwad, D. D., Jadhav, S. L., & Thorat, R. M. (2010). MICROENCAPSULATION : A REVIEW. *Vishal Institute of Pharmaceutical Education and Research in Pharmaceutical Sciences*, 1(2).
- Battaglia, L., Gallarate, M., Panciani, P. P., Ugazio, E., Sapino, S., Peira, E., & Chirio, a. D. (n.d.). Techniques for the Preparation of Solid Lipid Nano and Microparticles. Retrieved December 25, 2021, from <http://dx.doi.org/10.5772/58405>
- Benson, H. (2005). *Transdermal Drug Delivery: Penetration Enhancement Techniques (Vol. 2)*.
- Bhandary, B., Marahatta, A., Kim, H.-R., & Chae, H.-J. (2013). An Involvement of Oxidative Stress in Endoplasmic Reticulum Stress and Its Associated Diseases. *International Journal of Molecular Sciences*, 14(1), 434-456. doi:10.3390/ijms14010434
- Bodemer, C., de Prost, Y., Peuchmaur, M., Fraitag, S., Chatenoud, L., & Brousse, N. (2000). Role of Cytotoxic T Cells in Chronic Alopecia Areata. *Journal of Investigative Dermatology*, 114(1), 112-116. doi:<https://doi.org/10.1046/j.1523-1747.2000.00828.x>
- Bodemer, C., Peuchmaur, M., Fraitag, S., Chatenoud, L., Brousse, N., & De Prost, Y. (2000). Role of cytotoxic T cells in chronic alopecia areata. *J Invest Dermatol*, 114(1), 112-116. doi:10.1046/j.1523-1747.2000.00828.x
- Brito-Arias, M. (2007). Hydrolysis of Glycosides. In M. Brito-Arias (Ed.), *Synthesis and Characterization of Glycosides* (pp. 304-313). Boston, MA: Springer US.
- Buchi. (2016). *Operation Manual (Original)*, Mini Spray Dryer B-290. Flawil.

- Buonocore, D., Nobile, V., Michelotti, A., & Marzatico, F. (2013). Clinical Efficacy of a Cosmetic Treatment by Crescina(®) Human Follicle Stem Cell on Healthy Males with Androgenetic Alopecia. *Dermatology and Therapy*, 3(1), 53-62. doi:10.1007/s13555-013-0021-2
- C. Lauer, A., L. Flynn, G., Ramachandran, C., Weiner, N., & Margaret Lieb, L. (1995). *Transfollicular Drug Delivery* (Vol. 12).
- Devi, R., & Agarwal, S. (2019). SOME MULTIFUNCTIONAL LIPID EXCIPIENTS AND THEIR PHARMACEUTICAL APPLICATIONS. *International Journal of Pharmacy and Pharmaceutical Sciences*, 1-7. doi:10.22159/ijpps.2019v11i9.34194
- Dhurat, R., & Saraogi, P. (2009). Hair evaluation methods: merits and demerits. *International journal of trichology*, 1(2), 108-119. doi:10.4103/0974-7753.58553
- Dixit, M., Kini, A. G., & Kulkarni, P. K. (2010). Preparation and characterization of microparticles of piroxicam by spray drying and spray chilling methods. *Research in Pharmaceutical Sciences*, 5(2), 89-97.
- Ekoja, A. (2017). DEGRADATION PATHWAY OF PHARMACEUTICAL DOSAGE FORMS.
- Etemad, L., Zafari, R., Vahdati-Mashhadian, N., Moallem, S. A., Shirvan, Z. O., & Hosseinzadeh, H. (2015). Acute, Sub-Acute and Cell Toxicity of Verbascoside. *Research Journal of Medicinal Plant*, 9(7), 354-360.
- Fettelschoss, A., Kistowska, M., LeibundGut-Landmann, S., Beer, H.-D., Johansen, P., Senti, G., . . . Kündig, T. M. (2011). Inflammasome activation and IL-1 β target IL-1 α for secretion as opposed to surface expression. *Proceedings of the National Academy of Sciences*, 108(44), 18055-18060. doi:10.1073/pnas.1109176108
- Feughelman, M. (1997). *Hair and Hair Care* (Vol. 17). New York: Marcel Dekker.
- Filippin, L. I., Vercelino, R., Marroni, N. P., & Xavier, R. M. (2008a). Redox signalling and the inflammatory response in rheumatoid arthritis. *Clin Exp Immunol*, 152(3), 415-422. doi:10.1111/j.1365-2249.2008.03634.x

- Filippin, L. I., Verdelino, R., Marroni, N. P., & Xavier, R. M. (2008b). Redox signalling and the inflammatory response in rheumatoid arthritis. *Clin Exp Immunol*, 152(3), 415-422. doi:10.1111/j.1365-2249.2008.03634.x
- Fini, A., Cavallari, C., Rabasco Alvarez, A. M., & Rodriguez, M. G. (2011). Diclofenac salts, part 6: release from lipid microspheres. *J Pharm Sci*, 100(8), 3482-3494. doi:10.1002/jps.22581
- Freitas, C., & Muller, R. H. (1999). Correlation between long-term stability of solid lipid nanoparticles (SLN) and crystallinity of the lipid phase. *Eur J Pharm Biopharm*, 47(2), 125-132. doi:10.1016/s0939-6411(98)00074-5
- Gálvez, M., Martín-Cordero, C., & Ayuso, M. J. (2006). Pharmacological Activities of Phenylpropanoids Glycosides. In R. Atta ur (Ed.), *Studies in Natural Products Chemistry* (Vol. 33, pp. 675-718): Elsevier.
- Galvez Peralta, M., Martin-Cordero, C., & Ayuso, M. (2006). Pharmacological Activities of Phenylpropanoids Glycosides. *Studies in Natural Products Chemistry*, 33, 675-718. doi:10.1016/S1572-5995(06)80037-2
- Gandhi, B. R., Mundada, A. S., & Gandhi, P. P. (2011). Chronopharmaceutics: As a clinically relevant drug delivery system. *Drug Delivery*, 18(1), 1-18. doi:10.3109/10717544.2010.509358
- Garlanda, C., Dinarello, Charles A., & Mantovani, A. The Interleukin-1 Family: Back to the Future. *Immunity*, 39(6), 1003-1018. doi:10.1016/j.immuni.2013.11.010
- Garre Contreras, A., Piquero-Casals, J., Trullas, C., & Martinez, G. (2018). Efficacy and Safety of a New Topical Hair Loss-Lotion Containing Oleanolic Acid, Apigenin, Biotinyl Tripeptide-1, Diaminopyrimidine Oxide, Adenosine, Biotin and Ginkgo biloba in Patients with Androgenetic Alopecia and Telogen effluvium: A Six-month Open-Label Prospective Clinical Study. *Journal of Cosmetology & Trichology*, 04. doi:10.4172/2471-9323.1000132
- Ghosh, S., & Karin, M. (2002). Missing pieces in the NF-kappaB puzzle. *Cell*, 109 Suppl, S81-96.
- Gil Ede, S., Enache, T. A., & Oliveira-Brett, A. M. (2013). Redox behaviour of verbascoside and rosmarinic acid. *Comb Chem High Throughput Screen*, 16(2), 92-97.

- Grams, Y. Y. (2005). *Influence of molecular properties and delivery system design on the transfollicular transport across the skin*. (Doctoral Thesis), Leiden University, Leiden University, Faculty of Mathematics & Natural Sciences, Leiden-Amsterdam Center for Drug Research.
- Gregoriou, S., Papafragkaki, D., Kontochristopoulos, G., Rallis, E., Kalogeromitros, D., & Rigopoulos, D. (2010). Cytokines and other mediators in alopecia areata. *Mediators Inflamm*, 2010, 928030. doi:10.1155/2010/928030
- Gregoriou, S., Papafragkaki, D., Kontochristopoulos, G., Rallis, E., Kalogeromitros, D., & Rigopoulos, D. (2010). Cytokines and Other Mediators in Alopecia Areata. *Mediators Inflamm*, 2010, 928030. doi:10.1155/2010/928030
- Han, J. H., Kwon, O. S., Chung, J. H., Cho, K. H., Eun, H. C., & Kim, K. H. (2004). Effect of minoxidil on proliferation and apoptosis in dermal papilla cells of human hair follicle. *J Dermatol Sci*, 34(2), 91-98. doi:10.1016/j.jdermsci.2004.01.002
- Hausmann, M., Obermeier, F., Paper, D. H., Balan, K., Dunger, N., Menzel, K., . . . Rogler, G. (2007). In vivo treatment with the herbal phenylethanoid acteoside ameliorates intestinal inflammation in dextran sulphate sodium-induced colitis. *Clinical & Experimental Immunology*, 148(2), 373-381. doi:10.1111/j.1365-2249.2007.03350.x
- Hokputsa, S., Harding, S. E., Inngjerdigen, K., Jumel, K., Michaelsen, T. E., Heinze, T., . . . Paulsen, B. S. (2004). Bioactive polysaccharides from the stems of the Thai medicinal plant *Acanthus ebracteatus*: their chemical and physical features. *Carbohydrate Research*, 339(4), 753-762. doi:http://dx.doi.org/10.1016/j.carres.2003.11.022
- Hugh Rushton, D., Norris, M. J., & Van Neste, D. (2016). Hair regrowth in male and female pattern hair loss does not involve the conversion of vellus hair to terminal hair. *Experimental Dermatology*, 25(6), 482-484. doi:https://doi.org/10.1111/exd.12945

- Hwang, Y. P., Yun, H. J., Kim, H. G., Han, E. H., Lee, G. W., & Jeong, H. G. (2010). Suppression of PMA-induced tumor cell invasion by dihydroartemisinin via inhibition of PKC α /Raf/MAPKs and NF- κ B/AP-1-dependent mechanisms. *Biochem Pharmacol*, *79*(12), 1714-1726. doi:10.1016/j.bcp.2010.02.003
- Isacchi, B., Bergonzi, M. C., Iacopi, R., Ghelardini, C., Galeotti, N., & Bilia, A. R. (2017). Liposomal Formulation to Increase Stability and Prolong Antineuropathic Activity of Verbascoside. *Planta Med*, *83*(5), 412-419. doi:10.1055/s-0042-106650
- Ishino, A., Takahashi, T., Suzuki, J., Nakazawa, Y., Iwabuchi, T., & Tajima, M. (2014). Contribution of hair density and hair diameter to the appearance and progression of androgenetic alopecia in Japanese men. *British Journal of Dermatology*, *171*(5), 1052-1059. doi:10.1111/bjd.13230
- Jiménez, C., Villaverde, M. C., Riguera, R., Castedo, L., & Stermitz, F. (1989). Phenylpropanoid Glycosides from *Mussatia hyacinthina*. *Journal of Natural Products*, *52*(2), 408-410. doi:10.1021/np50062a036
- Jones, L. N. (2001). Hair structure anatomy and comparative anatomy 1. *Clinics in Dermatology*, *19*(2), 95-103. doi:http://dx.doi.org/10.1016/S0738-081X(00)00120-6
- Juráňová, J., Franková, J., & Ulrichová, J. (2017). The role of keratinocytes in inflammation. *Journal of Applied Biomedicine*, *15*(3), 169-179. doi:https://doi.org/10.1016/j.jab.2017.05.003
- Kanchanapoom, T., Kasai, R., Picheansoonthon, C., & Yamasaki, K. (2001). Megastigmane, aliphatic alcohol and benzoxazinoid glycosides from *Acanthus ebracteatus*. *Phytochemistry*, *58*(5), 811-817. doi:http://dx.doi.org/10.1016/S0031-9422(01)00306-5
- Kasumagic-Halilovic, E., Prohic, A., & Cavaljuga, S. (2011). Tumor necrosis factor- α in patients with alopecia areata. *Indian J Dermatol*, *56*(5), 494-496. doi:10.4103/0019-5154.87124
- Kataoka, T. (2009). Chemical biology of inflammatory cytokine signaling. *The Journal Of Antibiotics*, *62*, 655. doi:10.1038/ja.2009.98

- Kaufman, K. D., Olsen, E. A., Whiting, D., Savin, R., DeVillez, R., Bergfeld, W., . . . Gormley, G. J. (1998). Finasteride in the treatment of men with androgenetic alopecia. *Journal of the American Academy of Dermatology*, *39*, 578-589.
- Khalid, H., Zhari, I., Amirin, S., & Pazilah, I. (2011). Accelerated Stability and Chemical Kinetics of Ethanol Extracts of Fruit of Piper sarmentosum Using High Performance Liquid Chromatography. *Iranian Journal of Pharmaceutical Research : IJPR*, *10*(3), 403-413.
- Klimová, Z., Hojerová, J., Lucová, M., & Pažoureková, S. (2012). Dermal exposure to chemicals —evaluation of skin barrier damage. *Acta Chimica Slovaca*, *5*(1), 70—74.
- Koo, K. A., Kim, S. H., Oh, T. H., & Kim, Y. C. (2006). Acteoside and its aglycones protect primary cultures of rat cortical cells from glutamate-induced excitotoxicity. *Life sciences*, *79*(7), 709-716. doi:10.1016/j.lfs.2006.02.019
- Korkina, L. G., Mikhal'chik, E., Suprun, M. V., Pastore, S., & Dal Toso, R. (2007). Molecular mechanisms underlying wound healing and anti-inflammatory properties of naturally occurring biotechnologically produced phenylpropanoid glycosides. *Cell Mol Biol (Noisy-le-grand)*, *53*(5), 84-91.
- Koseki, J., Matsumoto, T., Matsubara, Y., Tsuchiya, K., Mizuhara, Y., Sekiguchi, K., . . . Kase, Y. (2015). Inhibition of Rat 5 α -Reductase Activity and Testosterone-Induced Sebum Synthesis in Hamster Sebocytes by an Extract of *Quercus acutissima* Cortex. *Evidence-based complementary and alternative medicine : eCAM*, 2015, 853846. doi:10.1155/2015/853846
- Kumar, S. (2011). Free Radicals and Antioxidants: Human and Food System Adv. *Appl. Sci. Res*, *2*(1), 129-135
- Laupattarakasem, P., Houghton, P. J., Houlst, J. R. S., & Itharat, A. (2003). An evaluation of the activity related to inflammation of four plants used in Thailand to treat arthritis. *Journal of Ethnopharmacology*, *85*(2–3), 207-215. doi:http://dx.doi.org/10.1016/S0378-8741(02)00367-7
- Lee, H.-J., Guo, H.-Y., Lee, S.-K., Jeon, B.-H., Jun, C.-D., Lee, S.-K., . . . Kim, E.-C. (2005). Effects of nicotine on proliferation, cell cycle, and differentiation in immortalized and malignant oral keratinocytes. *Journal of Oral Pathology & Medicine*, *34*(7), 436-443. doi:10.1111/j.1600-0714.2005.00342.x

- Lee, H. S., Jung, K.-H., Hong, S.-W., Park, I.-S., Lee, C., Han, H.-K., . . . Hong, S.-S. (2008). Morin protects acute liver damage by carbon tetrachloride (CCl₄) in rat. *Archives of Pharmacal Research*, *31*(9), 1160-1165. doi:10.1007/s12272-001-1283-5
- Lee, H. S., Jung, K. H., Hong, S. W., Park, I. S., Lee, C., Han, H. K., . . . Hong, S. S. (2008). Morin protects acute liver damage by carbon tetrachloride (CCl₄) in rat. *Arch Pharm Res*, *31*(9), 1160-1165. doi:10.1007/s12272-001-1283-5
- Lee, K.-W., Kim, H. J., Lee, Y. S., Park, H.-J., Choi, J.-W., Ha, J., & Lee, K.-T. (2007). Acteoside inhibits human promyelocytic HL-60 leukemia cell proliferation via inducing cell cycle arrest at G₀/G₁ phase and differentiation into monocyte. *Carcinogenesis*, *28*(9), 1928-1936. doi:10.1093/carcin/bgm126
- Lee, S. W., Juhasz, M., Mobasher, P., Ekelem, C., & Mesinkovska, N. A. (2018). A Systematic Review of Topical Finasteride in the Treatment of Androgenetic Alopecia in Men and Women. *J Drugs Dermatol*, *17*(4), 457-463.
- Li, L., Dai, H.-J., Ye, M., Wang, S.-L., Xiao, X.-J., Zheng, J., . . . Liu, J. (2012). Lycorine induces cell-cycle arrest in the G₀/G₁ phase in K562 cells via HDAC inhibition. *Cancer Cell International*, *12*, 49-49. doi:10.1186/1475-2867-12-49
- Li, Q., & Verma, I. M. (2002). NF-kappaB regulation in the immune system. *Nat Rev Immunol*, *2*(10), 725-734. doi:10.1038/nri910
- Lieb, L. M., Liimatta, A. P., Bryan, R. N., Brown, B. D., & Krueger, G. G. (1997). Description of the intrafollicular delivery of large molecular weight molecules to follicles of human scalp skin in vitro. *J Pharm Sci*, *86*(9), 1022-1029. doi:10.1021/js9700053
- Liebezeit, G., & Rau, M. T. (2006). New Guinean mangroves — traditional usage and chemistry of natural products. *Senckenbergiana maritima*, *36*(1), 1-10. doi:10.1007/bf03043698
- Lim, K. M., An, S., Lee, O.-K., Lee, M. J., Lee, J. P., Lee, K. S., . . . Bae, S. (2015). Analysis of changes in microRNA expression profiles in response to the troxerutin-mediated antioxidant effect in human dermal papilla cells. *Molecular Medicine Reports*, *12*(2), 2650-2660. doi:10.3892/mmr.2015.3717

- Little, J. C., Westgate, G. E., Evans, A., & Granger, S. P. (1994). Cytokine Gene Expression in Intact Anagen Rat Hair Follicles. *Journal of Investigative Dermatology*, *103*(5), 715-720. doi:<https://doi.org/10.1111/1523-1747.ep12398584>
- Liu, S., Zhang, J., Li, W., Zhang, T., & Hu, D. (2015). Acteoside reduces testosterone by inhibiting cAMP, p450scc, and StAR in rat Leydig cells. *Molecular & Cellular Toxicology*, *11*, 11-17. doi:10.1007/s13273-015-0002-x
- Lu, Z. F., Cai, S. Q., Wu, J. J., & Zheng, M. (2006). Biological characterization of cultured dermal papilla cells and hair follicle regeneration in vitro and in vivo. *Chin Med J (Engl)*, *119*(4), 275-281.
- Mahé, Y. F., Buan, B., Billoni, N., Loussouarn, G., Michelet, J. F., Gautier, B., & Bernard, B. A. (1996). Pro-inflammatory cytokine cascade in human plucked hair. *Skin Pharmacol*, *9*(6), 366-375. doi:10.1159/000211447
- Mahé, Y. F., Michelet, J.-F., Billoni, N., Jarrousse, F., Buan, B., Commo, S., & Saint-Léger, D. (2000). Androgenetic alopecia and microinflammation. *International Journal of Dermatology*, *39*(8), 576-584. doi:10.1046/j.1365-4362.2000.00612.x
- Mahe, Y. F., Michelet, J. F., Billoni, N., Jarrousse, F., Buan, B., Commo, S., . . . Bernard, B. A. (2000). Androgenetic alopecia and microinflammation. *Int J Dermatol*, *39*(8), 576-584.
- Mahesh, R., Bhuvana, S., & Hazeena Begum, V. M. (2009). Effect of Terminalia chebula aqueous extract on oxidative stress and antioxidant status in the liver and kidney of young and aged rats. *Cell Biochemistry and Function*, *27*(6), 358-363. doi:10.1002/cbf.1581
- Makoni, P. A., Wa Kasongo, K., & Walker, R. B. (2019). Short Term Stability Testing of Efavirenz-Loaded Solid Lipid Nanoparticle (SLN) and Nanostructured Lipid Carrier (NLC) Dispersions. *Pharmaceutics*, *11*(8). doi:10.3390/pharmaceutics11080397
- Marie, D. L. (2007). *Physical analysis of human hair*. Theses: Masters
- Martinho, N., Damgã, C., & Reis, C. P. (2011). Recent Advances in Drug Delivery Systems. *Journal of Biomaterials and Nanobiotechnology*, *2*(5), 17. doi:10.4236/jbmb.2011.225062

- Mirmirani, P., & Karnik, P. (2010). Comparative Gene Expression Profiling of Senescent and Androgenetic Alopecia Using Microarray Analysis. In R. M. Trüeb & D. J. Tobin (Eds.), *Aging Hair* (pp. 67-76). New York: Springer-Verlag Berlin Heidelberg
- Mohd, F., Todo, H., Yoshimoto, M., Yusuf, E., & Sugibayashi, K. (2016). Contribution of the Hair Follicular Pathway to Total Skin Permeation of Topically Applied and Exposed Chemicals. *Pharmaceutics*, 8(4), 32. doi:10.3390/pharmaceutics8040032
- Mori, O., & Uno, H. (1990). The effect of topical minoxidil on hair follicular cycles of rats. *J Dermatol*, 17(5), 276-281. doi:10.1111/j.1346-8138.1990.tb01641.x
- Müller, R. H., Mäder, K., & Gohla, S. (2000). Solid lipid nanoparticles (SLN) for controlled drug delivery – a review of the state of the art. *European Journal of Pharmaceutics and Biopharmaceutics*, 50(1), 161-177. doi:https://doi.org/10.1016/S0939-6411(00)00087-4
- Nagulsamy, P., Ponnusamy, R., & Thangaraj, P. (2015). Evaluation of antioxidant, anti-inflammatory, and antiulcer properties of *Vaccinium leschenaultii* Wight: A therapeutic supplement. *Journal of Food and Drug Analysis*, 23(3), 376-386. doi:https://doi.org/10.1016/j.jfda.2014.11.003
- Nazemiyeh, H., Rahman, M. M., Gibbons, S., Nahar, L., Delazar, A., Ghahramani, M.-A., . . . Sarker, S. D. (2008). Assessment of the antibacterial activity of phenylethanoid glycosides from *Phlomis lanceolata* against multiple-drug-resistant strains of *Staphylococcus aureus*. *Journal of natural medicines*, 62(1), 91-95. doi:10.1007/s11418-007-0194-z
- Ng, S.-F., Rouse, J. J., Sanderson, F. D., Meidan, V., & Eccleston, G. M. (2010). Validation of a Static Franz Diffusion Cell System for In Vitro Permeation Studies. *AAPS PharmSciTech*, 11(3), 1432-1441. doi:10.1208/s12249-010-9522-9
- Ngwuluka, N. C., Kotak, D. J., & Devarajan, P. V. (2017). Design and Characterization of Metformin-Loaded Solid Lipid Nanoparticles for Colon Cancer. *AAPS PharmSciTech*, 18(2), 358-368. doi:10.1208/s12249-016-0505-

- Nina, O., Alexa, P., Utkur, R., Timo, H., Michael, L., Ronald, S., . . . Jürgen, L. (2008). The role of hair follicles in the percutaneous absorption of caffeine. *British Journal of Clinical Pharmacology*, 65(4), 488-492. doi:10.1111/j.1365-2125.2007.03065.x
- OECD. (2004). OECD GUIDELINE FOR THE TESTING OF CHEMICALS *Skin Absorption: in vitro Method* OECD.
- Olsen, E. A., Dunlap, F. E., Funicella, T., Koperski, J. A., Swinehart, J. M., Tschien, E. H., & Trancik, R. J. (2002). A randomized clinical trial of 5% topical minoxidil versus 2% topical minoxidil and placebo in the treatment of androgenetic alopecia in men. *J Am Acad Dermatol*, 47(3), 377-385.
- Olsen, E. A., Weiner, M. S., DeLong, E. R., & Pinnell, S. R. (1985). Topical minoxidil in early male pattern baldness. *Journal of the American Academy of Dermatology*, 13(2, Part 1), 185-192. doi:https://doi.org/10.1016/S0190-9622(85)70157-0
- Olsen, E. A., Whiting, D. A., Savin, R., Rodgers, A., Johnson-Levonas, A. O., Round, E., . . . Kaufman, K. D. Global photographic assessment of men aged 18 to 60 years with male pattern hair loss receiving finasteride 1 mg or placebo. *Journal of the American Academy of Dermatology*, 67(3), 379-386. doi:10.1016/j.jaad.2011.10.027
- Parameswaran, N., & Patial, S. (2010). Tumor Necrosis Factor- α Signaling in Macrophages. *Critical reviews in eukaryotic gene expression*, 20(2), 87-103.
- Pesce, M., Franceschelli, S., Ferrone, A., De Lutiis, M. A., Patruno, A., Grilli, A., . . . Speranza, L. (2015). Verbascoside down-regulates some pro-inflammatory signal transduction pathways by increasing the activity of tyrosine phosphatase SHP-1 in the U937 cell line. *Journal of cellular and molecular medicine*, 19(7), 1548-1556. doi:10.1111/jcmm.12524
- Pesce, M., Franceschelli, S., Ferrone, A., De Lutiis, M. A., Patruno, A., Grilli, A., . . . Speranza, L. (2015). Verbascoside down-regulates some pro-inflammatory signal transduction pathways by increasing the activity of tyrosine phosphatase SHP-1 in the U937 cell line. *Journal of cellular and molecular medicine*, 19(7), 1548-1556. doi:10.1111/jcmm.12524

- Philpott, M. P., Sanders, D. A., Bowen, J., & Kealey, T. (1996). Effects of interleukins, colony-stimulating factor and tumour necrosis factor on human hair follicle growth in vitro: a possible role for interleukin-1 and tumour necrosis factor-alpha in alopecia areata. *British Journal of Dermatology*, *135*(6), 942-948. doi:10.1046/j.1365-2133.1996.d01-1099.x
- Phisalaphong, M., Thu Ha, N. T., & Siripong, P. (2006). Desalting of Aqueous Extract of *Acanthus ebracteatus* Vahl. by Nanofiltration. *Separation Science and Technology*, *41*(3), 455-470. doi:10.1080/01496390500524644
- Prasansuklab, A., & Tencomnao, T. (2018). *Acanthus ebracteatus* leaf extract provides neuronal cell protection against oxidative stress injury induced by glutamate. *BMC Complement Altern Med*, *18*(1), 278. doi:10.1186/s12906-018-2340-4
- Prausnitz, M. R., & Langer, R. (2008). Transdermal drug delivery. *Nature biotechnology*, *26*(11), 1261-1268. doi:10.1038/nbt.1504
- Prie, B. E., Iosif, L., Tivig, I., Stoian, I., & Giurcaneanu, C. (2016). Oxidative stress in androgenetic alopecia. *Journal of Medicine and Life*, *9*(1), 79-83.
- Qiao, Z., Tang, J., Wu, W., Tang, J., & Liu, M. (2019). Acteoside inhibits inflammatory response via JAK/STAT signaling pathway in osteoarthritic rats. *BMC Complementary and Alternative Medicine*, *19*(1), 264-271. doi:10.1186/s12906-019-2673-7
- Randall, V. A., & Botchkareva, N. I. (2009). The Biology of Hair Growth. In G. S. Ahluwalia (Ed.), *Cosmetic applications of laser & light-based systems* (pp. 4-13): William Andrew
- Rao, Y. K., Fang, S. H., Hsieh, S. C., Yeh, T. H., & Tzeng, Y. M. (2009). The constituents of *Anisomeles indica* and their anti-inflammatory activities. *J Ethnopharmacol*, *121*(2), 292-296. doi:10.1016/j.jep.2008.10.032
- Rostamkalaei, S. S., Akbari, J., Saeedi, M., Morteza-Semnani, K., & Nokhodchi, A. (2019). Topical gel of Metformin solid lipid nanoparticles: A hopeful promise as a dermal delivery system. *Colloids Surf B Biointerfaces*, *175*, 150-157. doi:10.1016/j.colsurfb.2018.11.072

- Ruktanonchai, U., Sakulkhu, U., Bejrappa, P., Opanasopit, P., Bunyapraphatsara, N., Junyaprasert, V., & Puttipipatkachorn, S. (2009). Effect of lipid types on physicochemical characteristics, stability and antioxidant activity of gamma-oryzanol-loaded lipid nanoparticles. *J Microencapsul*, 26(7), 614-626. doi:10.3109/02652040802586571
- Sakr, F. M., Gado, A. M. I., Mohammed, H. R., & Adam, A. N. I. (2013). Preparation and evaluation of a multimodal minoxidil microemulsion versus minoxidil alone in the treatment of androgenic alopecia of mixed etiology: A pilot study. *Drug Design, Development and Therapy*, 7, 413-423. doi:10.2147/DDDT.S43481
- Salminen, H., Helgason, T., Aulbach, S., Kristinsson, B., Kristbergsson, K., & Weiss, J. (2014). Influence of co-surfactants on crystallization and stability of solid lipid nanoparticles. *J Colloid Interface Sci*, 426, 256-263. doi:10.1016/j.jcis.2014.04.009
- Schembri, K., Scerri, C., & Ayers, D. (2013). Plucked Human Hair Shafts and Biomolecular Medical Research. *The Scientific World Journal*, 2013, 620531. doi:10.1155/2013/620531
- Schumann, R. R., Belka, C., Reuter, D., Lamping, N., Kirschning, C. J., Weber, J. R., & Pfeil, D. (1998). Lipopolysaccharide Activates Caspase-1 (Interleukin-1–Converting Enzyme) in Cultured Monocytic and Endothelial Cells. *Blood*, 91(2), 577.
- Sheng, G. Q., Zhang, J. R., Pu, X. P., Ma, J., & Li, C. L. (2002). Protective effect of verbascoside on 1-methyl-4-phenylpyridinium ion-induced neurotoxicity in PC12 cells. *Eur J Pharmacol*, 451(2), 119-124.
- Singh, M. N., Hemant, K. S. Y., Ram, M., & Shivakumar, H. G. (2010). Microencapsulation: A promising technique for controlled drug delivery. *Research in Pharmaceutical Sciences*, 5(2), 65-77.
- Speranza, L., Franceschelli, S., Pesce, M., Reale, M., Menghini, L., Vinciguerra, I., . . . Grilli, A. (2010). Antiinflammatory effects in THP-1 cells treated with verbascoside. *Phytother Res*, 24(9), 1398-1404. doi:10.1002/ptr.3173

- Su, D., Li, W., Xu, Q., Liu, Y., Song, Y., & Feng, Y. (2016). New metabolites of acetoacetic acid identified by ultra-performance liquid chromatography/quadrupole-time-of-flight MSE in rat plasma, urine, and feces. *Fitoterapia*, *112*, 45-55. doi:<https://doi.org/10.1016/j.fitote.2016.05.004>
- Todo, H., Kimura, E., Yasuno, H., Tokudome, Y., Hashimoto, F., Ikarashi, Y., & Sugibayashi, K. (2010). Permeation Pathway of Macromolecules and Nanospheres through Skin. *Biological and Pharmaceutical Bulletin*, *33*(8), 1394-1399. doi:10.1248/bpb.33.1394
- Trüeb, R. M. (2002). Molecular mechanisms of androgenetic alopecia. *Experimental Gerontology*, *37*(8-9), 981-990. doi:[http://dx.doi.org/10.1016/S0531-5565\(02\)00093-1](http://dx.doi.org/10.1016/S0531-5565(02)00093-1)
- Trüeb, R. M. (2015). The impact of oxidative stress on hair. *International journal of cosmetic science*, *37*(S2).
- Twist, J., & L. Zatz, J. (1988). *Membrane-solvent-solute interaction in a model permeation system (Vol. 77)*.
- Twist, J. N., & Zatz, J. L. (1986). Influence of solvents on paraben permeation through idealized skin model membranes. *Journal of the Society of Cosmetic Chemists*, *37*(6), 429-444.
- Uner, M., Wissing, S. A., Yener, G., & Muller, R. H. (2005). Solid lipid nanoparticles (SLN) and nanostructured lipid carriers (NLC) for application of ascorbyl palmitate. *Pharmazie*, *60*(8), 577-582.
- Upton, J. H., Hannen, R. F., Bahta, A. W., Farjo, N., Farjo, B., & Philpott, M. P. (2015). Oxidative Stress-Associated Senescence in Dermal Papilla Cells of Men with Androgenetic Alopecia. *Journal of Investigative Dermatology*, *135*(5), 1244-1252. doi:<https://doi.org/10.1038/jid.2015.28>
- Vallotton, P., & Thomas, N. (2008). Automated body hair counting and length measurement. *Skin Research and Technology*, *14*(4), 493-497. doi:10.1111/j.1600-0846.2008.00322.x
- Van Neste, D., Fuh, V., Sanchez-Pedreno, P., Lopez-Bran, E., Wolff, H., Whiting, D., . . . Kaufman, K. D. (2000). Finasteride increases anagen hair in men with androgenetic alopecia. *British Journal of Dermatology*, *143*(4), 804-810. doi:10.1046/j.1365-2133.2000.03780.x

- Varothai, S., & Bergfeld, W. F. (2014). Androgenetic Alopecia: An Evidence-Based Treatment Update. *American Journal of Clinical Dermatology*, *15*, 217–230.
- Vats, S., Saxena, C., Easwari, T. S., & Shukla, V. (2014). *Emulsion Based Gel Technique: Novel Approach for Enhancing Topical Drug Delivery of Hydrophobic Drugs* (Vol. 3).
- Vernon, C. A., & Perutz, M. F. (1967). The mechanisms of hydrolysis of glycosides and their relevance to enzyme-catalysed reactions. *Proceedings of the Royal Society of London. Series B. Biological Sciences*, *167*(1009), 389-401.
doi:10.1098/rspb.1967.0036
- Vertuani, S., Beghelli, E., Scalambra, E., Malisardi, G., Copetti, S., Dal Toso, R., . . . Manfredini, S. (2011). Activity and stability studies of verbascoside, a novel antioxidant, in dermo-cosmetic and pharmaceutical topical formulations. *Molecules*, *16*(8), 7068-7080. doi:10.3390/molecules16087068
- Wang, H., Xu, Y., Yan, J., Zhao, X., Sun, X., Zhang, Y., . . . Zhu, C. (2009). Acteoside protects human neuroblastoma SH-SY5Y cells against beta-amyloid-induced cell injury. *Brain Res*, *1283*, 139-147.
doi:10.1016/j.brainres.2009.05.101
- Wasko, C. A., Mackley, C. L., Sperling, L. C., Mauger, D., & Miller, J. J. (2008). Standardizing the 60-second hair count. *Arch Dermatol*, *144*(6), 759-762.
doi:10.1001/archderm.144.6.759
- Wester, R. C., & Maibach, H. I. (1992). Percutaneous Absorption of Drugs. *Clinical Pharmacokinetics*, *23*(4), 253-266. doi:10.2165/00003088-199223040-00002
- Whiting, D. A. (1993). Diagnostic and predictive value of horizontal sections of scalp biopsy specimens in male pattern androgenetic alopecia. *J Am Acad Dermatol*, *28*(5 Pt 1), 755-763.
- WHO. (2017). *Stability Testing of Active Pharmaceutical Ingredients and Finished Pharmaceutical Products*. Switzerland: WHO.
- Williams, A. C. (2015). *Topical and transdermal drug delivery*. N.P: n.p.
- Winiarska, A., Mandt, N., Kamp, H., Hossini, A., Seltmann, H., Zouboulis, C. C., & Blume-Peytavi, U. (2006). Effect of 5 α -Dihydrotestosterone and Testosterone on Apoptosis in Human Dermal Papilla Cells. *Skin Pharmacology and Physiology*, *19*(6), 311-321.

- Winyard, P. G., Ryan, B., Eggleton, P., Nissim, A., Taylor, E., Lo Faro, M. L., . . . Whiteman, M. (2011). Measurement and meaning of markers of reactive species of oxygen, nitrogen and sulfur in healthy human subjects and patients with inflammatory joint disease. *Biochem Soc Trans*, *39*(5), 1226-1232. doi:10.1042/bst0391226
- Wisuitiprot, V., Ingkaninan, K., Wisuitiprot, W., & Waranuch, N. (2016). Study of some medicinal plants on dermal papilla cells. In *Paper presented at the Naresuan Research Conference*. Phitsanulok, Thailand: Naresuan University.
- Wosicka, H., & Cal, K. (2010). Targeting to the hair follicles: Current status and potential. *Journal of Dermatological Science*, *57*(2), 83-89. doi:10.1016/j.jdermsci.2009.12.005
- Wu, K., Li, J., Wang, W., & Winstead, D. A. (2009). Formation and characterization of solid dispersions of piroxicam and polyvinylpyrrolidone using spray drying and precipitation with compressed antisolvent. *J Pharm Sci*, *98*(7), 2422-2431. doi:10.1002/jps.21598
- Wu, Y., Li, L., Zhou, S., Shen, Q., Lin, H., Zhu, Q., . . . Ge, R. S. (2017). Apigenin inhibits rat neurosteroidogenic 5 α -reductase 1 and 3 α -hydroxysteroid dehydrogenase. *Neurochem Int*, *110*, 84-90. doi:10.1016/j.neuint.2017.09.010
- Xiong, Q., Hase, K., Tezuka, Y., Namba, T., & Kadota, S. (1999). Acteoside inhibits apoptosis in D-galactosamine and lipopolysaccharide-induced liver injury. *Life Sci*, *65*(4), 421-430. doi:10.1016/s0024-3205(99)00263-5
- Yang, Y.-L. (2016). Verbascoside Reverses TGF- β 1-Induced Renal Cellular Fibrosis. *Journal of Diabetes, Metabolic Disorders & Control*, *3*, 122-127. doi:10.15406/jdmdc.2016.03.00083
- Yenin, J. Z., Serarslan, G., Yönden, Z., & Ulutaş, K. T. (2014). Investigation of oxidative stress in patients with alopecia areata and its relationship with disease severity, duration, recurrence and pattern. *Clinical and Experimental Dermatology*, *40*(6), 617-621. doi:10.1111/ced.12556
- York, K., Meah, N., Bhojrul, B., & Sinclair, R. (2020). A review of the treatment of male pattern hair loss. *Expert Opin Pharmacother*, *21*(5), 603-612. doi:10.1080/14656566.2020.1721463



APPENDIX

มหาวิทยาลัยนครพนม



OPEN **Effects of *Acanthus ebracteatus* Vahl. extract and verbascoside on human dermal papilla and murine macrophage**

Vanuchawan Wisuitiprot¹, Kornkanok Ingkaninan², Panlop Chakkavittumrong³, Wudtichai Wisuitiprot⁴, Nitra Neungchamnong⁵, Ruttanaporn Chantakul⁶ & Neti Waranuch^{1,7,✉}

Androgenic alopecia is a common type of hair loss, usually caused by testosterone metabolism generating dihydrotestosterone and hair follicular micro-inflammation. These processes induce dermal papilla cells to undergo apoptosis. Currently approved effective medications for alopecia are Finasteride, an oral 5 α -reductase inhibitor, Minoxidil, a topical hair growth promoter, and Diclofenac, an anti-inflammatory agent, all of which, however, have several adverse side effects. In our study, we showed the bioactivity of *Acanthus ebracteatus* Vahl. (AE) extract performed by 95% ethanol, and verbascoside (VB), a biomarker of AE extract. Both AE extract and VB were studied for their effects on dermal papilla cell viability and the cell cycle by using MTT assay and flow cytometry. The effect of an anti-inflammatory activity of AE extract and VB on IL-1 β , NO, and TNF- α , released from LPS induced RAW 264.7 cells, and IL-1 α and IL-6 released from irradiated dermal papilla cells were detected using ELISA technique. The preventive effect on dermal papilla cell apoptosis induced by testosterone was determined by MTT assay. In controlled in vitro assays it was found that AE extract and VB at various concentrations induced dermal papilla cell proliferation which was indicated by an increase in the number of cells in the S and G2/M phases of the cell cycle. AE extract at 250 μ g/mL concentration or VB at 62.50 μ g/mL concentration prevented cell apoptosis induced by testosterone at a statistically significant level. In addition, both AE extract and VB greatly inhibited the release of pro-inflammatory cytokines from RAW 264.7 and dermal papilla cells. The release of IL-1 β , TNF- α , and NO from RAW 264.7 cells, as well as IL-1 α and IL-6 from dermal papilla cells, was also diminished by AE extract 250 μ g/mL and VB 125 μ g/mL. Our results indicate that AE extract and VB are promising ingredients for anti-hair loss applications. However, further clinical study is necessary to evaluate the effectiveness of AE extract and VB as treatment for actual hair loss.

Androgenic alopecia (AGA) is the most common form of hair loss in men and women and can be serious enough to have a detrimental effect on an individual's social life and self-confidence. Several hypotheses regarding the mechanism and cause of hair loss have suggested that the most influential factor in hair loss is the metabolism of testosterone into the more potent androgen dihydrotestosterone (DHT) using enzyme 5 α -reductase. DHT then binds with the androgen receptor in the cytosol of dermal papilla cells to form a complex. The androgen receptor complex translocate into the nucleus and consequently activates androgen receptor-regulated genes¹. This results in stimulation of TGF- β mRNA synthesis in the dermal papilla cells. TGF- β is an important trigger of

¹Department of Pharmaceutical Technology, Faculty of Pharmaceutical Sciences and Center of Excellence for Innovation in Chemistry, Naresuan University, Phitsanulok 65000, Thailand. ²Department of Pharmaceutical Chemistry and Pharmacognosy, Faculty of Pharmaceutical Sciences, Naresuan University, Phitsanulok 65000, Thailand. ³Division of Dermatology, Department of Medicine, Faculty of Medicine, Thammasat University, Khlong Luang, Pathumthani 12121, Thailand. ⁴Department of Thai Traditional Medicine, Sirindhorn College of Public Health, Phitsanulok 65130, Thailand. ⁵Science Laboratory Centre, Faculty of Science, Naresuan University, Mueang, Phitsanulok 65000, Thailand. ⁶Bioscreening Unit, Department of Pharmaceutical Chemistry and Pharmacognosy, Faculty of Pharmaceutical Sciences, Naresuan University, Phitsanulok 65000, Thailand. ⁷Cosmetics and Natural Products Research Center, Faculty of Pharmaceutical Sciences, Naresuan University, Phitsanulok 65000, Thailand. ✉email: netiw@nu.ac.th

the intrinsic caspase network and programmed cell death, or apoptosis, of derma papilla cells². The apoptosis of dermal papilla cells also induces the catagen phase of the hair growth cycle, causing the hair to stop growing⁴.

Another contributing factor to hair loss is hair follicle microinflammation which has been identified in patients presenting baldness¹. Researchers have noted that some inflammatory cytokines in alopecia patients are higher than in the unaffected scalp. Others reported that inflammatory cytokines, such as IL-1 β , IL-1 α , IL-6, TNF- α , NO and prostaglandin D2, destroyed hair follicle structure and spurred dermal papilla to undergo apoptosis⁵⁻⁹. Inflammation and the apoptosis of cells involve the caspase-1 named inflammasome, which triggers an inflammatory chain reaction. Testosterone and DHT have also been found to contribute to inflammation¹⁰. According to two influential factors mentioned previously, anti-testosterone activity has been concerned particularly with 5 α -reductase inhibition activity.

Anti-inflammatory agents are often chosen for multimodal treatments for alopecia¹¹⁻¹⁶. However, many of these treatments have undesirable side effects. Finasteride is a synthetic 5 α -reductase inhibitor combined with an anti-inflammatory agent that is used to treat androgenic alopecia induced by the androgenic hormones¹⁷. Although finasteride is an effective treatment for AGA, patients taking this medication also suffer the detrimental side effect of sexual dysfunction. Moreover, finasteride is not approved for use in women with hair loss, particularly as it is especially dangerous for pregnant women, possibly causing abnormalities of the external genitalia in the male fetus¹³. Anti-inflammatory drugs in the NSAIDs group, used as a hair loss treatment, have diverse side effects such as GI disturbance and the potential negative effects during pregnancy^{18,19}. Minoxidil is also a common treatment for alopecia^{13,20}. However, common side effects of topical minoxidil administration are facial hypertrichosis and local intravascular spread of minoxidil. In some cases, patients using minoxidil have allergic reactions to propylene glycol, which is used in commercial minoxidil preparation^{21,22}.

There is, therefore, a need to develop new hair loss applications because of these various adverse side effects of current hair loss medications. Due to a growing understanding of the mechanisms causing AGA, researchers are interested in investigating herb-derived compounds that show anti-androgenic and anti-inflammatory activity as potential new ingredients for hair loss treatments.

Acanthus ebracteatus Vahl. (AE) is a medicinal plant that has been traditionally used as an anti-inflammatory agent, and has been used in traditional medicines as an ingredient in anti-cancer and anti-inflammatory formulations²³. One report from Malaysia recommends that the leaves of AE be used as an anti-hair loss remedy²⁴. A few reports have found that the ethanolic extract of AE contained various bioactive compounds including verbascoside (VB)²⁵, which is a promising phenylpropanoid compound in phytotherapy. Other studies have reported the anti-inflammatory activity of VB that has been isolated from many local herbs. Cyclooxygenase-1 (COX-1) and Cyclooxygenase-2 (COX-2) were inhibited by VB isolated from *Marrubium vulgare* with IC₅₀ at 1.00 mM and 0.69 mM concentrations, respectively²⁶. One article reported that VB decreased the expression of the COX enzyme by increasing the phosphorylation of the Src homology region 2 domain-containing phosphatase-1 (SHP-1). SHP-1 plays a crucial role in the synthesis of COX-2 and inducible nitric oxide synthase (iNOS)²⁷. In addition, recent studies reported that the anti-inflammatory activity of VB was due to the suppression of TGF- β gene expression^{27,28}. VB also affects the testosterone metabolism in Leydig cells and also decreases the testosterone level by down-regulating cAMP and preventing cell apoptosis²⁹. Thus, VB might be a promising compound for treating hair loss induced by testosterone metabolism and hair follicle inflammation. The objectives of our study were to identify the bioactivity of AE extract and VB, particularly their potential anti-androgenic and anti-inflammatory activities.

We investigated the inhibitory effect of AE extract and VB against the factors that contribute to hair loss in the human dermal papilla and mouse macrophage cells. Specifically, we examined 5 α -reductase inhibition activity, anti-inflammatory actions through the inhibition of IL-1 β , IL-1 α , TNF- α , NO, IL-6 expression, and protection against dermal papilla apoptosis.

Results

Plant extract preparation and VB analyzed using HPLC. AE extracts were prepared using 95% ethanol, 50% ethanol, water and hexane. The amount of VB in each extract was measured using the HPLC technique. The indicative HPLC method linearity was defined as having r^2 greater or equal to 0.9997 using concentrations ranging from 19.53 to 1000.00 $\mu\text{g/mL}$. The limit of detection (LOD) value of VB was 0.04 $\mu\text{g/mL}$ while the limit of quantification (LOQ) was 0.12 $\mu\text{g/mL}$. This method was precise with intra-day relative standard deviation (%RSD) less than 5.84% and inter-day values less than 5.05%. The method also showed high accuracy with percentage recovery ranging from 90 to 110%. Therefore, this HPLC method was accurate and reliable for the determination of the amount of VB in AE extract. Sample chromatogram of VB in AE extract with 95% ethanol is presented in Fig. 1.

VB contents in various AE extracts are shown in Table 1. The highest content of VB was found in an extract using 95% ethanol ($9.58 \pm 0.65\%$). In contrast, VB could not be detected in the AE extract using hexane. These results suggest that AE extract in 95% ethanol was a promising candidate for further study because it had the highest content of VB.

Determination of 5 α -Reductase Inhibition. One hundred micrograms per milliliter of each AE extract was determined for 5 α -reductase inhibitory activity. Finasteride was used as the positive control. Their inhibitory activities are shown in Table 2. The comparison of the inhibition activities indicated that AE extract with 95% ethanol showed the highest inhibition ($38.26 \pm 4.90\%$), followed by AE extract with hexane ($36.92 \pm 2.41\%$), 50% ethanol ($13.72 \pm 4.88\%$) and water ($6.75 \pm 4.20\%$) while, surprisingly, no inhibitory activity was found for VB. AE extract with 95% ethanol was selected for further bioactivity studies of both VB content and 5 α -reductase inhibitory activity.

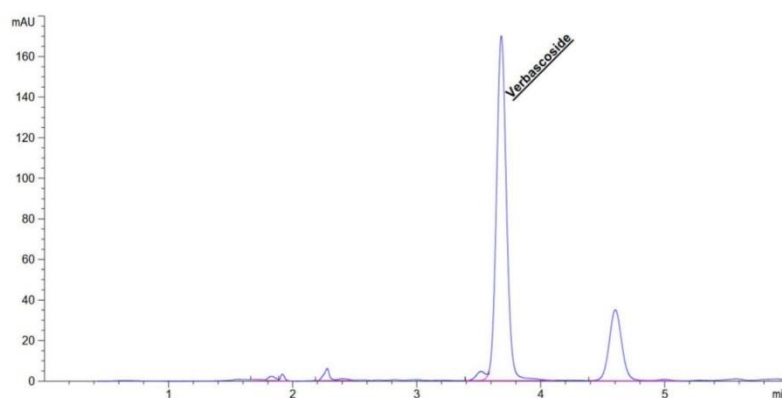


Figure 1. Sample high-performance liquid chromatography (HPLC) chromatogram of VB in 95% ethanol extract of AE.

Type of solvent for AE extract	VB (% \pm SD, w/w)
95% ethanol extract	9.58 \pm 0.65
50% ethanol extract	2.03 \pm 0.04
Water extract	3.10 \pm 0.10
Hexane extract	Below limit of detection

Table 1. Amount of VB in AE extracts obtained with various solvents, measured by high-performance liquid chromatography (HPLC) ($n \geq 3$).

Type of sample	5 α -reductase inhibition (% \pm SD)
AE extract in 95% ethanol	38.26 \pm 4.90
AE extract in 50% ethanol	13.72 \pm 4.88
AE extract in water	6.75 \pm 4.20
AE extract in hexane	36.92 \pm 2.41
VB	None
Finasteride	98.58 \pm 1.96

Table 2. 5 α -reductase inhibitory activity of Finasteride, VB and AE extracts of various solvents. ($n \geq 3$). AE extract and VB concentrations were 100 μ g/mL, finasteride concentration was 1.5 μ g/mL.

Cytotoxic effect of AE extract and VB on human dermal papilla cells. The cytotoxic effect of AE extract with 95% ethanol on dermal papilla cells was evaluated by MTT assay. The results indicated that AE extract and VB at a concentration of 0.98 to 500 μ g/mL did not show any cytotoxic effects on dermal papilla cells (Fig. 2). All of the treated cells presented relative cell viability of more than 80% compared to the control cells³⁰. Interestingly, VB at 31.25 to 500 μ g/mL concentration and AE extract at 62.50 to 500 μ g/mL concentration showed significantly increased relative cell viability of dermal papilla cells. This means that AE extract and VB at these concentrations might be able to activate dermal papilla cell proliferation.

Cell cycle analysis. Dermal papilla cells were treated with AE extract of 95% ethanol or VB at a concentration between 31.25 and 500 μ g/mL for 24 h. They were then analyzed at different points in the cell cycle with propidium iodide staining. AE extract showed different effects on the dermal papilla depending on concentrations (Fig. 3a). The dermal papilla cell growth (G1 phase) was stimulated by AE extract 500 μ g/mL. However, the preparation for cell division (G2/M phase) was lower than that of the control cells. On the contrary, AE extract at 250 μ g/mL and 125 μ g/mL concentrations showed a significantly increased number of cells in the G2/M

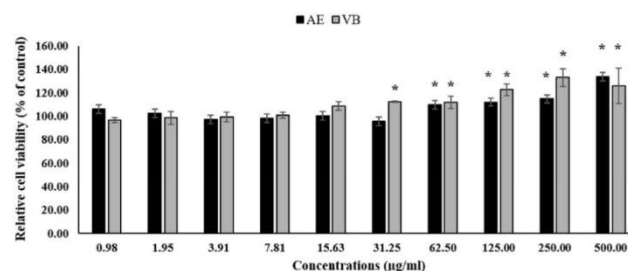


Figure 2. Relative cell viability of dermal papilla cells treated with AE extract or VB for 24 h (* significantly different from control cells at $p < 0.05$, Student's *t*-test). ($n \geq 3$).

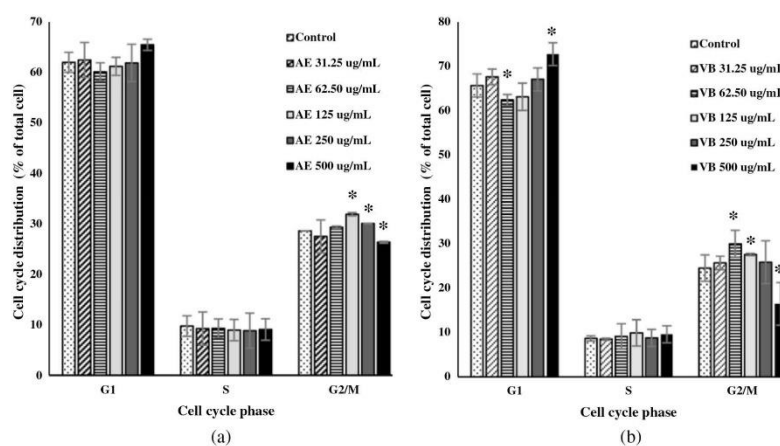


Figure 3. The effects of AE extract (a), VB (b) on the dermal papilla cell cycle; * significantly different from control at $p < 0.05$ Student's *t*-test. ($n \geq 3$).

phase compared to the control cells. In the case of VB, the concentration of 500 µg/mL significantly increased the number of cells in the G1 phase (Fig. 3b), but decreased the number of cells in the G2/M phase compared to the control cells. The positive effects of VB 62.50 µg/mL on the G2/M and G1 phases of the dermal papilla cells were significant. The number of cells in the G2/M phase significantly increased, while the number of cells in the G1 phase decreased after being treated by VB 62.50 µg/mL. In addition, treating the cells with VB 125 µg/mL resulted in an increased number of cells in the G2/M phase compared to the control cells while no difference of G1 phase from control cells was observed. All of the treatment concentrations had no effects on the number of cells in the DNA replication stage (S phase) of the cell cycle.

Inhibition effects of AE extract and VB on testosterone-induced cell apoptosis. Cell apoptosis was determined in terms of cell viability. The concentration of 250 µg/mL 95% ethanol AE extract was the optimal value identified in our cell cycle analysis and was therefore selected for these tests. Two hundred micromolar concentrations of testosterone caused a decrease in dermal papilla cells viability when the cells were treated for 4 days (Fig. 4). Cell viability remained close to 100% when the dermal papilla cells were treated with 200 µM testosterone and 250 µg/mL AE extract in combination. VB 62.50 µg/mL was also effective in preventing testosterone induced cell apoptosis, showing results similar to AE extract 250 µg/mL or 75 nM finasteride.

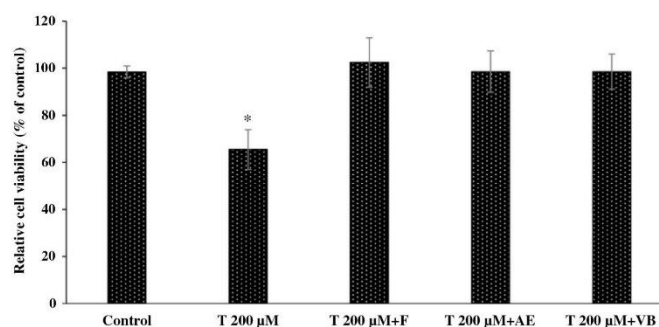


Figure 4. Relative cell viability of dermal papilla cells when being treated with testosterone 200 μM (T 200 μM), testosterone 200 μM plus AE extract 250 μg/ml (T 200 μM + AE), testosterone 200 μM plus finasteride 75 nM (T 200 μM + F) and testosterone 200 μM plus VB 62.50 μg/mL (T 200 μM + VB) (* significantly different from control at $p < 0.05$, Student's *t*-test). (n ≥ 3).

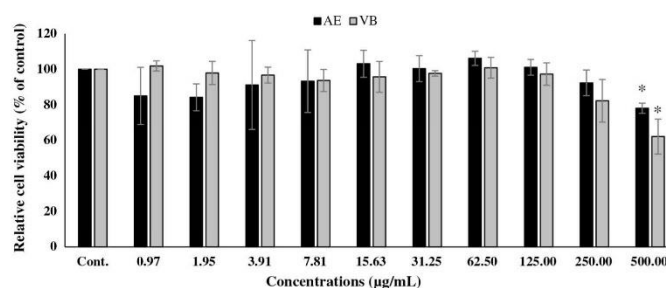


Figure 5. Relative cell viability of RAW 264.7 cells treated with different concentrations of AE extract or VB for 24 h; Cont. = Control. * Significantly different from control at $p < 0.05$ Student's *t*-test. (n ≥ 3).

Cytotoxic effect of AE extract and VB on murine macrophage RAW 264.7 cells. Cytotoxicity of various concentrations of 95% ethanol AE extract and VB on RAW 264.7 cells was determined using MTT assay. The results are shown in Fig. 5. The study found that both AE extract and VB were safe at concentrations up to 250 μg/mL. Thus, we selected these as the upper limit concentrations for further study on anti-inflammatory activity in macrophage cells.

Effects of AE extract and VB on IL-1 β , NO, and TNF- α production in LPS-stimulated macrophages. RAW 264.7 cells were treated by LPS to induce the release of IL-1 β , NO and TNF- α , and these cytokines were detected using the ELISA technique. AE ethanolic extract 250 μg/mL or VB 125 μg/mL was selected for IL-1 β and NO testing, while both AE extract and VB at 250 μg/mL were used for TNF- α determination. The different concentrations used in this study were taken from the potency screening previously undertaken in our previous work (data not shown). Hydrocortisone was a positive control. The amount of cytokines released from macrophage cells is shown in Figs. 6, 7 and 8.

LPS activated pro-inflammatory cytokines such as IL-1 β , NO and TNF- α were released from RAW 264.7 cells. Those cytokines can be inhibited by steroid agents such as hydrocortisone, a synthetic preparation of the steroid hormone cortisol, which has an anti-inflammatory response^{31–33}. Like hydrocortisone 5 μg/mL, AE extract 250 μg/mL showed successful downregulation of IL-1 β released from the RAW 264.7 cells treated with LPS (Fig. 6). Similarly, there was also significant inhibition but to a lesser degree when VB 125 μg/mL was used. RAW 264.7 cells treated with LPS also produced nitric oxide, which was represented by sodium nitrite content. N(G)-monomethyl-L-arginine (L-NMMA) was used as a positive control. As shown in Fig. 7, the results were that LPS effectively induced the synthesis of sodium nitrite in Raw 264.7 cells. L-NMMA inhibited the synthesis

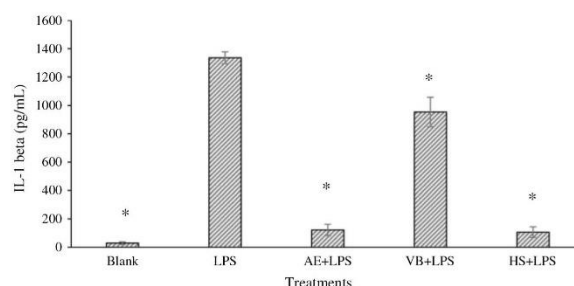


Figure 6. Amount of IL-1 β from RAW 264.7 cells treated with lipopolysaccharide 5 μ g/mL (LPS), AE extract 250 μ g/mL plus LPS 5 μ g/mL (AE + LPS), Hydrocortisone 5 μ g/mL plus LPS 5 μ g/mL (HS + LPS) and VB 125 μ g/mL plus LPS 5 μ g/mL (VB + LPS); * significantly different from LPS at $p < 0.05$ Student's t -test. ($n \geq 3$).

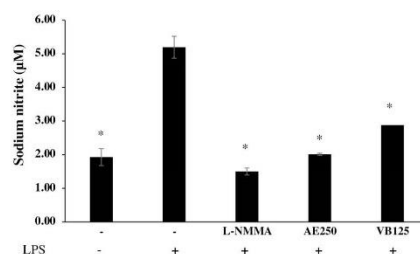


Figure 7. Amount of sodium nitrite from RAW 264.7 cells treated by lipopolysaccharide 1 μ g/mL (LPS), AE extract 250 μ g/mL plus LPS (AE + LPS), N(G)-monomethyl-L-arginine 10 μ g/mL (L-NMMA) plus LPS (L-NMMA + LPS), and VB 125 μ g/mL plus LPS (VB + LPS); * significantly different from LPS treated RAW 264.7 cell at $p < 0.05$ Student's t -test. ($n \geq 3$).

of NO activated by LPS due to the inhibition of nitric oxide synthase (NOS)³⁴. Both AE extract 250 μ g/mL and VB 125 μ g/mL also showed greater potency of inhibition of nitric oxide secretion than the LPS control cells.

Tumor necrosis factor (TNF- α) released from LPS treated macrophage cells was strongly inhibited by hydrocortisone (Fig. 8). Similar to hydrocortisone, 250 μ g/mL AE extract and 250 μ g/mL VB also significantly suppressed the release of TNF- α .

Effects of AE extract and VB on IL-1 α and IL-6 production in UVB irradiated dermal papilla cells. Dermal papilla cells released IL-1 α and IL-6 in the supernatant fluid after being irradiated with 20 J/cm² UVA and 100 mJ/cm² UVB, respectively. IL-6 and IL-1 α levels in the supernatant were measured using cytokine immunoassay (ELISA technique). Hydrocortisone 5 μ g/mL was a positive control. The amount of IL-1 α is shown in Fig. 9, and the amount of IL-6 is shown in Fig. 10.

Figure 9 shows that AE extract 250 μ g/mL or VB 125 μ g/mL significantly decreased the amount of IL-1 α released from the irradiated dermal papilla cells. Similar to IL-1 α , AE extract 250 μ g/mL and VB 125 μ g/mL significantly suppressed the release of IL-6 (Fig. 10).

Discussion

The bioactivity of AE extract and VB on murine macrophage RAW 267.4 and human dermal papilla cells was evaluated. The RAW 264.7 cells are normally used for evaluating anti-inflammatory activity because the macrophage can be stimulated by LPS to produce IL-1 β by activating Toll-like receptors^{35,36}. Although the release of pro-inflammatory cytokines in dermal papilla cells has been not fully understood, many reports also reveal the determination of those cytokines from dermal papilla cells and they play a crucial role in dermal papilla cell apoptosis and hair follicular damage^{1,8,9,37}. AE extracted with 95% ethanol had the highest content of VB of all tested AE extracts. Both AE extracted with 95% ethanol and VB were non-toxic to the dermal papilla and macrophage cells in the concentration range 0.98 to 500 μ g/mL. The inhibition activity of 5 α -reductase was evaluated

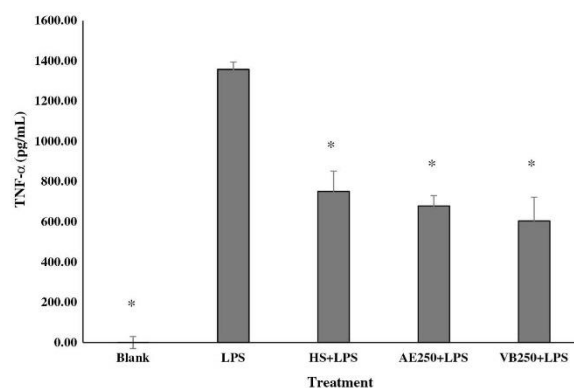


Figure 8. Amount of tumor necrosis factor (TNF- α) from RAW 264.7 cells treated with lipopolysaccharide 1 $\mu\text{g}/\text{mL}$ (LPS), hydrocortisone 10 $\mu\text{g}/\text{mL}$ + LPS 1 $\mu\text{g}/\text{mL}$ (HS + LPS), AE extract 250 $\mu\text{g}/\text{mL}$ plus LPS 1 $\mu\text{g}/\text{mL}$ (AE250 + LPS) and VB 250 $\mu\text{g}/\text{mL}$ plus 1 $\mu\text{g}/\text{mL}$ LPS (VB250 + LPS); * significantly different from LPS treated RAW 264.7 cell at $p < 0.05$ Student's *t*-test. ($n \geq 3$).

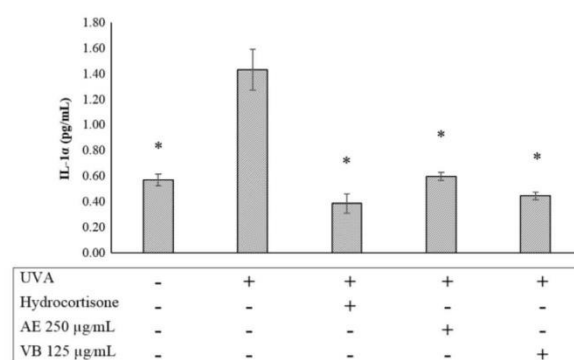


Figure 9. The release of IL-1 α from dermal papilla cells following UVA 20 mJ/cm^2 irradiation and after treatment with hydrocortisone 5 $\mu\text{g}/\text{mL}$, AE extract 250 $\mu\text{g}/\text{mL}$ and VB 125 $\mu\text{g}/\text{mL}$; * significantly different from irradiated cells at $p < 0.05$ Student's *t*-test. ($n \geq 3$).

by using an enzymatic activity assay. The enzyme used was isolated from LNCaP cell that presents the prominent quantity in 5 α -reductase^{38,39}. AE extracted with 95% ethanol possessed the highest 5 α -reductase inhibition activity ($38.26 \pm 4.90\%$ at 100 $\mu\text{g}/\text{mL}$). Surprisingly, this activity was not found for VB. These results indicate that other components than VB in the AE extract demonstrate 5 α -reductase inhibition activity. Although VB did not appear to affect 5 α -reductase inhibition, VB 62.50 $\mu\text{g}/\text{mL}$ inhibited dermal papilla cell apoptosis induced with 200 μM testosterone. Similar activity was also found with 250 $\mu\text{g}/\text{mL}$ AE extracted with 95% ethanol and 75 nM finasteride. This effect could be due to the down-regulation of cAMP, which prevents cell apoptosis induced by testosterone²⁹. AE extract and VB did not show any cytotoxic effects on dermal papilla cells, but these compounds did induce dermal papilla cell proliferation.

Cell cycle study indicated that both AE extract and VB at the concentration of 500 $\mu\text{g}/\text{mL}$ suppressed dermal papilla cell proliferation (G2/M phase). The increasing numbers of cells in the G1 phase were evidenced for 500 $\mu\text{g}/\text{mL}$ AE extract and 500 $\mu\text{g}/\text{mL}$ VB, which indicated the induction of G1 phase of dermal papilla cell cycle arrest^{40,41}. However, AE extract (125 $\mu\text{g}/\text{mL}$ and 250 $\mu\text{g}/\text{mL}$) and VB (62.50 $\mu\text{g}/\text{mL}$ and 125 $\mu\text{g}/\text{mL}$) promoted dermal papilla cell proliferation. At these concentrations, the cell numbers in the G2/M or S phases were greatly

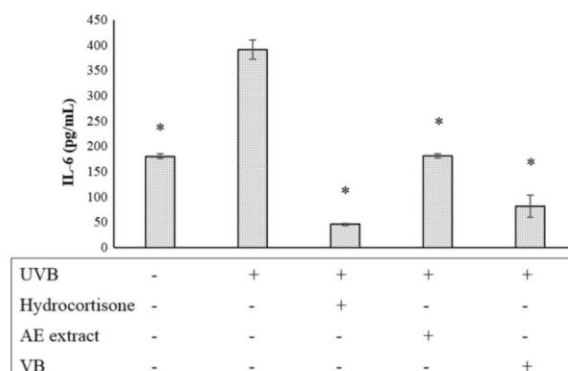


Figure 10. The release of IL-6 from dermal papilla cells following UVB 100 mJ/cm² irradiation and irradiated cell after treatment with hydrocortisone 5 µg/mL, AE extract 250 µg/mL and VB (VB) 125 µg/mL; * significantly different from irradiated cells at $p < 0.05$ Student's *t*-test. ($n \geq 3$).

increased compared to control cells. The increased numbers of cells in the G2/M or S phases in the cell cycle indicated that the cells were in the process of DNA synthesis and the proliferation stages^{42,43}. Although 125 µg/mL and 250 µg/mL of AE extracts did not show any effect on the G1 phase of the cell cycle, 62.50 µg/mL of VB significantly decreased the cell number in the G1 phase when compared to control cells. The decrease of cell number in the G1 phase has implied the increase of cell proliferation⁴². Those results were consistent with the results of anti-testosterone activity tests that showed that AE extracts (250 µg/mL) and VB (62.50 µg/mL) prevented cell apoptosis induced by testosterone. The human dermal papilla cell apoptosis induced by testosterone have been well documented⁴⁴. The prevention of cell apoptosis via down-regulating cAMP was reported as a mechanism of VB on testosterone activity²⁹. The decrease in testosterone metabolism diminished inflammation initiating cell apoptosis¹⁹.

IL-1 β and IL-1 α are pro-inflammatory cytokines that indicate cells are undergoing an inflammatory process⁴⁵. In various cell types, the IL-1 family can be induced to release several inflammatory cytokines, such as IL-6, prostaglandin E2, tumor necrotic factor- α (TNF- α), and nitric oxide (NO)^{36,46,47}. The release of NO can be detected by measuring nitrate and nitrite levels in cell culture supernatants. NO is a signaling molecule in the hair follicle. Overexpression of NO is involved in the regulation and differentiation of hair follicles resulting in hair loss⁵. RAW 264.7 cells were used to induce IL-1 β , TNF- α and NO-releasing by LPS^{35,48}. AE extract 250 µg/mL and VB 125 µg/mL were observed to inhibit the release of IL-1 β from RAW 264.7 cells. Similarly, the release of NO was inhibited by AE extract 250 µg/mL and VB 125 µg/mL. This is in agreement with previous reports which indicated that VB inhibited the expression of pro-inflammatory cytokines in immune cells^{49–51}. The inhibition occurs when VB binds to the two proinflammatory transcriptional factors, activator protein-1 and NF- κ B. This binding results in the downregulation of the two transcription factors⁵¹ and TGF- β expression⁵², which affects the synthesis of IL-1 β and TNF- α . In addition, another publication indicated that VB inhibits NO synthesis by suppressing iNOS enzyme activity⁵³. This mechanism can be used to explain the decrease of IL-1 β and NO released from RAW 264.7 cells.

Dermal papilla cells can release several inflammatory cytokines. IL-1 α , an inflammatory cytokine, was measured in irradiated dermal papilla cells. Generally, IL-1 α is found at the cell membrane surface and is released when the cell membrane is damaged^{54,55}. UVA 20 mJ/cm² was used to induce IL-1 α expression in dermal papilla cells. Both AE extract and VB effectively suppressed IL-1 α release. IL-6 has been recognized as an androgen inducible negative mediator for AGA development⁵⁶. IL-6 is also a proinflammatory mediator, which is upregulated in the hair follicles of AGA patients. There is a report⁵⁷ indicating that hair shaft elongation was inhibited by IL-6 treatment. IL-6 treatment is associated with suppressing the proliferation of matrix cells in cultures of human hair follicles and is known to promote the transition of hair follicles from the anagen to catagen phases in the hair cycle of mice which indicates that shortening the anagen phase results in less time for hair growth.

We induced IL-6 expression by UVB irradiation in the dermal papilla. AE extract 250 µg/mL and VB 125 µg/mL strongly decreased the level of IL-6 released from the irradiated dermal papilla cells. This inhibition could be due to the membrane stabilizing property of VB. We hypothesize that VB forms a stable lipid complex with the cell membrane which may prevent cell membrane damage from UV radiation⁵⁸. These findings suggest that anti-inflammatory, 5 α -reductase inhibitory, and dermal papilla growth promoter effects of AE extract were the rational use of AE extract in reducing alopecia. Although AE extract contains many active compounds, we are interested in VB and have used it as the biomarker because VB demonstrates an outstanding effect associated with the anti-hair loss pathway. VB can increase dermal papilla cell proliferation and protection of testosterone-induced dermal

papilla cell apoptosis concomitantly with anti-inflammation activity. These activities are an influence effect on the protection of hair loss and promote hair regrowth. VB in the AE extract is possible one component among others that contribute to this benefit. Further study needs to be done to identify other bioactive compounds.

Conclusion

AE has been used as a traditional medicine in some Asian countries to treat various diseases. AE also has numerous potential therapeutic effects such as being an anti-inflammatory and skin nourishing agent. VB possesses pharmacologically beneficial qualities for human health, including acting as an antioxidant and anti-inflammatory agent. In summary, AE extract and VB manifest positive effects on human dermal papilla and inflammatory conditions that can be used to reduce hair loss and promote hair growth. Our research suggests that AE extract and VB are potential ingredients for future alopecia therapy.

Materials and methods

Chemicals. 1-(4, 5-Dimethylthiazol-2-yl)-3, 5-diphenylformazan or thiazolyl blue formazan (MTT), finasteride and hydrocortisone were purchased from Sigma-Aldrich (St. Louis, USA). Fetal bovine, 2.5% trypsin serum, penicillin/streptomycin, phosphate buffer solution pH 7.4 were obtained from Gibco (Auckland, New Zealand). Dimethyl sulfoxide or DMSO (Analytical grade) was purchased from Labscan (V.S. Chem House, Thailand). Mouse IL-1 β ELISA Instant Kit was purchased from e-bio sciences (Bender-med systems Gmbh, Vienna, Austria). Follicle dermal papilla cell growth medium was purchased from PromoCell (Heidelberg, Germany).

Plant extraction. AE leaves were purchased from Khaokhoherbary (Phetchaboon, Thailand). The plant collection method and experimental use were in accordance with all the relevant guidelines. The specimens were identified by Assistant Professor Dr. Pranee Nangngam, of the Faculty of Science at Naresuan University. The voucher specimen, collection-number 004163, was deposited at the PNU herbarium also located at the Faculty of Science. The sample leaves of AE were dried at 50 °C for 24 h and then macerated with one or other of the following solvents: 50% ethanol, 95% ethanol, or hexane, and the leaf extracts were allowed to stand for 72 h. Each extract was filtered through Whatman No.1 filter paper before rotary evaporation at 40 °C. The average time for evaporation was 1 h/Liter of extract solution. To make the water extract, leaves of AE were boiled in hot water for 15 min and filtered, and the water was then removed from the extract by freeze-drying. All extracts were stored in vials at -20 °C and protected from light until use.

HPLC analysis of VB. The HPLC analysis of VB was performed on a Shimadzu HPLC (Bara Scientific, Japan) with a Luna Phenomenex analytical column. (150 mm \times 7 mm, 5- μ m particle size) (Phenomenex, Deerfield, IL, USA). The mobile phase consisted of 23% ACN (v/v) buffered with 50 mM Sodium Phosphate at pH 2.5. Elution was performed with a flow rate of 1.5 mL/min, detection wavelength at 332 nm, and volume of injection of 20 μ L.

Human dermal papilla cell culture. Human dermal papilla cells (PromoCell, Heidelberg, Germany) were cultured and maintained in a follicle dermal papilla cell growth medium. The growth medium contained growth factors of fetal calf serum 0.04 ml/ml, bovine pituitary extract 0.004 ml/ml, basic fibroblast growth factor recombinant human, 1 ng/ml, and insulin (recombinant human, 5 μ g/ml). The cells were incubated under cell culture conditions of 95% relative humidity (RH), 5% CO₂ and 37 °C. They were sub-cultured until they grew to about 80% confluence.

Murine macrophage RAW 264.7 cell culture. The RAW 264.7 (ATCC, Virginia, USA), a murine macrophage cell line, was cultured and maintained in DMEM medium (Gibco, Thermo scientific, MA, USA) containing 10% fetal bovine, 10,000 units/ml of penicillin and streptomycin. The cells were incubated under cell culture conditions of 95% RH, 5% CO₂ and 37 °C. They were sub-cultured until about 80% confluence.

MTT assay for cell viability and proliferation testing. Ten thousand dermal papilla cells or RAW 264.7 cells were seeded into each well of a 96-well plate. The cells were incubated under cell culture conditions of 95% relative humidity (RH), 5% CO₂ and 37 °C for 24 h. After incubation, they were treated with AE extract solutions at 0.98 – 500 μ g/mL. The incubation time of treatment was 24 h. Fifty micrograms per milliliter of MTT solution were added to each well and the plates incubated for 3 h. The formed formazan crystals were dissolved with 100 μ L of DMSO⁵⁹. An absorbance was determined at 595 nm. Relative cell viability was calculated by comparing the treated cells with control cells.

Cell cycle analysis. The cell cycle was analyzed by a published method⁶⁰ with slight modifications. One hundred thousand dermal papilla cells were seeded into each well of a 6-well plate and incubated under cell culture conditions of 95% relative humidity (RH), 5% CO₂ and 37 °C for 24 h. After incubation, the cells were treated with plant extract solutions at 31.25 – 500 μ g/mL. All cells were collected by trypsinizing and then fixed with 70% cold ethanol for 4 h at -20 °C. The fixed cells were stained using Muse[™] cell cycle kit (EMD Millipore Corporation, Hayward, CA), and kept for 30 min protected from light. The cell cycle was analyzed using Guava[®] easyCyte. The cell cycle profiles, which were represented by DNA contents of each cell cycle phase, were compared among treated cells versus control cells.

Inhibition effect on testosterone-induced cell apoptosis. The study of dermal papilla cell apoptosis induced by testosterone was slightly modified from the previous report⁴⁴. Ten thousand dermal papilla cells were seeded into each well of a 96-well plate and incubated under cell culture conditions of 95% relative humidity (RH), 5% CO₂ and 37 °C for 24 h and then pre-treated with 200 μM of testosterone before adding AE extract 250 μg/mL or VB 62.50 μg/mL. The treated cells were incubated for 4 days. On day four, cell viability was determined by MTT assay. The positive control was finasteride at 0.025 μg/mL concentration.

Determination of 5α-reductase inhibition. Anti-androgenic activity via the steroid 5α-reductase (5αR) inhibition mechanism was evaluated using a label-free enzymatic inhibitory assay, following the protocol developed by Srivilai and colleagues^{38,61,62}. Enzymatic activity was measured by analyzing the DHT formation after enzymatic reaction using liquid chromatography-mass spectrometry (LC-MS).

Enzymatic preparation. Androgen-dependent LNCaP cells (CRL-1740[™], American Type Culture Collection, VA, USA) provided the source of 5αR. Briefly, the LNCaP cells were cultured in RPMI-1640 medium (Gibco, Paisley, Scotland) supplemented with 10% fetal bovine serum (FBS) and 1% of 10,000 U/mL penicillin G and 10,000 μg/mL streptomycin (Gibco, Paisley, Scotland) at 37 °C under 5% CO₂ humidified atmosphere before harvesting at ≥ 80% confluent. The protein concentration of homogenized cells was measured using Pierce bicinchoninic acid (BCA) protein assay (Pierce, Rockford, IL, USA). The final total protein was not less than 75 μg in the 5αR inhibitory assay.

Enzymatic inhibitory assay. AE extracts were dissolved in DMSO and the inhibition activity determination followed the procedure in Srivilai and colleagues^{38,61}. Aliquots of these solutions were added to the assay solution. The enzymatic reaction was composed of test substances, 34.7 μM testosterone, and 1 mM NADPH in Tris buffer pH 7.4. The reaction was started by adding 200 μL of the homogenate enzyme (75 μg total protein). The mixture was incubated at 37 °C for 60 min. The reaction was stopped by adding 300 μL of hydroxylamine (10 mg/mL in 80% (v/v) ethanol) and incubating at 60 °C for 60 min for the derivatization process. The plate was then centrifuged at 1700 g for 10 min and the supernatants were transferred to another plate ready for injection into the LC-MS. C1 and C2 were the two control samples used. Both controls contained the complete reaction mixture as described above but C1 was stopped before enzymatic incubation, whereas, C2 was stopped after 60 min of incubation. The DHT production was measured using LC-MS. The extracted ion chromatogram (EIC) of derivatized DHT (m/z [M + H]⁺, 306.2428), the area under the curve was used to calculate enzymatic inhibition:

$$\% \text{Steroid } 5\alpha \text{-reductase inhibition} = [1 - (\text{Sample} - \text{C1}) / (\text{C2} - \text{C1})] \times 100$$

The standard steroid 5α-reductase inhibitor, finasteride, was used as a positive control.

LC-MS method for the measurement of DHT. The determination of DHT was done according to Srivilai and colleagues^{38,61}. The Agilent 1260 Infinity Series HPLC system with an auto-sampler accommodating either two 108-vial trays or two 96-well plates (Agilent Technologies, Santa Clara, CA, USA) was used. The analytical reversed-phase column was a Phenomenex Luna[®] C18 (2) (150 mm × 4.6 mm, 5 μm) with a guard column (Phenomenex C18, 4 mm × 3 mm, 5 μm). The HPLC was connected with an Agilent 6540 UHD Accurate-Mass Q-TOF LC/MS (Agilent Technologies, Santa Clara, CA, USA), equipped with dual electrospray ionization (ESI) in positive mode and m/z range 100–1200. Nitrogen was the nebulizing gas at 30 psi, and the drying gas (10 L/min; 350 °C). The mobile phase was 0.1% (v/v) formic acid in purified water (solvent A) and 0.1% (v/v) formic acid in acetonitrile (LC-MS grade, ACI Labscan, Bangkok, Thailand) as solvent B. The gradient program was used as follows: The initial mobile phase was 60% solvent B and 40% solvent A; solvent B was linearly increased up to 80% over 8 min then held constant for 4 min. Each run was followed by a 2-min post-run. The total run-time analysis was therefore 14 min with the column temperature controlled at 35 °C. The flow rate was 0.5 mL/min and the injection volume was 20 μL. Mass data were analyzed using Agilent Mass Hunter Qualitative Analysis software version B06.00. The data was identified, calculated and presented in term of inhibition activity.

Determination of IL-1β, NO, and TNF-α secretion inhibition in LPS-stimulated macrophages. One hundred thousand RAW 264.7 cells were seeded into each well of a 24-well plate and incubated under cell culture conditions of 95% relative humidity (RH), 5% CO₂ and 37 °C for 24 h. Next, the cells were treated with 1 μg/ml lipopolysaccharide (LPS) plus 250 μg/ml AE extracts or 125 μg/ml VB or 62.50 μg/ml VB depending on the tested cytokines. Five micrograms per milliliter of hydrocortisone were the positive control. The treated cells were incubated for 24 h and the supernatants were collected for determination of the amount of IL-1β and TNF-α using an ELISA Kit (Invitrogen, Vienna, Austria). The amount of nitric oxide was determined using the chemical reaction of Griess's reagent (Sigma-Aldrich, Steinheim, Germany).

Determination of IL-1α, IL-6 secretion inhibition in UV radiated dermal papilla cells. One hundred thousand dermal papilla cells were seeded into each well of a 24-well plate and incubated under cell culture conditions of 95% relative humidity (RH), 5% CO₂ and 37 °C for 24 h. The cells were irradiated by 100 mJ/cm² of UVB for the IL-6 study or 20 J/cm² of UVA for IL-1α study using UV irradiation chamber (Opsytec, Dr. Gröbel GmbH, Ettlingen, Germany). The irradiated cells were immediately treated with 250 μg/ml AE extract or 125 μg/ml VB solution and incubated for 24 h. The expression of IL-1α and IL-6 in the cell culture supernatants were assayed by an ELISA kit according to the manufacturer's protocol (BioLegend, San Diego, CA; Abcam, Cambridge CB2 OAX, UK).

Statistical analysis. All data were presented as a mean \pm standard deviation (S.D.). Individual differences were evaluated by t-test or one-way ANOVA.

Received: 30 August 2021; Accepted: 4 January 2022

Published online: 27 January 2022

References

- Trüeb, R. M. Molecular mechanisms of androgenetic alopecia. *Exp. Gerontol.* **37**, 981–990. [https://doi.org/10.1016/S0531-5565\(02\)00093-1](https://doi.org/10.1016/S0531-5565(02)00093-1) (2002).
- Ceruti, J. M., Leirós, G. J. & Balaña, M. E. Androgens and androgen receptor action in skin and hair follicles. *Mol. Cell. Endocrinol.* **465**, 122–133. <https://doi.org/10.1016/j.mce.2017.09.009> (2018).
- Chaturvedi, A. P. & Dehm, S. M. Androgen receptor dependence. *Adv. Exp. Med. Biol.* **1210**, 333–350. https://doi.org/10.1007/978-3-030-32656-2_15 (2019).
- Inui, S. & Itami, S. Androgen actions on the human hair follicle: perspectives. *Exp. Dermatol.* **22**, 168–171. <https://doi.org/10.1111/exd.12024> (2013).
- Wolf, R., Schonfelder, G., Paul, M. & Blume-Peytavi, U. Nitric oxide in the human hair follicle: constitutive and dihydrotestosterone-induced nitric oxide synthase expression and NO production in dermal papilla cells. *J. Mol. Med.* **81**, 110–117. <https://doi.org/10.1007/s00109-002-0402-y> (2003).
- Garza, L. A. *et al.* Prostaglandin D(2) inhibits hair growth and is elevated in bald scalp of men with androgenetic alopecia. *Sci. Transl. Med.* **4**, 1–21. <https://doi.org/10.1126/scitranslmed.3003122> (2012).
- Xiong, Y. & Harmon, C. S. Interleukin-1 β is differentially expressed by human dermal papilla cells in response to PKC activation and is a potent inhibitor of human hair follicle growth in organ culture. *J. Interferon Cytokine Res.* **17**, 151–157. <https://doi.org/10.1089/jir.1997.17.151> (1997).
- Philpott, M. P., Sanders, D. A., Bowen, J. & Kealey, T. Effects of interleukins, colony-stimulating factor and tumour necrosis factor on human hair follicle growth in vitro: a possible role for interleukin-1 and tumour necrosis factor- α in alopecia areata. *Br. J. Dermatol.* **135**, 942–948. <https://doi.org/10.1046/j.1365-2133.1996.d01-1099.x> (1996).
- Mahé, Y. F. *et al.* Androgenetic alopecia and microinflammation. *Int. J. Dermatol.* **39**, 576–584. <https://doi.org/10.1046/j.1365-4362.2000.00612.x> (2000).
- Gilliver, S. C., Ashworth, J. J., Mills, S. J., Hardman, M. J. & Ashcroft, G. S. Androgens modulate the inflammatory response during acute wound healing. *J. Cell Sci.* **119**, 722–731. <https://doi.org/10.1242/jcs.02786> (2006).
- Health, R. New cure for baldness? *Nat. Rev. Immunol.* **2**, 382–382. <https://doi.org/10.1038/nri835> (2002).
- Anzai, A., Pereira, A. F., Malaquias, K. R., Guerra, L. O. & Mercuri, M. Efficacy and safety of a new formulation kit (shampoo + lotion) containing anti-inflammatory and antioxidant agents to treat hair loss. *Dermatol. Ther.* **33**, 1–6. <https://doi.org/10.1111/dth.13293> (2020).
- York, K., Meah, N., Bhojru, B. & Sinclair, R. A review of the treatment of male pattern hair loss. *Expert Opin. Pharmacother.* **21**, 603–612. <https://doi.org/10.1080/14656566.2020.1721463> (2020).
- Majid, I. & Keen, A. Management of alopecia areata: An update. *Br. J. Med. Pract.* **5**, a530 (2012).
- Chen, C. A., Costa, D. B. & Wu, P. A. Successful treatment of epidermal growth factor receptor/inhibitor-induced alopecia with doxycycline. *JAAD Case Rep.* **1**, 289–291 (2015).
- Ellis, C. N., Brown, M. E. & Voorhees, J. J. Sulfasalazine for alopecia areata. *J. Am. Acad. Dermatol.* **46**, 541–544. <https://doi.org/10.1067/mjd.2002.119671> (2002).
- Mysore, V. & Shashikumar, B. M. Guidelines on the use of finasteride in androgenetic alopecia. *Indian J. Dermatol. Venereol. Leprol.* **82**, 128–134. <https://doi.org/10.4103/0378-6323.177432> (2016).
- Wongrakpanich, S., Wongrakpanich, A., Melhado, K. & Rangaswami, J. A comprehensive review of non-steroidal anti-inflammatory drug use in the elderly. *Aging Dis* **9**, 143–150. <https://doi.org/10.14336/AD.2017.0306> (2018).
- Antonucci, R. *et al.* Use of non-steroidal anti-inflammatory drugs in pregnancy: impact on the fetus and newborn. *Curr. Drug Metab.* **13**, 474–490. <https://doi.org/10.2174/138920012800166607> (2012).
- Sriviriyakul, P. & Chokdeesumrit, W. A comparative study of the efficacy of topical 10% curcuma aeruginosa solution and topical 5% minoxidil solution on the treatment of male androgenetic alopecia. *J. Med. Health Sci.* **27**, 28–38 (2020).
- Scheman, A. Alternative formulation for patients with contact reactions to topical 2% and 5% minoxidil vehicle ingredients. *Contact Dermatitis* **42**, 241 (2000).
- Rossi, A. *et al.* Minoxidil use in dermatology, side effects and recent patents. *Recent Pat. Inflamm. Allergy Drug Discov.* **6**, 130–136 (2012).
- Laupattarakasem, P., Houghton, P. J., Hoult, J. R. S. & Itharat, A. An evaluation of the activity related to inflammation of four plants used in Thailand to treat arthritis. *J. Ethnopharmacol.* **85**, 207–215. [https://doi.org/10.1016/S0378-8741\(02\)00367-7](https://doi.org/10.1016/S0378-8741(02)00367-7) (2003).
- Liebezit, G. & Rau, M. T. New Guinean mangroves—Traditional usage and chemistry of natural products. *Senckenb. Marit* **36**, 1–10. <https://doi.org/10.1007/bf03043698> (2006).
- Kanchanapoom, T., Kasai, R., Picheansoonthon, C. & Yamasaki, K. Megastigmane, aliphatic alcohol and benzoxazinoid glycosides from *Acanthus ebraacteatus*. *Phytochemistry* **58**, 811–817. [https://doi.org/10.1016/S0031-9422\(01\)00306-5](https://doi.org/10.1016/S0031-9422(01)00306-5) (2001).
- Sahpaz, S., Garbacki, N., Tits, M. & Bailleul, F. Isolation and pharmacological activity of phenylpropanoid esters from *Marrubium vulgare*. *J. Ethnopharmacol.* **79**, 389–392. [https://doi.org/10.1016/S0378-8741\(01\)00415-9](https://doi.org/10.1016/S0378-8741(01)00415-9) (2002).
- Pesce, M. *et al.* Verbascoside down-regulates some pro-inflammatory signal transduction pathways by increasing the activity of tyrosine phosphatase SHP-1 in the U937 cell line. *J. Cell Mol. Med.* **19**, 1548–1556. <https://doi.org/10.1111/jcmm.12524> (2015).
- Yang, Y.-L. Verbascoside reverses TGF- β 1-induced renal cellular fibrosis. *J. Diabetes Metab. Disord. Control* **3**, 122–127. <https://doi.org/10.15406/jdmdc.2016.03.00083> (2016).
- Liu, S., Zhang, J., Li, W., Zhang, T. & Hu, D. Acteoside reduces testosterone by inhibiting cAMP, p450sec, and STAR in rat Leydig cells. *Mol. Cell. Toxicol.* **11**, 11–17. <https://doi.org/10.1007/s13273-015-0002-x> (2015).
- Meerlo, J. V., Kaspers, G. J. L. & Cloos, J. In *Cancer Cell Culture Methods and Protocols* (ed. Cree, I. A.) 237–246 (Humana Press, 2011).
- Hirooka, Y., Mitsuma, T., Nogimori, T. & Ishizuki, Y. Effect of hydrocortisone on interleukin-6 production in human, peripheral blood mononuclear cells. *Mediators Inflamm.* **1**, 9–13. <https://doi.org/10.1155/S0962935192000036> (1992).
- Rautava, S., Walker, W. A. & Lu, L. Hydrocortisone-induced anti-inflammatory effects in immature human endotocytes depend on the timing of exposure. *Am. J. Physiol. Gastrointest. Liver Physiol.* **310**, G920–G929. <https://doi.org/10.1152/ajpgi.00457.2015> (2016).
- Hindmarsh, P. C. & Geertsma, K. In *Congenital Adrenal Hyperplasia* (eds Hindmarsh, P. C. & Geertsma, K.) 231–249 (Academic Press, 2017).
- Kithas, A. C. *et al.* Nitric oxide synthase inhibition with N(G)-monomethyl-L-arginine: Determining the window of effect in the human vasculature. *Nitric Oxide* **104–105**, 51–60. <https://doi.org/10.1016/j.niox.2020.09.001> (2020).

35. Pestka, J. & Zhou, H.-R. Toll-like receptor priming sensitizes macrophages to proinflammatory cytokine gene induction by deoxy-nivalenol and other toxicants. *Toxicol. Sci.* **92**, 445–455. <https://doi.org/10.1093/toxsci/ki012> (2006).
36. Dinarello, C. A. Interleukin-1. *Cytokine Growth Factor Rev.* **8**, 253–265. [https://doi.org/10.1016/s1359-6101\(97\)00023-3](https://doi.org/10.1016/s1359-6101(97)00023-3) (1997).
37. Mahe, Y. F. et al. Pro-inflammatory cytokine cascade in human plucked hair. *Skin Pharmacol.* **9**, 366–375. <https://doi.org/10.1159/000211447> (1996).
38. Srivilai, J. et al. Anti-androgenic curcumin analogues as steroid 5-alpha reductase inhibitors. *Med. Chem. Res.* **26**, 1550–1556. <https://doi.org/10.1007/s00044-017-1869-y> (2017).
39. Li, J. et al. Androgen regulation of 5 α -reductase isoenzymes in prostate cancer: implications for prostate cancer prevention. *PLoS ONE* **6**, e28840–e28840. <https://doi.org/10.1371/journal.pone.0028840> (2011).
40. Hashimoto, T. et al. Caffeine inhibits cell proliferation by G0/G1 phase arrest in JB6 cells. *Can. Res.* **64**, 3344–3349. <https://doi.org/10.1158/0008-5472.can-03-3453> (2004).
41. Reja, B. et al. Simvastatin inhibits cell growth and induces apoptosis and G0/G1 cell cycle arrest in hepatic cancer cells. *Int. J. Mol. Med.* **26**, 735–741 (2010).
42. Zanni, G. et al. Lithium increases proliferation of hippocampal neural stem/progenitor cells and rescues irradiation-induced cell cycle arrest in vitro. *Oncotarget* **6**, 37083–37097 (2015).
43. Lee, H.-J. et al. Effects of nicotine on proliferation, cell cycle, and differentiation in immortalized and malignant oral keratinocytes. *J. Oral Pathol. Med.* **34**, 436–443. <https://doi.org/10.1111/j.1600-0714.2005.00342.x> (2005).
44. Winiarska, A. et al. Effect of 5 α -dihydrotestosterone and testosterone on apoptosis in human dermal papilla cells. *Skin Pharmacol. Physiol.* **19**, 311–321 (2006).
45. Chen, L. et al. Inflammatory responses and inflammation-associated diseases in organs. *Oncotarget* **9**, 7204–7218. <https://doi.org/10.18632/oncotarget.23208> (2017).
46. Pawluk, H. et al. The role of selected pro-inflammatory cytokines in pathogenesis of ischemic stroke. *Clin. Interv. Aging* **15**, 469–484 (2020).
47. Garlanda, C., Dinarello, C. A. & Mantovani, A. The interleukin-1 family: Back to the future. *Immunity* **39**, 1003–1018. <https://doi.org/10.1016/j.immuni.2013.11.010> (2013).
48. Joo, T. et al. Inhibition of nitric oxide production in LPS-stimulated RAW 264.7 cells by stem bark of *Ulmus pumila* L. *Saudi J. Biol. Sci.* **21**, 427–435. <https://doi.org/10.1016/j.sjbs.2014.04.003> (2014).
49. Xiong, Q., Hase, K., Tezuka, Y., Namba, T. & Kadota, S. Acteoside inhibits apoptosis in D-galactosamine and lipopolysaccharide-induced liver injury. *Life Sci.* **65**, 421–430. [https://doi.org/10.1016/s0024-3205\(99\)00263-5](https://doi.org/10.1016/s0024-3205(99)00263-5) (1999).
50. Hausmann, M. et al. In vivo treatment with the herbal phenylethanoid acteoside ameliorates intestinal inflammation in dextran sulphate sodium-induced colitis. *Clin. Exp. Immunol.* **148**, 373–381. <https://doi.org/10.1111/j.1365-2249.2007.03350.x> (2007).
51. Qiao, Z., Tang, J., Wu, W., Tang, J. & Liu, M. Acteoside inhibits inflammatory response via JAK/STAT signaling pathway in osteoarthritic rats. *BMC Complement. Altern. Med.* **19**, 264–271. <https://doi.org/10.1186/s12906-019-2673-7> (2019).
52. You, S.-P., Ma, L., Zhao, J., Zhang, S.-L. & Liu, T. Phenylethanoid glycosides from *Cistanche tubulosa* suppress hepatic stellate cell activation and block the conduction of signaling pathways in TGF- β 1/sm α d as potential anti-hepatic fibrosis agents. *Molecules* **21**, 102–117. <https://doi.org/10.3390/molecules21010102> (2016).
53. Lee, J. Y., Woo, E.-R. & Kang, K. W. Inhibition of lipopolysaccharide-inducible nitric oxide synthase expression by acteoside through blocking of AP-1 activation. *J. Ethnopharmacol.* **97**, 561–566. <https://doi.org/10.1016/j.jep.2005.01.005> (2005).
54. Tebbe, B. et al. L-ascorbic acid inhibits UVA-induced lipid peroxidation and secretion of IL-1 α and IL-6 in cultured human keratinocytes in vitro. *J. Invest. Dermatol.* **108**, 302–306. <https://doi.org/10.1111/1523-1747.ep12286468> (1997).
55. Batista, S. J. et al. Gasdermin-D-dependent IL-1 α release from microglia promotes protective immunity during chronic *Toxoplasma gondii* infection. *Nat. Commun.* **11**, 1–13. <https://doi.org/10.1038/s41467-020-17491-z> (2020).
56. Yu, M. et al. Interleukin-6 cytokine family member oncostatin M is a hair-follicle-expressed factor with hair growth inhibitory properties. *Exp. Dermatol.* **17**, 12–19. <https://doi.org/10.1111/j.1600-0625.2007.00643.x> (2008).
57. Kwack, M. H., Ahn, J. S., Kim, M. K., Kim, J. C. & Sung, Y. K. Dihydrotestosterone-inducible IL-6 inhibits elongation of human hair shafts by suppressing matrix cell proliferation and promotes regression of hair follicles in mice. *J. Invest. Dermatol.* **132**, 43–49. <https://doi.org/10.1038/jid.2011.274> (2012).
58. Lorena Funes, O. L., Cerdán-Calero, M. & Mico, V. Effects of verbascoside, a phenylpropanoid glycoside from *Lemon verbena*, on phospholipid model membranes. *Chem. Phys. Lipids* **163**, 190–199 (2009).
59. Sylvester, P. W. In *Drug Design and Discovery Methods and Protocols* (ed. Satyanarayanan, S. D.) 157–168 (Humana Press, 2011).
60. Kang, M. R. et al. Lipid-soluble ginseng extract induces apoptosis and G0/G1 cell cycle arrest in NCI-H460 human lung cancer cells. *Plant Foods Hum. Nutr.* **66**, 101–106 (2011).
61. Srivilai, J. et al. A new label-free screen for steroid 5 α -reductase inhibitors using LC-MS. *Steroids* **116**, 67–75. <https://doi.org/10.1016/j.steroids.2016.10.007> (2016).
62. Fachrunniza, Y. et al. *Tectona grandis*, a potential active ingredient for hair growth promotion. *Songklanakarinn J. Sci. Technol.* **42**, 1352–1359 (2020).

Acknowledgements

This study was supported by (i) the Thailand Center of Excellence for Life Sciences (TCELS) (TC-A 6/61), (ii) the National Research Council of Thailand (NRCT) (DBG6080005, IRN61W0005), (iii) the Center of Excellence for Innovation in Chemistry (PERCH-CIC), Ministry of Higher Education, Science, Research and Innovation. We thank Mr. Roy I. Morien of the Naresuan University Graduate School for his assistance in editing the English expression and grammar in this document.

Author contributions

Conceptualization, V.W. (Vanuchawan Wisuitiprot), N.W. (Neti Waranuch) P.C. (Panlop Chakkavittumrong) W.W. (Wudtichai Wisuitiprot) and K.I. (Kornkanok Inkaninan); methodology and experimental design, V.W., P.C., K.I., W.W., N.N. (Nitra Neungchamnon), R.C. (Ruttanaporn Chantakul) and N.W.; Validation, V.W., N.N., R.C., K.I. and N.W.; formal analysis, V.W., P.C., K.I. and N.W.; investigation, V.W., R.C., N.N., K.I. and N.W.; resources, V.W., P.C., and N.W.; data curation and interpretation, V.W., P.C., W.W., K.I. and N.W.; writing-original draft preparation, V.W., K.I., W.W. and N.W.; writing-review and editing, V.W., K.I. and N.W.; visualization, V.W. and N.W.; supervision, V.W., P.C., K.I. and N.W.; project administration, N.W.; funding acquisition, N.W. All authors have read and agree to published version of the manuscript.

Competing interests

The authors declare no competing interests.

Additional information

Correspondence and requests for materials should be addressed to N.W.

Reprints and permissions information is available at www.nature.com/reprints.

Publisher's note Springer Nature remains neutral with regard to jurisdictional claims in published maps and institutional affiliations.

 **Open Access** This article is licensed under a Creative Commons Attribution 4.0 International License, which permits use, sharing, adaptation, distribution and reproduction in any medium or format, as long as you give appropriate credit to the original author(s) and the source, provide a link to the Creative Commons licence, and indicate if changes were made. The images or other third party material in this article are included in the article's Creative Commons licence, unless indicated otherwise in a credit line to the material. If material is not included in the article's Creative Commons licence and your intended use is not permitted by statutory regulation or exceeds the permitted use, you will need to obtain permission directly from the copyright holder. To view a copy of this licence, visit <http://creativecommons.org/licenses/by/4.0/>.

© The Author(s) 2022

1 Thermal Degradation Kinetics and pH–Rate Profile of Verbasicoside 2 and Stability Improvement by Solid Lipid Nanoparticles

3 Vanuchawan Wisuitiprot, Kornkanok Ingkaninan, Panlop Chakkavittumrong, Wudtichai Wisuitiprot,
4 Eakkaluk Wongwad, and Neti Waranuch*

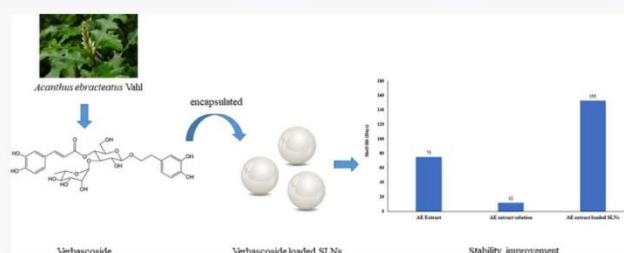
Cite This: <https://doi.org/10.1021/acsmchemlett.2c00145>

Read Online

ACCESS |

Metrics & More

Article Recommendations



5 **ABSTRACT:** Thermal degradation of verbasicoside (VB) in *Acanthus ebracteatus* Vahl (AE) always affects its health benefit. Here
6 the temperature effect on VB in both AE extract and solid lipid nanoparticles (SLNs)-encapsulated AE extract was demonstrated
7 using the Arrhenius plot. The reaction rate constants were calculated for shelf life and plotted to obtain pH–rate profiles. VB
8 degradation was a first-order reaction. The reaction rate in a neutral to alkaline solution was faster than in an acidic solution. VB in
9 AE extract-loaded SLNs was more stable than in uncapsulated AE extract. The shelf life of VB in SLNs was 153 days with activation
10 energy (E_a) of $76.16 \text{ kJ mol}^{-1}$, whereas those of VB in AE extract and in AE extract solution were 75 days with $E_a = 78.03 \text{ kJ mol}^{-1}$
11 and 12 days with $E_a = 49.24 \text{ kJ mol}^{-1}$, respectively. Therefore, we anticipate that the AE extract-loaded SLNs will be beneficial for
12 product development.

13 **KEYWORDS:** Verbasicoside, Stability, Arrhenius equation, Solid lipid nanoparticles, *Acanthus ebracteatus*

14 **P**lants and their chemical constituents have gained
15 attention and been studied for their biological activities
16 both *in vitro* and in the clinic.^{1–4} Verbasicoside (VB), or
17 acteoside, is a phenylpropanoid glycoside found in some
18 medicinal plants such as *Verbena officinalis*, *Syringa vulgaris*,
19 *Clerodendrum trichotomum* Thunb., *Orobanchae rapum-genistae*
20 Thuill., and *Acanthus ebracteatus* Vahl (AE),^{5–9} Many reports
21 document the beneficial bioactivities of VB, which include
22 antioxidant, anti-inflammatory, antimicrobial, and anti-andro-
23 gen activities.^{5,8,10,11} VB's bioactivities have inspired the
24 development of these plants into health applications. Previous
25 reports have identified AE as containing high amounts of VB,
26 and AE has been traditionally used as the main ingredient in an
27 anti-inflammation recipe for treating skin and musculoskeletal
28 inflammation.^{12,13} Thus, AE is a promising natural ingredient
29 for the development of health products.

30 Unfortunately, instability is an important problem of
31 bioactive compounds in plant extracts and herbal preparations.
32 Thermal degradation kinetics and shelf life evaluation using
33 Arrhenius' theory can be used for predicting and controlling

the quality of plant extracts and products.^{14,15} However, the
34 stability of VB has not yet been fully explored, and no
35 instability problem of AE extract has been identified. VB is
36 degraded by the hydrolysis reaction of its ester bond (Figure
37 1),¹⁰ which is induced by high temperatures or by being
38 contained in a neutral solution.^{10,16} Liposomes were used to
39 entrap VB, which improved its stability.^{17,18} Although VB was
40 successfully stabilized in a lipid vesicle, stability testing under
41 elevated temperatures and for extended shelf life has not been
42 reported.

The objectives of our study were to evaluate the effects of
43 pH and temperature on the degradation of VB in a semi-solid
44

Received: March 29, 2022

Accepted: June 7, 2022

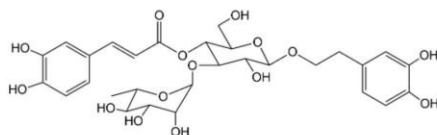


Figure 1. Chemical structure of verbasoside.

46 form of AE extract, in a solution form of AE extract, and in AE
47 extract-loaded solid lipid nanoparticles (SLNs). Arrhenius's
48 theory was used to determine the thermal degradation kinetic
49 parameters, such as the order of reaction and reaction rate
50 constant. These parameters were then used to predict the shelf
51 life of VB.

52 The SLN is a delivery system created from Compritol 888
53 ATO (glyceryl dibehenate), which was used for encapsulating
54 AE extract. The thermal degradation behavior of VB in the AE
55 extract-loaded SLNs was evaluated. Finally, the thermal
56 degradation behaviors of VB in the AE extract in three
57 different forms, e.g., liquid, semi-solid, and AE-loaded SLNs,
58 were evaluated and compared.

59 **Chemicals.** Verbasoside (VB) was purchased from Abcam
60 (Cambridgeshire, UK). Sodium dihydrogen orthophosphate
61 and potassium chloride were purchased from Ajax Finechem
62 (NSW, Australia). Glacial acetic acid, hydrochloric acid, and
63 sodium hydroxide were purchased from RCI Labscan
64 (Bangkok, Thailand). Acetonitrile was HPLC grade (Mallinck-
65 rodt Baker Inc., Phillipsburg, NJ, USA). All reagents were of
66 analytical grade. Compritol ATO 888 (glyceryl dibehenate)
67 was purchased from PT Intertrade Co., Ltd. (Nonthaburi,
68 Thailand). Water was produced from a Milli-Q water
69 purification system (Millipore, Billerica, MA, USA).

70 **Plant Extraction.** Fresh AE leaves were purchased from
71 Khaokhoherbary organic farm (Phetchaboon, Thailand). The
72 plant collection method and experimental use were in
73 accordance with all the relevant guidelines. The specimens
74 were identified by Assistant Professor Dr. Pranee Nangngam of
75 the Faculty of Science at Naresuan University. The voucher
76 specimen, collection no. 004163, was deposited at the PNU
77 herbarium, also located at the Faculty of Science. The fresh
78 leaves were dried at 50 °C for 24 h. Five-hundred gram
79 samples of the dried leaves were weighed and then macerated
80 with 2000 mL of 95% ethanol for 3 days. The extract solutions
81 were filtered, and the solvent was removed using a rotary
82 evaporator at 40 °C. The extract was then kept at -20 °C and
83 protected from light until use.

High-Performance Liquid Chromatography (HPLC)

84 **Analysis of VB.** HPLC analysis of VB was performed using a
85 Shimadzu HPLC (Bara Scientific, Japan) with a Luna
86 Phenomenex analytical column (250 mm × 7 mm, 5- μ m
87 particle size) (Phenomenex, Deerfield, IL, USA). The mobile
88 phase consisted of 23% acetonitrile (vol%) buffered with 50
89 mM sodium phosphate at pH 2.5. Elution was performed with
90 a flow rate of 1.5 mL/min, detection wavelength at 332 nm,
91 and injection volume of 20 μ L. The system was validated to
92 achieve the following parameters: linearity, limit of detection
93 (LOD), limit of quantification (LOQ), precision, and accuracy.
94

Preparation of AE Extract-Loaded Solid Lipid Nano-

95 **particles.** AE extract was encapsulated into SLNs using the
96 hot melt homogenization technique. The lipid carrier,
97 Compritol ATO 888 (HLB = 2), was used to formulate the
98 lipid particles, which were stabilized by using Tween 80 (HLB
99 = 15) and Span 80 (HLB = 4) as the co-surfactants (HLB = 100
hydrophilic-lipophilic balance). The formulation of the
101 particle preparation is shown in Table 1. Briefly describing
the preparation process, the lipid phase containing Compritol
103 888 ATO and Span 80 was melted at 80 °C. AE extract was
104 then added to the melted lipid, and the mixture was stirred
105 until it was homogeneous. Distilled water containing Tween 80
106 was separately heated to 90 °C, and the lipid part was poured
107 into the aqueous phase. The mixture was then emulsified by
108 using a high-speed homogenizer (Silverson LSM, Silverson
109 Machines Ltd., Waterside, UK) at 10 000 rpm for 15 min. The
110 particle was solidified at room temperature and then dried
111 using a freeze-dryer. A free-flowing powder was achieved using
112 maltodextrin as a cryoprotectant. No unexpected or unusually
113 high safety hazards were encountered. The particle size was
114 evaluated by using a dynamic light scattering (DLS) particle
115 size analyzer (ZetaPals, Brookhaven, New York, USA).
116 Encapsulation efficacy was calculated as the amount of VB
117 remaining encapsulated in the particles as a percentage of the
118 original amount of VB in the extract, calculated from the
119 HPLC chromatogram. The influential parameters affecting the
120 particle characteristics were the amount of Compritol ATO
121 888 and concentration of surfactant, and these were varied and
122 optimized.
123

124 **Effect of pH on VB in AE Extract.** The effect of pH on the
125 stability of VB was determined by dissolving AE extract in
126 buffer solutions at various pH values—pH 2.0 (0.2 M HCl +
0.2 M KCl), pH 5.5 (0.1 M citric acid and 0.1 M trisodium
127 citrate), pH 7.4 (0.2 M HCl and 0.2 M KCl), pH 8 (0.1 M
128 trimethylamine and 0.1 M HCl), and pH 11.0 (0.05 M
129 NaHCO₃ + 0.1 M NaOH)—to produce 10 mg/mL solutions
130

Table 1. Formulations for Preparing AE Extract-Loaded SLNs and Particle Characteristics^a

formula	parameters			particle characteristics			
	Compritol ATO 888 (g)	Tween 80 (%)	Span 80 (%)	PS (nm) \pm SD	PDI \pm SD	ZP (mV) \pm SD	entrapment efficiency (%) \pm SD
F1	10.00	1.00	0.00	1240.05 \pm 365.44	0.564 \pm 0.08	-23.10 \pm 4.55	4.21 \pm 2.01
F2	10.00	0.50	0.00	3546.77 \pm 548.78	0.321 \pm 0.01	-19.75 \pm 3.78	40.84 \pm 1.42
F3	1.50	0.50	0.25	2692.93 \pm 218.86	0.293 \pm 0.04	-31.42 \pm 2.06	13.51 \pm 0.27
F4	1.50	0.50	0.50	2606.76 \pm 125.83	0.248 \pm 0.03	-31.09 \pm 0.61	18.24 \pm 1.07
F5	1.50	0.50	1.00	2056.5 \pm 407.20	0.393 \pm 0.07	-33.07 \pm 3.33	15.87 \pm 2.22
F6	1.50	0.50	2.00	1372.3 \pm 100.36	0.120 \pm 0.05	-37.48 \pm 0.90	21.73 \pm 1.79
F7	1.50	0.50	3.00	628.06 \pm 159.36	0.210 \pm 0.04	-37.65 \pm 0.90	31.28 \pm 0.98
F8	1.50	0.50	4.00	1450.96 \pm 66.10	0.324 \pm 0.08	-39.77 \pm 0.86	24.99 \pm 0.44
F9	1.50	0.50	5.00	1129.16 \pm 61.88	0.355 \pm 0.02	-44.46 \pm 1.12	25.37 \pm 0.56

^aPS = particle size, PDI = polydispersity index, ZP = zeta potential, SD = standard deviation.

131 of each, which were then kept in a saturated sodium chloride
132 solution box at 25 °C for 30 days. The collection of samples for
133 analysis was done on days 0, 3, 7, 14, 21, and 28. The
134 remaining VB was evaluated by using a HPLC.

135 **Thermal Degradation Kinetic Analysis of VB in AE**
136 **Extract.** Ten milligrams of AE extract (semi-solid), 1 mL of
137 AE extract solution (10 mg of AE extract dissolved in 10 mL of
138 pH 7.4 phosphate buffer solution), and 50 mg of the AE
139 extract-loaded SLNs were separately put into microcentrifuge
140 tube (Thermo Fisher Scientific, Waltham, MA, USA) that were
141 then sealed with laboratory parafilm tape. These tubes were
142 then kept in saturated sodium chloride solution environments
143 in an incubator (Memmert GmbH, Selecta Biosciences,
144 Germany) at temperatures ranging from 50 to 80 °C, 16
145 days for AE extract, and 60 to 90 °C, 28 days for AE extract
146 solution, while the AE extract-loaded SLNs were stored
147 between 40 and 70 °C, 28 days. Samples were collected at days
148 0, 4, 8, 12, and 16 for the AE extract and AE extract solution,
149 while the AE extract-loaded SLNs were collected at days 0, 7,
150 14, 21, and 28. All samples were kept at -20 °C until
151 quantification of the remaining VB by using the HPLC
152 method. The remaining VB was used to identify the reaction
153 order and calculate the rate of reaction constant (K) and shelf
154 life (T_{90}).

155 The ethanolic extract of AE was successfully prepared with a
156 percentage yield of $18.19\% \pm 0.75$. VB content in this extract
157 was quantitated by the HPLC technique that was validated to
158 achieve the parameters of linearity, limit of detection (LOD),
159 limit of quantification (LOQ), precision, and accuracy.
160 Achieving linearity was defined as having R^2 greater than or
161 equal to 0.9997 using concentrations ranging from 19.53 to
162 1000.00 $\mu\text{g/mL}$. The LOD value of VB was 0.04 $\mu\text{g/mL}$, while
163 the LOQ was 0.12 $\mu\text{g/mL}$. We found that this method was
164 precise, with intraday and interday relative standard deviations
165 (%RSD) of less than 5.84% and 5.05%, respectively. We also
166 observed high accuracy of our procedure, with percentage
167 recovery ranging from 90% to 110%. The evaluation results
168 indicated that the HPLC method was accurate and reliable for
169 the determination of the amount of VB in AE extract. The
170 chromatogram of VB in ethanolic extract of AE is shown in
171 Figure 2. VB content in AE extract was $9.58 \pm 0.65\%$ (w/w).

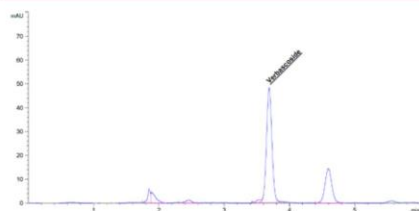


Figure 2. Chromatogram of VB in AE extract.

172 AE extract-loaded SLNs were successfully prepared by using
173 the hot melt homogenization technique. The particle
174 characteristics are presented in Table 1. The ratios of co-
175 surfactant and lipid content were varied, and the particle
176 properties were observed. The properties of lipid particles were
177 dependent on several factors, particularly surfactant concen-
178 trations. Formulas F1 and F2 indicated that the high content of
179 Tween 80 caused the particles to be smaller in size, while the

entrapment efficiency also distinctly decreased. Formulas F2
and F3 showed that an increased amount of Compritol ATO
888 increased both particle size and entrapment efficiency. A
co-surfactant system is usually recommended for effectively
inducing and stabilizing lipid particles. This study optimized
the concentrations of Tween 80 and Span 80 for forming lipid
particles of the appropriate size and entrapment efficiency.
Particle entrapment efficiency was increased by increasing the
amount of Span 80. However, the entrapment efficiency
tended to decrease when the Span 80 concentration was higher
than 3.00%. In addition, the zeta potential (ZP) of particles
tended to increase the value of negative charge when the
concentration of Span 80 was increased. The results in Table 1
also show that optimized proportions of 0.50% of Tween 80
and 3.00% of Span 80 along with 1.50 g of Compritol ATO
888 formed lipid particles with the highest entrapment
efficiency of 31.28% and a particle size of approximately 628
nm. With this formulation, smooth and spherical particles were
obtained (Figure 3).

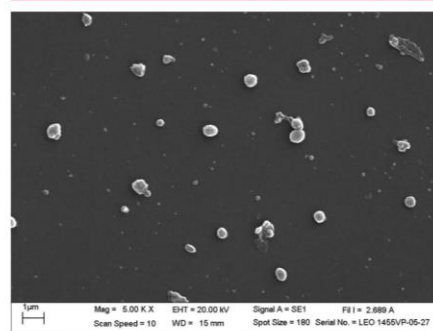


Figure 3. Morphology of AE extract-loaded SLNs observed under the scanning electron microscope.

AE extracts were dissolved in various pH buffer solutions. 199
The remaining VB was quantitated at designated times to 200
determine the degradation reaction. The order of the VB 201
degradation rate was predicted by the graphical method.¹⁹ 202
Zero-order, first-order, and second-order profiles were plotted 203
for each temperature. The reaction rate constant (K) of 204
chemical reaction at each temperature was calculated from 1% 205
the slope of the curve of remaining VB concentration versus 206
time for zero-order, 2% natural logarithm of remaining VB 207
versus time for first order, and 3% inverse of remaining VB 208
versus time for second order. In addition, the correlation 209
coefficient (R^2) of each graph was calculated to find the best 210
linearity that correlated with the order of a chemical reaction. 211
The degradation of VB at each pH was found to be a first- 212
order reaction. The reaction rate constant (K) of VB was 213
calculated from the slope and was then plotted against the pH 214
values to generate the degradation pH-rate profile of VB 215
(Figure 4). VB was more stable in acidic solutions than in 216
alkaline solutions, with the fastest decrease at pH 8. 217

The pH-rate profile of VB can be used to optimize VB 218
stability in a solution. However, valid estimates of shelf life of 219
VB in solution and other forms are needed for the 220

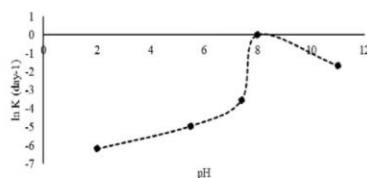


Figure 4. pH–rate profile of VB in solution form of AE extract at 25 °C ($n \geq 3$).

development of VB products. This was an important aspect of our study, to evaluate the thermal and chemical kinetics stability of VB in the semi-solid form of an AE extract, solution form of an AE extract, and AE extract-loaded SLNs by using Arrhenius' theory. The amount of VB remaining in all 16 sample forms after being stored at various temperatures for 16–28 days is presented in Figure 5.

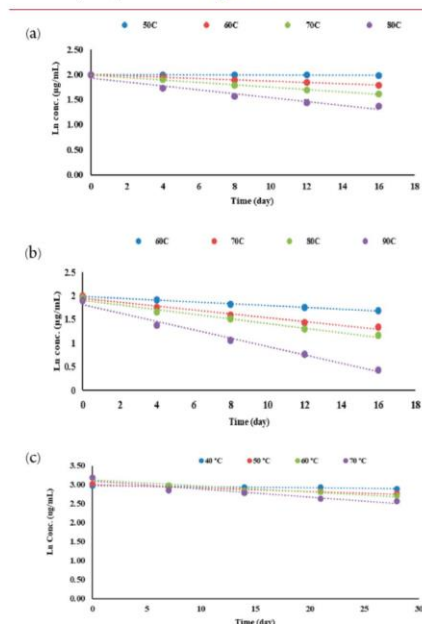


Figure 5. Thermal degradation kinetics for VB in (a) AE extract, (b) AE extract solution, and (c) AE extract-loaded SLNs as fitted to a first-order kinetic model.

These results indicated that the rate of VB decomposition was faster at elevated temperatures. The correlation between the natural logarithm of remaining VB in each sample form versus time was linear, which indicates a first-order reaction of VB in thermal degradation. The degradation rate constants (K) of VB at each tested temperature were calculated from the slope of the curve plotting the natural logarithm of remaining

VB concentration versus time elapsed. The reaction rate constants are presented in Table 2. The slope of the semi-logarithmic curve multiplied by the gas constant ($R = 8.3145 \text{ J/mol}\cdot\text{K}$) represents the activation energy (E_a). The Arrhenius frequency factor (A) for the accelerated breakdown over the tested temperature of each compound can be calculated from eq 1. The natural logarithm of each rate reaction constant

$$\ln K = \ln A - E_a/RT \quad (1)$$

($\ln K$) was plotted against the inverse of absolute temperature ($1/T$). The reaction rate constant at 25 °C was calculated from the linear equation.

As shown in Table 2, the temperature played a crucial role in the degradation rate constants of VB. The rate constants increased with increasing temperatures. In addition, the reaction rate constant of VB in AE extract solution was faster than those of VB in AE extract and AE extract-loaded SLNs, respectively. This implies that VB in AE extract solution was less stable than the forms. The shelf life of VB at 25 °C was predicted by using eq 2, where the reaction rate constant (K) for this temperature was obtained by utilizing the linear equation expressing the relationship between the natural logarithm of rate constant ($\ln K$) and the inverse of absolute temperature ($1/T$) (Figure 6).

$$\text{shelf life } (T_{90}) = 0.105/K \quad (2)$$

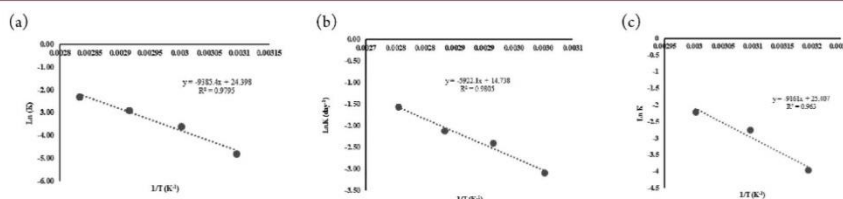
The estimated reaction rate constants and shelf life at 25 °C of VB in three forms, as well as activation energy (E_a), are shown in Table 3. The results indicated that VB in AE extract solution showed the highest rate constant, followed by VB in AE extract and VB in AE extract-loaded SLNs. The VB in AE extract-loaded SLNs showed the highest shelf life (153 days), followed by the VB in AE extract (75 days) and the VB in AE extract solution (12 days).

VB is a naturally occurring water-soluble phenylpropanoid glycoside that is widely distributed in the plant kingdom. Most commonly, VB has been isolated from medicinal plants. Several biological properties have been documented including anti-inflammatory, antimicrobial, antitumor, and antioxidant activities. Although VB is a promising compound due to its bioactivities, its usage is limited because of chemical degradation. Previous studies have shown that the hydrolysis reaction is the cause of the instability of VB^{10,16} and that the glycosidic bond is hydrolyzed in an alkaline solution.²² Similarly, VB in AE extract is further degraded by basic hydrolysis. However, the degradation rate of VB tends to decrease, implying an increase in VB stability, when the pH of the solution is more than 8. This increase in VB stability in a strongly alkaline solution is not fully understood. In addition to the pH of the aqueous solution, temperature also shows a major effect on VB stability. Elevated temperatures of 50 °C or more induce more degradation of VB in both AE extract and AE extract solution. At these elevated temperatures, the degradation rate constant of VB tends to be higher. Increasing pH in an aqueous preparation also increases the degradation rate constant of VB. Therefore, since VB is water-soluble, it can be degraded by hydrolysis and oxidation reactions. Thus, increasing the hydrophobicity or preventing water exposure are alternative ways for increasing VB's stability. Some reports have revealed that derivatized VB¹⁰ or encapsulated VB^{17,18} can decrease water exposure and increase VB's stability.

D

Table 2. Effect of Temperature on the Reaction Rate Constant (K) of VB in AE Extract, AE Extract Solution, and AE Extract-Loaded SLNs^a

temp (°C)	K ($\times 10^3$ day ⁻¹)			R^2		
	AE extract (semi-solid form)	AE extract (solution form)	AE extract-loaded SLNs	AE extract (semi-solid form)	AE extract (solution form)	AE extract-loaded SLNs
40	—	—	0.270 \pm 0.078	—	—	0.8936
50	0.691 \pm 0.044	10.778 \pm 0.078	0.910 \pm 0.014	0.9410	—	0.9421
60	3.086 \pm 0.879	4.514 \pm 0.085	1.570 \pm 0.096	0.9963	0.9954	0.9138
70	5.573 \pm 0.975	9.488 \pm 1.779	2.140 \pm 0.034	0.9967	0.9786	0.9068
80	8.982 \pm 1.879	11.216 \pm 3.451	—	0.9446	0.9821	—
90	—	20.957 \pm 2.441	—	—	0.9853	—

^a K = degradation rate constants \pm standard deviation ($n = 3$), R^2 = coefficient of determination.**Figure 6.** Arrhenius plot for thermal degradation of VB in (a) AE extract, (b) AE extract solution, and (c) AE extract-loaded SLNs over the temperature range 40–90 °C.**Table 3.** Reaction Rate Constant and Shelf Life of VB at 25 °C: Comparison among AE Extract, AE Extract Solution, and AE Extract-Loaded SLNs

forms	K ($\times 10^{-2}$ day ⁻¹)	E_a (kJ mol ⁻¹)	shelf life (days)
AE extract	0.1398	78.03	75
AE extract solution	0.8189	49.24	12
AE extract-loaded SLNs	0.0048	76.16	153

293 In our study, we encapsulated AE extract into lipid carriers
 294 to make SLNs loaded with VB. Some previous studies had
 295 reported that high amounts of lipid carrier significantly affect
 296 the particle size.^{23,24} We found that increasing the concentration
 297 of Compritol ATO 888, and thus increasing the
 298 amount of lipid in the formulation, resulted in increased
 299 particle size. High entrapment efficiency was obtained from the
 300 high amount of lipid due to the increased particle capacity.
 301 However, some reports revealed that the increase in lipid
 302 quantity made the particles become unstable because of drug
 303 expulsion induced by the lipid recrystallization process.^{24,25} We
 304 also found that doubling the concentration of Tween 80
 305 decreased the entrapment efficiency 10 times because the high
 306 amount of Tween 80 increased the amount of VB solubilized
 307 into the outer phase. Although a decrease of Tween 80
 308 increases VB encapsulation, a low concentration of surfactant
 309 causes instability of the lipid particles.²⁶ Co-surfactants are
 310 normally recommended for improving the stability and
 311 entrapment efficiency of particles.^{27,28} Previous studies
 312 reported that Span 80 and Tween 80 were effective in forming
 313 and stabilizing SLNs.^{27,29} Span 80 influences the entrapment
 314 efficiency, where an increase in the amount of Span 80 results
 315 in an increase in the entrapment efficiency of the particles.
 316 However, the entrapment efficiency is decreased when the
 317 concentration of Span 80 is more than 3%. It can be
 318 concluded, based on our study results, that an increase of Span

80 over 3% causes the entrapment efficiency to decrease
 319 because Span 80 alters the layer formation of Tween 80.²⁸ The
 320 layer alteration causes VB to be solubilized in the outer
 321 phase.³⁰ Moreover, the increased amount of Span 80 also
 322 decreased the HLB value of the system; therefore, VB's
 323 solubility and miscibility in the lipid matrix decreased. On the
 324 other hand, a decrease of Span 80 to less than 3% also reduced
 325 VB's entrapment efficiency, because the decrease of Span 80
 326 allows the HLB value to increase. In this scenario, VB tends to
 327 be solubilized in the aqueous phase.²⁸ In the optimization
 328 process for preparing AE extract-loaded SLNs, the percentage
 329 ratio of Compritol ATO 888, Tween 80, and Span 80 was
 330 15.00:0.50:3.00.
 331

We also examined the thermal degradation kinetics of VB in
 332 AE extract-loaded SLNs using Arrhenius's theory. We used the
 333 reaction rate constant to infer VB's degradation trend. The
 334 reaction rate constant of VB in AE extract-loaded SLNs
 335 presented the lowest value when compared with the reaction
 336 rate constants of VB in AE extract and AE extract solution. The
 337 shelf life times of VB in AE extract-loaded SLNs, AE extract
 338 solution, and AE extract were 153 days, 12 days, and 75 days,
 339 respectively. These results indicate that VB in AE extract-
 340 loaded SLNs is more stable than VB in the two other forms.
 341 The improvement of VB's stability might be due to the SLN
 342 preventing encapsulated active substances from undergoing
 343 chemical reactions induced by environmental conditions.³¹
 344 Although lipid particles can protect VB from being influenced
 345 by some external factors, the elevated temperature still
 346 obviously affects encapsulated VB. High temperatures can
 347 induce lipid particles to become gelled and encapsulated
 348 compounds to be expelled from the SLN.^{32,33} Recrystallization
 349 can also occur due to a change of temperature,³³ the lipid
 350 structure alteration allows more of the encapsulated compound
 351 to be liberated from lipid particles.^{25,33} Hence, the degradation
 352 of encapsulated VB is exacerbated at high temperatures.
 353

E

<https://doi.org/10.1021/acsmchemlett.2c00145>
 ACS Med. Chem. Lett. XXXX, XXX, XXX–XXX

354 Although VB is a promising component of *Acanthus*
 355 *ebracteatus* Vahl. (AE) for health applications due to its
 356 bioactivities, its degradation is a limitation to potential uses.
 357 Our thermal degradation kinetics study reveals that the
 358 degradation of VB is a first-order reaction. The chemical
 359 reaction parameters according to Arrhenius's theory indicate
 360 that VB is unstable when it dissolves in aqueous solution. The
 361 reaction rate in neutral to alkaline solutions was faster than in
 362 acidic solution. The stability of VB is successfully improved by
 363 encapsulating VB into SLNs that can substantially extend VB's
 364 shelf life. The shelf life of VB in SLNs was 153 days with $E_a =$
 365 $76.16 \text{ kJ mol}^{-1}$, whereas those of VB in AE extract and in AE
 366 extract solution were 75 days with $E_a = 78.03 \text{ kJ mol}^{-1}$ and 12
 367 days with $E_a = 49.24 \text{ kJ mol}^{-1}$, respectively. Therefore, we
 368 anticipate that the AE extract-loaded SLNs will be beneficial
 369 for product development. However, they should be further
 370 examined in both *in vitro* and clinical studies to evaluate their
 371 safety and efficacy.

372 ■ AUTHOR INFORMATION

373 Corresponding Author

374 **Neti Waranuch** – Department of Pharmaceutical Technology,
 375 Faculty of Pharmaceutical Sciences, and Center of Excellence
 376 for Innovation in Chemistry and Cosmetics and Natural
 377 Products Research Center, Faculty of Pharmaceutical
 378 Sciences, Naresuan University, Phitsanulok 65000,
 379 Thailand; orcid.org/0000-0001-7476-7288;
 380 Phone: +66-815339002; Email: netiw@nu.ac.th

381 Authors

382 **Vanuchawan Wisuitiprot** – Department of Pharmaceutical
 383 Technology, Faculty of Pharmaceutical Sciences, and Center
 384 of Excellence for Innovation in Chemistry, Naresuan
 385 University, Phitsanulok 65000, Thailand
 386 **Kornkanok Ingkaninan** – Department of Pharmaceutical
 387 Chemistry and Pharmacognosy, Faculty of Pharmaceutical
 388 Sciences, Naresuan University, Phitsanulok 65000, Thailand
 389 **Panlop Chakkavittumrong** – Division of Dermatology,
 390 Department of Medicine, Faculty of Medicine, Thammasat
 391 University, Pathumthani 12121, Thailand
 392 **Wudtichai Wisuitiprot** – Sirindhorn College of Public Health
 393 Phitsanulok, Faculty of Public Health and Allied Health
 394 Sciences, Praboromarajchanok Institute, Ministry of Public
 395 Health, Nonthaburi 65130, Thailand
 396 **Eakkaluk Wongwad** – Department of Pharmaceutical
 397 Chemistry and Pharmacognosy, Faculty of Pharmaceutical
 398 Sciences, Naresuan University, Phitsanulok 65000, Thailand;
 399 Department of Cosmetic Sciences, School of Pharmaceutical
 400 Sciences, University of Phayao, Phayao 66000, Thailand

401 Complete contact information is available at:

402 <https://pubs.acs.org/10.1021/acsmchemlett.2c00145>

403 Author Contributions

404 Conceptualization, V.W., N.W., P.C., and K.L.; methodology
 405 and experimental design, V.W., K.L., W.W., E.W., and N.W.;
 406 validation, V.W., E.W., and N.W.; formal analysis, V.W. and
 407 N.W.; investigation, V.W., K.L., and N.W.; resources, V.W. and
 408 N.W.; data curation and interpretation, V.W., W.W., and N.W.;
 409 writing - original draft preparation, V.W., W.W., and N.W.;
 410 writing - review and editing, V.W., K.L., and N.W.; visual-
 411 ization, V.W. and N.W.; supervision, V.W., P.C., K.L., and
 412 N.W.; project administration, N.W.; funding acquisition, N.W.

All authors have read and agreed to the published version of
 the manuscript.

Notes

The authors declare no competing financial interest.

■ ACKNOWLEDGMENTS

This study was supported by Thailand Center of Excellence for
 Life Sciences (TCELS), and the Center of Excellence for
 Innovation in Chemistry (PERCH-CIC), Ministry of Higher
 Education, Science, Research and Innovation, Thailand. We
 thank Mr. Roy I. Morien of the Naresuan University Graduate
 School for his assistance in editing the English expression and
 grammar in this document.

■ ABBREVIATIONS

AE, *Acanthus ebracteatus*; E_a , activation energy; HLB, hydro-
 philic–lipophilic balance; LOD, limit of detection; LOQ, limit
 of quantification; PS, particle size; PDI, polydispersity index;
 SLN, solid lipid nanoparticle; VB, verbascoside; ZP, zeta
 potential

■ REFERENCES

- (1) Srivilai, J.; Phimnuan, P.; Jaisabai, J.; Luangtoomma, N.;
 Waranuch, N.; Khorana, N.; Wisuitiprot, W.; Scholfield, C. N.;
 Champachaisri, K.; Ingkaninan, K. Curcuma aeruginosa Roxb.
 essential oil slows hair-growth and lightens skin in axillae; a
 randomised, double blinded trial. *Phytotherapy* **2017**, *25*, 29–38.
- (2) Therdphapiyanak, N.; Jaturanpinyo, M.; Waranuch, N.;
 Kongkanermit, L.; Sarisuta, N. Development and assessment of
 tyrosinase inhibitory activity of liposomes of Asparagus racemosus
 extracts. *Asian Journal of Pharmaceutical Sciences* **2013**, *8* (2), 134–
 142.
- (3) Viyoch, J.; Buranajaree, S.; Grandmottet, F.; Robin, S.; Binda,
 D.; Viennet, C.; Waranuch, N.; Humbert, P. Evaluation of the effect
 of Thai breadfruit's heartwood extract on the biological functions of
 fibroblasts from wrinkles. *J. Cosmet. Sci.* **2010**, *61* (4), 311–324.
- (4) Khunkitti, W.; Veerapan, P.; Hahnvajanawong, C. *In vitro*
 bioactivities of clove buds oil (Eugenia caryophyllata) and its effect on
 dermal fibroblast. *International Journal of Pharmacy and Pharmaceuti-
 cal Sciences* **2012**, *4*, 556–560.
- (5) Kubica, P.; Szopa, A.; Kokotkiewicz, A.; Miceli, N.; Taviano, M.
 F.; Maugeri, A.; Cirni, S.; Synowiec, A.; Gniewosz, M.; Elansary, H.
 O.; Mahmoud, E. A.; El-Ansary, D. O.; Nasif, O.; Luczkiewicz, M.;
 Ekiert, H. Production of Verbascoside, Isoverbascoside and Phenolic
 Acids in Callus, Suspension, and Bioreactor Cultures of Verbena
 officinalis and Biological Properties of Biomass Extracts. *Molecules*
2020, *25* (23), 5609.
- (6) Kanchanapoom, T.; Kasai, R.; Picheansoonthon, C.; Yamasaki,
 K. Megastigmane, aliphatic alcohol and benzoxazinoid glycosides
 from *Acanthus ebracteatus*. *Phytochemistry* **2001**, *58* (5), 811–817.
- (7) Paola, R. D.; Oteri, G.; Mazzon, E.; Crisafulli, C.; Galuppo, M.;
 Toso, R. D.; Pressi, G.; Cordasco, G.; Cuzzocrea, S. Effects of
 verbascoside, biotechnologically purified by *Syringa vulgaris* plant cell
 cultures, in a rodent model of periodontitis. *J. Pharm. Pharmacol.*
2011, *63* (5), 707–17.
- (8) Kim, K. H.; Kim, S.; Jung, M. Y.; Ham, I. H.; Whang, W. K. Anti-
 inflammatory phenylpropanoid glycosides from *Clerodendron*
trichotomum leaves. *Arch. Pharm. Res.* **2009**, *32* (1), 7–13.
- (9) Andary, C.; Wylde, R.; Laffite, C.; Privat, G.; Winternitz, F.
 Structures of verbascoside and orobanchoside, caffeic acid sugar esters
 from *Orobancha rapum-genistae*. *Phytochemistry* **1982**, *21* (5), 1123–
 1127.
- (10) Vertuani, S.; Beghelli, E.; Scalambra, E.; Malisardi, G.; Copetti,
 S.; Dal Toso, R.; Baldisserotto, A.; Manfredini, S. Activity and stability
 studies of verbascoside, a novel antioxidant, in dermo-cosmetic and

F

<https://doi.org/10.1021/acsmchemlett.2c00145>
 ACS Med. Chem. Lett. XXXX, XXX, XXX–XXX

- 475 pharmaceutical topical formulations. *Molecules (Basel, Switzerland)* 2011, 16 (8), 7068–7080.
- 477 (11) Wisuitiprot, V.; Ingkaninan, K.; Chakkavittumrong, P.;
478 Wisuitiprot, W.; Neungchamnong, N.; Chantakul, R.; Waranuch, N.
479 Effects of *Acanthus ebracteatus* Vahl. extract and verbascoside on
480 human dermal papilla and murine macrophage. *Sci. Rep.* 2022, 12 (1),
481 1491.
- 482 (12) Adebayo, S. A.; Dzoyem, J. P.; Shai, L. J.; Eloff, J. N. The anti-
483 inflammatory and antioxidant activity of 25 plant species used
484 traditionally to treat pain in southern African. *BMC Complementary*
485 *and Alternative Medicine* 2015, 15, 159.
- 486 (13) Laupattarakasem, P.; Houghton, P. J.; Houlst, J. R. S.; Itharat, A.
487 An evaluation of the activity related to inflammation of four plants
488 used in Thailand to treat arthritis. *Journal of Ethnopharmacology* 2003,
489 85 (2–3), 207–215.
- 490 (14) Jaidee, W.; Siridechakorn, I.; Nessopa, S.; Wisuitiprot, V.;
491 Chaiwangrach, N.; Ingkaninan, K.; Waranuch, N. Kinetics of CBD,
492 $\Delta(9)$ -THC Degradation and Cannabinol Formation in Cannabis
493 Resin at Various Temperature and pH Conditions. *Cannabis*
494 *Cannabinoid Res.* 2021, DOI: 10.1089/can.2021.0004.
- 495 (15) Wongwad, E.; Ingkaninan, K.; Wisuitiprot, W.; Sritularak, B.;
496 Waranuch, N. Thermal Degradation Kinetics and pH-Rate Profiles of
497 Iridophenone 3,5-C- β -d-diglucoiside, Iridophenone 3-C- β -d-Glucoside
498 and Mangiferin in *Aquilaria crassna* Leaf Extract. *Molecules* 2020, 25
499 (21), 4898.
- 500 (16) Zhou, F.; Zhao, Y.; Li, M.; Xu, T.; Zhang, L.; Lu, B.; Wu, X.;
501 Ge, Z. Degradation of phenylethanoid glycosides in *Osmanthus*
502 *fragrans* Lour. flowers and its effect on anti-hypoxia activity. *Sci. Rep.*
503 2017, 7 (1), 10068.
- 504 (17) Isacchi, B.; Bergonzi, M. C.; Iacopi, R.; Ghelardini, C.; Galeotti,
505 N.; Bilia, A. R. Liposomal Formulation to Increase Stability and
506 Prolong Antineuropathic Activity of Verbascoside. *Planta Med.* 2017,
507 83 (5), 412–419.
- 508 (18) Sinico, C.; Caddeo, C.; Valenti, D.; Fadda, A. M.; Bilia, A. R.;
509 Vincieri, F. F. Liposomes as carriers for verbascoside: stability and
510 skin permeation studies. *J. Liposome Res.* 2008, 18 (1), 83–90.
- 511 (19) Sinko, P. J. Chemical Kinetics and Stability. In *Martin's Physical*
512 *Pharmacy and Pharmaceutical Sciences*; Sinko, P. J., Ed.; Lippincott
513 Williams & Wilkins: China, 2006; Vol. 6, p 318.
- 514 (20) Akdemir, Z.; Kahraman, C.; Tatlı, I. I.; Küpeli Akkol, E.;
515 Süntar, I.; Keles, H. Bioassay-guided isolation of anti-inflammatory,
516 antinociceptive and wound healer glycosides from the flowers of
517 *Verbascum mucronatum* Lam. *J. Ethnopharmacol.* 2011, 136 (3),
518 436–43.
- 519 (21) Jiménez, C.; Villaverde, M. C.; Riguera, R.; Castedo, L.;
520 Stermitz, F. Phenylpropanoid Glycosides from *Mussatia hyacinthina*.
521 *J. Nat. Prod.* 1989, 52 (2), 408–410.
- 522 (22) Brito-Arias, M., Hydrolysis of Glycosides. In *Synthesis and*
523 *Characterization of Glycosides*; Brito-Arias, M., Ed.; Springer US:
524 Boston, MA, 2007; pp 304–313.
- 525 (23) Madan, J. R.; Khude, P. A.; Dua, K. Development and
526 evaluation of solid lipid nanoparticles of Mometasone furoate for
527 topical delivery. *International journal of pharmaceutical investigation*
528 2014, 4 (2), 60–4.
- 529 (24) Müller, R. H.; Mäder, K.; Gohla, S. Solid lipid nanoparticles
530 (SLN) for controlled drug delivery - a review of the state of the art.
531 *Eur. J. Pharm. Biopharm.* 2000, 50 (1), 161–177.
- 532 (25) Aburahma, M. H.; Badr-Eldin, S. M. Compritol 888 ATO: a
533 multifunctional lipid excipient in drug delivery systems and nano-
534 pharmaceuticals. *Expert opinion on drug delivery* 2014, 11 (12), 1865–
535 83.
- 536 (26) Helgason, T.; Awad, T. S.; Kristbergsson, K.; McClements, D.
537 J.; Weiss, J. Effect of surfactant surface coverage on formation of solid
538 lipid nanoparticles (SLN). *J. Colloid Interface Sci.* 2009, 334 (1), 75–
539 81.
- 540 (27) Salminen, H.; Helgason, T.; Aulbach, S.; Kristinsson, B.;
541 Kristbergsson, K.; Weiss, J. Influence of co-surfactants on crystal-
542 lization and stability of solid lipid nanoparticles. *J. Colloid Interface Sci.*
543 2014, 426, 256–63.
- (28) Rostamkalaei, S. S.; Akbari, J.; Saeedi, M.; Morteza-Semnani, 544
K.; Nokhodchi, A. Topical gel of Metformin solid lipid nanoparticles: 545
A hopeful promise as a dermal delivery system. *Colloids Surf., B* 2019, 546
175, 150–157. 547
- (29) Bhalekar, M.; Upadhaya, P.; Madgulkar, A. Formulation and 548
characterization of solid lipid nanoparticles for an anti-retroviral drug 549
darunavir. *Applied Nanoscience* 2017, 7 (1), 47–57. 550
- (30) Ngwuluka, N. C.; Kotak, D. J.; Devarajan, P. V. Design and 551
Characterization of Metformin-Loaded Solid Lipid Nanoparticles for 552
Colon Cancer. *AAPS PharmSciTech* 2017, 18 (2), 358–368. 553
- (31) Singh, H.; Bhandari, R.; Kaur, I. P. Encapsulation of Rifampicin 554
in a solid lipid nanoparticulate system to limit its degradation and 555
interaction with Isoniazid at acidic pH. *International journal of* 556
pharmaceutics 2013, 446 (1–2), 106–11. 557
- (32) Makoni, P. A.; Wa Kasongo, K.; Walker, R. B. Short Term 558
Stability Testing of Efavirenz-Loaded Solid Lipid Nanoparticle (SLN) 559
and Nanostructured Lipid Carrier (NLC) Dispersions. *Pharmaceutics* 560
2019, 11 (8), 397. 561
- (33) Freitas, C.; Muller, R. H. Correlation between long-term 562
stability of solid lipid nanoparticles (SLN) and crystallinity of the lipid 563
phase. *Eur. J. Pharm. Biopharm.* 1999, 47 (2), 125–32. 564



BIOGRAPHY

มหาวิทยาลัยนครพนม

BIOGRAPHY

Name-Surname	Vanuchawan Wisuitiprot
Date of Birth	
Address	
Current Workplace	Mohya Pharmacy 83/255 Phra Ruang Road Ampoe Muang Phitsanulok 65000
Current Position	Owner
Education Background	2000 B.Sc. (Physiotherapy), Khonkaen University 2016 M.Sc. (Cosmetic Sciences), Naresuan University
Publication	Fachrunniza, Y., Srivilai, J., Wisuitiprot, V., Wisuitiprot, W., Suphrom, N., Temkitthawon, P., Ingkaninan, K. (2020). <i>Tectona grandis</i> , a potential active ingredient for hair growth promotion. <i>Songklanakarin Journal of Science and Technology</i> , 42(6), 1352-1359. Wisuitiprot, V., Bumrungrachaichana, W., Kaewtai, N., Rawangking, A., Saiphanit, S., Lasongmuang, K., . . . Wisuitiprot, W. (2019). Effectiveness of a Plai Oil Prepared by Thai Traditional Medicine Process in the Treatment of Myofascial Pain Syndrome: A Randomized Placebo Controlled Trial. <i>Journal of Health Science and Medical Research</i> , 37(4), 16-21. Wisuitiprot, W., Wisutthathum, S., Pitiporn, S., Wisuitiprot, V., Kwankhao, P., & Waranuch, N. (2019). Effect of <i>Garcinia Mangostana</i> Linn Fruit Peel Ethanolic Extract on Fibroblast Cell Migration. <i>Journal of Scientific & Medical Research</i> , 19(3), 1439-14397. Wisuitiprot, W., Wisuitiprot, V., Keawtai, N., & Sreenoukrow, P. (2020). Bioactivity Study of <i>Tadehagi triquetrum</i> (L.) H. Extracts Used in Thai Folk Medicine. <i>Journal of Thai Traditional and Alternative Medicines</i> , 18(2), 259-269. Jaidee W, Siridechakorn I, Nessopa S, Wisuitiprot V, Chaiwangrach N, Ingkaninan K, Waranuch N. Kinetics of CBD, Δ^9 -THC Degradation and Cannabinol Formation in Cannabis Resin at Various Temperature and pH Conditions. <i>Cannabis Cannabinoid Res.</i> 2021 Jun 4. doi: 10.1089/can.2021.0004. Epub ahead of print. PMID: 34096805.
Awards	2021: Best Oral Presentation in Biological Sciences, The 38th International Conference of the Microscopy Society of Thailand. Chonburi: Burapha university

